Investigation Of Hypoxia And Mitochondrial Dysfunction In The Central Nervous System Resulting From Focal And Systemic Inflammation

Kim Imogen Chisholm

UCL Institute of Neurology

Supervised by:

Professor Kenneth Smith

Professor Michael Duchen

A thesis submitted for the degree of Doctor of Philosophy (Ph.D)

I, Kim Imogen Chisholm, confirm that the work presented in this thesis is my own. Where information has been derived from other sources, I confirm that this has been indicated in the thesis.

Acknowledgements Please excuse the unscientific nature of these but so rarely does one get the opportunity to officially thank all the people that have supported one so much

My most severe and humble gratitude goes to the numerous non-human animals that have provided the very basis for the advancement of human health and wellbeing. Many years of my life have been spent genuinely appreciating the sacrifices made in the name of science and in a very futile attempt I would like to thank all the mice and rats I have used for my own research. Thank you.

I would also like to extend my most sincere thanks to my supervisors Professor Kenneth Smith and Professor Michael Duchen who took me on despite my complete lack of experience. You took quite a risk and I hope I have not disappointed you as you truly provided me with a wonderful support network that has made my PhD not only possible but hugely enjoyable. Thank you very much for all your continuous support and guidance. They have not gone unappreciated.

Image from https://www.tumblr.com/search/dna%20lab. Monument in Novosibirsk dedicated to laboratory rodents

Despite the "rollercoaster" that is one's PhD one thing has always been stable. The unshakable support provided by my friends in the "Department of Neuroinflammation". Every one of the lab members has enriched my PhD experiences in ways that I did not think was possible but I would like to extend my particular thanks to a few very special people. Thank you, Dr Andrew Davies and Dr Roshni Patel for their patient help and support, Fabian Peters for so many exceptional conversations and suggestions, Dr Radha Desai for being the best mentor in the whole world and a huge inspiration, Mario Amatruda for being the calmest pillar in the storm, Alex Phillips for putting everything in context and the lovely marmalade, and finally to those who are most dear to me and have made everything shiny and sparkling: Thank you from the very bottom of my heart to Keila Ida and Dimitra Schiza who are simply the best scientific and social support I could have hoped for. Without your support I would not have been able to complete half my PhD and more importantly I would have not been able to enjoy it to the extent that I did. We have spent so many amazing days together that I feel deeply unhappy about leaving this seat of happiness I have found but I remind myself: "How lucky am I to have something that makes saying goodbye so hard" WtP.

Without my dearest friends, Anna Karra and Dr Laura de Molière, I would have never had the courage to attempt any scientific exploration. Thanks to your relentless support and uncompromising friendship, I can dare everything because I know I have you to fall back on. You have ALWAYS provided the relief from emotional and physical stress and ALWAYS manage to build me up again, no matter how badly the experiment went or how little one thinks one has achieved. Many evenings have been spent discussing the basics of science, hypothesis testing and statistics as well as other fun topics, and without this my horizon would be so much narrower. Thank you!

I am also acutely aware that my family is the main reason I have had this incredible opportunity. Daniel and Sarah, you have always been the best role models to me and have taught me what is desirable and what is possible. Looking up to you meant that I always had a light to follow. Sarah, so many times have you been the reason why I believed in myself with your continuous encouragement and support. Daniel, so often have I turned to you for advice and guidance and I have never been disappointed. Mum and Dad, it is rare that I am short of words but I don't quite know how to say 'thank you'. I know that any achievement, no matter how small, is only thanks to you. Everything you have built for me, every strength you have fostered in me is embedded in the loving sacrifices you have made and the undiluted kindness you have always shown. I have been given the greatest privilege in the world to have had you support me through this PhD because I know no matter how badly I fail I will always find love and support from you.

Everyone needs someone who is there for you day and night no matter what. Especially the often discouraging experience of a PhD drives you right to those who take care of you. For me this support has always and unyieldingly been provided by Dr Tommaso Tufarelli who has shared this experience with me from start to finish and who has very often suffered the consequences. Thank you for always supporting me, even when I have not made it easy, and giving me the courage to do this.

ABSTRACT

Inflammation is an important feature of several seemingly disparate neurological disorders, including multiple sclerosis, Parkinson's disease and sepsis-related brain dysfunction. Inadequate oxygenation and mitochondrial dysfunction have been implicated in these and other CNS pathologies in which inflammation is found. Indeed, inflammation can have direct or indirect effects on mitochondrial function, for example, via reactive oxygen/nitrogen species, or through compromised perfusion respectively. However, the study of oxygenation and mitochondrial function in the CNS has been limited as tissues are typically excised for study *in vitro*, invariably exposing cells and their mitochondria to non-physiological environments. To overcome these limitations, the work described in this thesis involved the study of mitochondrial dysfunction and tissue oxygenation in the CNS during local and systemic inflammation in whole-animal preparations under physiological and pathophysiological conditions.

The experiments include development of *in vivo* optical imaging techniques to assess the redox potential of mitochondria, without the application of dyes, and with an intact blood supply. Using this technique in conjunction with established methods we investigated mitochondrial function and tissue oxygen concentrations in cortical and retinal models of local and systemic inflammation.

Our findings reveal that mitochondrial flavoprotein autofluorescence imaged in the cortex of anaesthetised mice can be used to assess an aspect of mitochondrial function (redox potential) in the CNS *in vivo*. Additionally, we show that certain types of inflammation are associated with tissue hypoxia in the brain and retina, and that this can have profound functional consequences for cerebral mitochondria during systemic inflammation. Hypothermia was also explored as a potential therapeutic strategy to attenuate inflammation-induced functional deficits.

Collectively, these findings further our understanding of the mechanisms underlying neurological deficits associated with inflammation, and reveal mitochondrial redox state imbalances in certain inflammatory conditions with potential implications for the treatment of CNS disorders in which inflammation plays a role.

TABLE OF CONTENT

LIST OF FIGURES

1. Introduction

Page

2. Flavoproteins in the cortex

3. Mitochondrial function in the CNS during systemic inflammation

4. Retinal inflammation

LIST OF TABLES

Page

1. Introduction

2. Mitochondrial function in the CNS during systemic inflammation

3. Retnal inflammation

ABBREVIATIONS

αKGDH	Alpha Ketoglutarate Dehydrogenase
AMD	Age-Related Macular Degeneration
ANOVA	Analysis of Variance
ATP	Adenosine Triphosphate
BN	Brown Norway
CC	Choriocapillaris
CFA	Complete Freud's Adjuvant
CFH	Complement Factor H
CNS	Central Nervous System
DAB	3,3′-Diaminobenzidine
DAF-FM	4-Amino-5-Methylamino-2',7'-Difluorofluorescein
DMSO	Dimethyl Sulfoxide
DNA	Deoxyribonucleic Acid
DPI	Diphenyleneiodonium
DPX	Dibutyl Phthalate Xylene
EAE	Experimental Autoimmune Encephalomyelitis
ECG	Electrocardiogram
EIU	Endotoxin-Induced Uveitis
eNOS	Endothelial Nitric Oxide Synthase
ERG	Electroretinogram
ETC	Electron Transport Chain
ETF	Electron Transfer Flavoproteins
FAD	Flavin Adenine Dinucleotide
FCCP	Carbonyl Cyanide 4-(trifluoromethoxy)phenylhydrazone
FiO_2	Fraction of Inspired Oxygen
FLIM	Fluorescence Lifetime Imaging
FMN	Flavin Mononucleotide
GCL	Ganglion Cell Layer
GSH	Reduced Glutathione
GSSG	Oxidized Glutathione
H&E	Haematoxylin and Eosin
HEPES	4-(2-hydroxyethyl)-1-piperazineethanesulfonic acid
IL-1	Interleukin-1
INL	Inner Nuclear Layer
iNOS	Inducible Nitric Oxide Synthase
i.p.	Intraperitoneally
IPL	Inner Plexiform Layer
IS	Inner Segment (of photoreceptors)
LipDH	Lipoamide Dehydrogenase
L-NMMA	N-Monomethyl-L-Arginine
LPS	Lipopolysaccharide
MHC	Major Histocompatibility Complex
MHCII	Major Histocompatibility Complex Class II
MOG	Myelin Oligodendrocyte Glycoprotein

MON	Myelinated Optic Nerve	PFA	Paraformaldehyde
MS	Multiple Sclerosis	Pfkfb3	6-Phosphofructo-2-Kinase/Fructose-2,6-Biphosphatase 3
NaCN	Sodium Cyanide	p.i.	Post injection
NAD(P)	Oxidized Nicotinamide Adenine Dinuclerotide (Phosphate)	PRL	Photoreceptor Layer
NAD(P)H	Reduced Nicotinamide Adenine Dinuclerotide (Phosphate)	PtPFPP	Platinum(II)-5,10,15,20-Tetrakis(2,3,4,5,6-Pentafluorophenyl)Porphyrin
NFL	Nerve Fibre Layer	rMOG	Recombinant Myelin Oligodendrocyte Glycoprotein
NO	Nitric Oxide	RPE	Retinal Pigment Epithelium
O_2	Oxygen	SEM	Standard Error of the Mean
OCT	Optimal Cutting Temperature	TCA	Tricarboxylic Acid Cycle
ONL	Outer Nuclear Layer	TLR4	Toll-Like Receptor 4
OPL	Outer Plexiform Layer	TMRM	Tetramethylrhodamine Methyl Ester
OS	Outer Segment (of photoreceptors)	TNF-α	Tumour necrosis factor alpha
PBS	Phosphate Buffered Saline	VDAC-1	Voltage-Dependent Anion- Channel 1
PDH	Pyruvate Dehydrogenase Complex	VEGF	Vascular Endothelial Growth Factor

HYPOTHESES

1) Both local and systemic inflammation can lead to reduction in tissue oxygen concentrations in the central nervous system
2) Such reductions in tissue oxygen can have consequences on mitochondrial function
3) Flavoprotein fluorescence can be used to assess the consequences of inflammation on an aspect of mitochondrial function (redox potential) in the brain and retina

CHAPTER ONE

1. Introduction

1.1. Inflammation

Inflammation is an adaptive mechanism aimed at limiting tissue damage by, for example, preventing the spread of infiltrating pathogens, and promoting recovery. However, chronic or excessive inflammation can lead to large scale damage. Despite the 'immune privilege' enjoyed by the central nervous system (CNS), including a blood brain/retinal/spinal cord barrier and the absence of a conventional lymphatic system, it is now appreciated that inflammation plays a key role in many physiological and pathological processes in the CNS (Carson et al. 2006; Galea et al. 2007). As such, CNS inflammation has been associated with several neurological conditions, including Alzheimer's disease, Parkinson's disease, multiple sclerosis (MS) and sepsis-related brain dysfunction (Akiyama 2000; Bennett and Stuve 2009; Mcgeer and Mcgeer 2004; Trapp et al. 1998; Young et al. 1990). Additionally, inflammation has been implicated in ocular pathology of various types, such as uveitis (which can occur for example in MS, juvenile rheumatoid arthritis or inflammatory bowel disease) or age-related macular degeneration (AMD) (Calabresi et al. 2010; Coffey et al. 2007; Flemming 2011; Hageman et al. 2005; Hollyfield et al. 2008). Therefore, the study of the consequences of CNS inflammation remains an important topic and both the effect of local inflammation, as well as peripheral inflammation on CNS organs, is of great importance.

A large body of evidence now implicates the failure of bioenergetics in inflammatory pathology, including both mitochondrial damage leading to dysfunctional oxygen uptake, as well as vascular complications which result in inadequate oxygen delivery and secondary mitochondrial dysfunction.

Inflammation in the CNS involves several characteristic changes, including the activation of resident immune cells, such as microglia, and the recruitment of other immune cells, including macrophages and/or lymphocytes. Inflammation often also involves the production of reactive oxygen and nitrogen species such as superoxide and nitric oxide (NO) as well as changes in the vasculature, such as increased permeability or disturbed blood-flow.

Microglial activation is characteristic of CNS inflammation (Kreutzberg 1996) and is an early indicator of inflammation (Banati et al. 1993; Gehrmann et al. 1995; Kreutzberg 1996). Microglial/macrophage activation, following trauma or pathogen entry, involves their proliferation and migration towards the pathological stimulus (Kreutzberg 1996) as well as an upregulation of major histocompatibility complexes (MHC) and enhanced phagocytic activity (Kreutzberg 1996). Their activation can be assessed by morphological changes (Nakajima and Kohsaka 2005; Streit 2005) or by the expression of certain markers including CD68. Microglia and macrophages, as well as other activated cells, including endothelial cells (Kroll and Waltenberger 1998; Nussler and Billiar 1993), can then produce reactive nitrogen and oxygen species as well as a host of inflammatory cytokines and chemokines (Banati et al. 1993; Gibson et al. 2005) which amplify the immune response by recruiting other immune cells to the site of injury. Such responses are primarily aimed at pathogen destruction but can be associated with host tissue damage (Bennett and Stuve 2009; Block and Hong 2005), including damage to mitochondria and the vasculature. Oxidative stress is particularly important in situations of inadequate antioxidant defences, such as occur in several inflammatory conditions (Goode et al. 1995; LihBrody et al. 1996; Spronk et al. 2005). Under such circumstances, reactive oxygen species can more readily result in DNA damage and lipid peroxidation, including in both mitochondria (Richter et al. 1988; Shigenaga et al. 1994; Yakes and VanHouten 1997) and endothelial cells (Spronk et al. 2005). Such damage can be particularly important in mitochondria which are themselves a major source of free radicals when leaking

electrons from the electron transport chain (ETC) to reduce oxygen into superoxide anions (Boveris and Chance 1973; Murphy 2009; Turrens 1997; Turrens 2003).

Inflammation can also lead to an up-regulation of inducible NO synthase (iNOS) (Bruins et al. 2002; Sato et al. 1995; Wong et al. 1996), which can produce high levels of NO in many cell types, including inflammatory cells and endothelial cells (Nussler and Billiar 1993). NO can be a potent reversible as well as irreversible inhibitor of mitochondrial function (see below: 'Mitochondria in inflammation') and also plays an important role in physiological and pathological regulation of the vascular network. Under physiological conditions NO (including NO produced by endothelial NOS (eNOS)) can influence vasodilation and blood flow in response to a variety of stimuli (Dirnagl et al. 1993; Lowenstein et al. 1994; Minson et al. 2001; Palmer et al. 1987; Vallance et al. 1989). Additionally, pathological up-regulation of iNOS can reduce vascular resistance and vascular reactivity to changes in oxygen supply/demand, and can reduce vascular contraction in response to agents such as noradrenaline (da Silva-Santos et al. 2002; Fernandes and Assreuy 2008; Fleming et al. 1991). Despite the extensive body of research implicating NO in inflammatory damage, a randomized controlled phase III trial on the effect of N-monomethyl-L-arginine (L-NMMA; non-specific NOS inhibitor) in septic patients had to be prematurely terminated due to higher mortality in the treatment group (Grover et al. 1999). Thus, the 28-day mortality rate in the treatment group was 10% higher compared to the placebo group. This effect could be attributed to NOs role as a competitor to oxygen for the binding site on complex IV. This competition with O_2 has been suggested to regulate mitochondrial respiration in response to changes in available oxygen, allowing mitochondria to sense oxygen changes effectively (Brown 1995). Such a regulation of oxygen consumption could prove beneficial in situations of reduced oxygen supply. Therefore, even if NO inhibition improves oxygen delivery in sepsis through improved haemodynamics, the beneficial effects might be counteracted by increased oxygen consumption, which is in line with findings suggesting increased oxygen consumption during inhibition of NOS (Laycock et al. 1998;

Shen et al. 1994). This would suggest that respiratory inhibition might prove beneficial in inflammatory conditions in which oxygenation is compromised (see chapter 3).

Additionally, other inflammatory mediators can influence vascular function during inflammation. Examples include neutrophil and/or cytokine-mediated endothelial cell damage (Fujita et al. 1991; Meyrick et al. 1991), up-regulation of adhesion molecule expression (Astiz et al. 1995; Smith 1993), a decrease in red blood cell deformability (Astiz et al. 1995; Machiedo et al. 1989; Powell et al. 1991; Todd et al. 1993), an increase in vascular permeability (Wedmore and Williams 1981), coagulation (Schouten et al. 2008) and vascular flow heterogeneity (De Backer et al. 2002). All these factors have potential to influence organ perfusion and it is therefore not surprising that inflammation has been associated with tissue hypoxia (Eltzschig and Carmeliet 2011; Karhausen et al. 2005), including in animal models of MS (Davies et al. 2013) and sepsis (Goldman et al. 2004; Ince 2005; Vallet et al. 1994). Indeed, deficiencies in motor function associated with the clinical onset of experimental autoimmune encephalomyelitis (EAE, a rodent model of MS) were attenuated by oxygen therapy (Davies et al. 2013) and treatment aimed at microcirculatory recovery in sepsis have shown promise (Anning et al. 1999; Bateman and Walley 2005; Spronk et al. 2002). However, limited information exists on the spatial distribution of hypoxia during inflammatory diseases.

1.1.1. Inflammation in sepsis

During conditions of severe infection, the associated pathogen may enter the bloodstream and cause a whole-body inflammatory response which can result in systemic inflammatory response syndrome and sepsis. Sepsis is therefore an often fatal condition of systemic inflammation, occurring distal from the original insult. Sepsis can lead to its hallmark multiple organ dysfunction and eventually death by combined damage from the invading pathogen and, more importantly, from the over-activity of the host immune system (Cohen 2002; Schouten et al. 2008). During the initial

infection pathogenic components, such as lipopolysaccharides (LPS, or endotoxin) from the cell wall of Gram-negative bacteria, can result in the activation of immune and endothelial cells via pattern recognition receptors, including toll-like receptor 4 (TLR4) (Chow et al. 1999; Henneke and Golenbock 2002). Complex inflammatory cascades follow which can influence both mitochondrial and endothelial cells resulting in, for example, mitochondrial swelling (Crouser et al. 2002a; Crouser et al. 2002b; Zapelini et al. 2008), cytochrome c release (Zapelini et al. 2008), mitochondrial depolarisation (Lowes et al. 2008), dysfunctional energy production (Brown and Bal-Price 2003; Chaudry et al. 1979; Leist et al. 1999) as well as endothelial cell damage and apoptosis (Frey and Finlay 1998), enhanced adhesion molecule expression (Albelda et al. 1994; Parent and Eichacker 1999), increased vascular permeability (Pickkers et al. 2005; Wilhelm 1962), hypovolaemia (Wilson et al. 1971) and hypotension (Kumar et al. 2006) which provide the hallmarks of sepsis-related dysfunction. LPS are very important molecules in sepsis, as ~45% of sepsis cases are caused by Gram-negative bacteria (Alberti et al. 2002) and even the more severe toxic shock sepsis, associated with an initial Gram-positive bacterial infection (typically seen in women after prolonged retention of tampons or intrauterine devices), has been associated with hypersensitivity towards LPS (Cohen 2002). After binding to the TLR4 (Chow et al. 1999), LPS induced a strong inflammatory reaction mediated for example by the rapid expression of tumour necrosis factor α (TNF-α) and interleukin-1 (IL-1). TNF-α and IL-1 are then able to affect the transcription and translation of numerous other inflammatory mediators, including iNOS (Dinarello 1997) which produces NO and thereby affects both the vasculature and the local tissue environment, including mitochondria as mentioned before. During or following a period of intense inflammation, compensatory anti-inflammatory activity can be initiated, including the production of interleukin-10 (Marchant et al. 1994) and transforming growth factor-β (Marie et al. 1996). This compensatory anti-inflammatory reaction has been suggested to be an adaptive response to limit the spread of immune-mediated damage but which can also play a detrimental role in the pathogenesis of multiple

organ dysfunction and death, leaving some patients immune-suppressed and unable to combat infection (for reviews see (Adib-Conquy and Cavaillon 2009; Bone et al. 1997)).

Although comparatively understudied it is now clear that the brain plays an essential role in the disease course of sepsis. In fact studies have shown that brain dysfunction, including delirium, confusion and even coma, occurs in around 70% of patients (Young et al. 1990), is associated with increased mortality (Eidelman et al. 1996; Sprung et al. 1988) and can result in prolonged cognitive impairment in survivors of sepsis (Semmler et al. 2013). Such symptoms can occur even in the absence of local CNS inflammation (Sonneville et al. 2013) and instead systemic inflammation can be relayed to the brain via the vagus nerve and/or circumventricular organs (Sonneville et al. 2013). These pathways can then lead to an increase in the transcription of several inflammatory mediators and to microglial cell activation (Hannestad et al. 2012; Semmler et al. 2005). In addition, vascular changes have been observed also in cerebral structures, including endothelial cell dysfunction (Handa et al. 2008), altered cerebral perfusion (Bowton et al. 1989; Maekawa et al. 1991) and vascular autoregulation (Taccone et al. 2010), swelling of perivascular astrocytes (Papadopoulos et al. 1999), blood brain barrier breakdown (Jeppsson et al. 1981; Young et al. 1992) and oedema (Papadopoulos et al. 1999), suggesting an additional, more direct pathway for brain damage in sepsis. Indeed, in a porcine faecal peritonitis model, brain damage was evident not only in terms of vascular abnormalities and oedema, but also in terms of neuronal shrinkage, and darkening of neurons as assessed by electron microscopy, 8 hours after the induction of peritonitis (Papadopoulos et al. 1999). The authors suggest that these alterations stem from early neuronal degeneration and point out that more prolonged disease, as seen in patients, is likely to result in greater damage (Papadopoulos et al. 1999). Other models of sepsis have also resulted in neuronal damage and apoptosis, including systemic LPS in rodents (Semmler et al. 2005). Here the authors report activation of glia (astrocytes and microglia), up-regulation of iNOS and neuronal apoptosis.

Neuronal apoptosis was attenuated by administration of L-NMMA, a non-specific nitric oxide synthase inhibitor (Semmler et al. 2005).

In summary, it is clear that the immune system plays an essential role in the development of sepsis, and sepsis-related multiple organ dysfunction, and that LPS is commonly a prime mediator of this inflammatory reaction. Additionally, the brain is not spared from inflammatory damage during sepsis and can significantly affect the survival of the septic patient. Therefore the study of the effect of systemic LPS on the brain is important to aid the understanding of the pathogenesis of sepsis and its sequelae.

1.1.2. Inflammation in the retina

Ocular inflammation is associated with numerous diseases including MS (Zein et al. 2004), juvenile rheumatoid arthritis (Anesi and Foster 2012; Wolf et al. 1987), inflammatory bowel disease (Orchard et al. 2002), Reiter's syndrome (Kiss et al. 2003) and others (Kongyai et al. 2012; Rothova et al. 1992). As such it is considered to be the most common form of ocular inflammation, responsible for 10% of visual impairments in the western world (Nussenblatt 1990). Uveitis can be caused both by external infectious agents entering the eye (i.e. exogenous inflammation), or through endogenous mechanisms if no infectious agent is involved (Forrester 1991). The latter type has been associated with autoimmunity, including immunity against inter-retinal binding protein and retinal soluble antigen (Desmet et al. 1990; Fukushima et al. 1997; Gupta et al. 1996; Matsuo et al. 1986; Nussenblatt et al. 1980; Selmi 2014). Uveitis can influence the anterior portions of the eye (e.g. iris and ciliary bodies of the eye) and/or the posterior segments, including the retina. The work presented here will focus only on retinal inflammation.

Inflammatory infiltrates in the eye can cause loss of vision directly by clouding of the ocular compartments, or indirectly through pathological effects on aqueous fluid dynamics (Forrester

1991). Additionally, more severe damage is associated with inflammatory oedema and macular damage, as well as neovascularisation which can significantly impair vision (Forrester 1991). Numerous immune cell types have been implicated in uveitis, with neutrophils characteristically involved in early acute stages of uveitis, lymphocytes driving chronic inflammation, activated macrophages/microglia providing both antigen presenting and phagocytic roles and endothelial cells together with glial cells contributing important resident immune functions (Chan et al. 1987; Chan and Li 1998; Deschenes et al. 1988).

As with systemic inflammation, the vasculature of the retina is not spared from the effects of ocular inflammation. Indeed, in a mouse model of posterior uveitis the infiltration of inflammatory cells (including lymphocytes and macrophages) into the retina was preceded by a breakdown of the blood-retinal barrier and endothelial expression of adhesion molecules, including intercellular adhesion molecule 1 and p-selectin (Xu et al. 2003). Additionally the number of non-perfused vessels was increased and morphological changes in the vasculature were observed, including straightening of naturally curved vessels (Xu et al. 2003). The vascular pathology occurring during retinal inflammation has been attributed to the activity of inflammatory cytokines, including vascular endothelial growth factor (VEGF), TNF-α and IL-1β, as well as NO, which are capable of activating endothelial cells, opening tight junctions and recruiting and activating other immune cells (Bamforth et al. 1996; Carmo et al. 2000; Claudio et al. 1994; Leal et al. 2007; Luna et al. 1997). Together, these factors are capable of causing blood retinal barrier breakdown as well as immune cell infiltration. Such effects on the retinal vasculature, together with the occurrence of inflammation-associated oedema (Kapin et al. 2003) and increased intraocular pressure (Panek et al. 1990), which can lead to vascular compression, can conceivably result in tissue hypoxia. Indeed, ocular inflammation has been associated with neovascularisation (Graham et al. 1987; Shorb et al. 1976), suggesting inadequate oxygen concentrations in the inflamed retina. Therefore, the

relationship between different types of retinal inflammation and tissue hypoxia remain important, especially given the retina's inherent vulnerability towards hypoxia (see chapter 4).

1.1.2.1. Ocular inflammation in multiple sclerosis

MS is a neurodegenerative and demyelinating disease of the CNS (Dutta et al. 2006; Qi et al. 2007) which typically takes an initially relapse/remitting disease course (with symptomatic phases being alleviated by symptomless periods) followed by incomplete recovery and eventually gradual, progressive degeneration (Maurer and Rieckmann 2000). A subset of patients will instead develop primary progressive MS which omits the relapse-remitting phase and is a continuous, progressive degenerative disorder (Thompson et al. 1997). Symptoms include weakness, depression, fatigue, cognitive impairment, paralysis and visual loss (Chwastiak et al. 2002). Visual defects are often the earliest disease manifestation (Leibowitz and Alter 1968) and are in fact common throughout the disease, being expressed by 80% of MS patients (Fisher et al 2006). Additionally, it has been reported that most MS patients show pathology in the optic nerve tract (Mogensen 1990; Toussaint et al. 1983; Ulrich and Groebkelorenz 1983).

Although most work on optic pathology in MS focusses on myelin containing structures, such as the optic nerves, some observations have also been made in retinal MS pathology. These advances have been accelerated by the development of clinical techniques for the assessment of retinal damage in MS patients, including optical coherence tomography, which noninvasively provides cross-sectional images of retinal morphology (Huang et al. 1991). Such techniques have revealed thinning of the nerve fibre layer and macular (Henderson et al. 2008; Toledo et al. 2008; Trip et al. 2005) even in eyes without a history of optic neuritis (Fisher et al. 2006). The latter finding suggests that not all MS-related retinal atrophy may originate in the optic nerve, but that primary retinal damage may be important. And indeed, despite an absence of myelin, retinal inflammation occurs in a subset of MS patients (Biousse et al. 1999; Graham et al. 1989; Green et

al. 2010; Kerrison et al. 1994; Le Scanff et al. 2008). A histochemical assessment of a large number of patients' samples showed enhanced nerve fibre and ganglion cell layer loss in keeping with previous reports (Henderson et al. 2008; Toledo et al. 2008; Trip et al. 2005), but also an additional atrophy of the inner nuclear layers which is composed mainly of bipolar, horizontal and amacrine cells (Green et al. 2010). They also reported the presence of retinal inflammation, which was predominantly found in relapsing-remitting MS (29%), with fewer (5%) primary progressive MS patients exhibiting retinal inflammation (Green et al. 2010). Additionally, gliosis was noted together with some vascular abnormalities, including thickening of vessel walls (Green et al. 2010), retinal phlebitis (inflammation of the veins and surrounding tissues) (Kerrison et al. 1994), and increased retinal vascular permeability in optic neuritis patients which was predictive of a later diagnosis of MS (Lightman et al. 1987).

Authors	**Year**	**Findings**
Henderson et al	2008	Thinning of the nerve fibre layer and macula
Toledo et al	2008	
Trip et al	2005	
Fisher et al	2006	Thinning of the nerve fibre layer and macula even in eyes without a history of optic neuritis
Biousse et al	1999	Retinal inflammation in a subset of patients
Graham et al	189	
Green et al	2010	
Kerrison et al	1994	
Le Scanff et al	2008	
Green et al	2010	Atrophy of the inner nuclear layers, gliosis and vascular abnormalities, including thickening of vessel wall
Kerrison et al	1994	Retinal phlebitis
Lightman et al	1987	Increased retinal vascular permeability in optic neuritis patients, predictive of a later diagnosis of MS

Table 1.1.2.1.1. **Summary of retinal findings in MS**

1.1.2.2. Inflammation in the aged eye

Inflammation has been extensively implicated in normal ageing (Chung et al. 2006; Chung et al. 2009; Harman 1956). It has been stated that an altered redox state, characterised by an up-regulation of reactive oxygen and nitrogen species and loss of antioxidant defences, occurs in normal ageing (Chung et al. 2006; Chung et al. 2009). Such reports have led to the development of the molecular "Inflammation Hypothesis of Ageing" (Chung et al. 2006). This theory suggests that continuous low-level inflammation during ageing could provide the bridging link between normal ageing and age-related diseases. This is founded on several reports of increased inflammatory mediators in aged tissues, including increased cyclooxygenase-2 gene expression in the aged kidney (Kim et al. 2000), upregulation of eNOS and iNOS in vessel walls (Cernadas et al. 1998), an augmented iNOS expression and NO production in response to LPS (Chorinchath et al. 1996; Poynter and Daynes 1999), enhanced cytokine secretion by T cells (Hobbs et al. 1993; Riancho et al. 1994; Roubenoff et al. 1998), and increased nuclear factor-κB DNA-binding (Helenius et al. 1996; Korhonen et al. 1997). The link between ageing and inflammation is further supported by evidence of an attenuation of this age-related inflammation by factors known to increase longevity, including calorific restriction and exercise (Chung et al. 2009). Other theories, including the free radical theory of ageing (Harman 1956), have also implicated inflammation, particularly free radical generation, in normal ageing and age-related diseases. This theory also highlights the importance of a balance of pro- and anti-oxidant systems which may be derailed in ageing and age-related diseases (Chung et al. 2009; Harman 1992). Again, despite a loss of antioxidant defences with age, interventions, including calorific restriction and exercise, can attenuate this imbalance (Carter et al. 2007; Cho et al. 2003) supporting the suggestions of a link between inflammation and physiological ageing.

The retina is not spared from age-associated inflammation. A study employing fundus autofluorescence in young and aged mice revealed an increase in the number of retinal microglia

with age (Xu et al. 2008). This finding is complemented by observations of enhanced microglial activation in the aged retina, as assessed by MHC class II and ED1 labelling, suggesting increased antigen presenting and phagocytic capacity (Chan-Ling et al. 2007). The same study also reported a significant increase in blood-retinal barrier breakdown (as assessed by leakage of intravascular tracers and occludin expression) and altered vascular morphology in agreement with previous observations (Hughes et al. 2006). This previous study detected structural vascular changes using flat-mount histochemistry, which included broadening of veins and capillaries, as well as thickening of their basement membrane, increased vessel tortuosity and kinking as well as the formation of arteriovenous shunts (Hughes et al. 2006). Additionally, increased vessel blockage was observed in the peripheral retina together with increases in vascular loops and spirals which were suggested to indicate angiogenesis (Hughes et al. 2006). The authors of this study argue that some of the changes observed, including the thickening of the basement membrane and altered expression of calponin (a calcium regulating protein), lead to impaired vascular autoregulation as well as reduced nutrient and oxygen exchange across the vessel walls (Hughes et al. 2006). These factors were suggested to result in 'physiological hypoxia' in the aged retina which in turn explains the putative compensatory angiogenesis observed (Hughes et al. 2006).

Another study found increased amyloid beta deposition in aged retinal vessels and around Bruch's membrane which was suggested to negatively affect retinal perfusion (Kam et al. 2010). Such deposits of amyloid β are expected to increase immune cell activation (Akiyama et al. 2000; Davis et al. 1992; Giovannini et al. 2002; Kam et al. 2010; Meda et al. 1995a; Meda et al. 1995b), leading to an age-related increase in retinal inflammation together with compromised perfusion.

Inflammation has additionally been implicated in the formation of age-related drusen, the hallmark of age-related macular degeneration (AMD) (Anderson et al. 2002). AMD is the leading cause of blindness in the over 50s in the western world (Bressler et al. 1988) and is characterised by the presence of druses, choroidal neovascularisation, atrophy of the retinal pigment epithelium

(RPE) and visual loss (Bressler et al. 1988). Drusen are hydrophobic deposits, which include lipoproteins as well as pro-inflammatory components (Englander and Singh 2013), and are located between Bruch's membrane and the RPE (Strauss 2005). While dry AMD is primarily charcterised by such drusen deposits, wet or exudative AMD includes neovascularisation of the choroid with infiltration of vessels into the outer retina, which is normally avascular (Nowak 2006). *Post-mortem* assessment of drusen shows a clear link between drusen and inflammation through, for example, enhanced presence of components of the complement cascade, including C3, C5 and the membrane attack complex (Anderson et al. 2002). The complement cascade is further implicated in AMD as single-nucleotide substitutions of the complement factor H gene (a regulator of the alternative pathway of the complement system; for more detail see chapter 4) are commmon in AMD patients (Coffey et al. 2007; von Leithner et al. 2009) and a mouse knockout results in visual deficit and a phenotype similar to human AMD (Coffey et al. 2007).

1.1.3. Mitochondria in inflammation

Mitochondria are essential organelles, involved in adenosine triphosphate (ATP) production, calcium buffering, apoptosis and redox signalling. As such, damage to mitochondria has been associated with several neurodegenerative diseases including MS (Erecinska and Silver 2001; Mahad et al. 2008), Parkinson's disease (Schapira et al. 1998), sepsis (Fink 2002a) as well as others (DiMauro and Schon 2003; DiMauro and Schon 2008; Kang and Hamasaki 2005). Inflammation is known to have a significant damaging effect on mitochondrial function as several inflammatory mediators are capable of inducing mitochondrial dysfunction, including reactive oxygen and nitrogen species. Nitric oxide, for example, is capable of reversibly inhibiting mitochondrial function through competition with oxygen for binding to cytochrome c oxidase (Brown 2001; Brown and Cooper 1994; Cassina and Radi 1996; Cleeter et al. 1994; Schweizer and Richter 1994). Prolonged exposure to NO, or its reactive derivatives (reactive nitrogen species),

can also irreversibly inhibit mitochondrial function through several mechanisms, including the inhibition of mitochondrial complexes (Clementi et al. 1998), the induction of proton leak (Brookes et al. 1998) and/or the initiation of mitochondrial permeability transition and apoptosis (Hortelano et al. 1997). The combination of NO and superoxide can cause additional damage via the highly reactive intermediate peroxynitrite (Bolanos et al. 1995). Mitochondria are believed to be particularly susceptive to oxidizing agents as they themselves are sources of these inflammatory mediators. Indeed oxidative phosphorylation produces reactive oxygen species via electron leakage from the ETC primarily in complex I, but also from complex III under certain conditions (Cadenas et al. 1977; Murphy 2009; Turrens and Boveris 1980), although other mitochondrial sources have also been implicated (Andreyev et al. 2005). Baseline production of reactive oxygen species is considered to be an important element of mitochondrial signalling (Hamanaka and Chandel 2010). However, under pathological conditions, including hypoxia and inflammation, the electron leak can be intensified (Andreyev et al. 2005; Murphy 2009), resulting in mitochondria becoming a potent source of free radicals and creating a vicious cycle of mitochondrial damage and enhanced ROS production. In addition to their proximity to a potent free radical source, mitochondria are also particularly vulnerable to free radical mediated damage due to the 'naked' nature of their DNA, lacking protective proteins, such as histones (Bandy and Davison 1990; Larsson and Clayton 1995; Richter et al. 1988), and their limited DNA repair mechanisms, when compared with nuclear DNA (Bandy and Davison 1990; Clayton et al. 1974; Clayton 1982; Larsson and Clayton 1995). As a result mitochondrial DNA exhibits significantly more damage compared to its nuclear counterpart (Mecocci et al. 1993; Richter et al. 1988; Wang et al. 2005; Yakes and VanHouten 1997), highlighting the important role played by mitochondria in inflammatory pathogenesis. Such mitochondrial damage is expected to be particularly detrimental in large, post mitotic neurons, which perform limited glycolysis (Almeida et al. 2001) and require a functional pool of mitochondria to sustain high levels of energetically demanding activities (see next section "Neuronal sensitivity to mitochondrial damage").

1.1.3.1. Neuronal sensitivity to mitochondrial damage

Neurons are believed to rely primarily on oxidative phosphorylation as their primary source of ATP production (Almeida et al. 2001; Belanger et al. 2011; Sperlagh and Vizi 1996). As such they have been reported to undertake a higher level of oxidative phosphorylation when compared with glial cells (Bouzier-Sore et al. 2006; Lebon et al. 2002) and they are not able effectively to upregulate glycolysis when oxidative phosphorylation is inhibited, e.g. by NO (Almeida et al. 2001). The inability of neurons to use glycolysis as a source for ATP was suggested to be related to the rapid degradation of Pfkfb3 (6-phosphofructo-2-kinase/fructose-2, 6-bisphosphatase-3) in neurons compared with for example astrocytes (Herrero-Mendez et al. 2009). Pfkfb3 is involved in the regulation of glycolytic enzymes via the synthesis of fructose-2,6-bisphosphate and therefore indirectly leads to the activation of the rate-limiting enzyme in glycolysis, 6-phosphofructo-1-kinase (Yalcin et al. 2009). As such, the degradation of Pfkfb3 results in a suppression of glycolysis in neurons (Herrero-Mendez et al. 2009). This inhibition of the glycolytic pathway was found to be beneficial to the survival of neurons as an artificial increase in glycolysis, by the inhibition of the E3 ubiquitin ligase, responsible for the degradation of Pfkfb3, was found to divert glucose utilisation away from reduced glutathione production and subsequently led to increased levels of apoptosis (Herrero-Mendez et al. 2009). These findings therefore suggest that glycolysis cannot effectively sustain neuronal energetic demands and that glucose is instead preferentially used for antioxidant production in neurons.

Such investigations also support evidence suggesting that glucose does not provide the primary fuel for ATP production in neurons but that other substrates may be more important for neuronal oxidative phosphorylation (Schurr 2006). Several lines of evidence now implicate lactate in neuronal energetic homeostasis (for review see (Belanger et al. 2011)). The astrocyte-neuron lactate shuttle hypothesis (Magistretti et al. 1999; Pellerin and Magistretti 1994) suggests that glutamate, released upon neuronal stimulation, gets taken up by astrocytes, with sodium being

cotransported. The resulting increase in astrocytic sodium levels stimulates ATP consumption by sodium-potassium-ATPases which actively pump sodium into the extracellular space. As a result of the decline in intracellular ATP, astrocytic glycolysis is activated and results in lactate production. This lactate is then made available to neurons as it is moved out of astrocytes and into neurons by monocarboxylate transporters where it fuels oxidative phosphorylation in neuronal mitochondria (reviewed in (Magistretti and Pellerin 1999)). Despite some controversy surrounding the astrocyte-neuron lactate shuttle hypothesis (Chih and Roberts 2003; Hall et al. 2012) there is significant evidence that lactate can provide an efficient fuel for oxidative phosphorylation in neurons (Schurr 2006).

However, regardless of the substrate used, the reports summarised above suggest that neurons support their energetic needs mainly through oxidative phosphorylation resulting in great sensitivity towards mitochondrial dysfunction and oxygen deprivation. Together with the very high metabolic demand of cerebral tissue, which utilises 20% of the oxygen and 25% of the glucose consumption despite constituting only 2% of the body mass (Belanger et al. 2011; Lassen 1959), these findings suggest that neuronal function and survival relies fundamentally on mitochondrial oxidative phosphorylation and an adequate supply of oxygen. Such a reliance on mitochondrial function is demonstrated by the numerous neurodegenerative diseases in which mitochondrial dysfunction has been implicated (for review see (Federico et al. 2012; Lin and Beal 2006)), providing additional importance to the study of mitochondrial dysfunction and oxygen deprivation in the CNS.

Overall, we have summarised putative links between inflammatory conditions and hypoxia. This combination is particularly detrimental in an environment of high NO production, which is capable of competing with oxygen for binding on complex IV, thereby increasing the apparent K_m for oxygen and resulting in mitochondrial inhibition and eventually neuronal death even under mild hypoxic conditions (Mander et al. 2005). Furthermore, these partially inhibited mitochondria are

likely to be suffering from additional inflammatory insults, including DNA and protein damage from other inflammatory mediators, including reactive oxygen species. These factors together, suggest that inflammatory environments are likely to lead to significant bioenergetic dysfunction which could be of particular detriment to highly active and large cells, such as neurons, which rely primarily on oxidative phosphorylation for the production of ATP. Therefore, the study of oxygenation and mitochondrial function in neuroinflammatory conditions is of paramount importance in understanding and overcoming the putative energetic failures associated with inflammation of the CNS.

1.2. Why *in vivo*

Mitochondrial dysfunction is associated with a wide range of neurodegenerative diseases as described above. Notwithstanding the importance of mitochondria both as victims of inflammatory disease and as propagators of the damage, the assessment of their function in disease states has been slowed by limitations in traditional methods which are comprised principally of the *post-mortem* assessment of mitochondrial structure and morphology or *in vitro* assessment of mitochondrial function. These techniques provide a trade-off between dynamic assessment capabilities (during *in vitro* imaging for example) in the absence of physiological environments and fixation of more physiological preparations for *post-mortem* assessment which provides only very static snapshots of morphology with fewer opportunities to assess mitochondrial function. However, recent advances in *in vivo* imaging techniques have provided an opportunity to overcome some of these limitations and provide an additional technique to assess mitochondrial function. Indeed, intravital imaging offers the opportunity to maintain mitochondria within a physiological environment while also providing dynamic assessment capabilities with high spatial and temporal resolution. Unfortunately the tight experimental control which is relatively easily achieved *in vitro* is often more challenging within more complex preparations and may make causal attributions and

pathways difficult to assess. Additionally even physiological *in vivo* studies will have limitations in their applicability to human research, being constrained by the choice of the animal model, the organ system studied and type and depth of anaesthetic. Furthermore, *in vivo* optical imaging is only capable of probing the surface of the chosen organ, even using two-photon microscopy, as both the excitation and emitted light are readily scattered by overlying tissue.

However, despite the complexity and limitations of intravital experimental design, it provides the opportunity to make more meaningful observations within more physiological preparations and is essential to the study of mitochondrial function in neurodegenerative diseases. Additionally, technical advancements are continuously being made, including the use of chronic *in vivo* imaging techniques which allow longitudinal assessment (Holtmaat et al. 2009; Yang et al. 2010) even without anaesthetic (Dombeck et al. 2007) or the use of *in vivo* microscopy on human subjects including assessment of the retina (Webb et al. 1987) or skin (Masters et al. 1997).

The benefits of intravital imaging are particularly relevant to the investigation of mitochondrial function in which the availability of oxygen and substrates can be of vital importance in the physiological and pathological regulation of this organelle. Particularly the substantial difference between the *in vitro* environment that mitochondria are exposed to, including aggressive extraction processes, elevated oxygen concentrations and non-physiological substrate levels, compared with the much more constrained situation faced by mitochondria *in vivo*, warrants significant investment into sound intravital imaging techniques. Such a highly physiological technique includes the visualisation of mitochondria even without external dye application, using the autofluorescent properties of electron carriers. This method provides a convenient signal for the minimally invasive assessment of mitochondrial function and neuronal activity in the superficial layers of the CNS *in vivo* as described below.

1.2.1. Mitochondrial redox potential *in vivo*

Since the pivotal work of Britton Chance and his colleagues in the 1950s it has been apparent that the mitochondrial redox state can be assessed using the autofluorescent properties of redox cofactors. The mitochondrial cofactors, pyridine nucleotides (nicotinamide adenine dinucleotide (phosphate) NAD(P)/NAD(P)H) and flavoproteins (flavin mononucleotide and flavin adenine dinucleotide), transfer electrons to the electron transport chain, changing their redox potential in the process. Helpfully, only oxidized flavoproteins emit fluorescence when excited with blue light, while only reduced pyridine nucleotides are capable of fluorescing when excited with UV light. The respective reduced and oxidised counterparts of these cofactors do not have the same fluorescent properties, allowing the fluorescence, fluorometric and spectrofluorimetric assessment of the relative presence of oxidised flavoproteins and reduced pyridine nucleotides (e.g. (Chance et al. 1962; Chance and Baltscheffsky 1958; Chance and Connelly 1957; Chance and Jobsis 1959; Lewis and Schuette 1976; Lothman et al. 1975; Mayevsky et al. 1974; Mayevsky 1984; Mayevsky and Chance 1973; Mayevsky and Chance 1974; Quistorff et al. 1985)). The endogenous autofluorescent properties of these electron carriers have more recently been used to visualize mitochondrial redox potential *in vivo*, with the high spatial and temporal resolution afforded by standard fluorescence and laser based microscopy. NAD(P)H has additionally been imaged *in vivo* using two-photon microscopy (Kasischke et al. 2011; Takano et al. 2007) which allows better tissue penetration and less photodamage outside the focal area, when compared with single-photon UV excitation (Piston et al. 1995). As the signal generated by oxidized flavoproteins is weaker compared with that of reduced pyridine nucleotides (Chance et al. 1979; Koke et al. 1981) their assessment using two-photon excitation might be more difficult due to the localised excitation of two-photon lasers. To our knowledge two-photon microscopy has not been used *in vivo* to assess mitochondrial flavoprotein autofluorescence in the central nervous system, and anecdotal reports indicate that the technique has been applied, but attempts failed. In the current thesis, confocal

methods have been developed (despite some limitations, including low resolution in depth) to overcome the limitations of the two-photon approach.

Because of the close relationship between neuronal activity, mitochondrial oxygen consumption and aerobic metabolism (Fein and Tsacopoulos 1988; Kann et al. 2003; Shibuki 1989; Shibuki et al. 2003) flavoprotein fluorescence has been used as a proxy for neuronal activation and the associated rise in oxidative metabolism (Gao et al. 2006; Husson et al. 2007; Reinert et al. 2004; Reinert et al. 2007; Reinert et al. 2011; Shibuki et al. 2003), as confirmed by optical imaging of intrinsic signals (Husson et al. 2007; Kitaura et al. 2007; Takahashi et al. 2006; Tohmi et al. 2006), calcium imaging (Gao et al. 2006), and field potential recordings (Kitaura et al. 2007; Takahashi et al. 2006; Tohmi et al. 2006). Additionally it was found that flavoprotein fluorescence can provide enhanced resolution for the localisation of cortical activity compared with changes in blood flow (Weber et al. 2004), which are the basis for the commonly used blood-oxygen-level dependent contrast imaging. The endogenous autofluorescence of oxidized flavoproteins therefore provides a very sensitive tool for the visualisation and assessment of the relationship between neuronal activation and oxidative metabolism, without the need for the application of dyes.

For example, a series of experiments showed that stimulation of parallel fibres in the cerebellar cortex resulted in a temporary "beam-like" increase in flavoprotein fluorescence followed by a superimposed, delayed reduction in fluorescence (Gao et al. 2006; Reinert et al. 2004; Reinert et al. 2007; Reinert et al. 2011) (see Figure 1.2.1.1). It was possible to confirm the mitochondrial origin of the signal by its response to the mitochondrial inhibitors, cyanide (NaCN, blocks complex IV, preventing the transfer of electrons to oxygen and thereby maximally reducing the entire electron transport chain, including flavoproteins) and diphenyleneiodonium (DPI, inactivates flavoproteins) which abolished both phases of the signal without affecting neuronal excitability (Reinert et al. 2004). However, debate is still ongoing regarding the nature and origin of the components of this signal, with the initial increase in flavoprotein fluorescence suggested to

be due to the activation and depolarisation of neurons leading to a rapid increase in oxidative metabolism (Reinert et al. 2004; Reinert et al. 2011), while the subsequent dark phase was suggested to have at least a partial glial origin (Reinert et al. 2011). Other investigations have questioned the glial origin of the dark phase (Brennan et al. 2006).

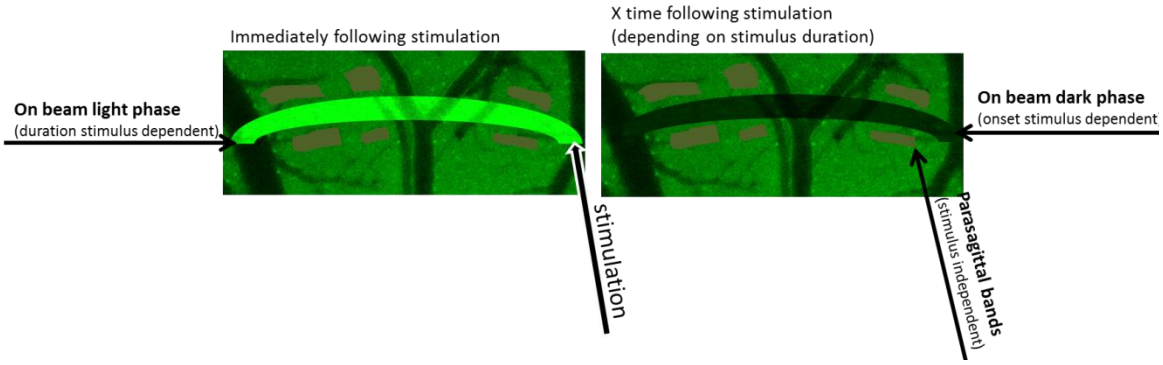

Figure 1.2.1.1: **Diagrammatic representation of "beam like" autofluorescence changes following stimulation (as described in (Gao et al. 2006; Reinert et al. 2004; Reinert et al. 2007; Reinert et al. 2011)).**
Stimulation of parallel fibres in the cerebellar cortex leads to a characteristic change in the flavoprotein autofluorescence including an initial increase in fluorescence in a "beam like" manner followed, after a stimulus dependent interval, by a superimposed decrease in fluorescence intensity. Additionally, parasagittal bands were described which appear along and across the "beam like" fluorescence changes and are stimulus independent. This diagram is roughly to scale with one cortical image representing around 1mm width.

Together with this biphasic, beam-like signal, an 'off-beam' dark phase was also reported to be organised into parasagittal bands along and across the on-beam signal (Gao et al. 2006) (see also Figure 1.2.1.1.). This dark phase was suggested to originate from inhibitory interneurons, demonstrating the potential for mitochondrial redox state to offer information on inhibition (reduction of flavoproteins) as well as excitation (oxidation of flavoprotein pool) of postsynaptic neurons (Gao et al. 2006). In a separate study it was found that the off-beam reduction in the flavoprotein signal following stimulation was diminished in spinocerebellar ataxia type 8, while the

on-beam increase in fluorescence was augmented, suggesting reduced inhibition by cerebellar interneurons and altered cerebellar circuity (Moseley et al. 2006). Such findings demonstrate that the endogenous flavoprotein signal is sensitive enough to provide clinically relevant information.

In comparison with the effects of physiological stimulation, cortical spreading depression, which has been associated with pathological mechanisms after traumatic brain injury, stroke, subarachnoid haemorrhage and migraine (Ayata et al. 2006; Lauritzen et al. 2011; van den Maagdenberg et al. 2004), has been reported to result in larger changes in redox state *in vivo* (Takano et al. 2007). By virtue of the high spatial and temporal resolution of two-photon NAD(P)H imaging it was possible to visualise a striking spatial relationship between the cortical redox state and the cortical vasculature during cortical spreading depression. This relationship was comprised of an initial, global decline in NAD(P)H fluorescence, which remained stable close to vessels, but was replaced by a localised increase in fluorescence further away from vessels (Takano et al. 2007). This therefore revealed a close relationship between the cortical vascular network and redox state, which is not evident during rest but is uncovered during situations of high oxygen demand which are capable of exceeding the rate of oxygen delivery, revealing areas of greater ischemic vulnerability and enhanced pyridine nucleotide fluorescence. It is not surprising therefore, that the application of oxygenated cerebral spinal fluid to the cortex prevented the spreading depression induced and spatially selective increase in NAD(P)H fluorescence, as the spatial relationship to the oxygen source was lost (Takano et al. 2007). These findings therefore highlight the importance of a preserved vascular network within a physiological preparation when investigating mitochondrial function during physiological and pathological events.

Physiological, intact, whole animal preparations are also beneficial when investigating cortical networks, long-range plasticity and the mitochondrial involvement in them. For example, *in vivo* autofluorescence of flavoproteins was used to assess cortical plasticity in the visual, auditory and somatosensory cortex (Shibuki et al. 2006; Takahashi et al. 2006; Tohmi et al. 2006), and to

investigate long-range neural plasticity pathways in response to tetanic stimulation (Murakami et al. 2004). It was even possible to use flavoprotein autofluorescence to visualise the retinotopic and tonotopic maps of the visual and auditory cortex respectively (Husson et al. 2007; Takahashi et al. 2006; Tohmi et al. 2006). Therefore, the possibility of instantaneous assessment of mitochondrial redox potential over a large area, spanning both hemispheres, permits the mapping of neural plasticity *in vivo*. Indeed such large and complex networks cannot easily be investigated with electrodes (due to the number of recordings needed) or *ex vivo* preparations in which long-range pathways are unlikely to be intact.

The absorbing properties of flavoproteins have been useful not only in terms of visualisation of fluorescence but also for the inhibition of neuronal function. Prolonged (50 minutes) blue light exposure allows for the targeted inactivation of flavoprotein fluorescence and therefore oxidative metabolism (Kubota et al. 2008). Using this technique Kubota et al were able to show that information processing in the primary auditory cortex is partly driven by signals originating from the anterior auditory field, as photo-inactivation of the latter area reduced subsequent stimulus processing (visualised by flavoprotein fluorescence) in the former, while inactivation of the primary auditory cortex left stimulus processing in the anterior auditory field intact (Kubota et al. 2008). By virtue of the high spatial sensitivity of optical techniques, photo-inactivation of mitochondrial metabolism and neuronal function can be achieved in a highly localised manner, providing greater sensitivity compared with many pharmacological interventions.

Overall, many benefits are associated with the use of flavoprotein and pyridine nucleotide autofluorescence in the assessment of neuronal and mitochondrial function. Without the use of dyes, issues associated with loading, distribution and toxicity are avoided while a stable signal (Shibuki et al. 2003) with excellent spatial (Husson et al. 2007; Shuttleworth et al. 2003) and temporal resolution (Husson et al. 2007; Weber et al. 2004) is maintained over large areas. Nonetheless, the autofluorescent signals generated are relatively weak, and the endogenous NAD(P)H and

flavoprotein fluorescence strength can vary depending on the laser intensity and imaging depth, as well as the preparation quality. These limitations can make absolute and baseline measurements meaningless, and instead the experimental design needs to assess longitudinal changes across the duration of the experiment.

Generally the autofluorescence of mitochondrial electron carriers can offer a convenient, spatially and temporally sensitive, and minimally invasive, readout of mitochondrial redox potential and neuronal activity in a physiological, whole-animal preparation with an intact blood supply, in the superficial layers of the central nervous system *in vivo*.

CHAPTER TWO

2. Flavoproteins in the cortex

2.1. Introduction

A wide range of diseases, including MS (Erecinska and Silver 2001; Mahad et al. 2008), Parkinson's disease (Schapira et al. 1998), and sepsis (Fink 2002a), have been associated with mitochondrial dysfunction. This extensive involvement of mitochondria in a multitude of pathological processes emphasizes the need for a better understanding of the role of mitochondrial function in health and disease. However, assessment of mitochondria in large parts of the published literature relies on *in vitro* assays, which are far removed from physiological reality. Therefore, the need for dynamic *in vivo* assessment of mitochondrial function with both spatial and temporal resolution remains, as discussed above.

2.1.1. Flavoprotein fluorescence as a measure of mitochondrial function

Mitochondrial function can be assessed *in vitro* and more recently *in vivo* using confocal or two-photon microscopy and membrane potential-sensitive dyes, like tetramethylrhodamine methyl ester (TMRM) or through autofluorescent markers, including oxidized flavoproteins and reduced nicotinamide adenine dinucleotide (phosphate) (NAD(P)H). As mentioned in the introduction (chapter 1), oxidized flavoproteins and reduced NAD(P)H (pyridine nucleotides) exhibit fluorescent properties (Reinert et al. 2004) that differ significantly from those of their reduced and oxidized counterparts, respectively (Figure 2.1.1.1). This allows the mitochondrial

redox potential to be mapped with the spatial and temporal resolution provided by the chosen imaging technique.

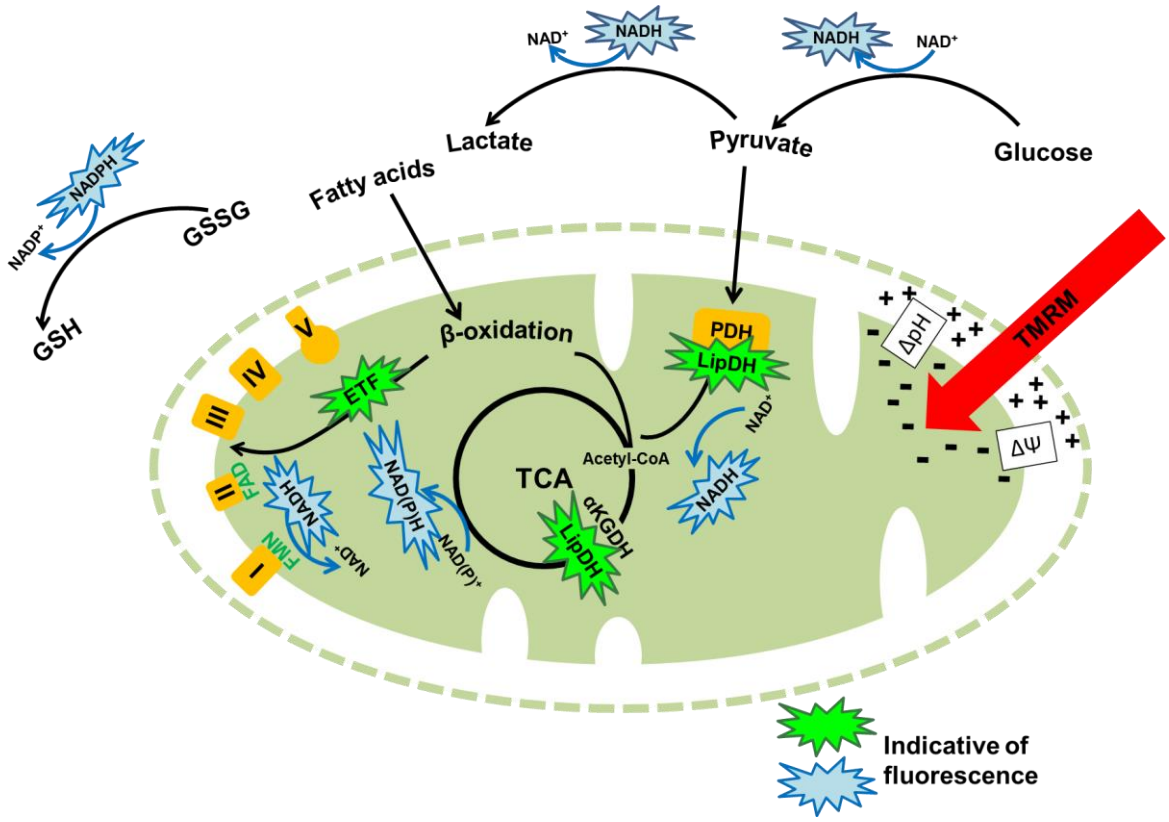

Figure 2.1.1.1: **Diagrammatic representation of flavoprotein, pyridine nucleotide and TMRM fluorescence.**

Abbreviations: GSH, reduced glutathione; GSSG, oxidized glutathione; FMN, flavin mononucleotide; FAD, flavin dinucleotide; ETF, electron transfer flavoproteins; LipDH, lipoamide dehydrogenase; αKGDH, alpha ketoglutarate dehydrogenase; PDH, pyruvate dehydrogenase complex; TCA, tricarboxylic acid cycle.

Flavoproteins are primarily found in mitochondria (Huang et al. 2002; Koke et al. 1981; Scholz et al. 1969). Here both flavin adenine dinucleotide (FAD) and flavin mononucleotide (FMN) are present. Although several enzymes in mitochondria contain these molecules the local environment mostly quenches their fluorescent properties (Kunz and Kunz 1985; Ragan and Garland 1969) and instead mainly flavins from electron transfer flavoproteins (transferring

electrons from β-oxidation of fatty acids to ubiquinone) and α-lipoamide dehydrogenase (involved in the conversion of pyruvate to acetyl-CoA and in the tricarboxylic acid cycle, as a component in the α-ketoglutarate dehydrogenase complex) seem to contribute significantly to redox linked flavoprotein autofluorescence (Kunz and Gellerich 1993; Kunz and Kunz 1985) (Figure 2.1.1.1). It should be noted however, that β-oxidation is limited in the brain as fat is not a major fuel source. In line with this the brain shows a limited uptake of fatty acids (Hawkins 1986) and has a reduced pool of enzymes for the β-oxidation pathway (Yang et al. 1987), including electron transfer flavoproteins (Kunz and Gellerich 1993). Therefore, the brain's flavoprotein signal is likely to be dominated by α-lipoamide dehydrogenase, together with a proportion of green fluorescence which does not seem to be redox sensitive (Kunz and Gellerich 1993; Kunz and Kunz 1985).

NAD(P)H fluorescence refers to the combined signal from NADH and NADPH. While NADH, as a cofactor for the ETC, provides a proxy for oxidative metabolism, it is also involved in glycolysis and thereby anaerobic metabolism (Kasischke et al. 2004). In contrast, the phosphorylated form, NADPH, is involved in biosynthetic reactions and antioxidant production as a reducing equivalent in, for example, nucleotide and lipid synthesis as well as glutathione reduction (Ying 2008) (Figure 2.1.1.1). NADH and NADPH are spectrally indistinguishable, preventing separation of the two signals using standard confocal or two-photon microscopy. Therefore, given the involvement of pyridine nucleotides also in reactions outside mitochondria, for example biosynthetic pathways or glycolysis (Ying 2008) they have also been detected in the cytosolic compartment (Blacker et al. 2014; Kasischke et al. 2004; Patterson et al. 2000). Nevertheless an inverse relationship has been reported between flavoprotein and pyridine nucleotide fluorescence (Chisholm et al. 2015; Mayevsky 1984; Shuttleworth et al. 2003) partly attributed to the dominance of the mitochondrial NAD(P)H signal in the brain (Klaidman et al. 1995; Shuttleworth 2010).

2.1.2. Oxygen supply to the cortex

Mitochondrial respiratory function depends on the availability of oxygen. As electrons are passed to the successively higher affinity electron acceptors along the ETC, O_2 acts as the final acceptor of these electrons. Therefore, hypoxic conditions can result in the blockage of electron flow, accumulation of electrons along the ETC and the reduction of a number of components of the ETC (e.g. (Scholz et al. 1969; Sugano et al. 1974)). This mitochondrial reduction, in the absence of oxygen, can be visualized using flavoprotein and/or pyridine nucleotide fluorescence (Chisholm et al. 2015; Kasischke et al. 2011).

Despite the relatively small mass of the brain (2% of body mass (Raichle and Gusnard 2002)) it has been reported to consume 20% of the oxygen taken up by the human body at rest (Lassen 1959), emphasizing the essential need for a functional oxygen supply to the brain. Indeed, unconsciousness ensues only 5-6 seconds following the arrest of cerebral blood flow (Rossen et al. 1943). However, despite large regional variations in cortical oxygen concentrations (Erecinska and Silver 2001), oxygen is usually provided to cells at a sufficient rate to sustain tissue oxygen levels above the concentration necessary for function under basal conditions (Erecinska and Silver 2001). Historically the capillary network has been accredited with the supply of oxygen to tissues with each capillary suggested to supply a distinct cylindrical region (Krogh 1919). More recently however it has been suggested that oxygen diffusion can also occur from arteries and arterioles, including pial vessels (Duling et al. 1979; Duling and Berne 1970; Ivanov et al. 1982; Ivanov et al. 1999; Sakadzic et al. 2010; Vovenko 1999). However, the published literature has largely relied on oxygen probe measurements, which lack spatial resolution. A separate study has made use of the phosphorescent quenching properties of oxygen and utilized the resulting lifetime changes of phosphorescent bead to assess changes in vascular and tissue oxygen concentrations throughout the cortex (Sakadzic et al. 2010). However, to our knowledge only one study investigated the spatial relationship between the oxygenation provided via pial arterioles and mitochondrial function

(Kasischke et al. 2011). Further studies are necessary to confirm the spatial and temporal responsiveness of mitochondrial function to changes in pial arterial oxygenation.

2.2. Hypotheses

1) The endogenous fluorescence of flavoproteins can be used to assess mitochondrial redox state *in vivo* in the CNS of anaesthetized mice
2) Hypoxaemia results in selective reduction of mitochondrial flavoproteins with preserved oxidation in well oxygenated areas

2.3. Aims and objectives

In order to assess the spatial distribution of mitochondrial redox potential in relation to the cortical vasculature in real time in the mouse cerebral cortex during normoxaemia, hyperoxaemia and hypoxaemia, our initial aim is to assess the applicability of endogenous flavoprotein fluorescence as a proxy for mitochondrial redox state in the exposed murine cerebral cortex *in vivo* using confocal microscopy. To achieve this aim our first objective was to confirm the mitochondrial origin of the endogenous green fluorescence imaged in the cerebral cortex of anaesthetised mice using pharmacological agents known to manipulate mitochondrial redox potential. Having established a measure of mitochondrial redox potential we then aim to determine the effects of changes in cerebral oxygenation on flavoprotein fluorescence by manipulating the inspired oxygen fraction (FiO_2). Finally changes in flavoprotein fluorescence will be compared to changes in other markers known to be influenced by the mitochondrial redox potential.

2.4. Methods

C57bl/6 mice (~20 g) were housed in a 12 hour light/dark cycle with food and water *ad libitum*. All experiments were performed in accordance with the UK Home Office Animals (Scientific Procedures) Act (1986).

2.4.1. Surgery

Mice were anaesthetised with ~2% isoflurane in room air for most experiments, but a mixture or ketamine (20mg/kg) and urethane (2g/kg), injected intraperitoneally (i.p.), was used when NAD(P)H and flavoprotein fluorescence were imaged together. Mice were then placed on a homeothermic heating mat to maintain their rectal temperature at 37ºC, and an incision was made in the scalp to expose the skull. The skull was subsequently cleaned of connective tissue, and affixed to a titanium bar for stability using dental cement (Contemporary Ortho-Jet Powder, USA) mixed with cyanoacrylate glue (Loctite, Henkel Ltd., UK). A craniotomy (~5mm diameter) was performed to expose part of the right hemisphere, between bregma and lambda and lateral to the sagittal suture. The exposed dura was moistened and cleaned with saline. The opening was surrounded by a ring of petroleum jelly (Vasline, Unilever, UK) over which a circular glass coverslip (6mm) was placed to seal the craniotomy and prevent evaporation during imaging. Following surgery, the mice were moved to a custom-made stage for confocal or two-photon microscopy.

2.4.2. Dyes

In a subset of experiments, oxygen-sensitive microbeads impregnated with a phosphorescent dye, platinum(II)-5,10,15,20-tetrakis(2,3,4,5,6-pentafluorophenyl)porphyrin

(PtPFPP, courtesy of Dmitri Papkovsky; excitation 543 nm; emission: 650 nm, collected with 585 nm long pass filter) were added to cover the dura (5 µl of 5 mg/ml aqueous suspension, 5 minutes incubation before the application of a coverslip). Alternatively, the dura was removed and the exposed cortex incubated with TMRM (Molecular Probes, Invitrogen, UK; 1µM; excitation: 561nm, emission: 584-656), isolectin GS–IB4 from *Griffonia simplicifoli*a (Life technologies, Thermo Fisher Scientific, UK, 400µM, excitation: 488nm, emission: 505-570nm) and/or 4-amino-5-methylamino-2',7'-difluorofluorescein (DAF-FM, Life Technologies, Molecular Probes, Invitrogen, UK; 1µM, excitation: 488nm, emission: 505-570nm) for 30 minutes before the coverslip was added as described before (see Figure 2.4.2.1).

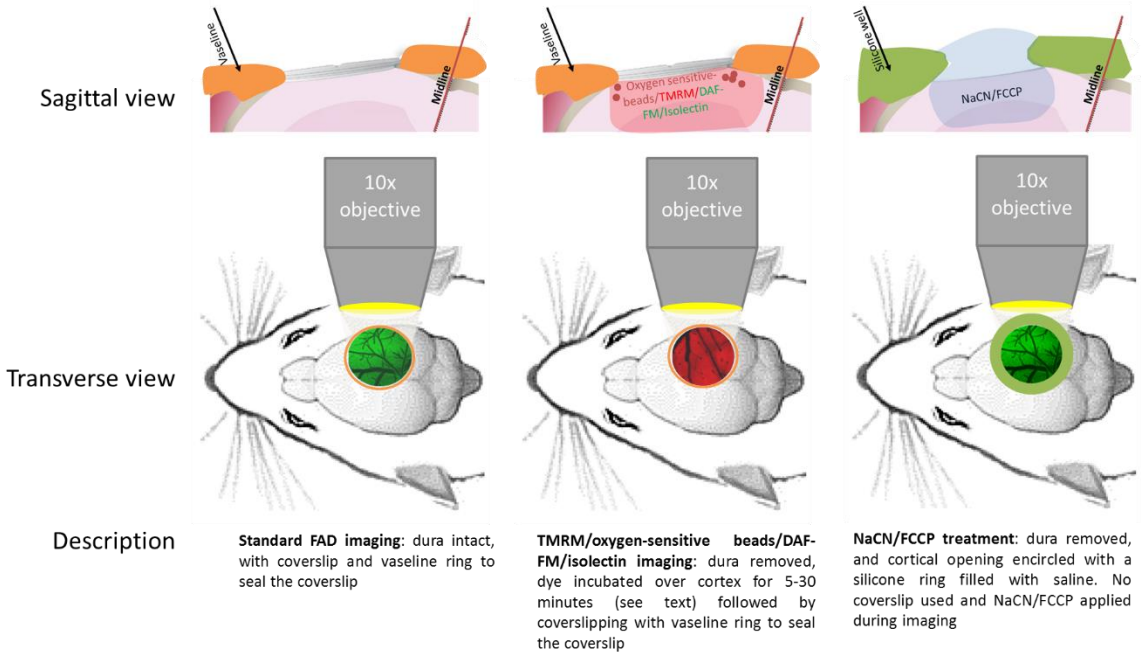

Figure 2.4.2.1. **Summary of the protocol used for dyes and treatments**

2.4.3. Interventions

In experiments using carbonyl cyanide 4-(trifluoromethoxy)phenylhydrazone (FCCP) or sodium cyanide (NaCN) the dura was removed and no coverslip was used. Instead a silicone well

was drawn around the exposed cortex (Body Double, Smooth-On Inc., USA) and filled with 40µl saline. During time lapse imaging 2µl of saline from the well was replaced with NaCN or FCCP (working concentration of 5mM and 10µM, respectively, see Figure 2.4.2.1). Five of the time lapse images were averaged, seconds or minutes after application, once the image stabilized.

Room air exposure was achieved with a room air pump while other variations of FiO_2 were controlled by mixing oxygen and nitrogen at appropriate concentrations. Oxygen variations were conducted as a gradual decrease from 21% O_2 downwards in 1% increments until death occurred or as 5 minutes interval variations as follows: 21%, 100%, 21%, 15%, 21%, 10%, 21% and 5% oxygen, until death.

2.4.4. Microscopy

The endogenous flavoprotein signal (excitation: 488nm, emission: 505-570nm) and all dyes described were imaged with a LSM 5 Pascal laser-scanning confocal microscope (Zeiss, Germany), using time lapse recordings with an in-plane resolution of 512 by 512 pixels and an optical slice thickness of 896 µm. Endogenous NAD(P)H (excitation: 720, emission: 430-480) was imaged using a Zeiss 510 NLO META equipped with a Coherent Chameleon Ti:sapphire laser.

2.4.5. Image analysis

Images were processed using Fiji/ImageJ Version 1.48v (NIH, USA). Time-lapse sequences were aligned using the 'Stackreg'-Plugin. Areas of interest were selected using the free hand selection tool. To assess the flavoprotein fluorescence three regions of interest were selected around arteries, and three around veins, followed by a calculation of the ratio of these areas. The change in the ratio of periarterial over perivenular fluorescence intensity was compared during different FiO_2 conditions. To assess changes in cortical oxygenation the average intensity of

phosphorescent microbeads close to arteries and close to veins was determined separately and compared across conditions of variable FiO_2. Statistical significance was assessed using the IBM SPSS Statistics 22 package and a $p \leq 0.05$ was considered significant.

2.5. Results

2.5.1. Endogenous fluorescence in the naïve cortex

During normoxia (21% inspired O_2) a green autofluorescent signal was present uniformly throughout the cortex, except where obscured by the vasculature, which was highlighted in negative contrast. We distinguished arteries from veins by their morphology, and their uniform outline, which was typically highlighted as brightly fluorescent walls (Figure 2.5.1.1). The arterial nature of these vessels was confirmed using DAF-FM diacetate (Figure 2.5.1.1) which is non-fluorescent until it reacts with nitric oxide, as nitric oxide is expressed by the endothelial cells of arteries, from where it diffuses to the surrounding smooth muscle (Bateman et al. 2003).

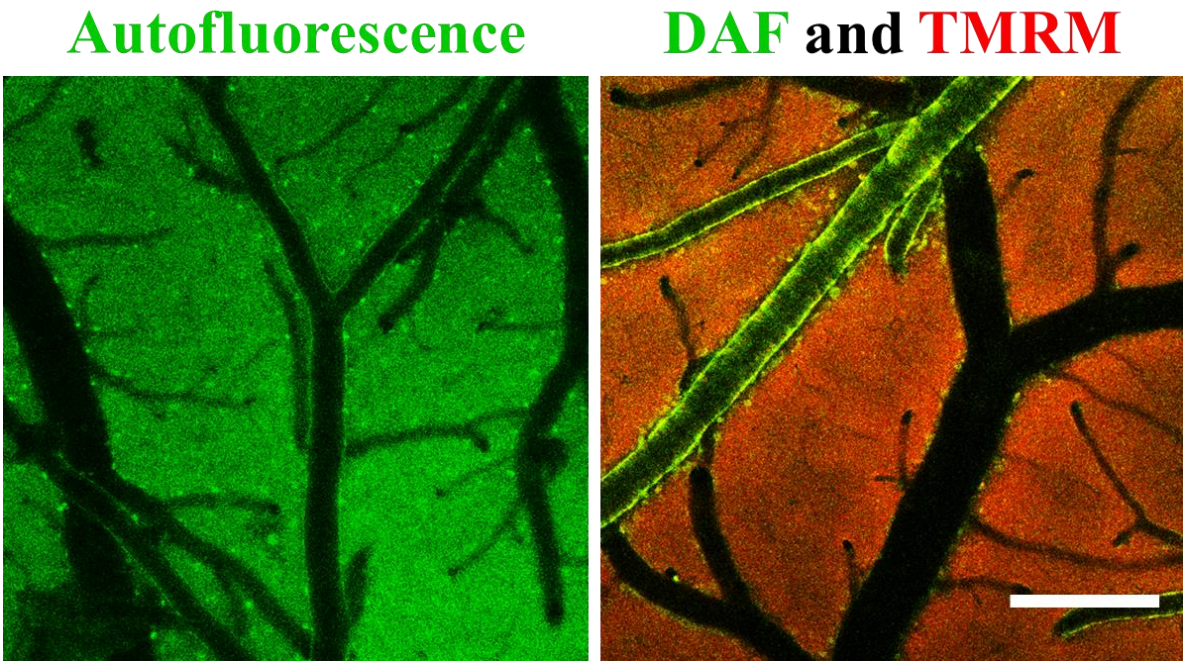

Figure 2.5.1.1: **Arteries can be distinguished morphologically and by their arterial wall** Left: green autofluorescence; right DAF-FM (green) and TMRM (red) fluorescence. The nitric oxide label, DAF-FM, confirms the arterial nature of vessels with thicker, DAF-FM positive walls compared with veins. Scale bar = 200µm

Brightly fluorescent puncta can be seen in the naïve cortex imaged for green autofluorescence (Figure 2.5.1.1). When time lapse recordings are taken at higher magnification (63x) it is possible to see movement of the brightly fluorescent puncta (data not shown). These puncta also labelled with isolectin (Figure 2.5.1.2) suggesting that these are perivascular macrophage/microglia (Kaur and Ling 1991).

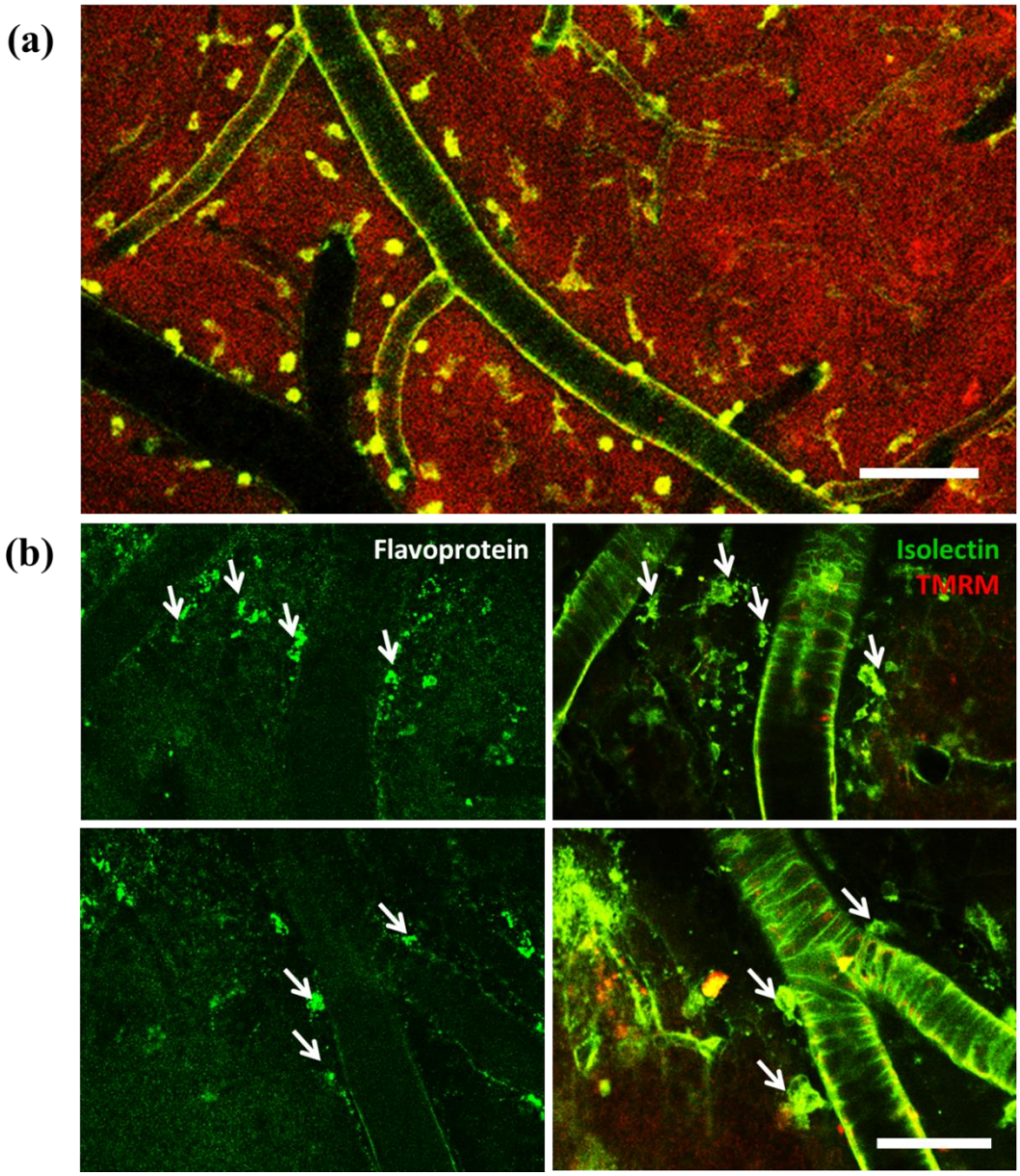

Figure 2.5.1.2: **Isolectin mirrors the punctate pattern of green autofluorescence in the murine cortex.**

(a) Isolectin (green) / TMRM (red) in 10x magnification, scale bar = 200µm. Bright puncta in isolectin labelled cells replicate the pattern seen with autofluorescence imaging. **(b)** Higher magnification (63x) reveals direct colabelling of bright perivascular autofluorescent puncta with isolectin (arrows). Scale bar = 100µm.

2.5.2. Endogenous fluorescence is mitochondrial in origin

The putative mitochondrial origin of the green autofluorescence in the cerebral cortex was explored by use of agents known to influence the redox state of flavoproteins. Application of NaCN is known to result in the reduction of a number of components of the ETC (Hackenbr 1968) and this was confirmed by a significant reduction in fluorescence intensity (~35%). Application of FCCP instead oxidizes the ETC and also significantly increased the fluorescence intensity (~23%; Figure 2.5.2.1), as expected. The control treatments (application of HEPES (4-(2-hydroxyethyl)-1-piperazineethanesulfonic acid) buffered saline or DMSO (Dimethyl sulfoxide) in saline (1:500) for NaCN and FCCP respectively) did not significantly affect the autofluorescence signal. These data are therefore in line with the proposition that the endogenous green fluorescence imaged here originates from oxidized mitochondrial flavoproteins.

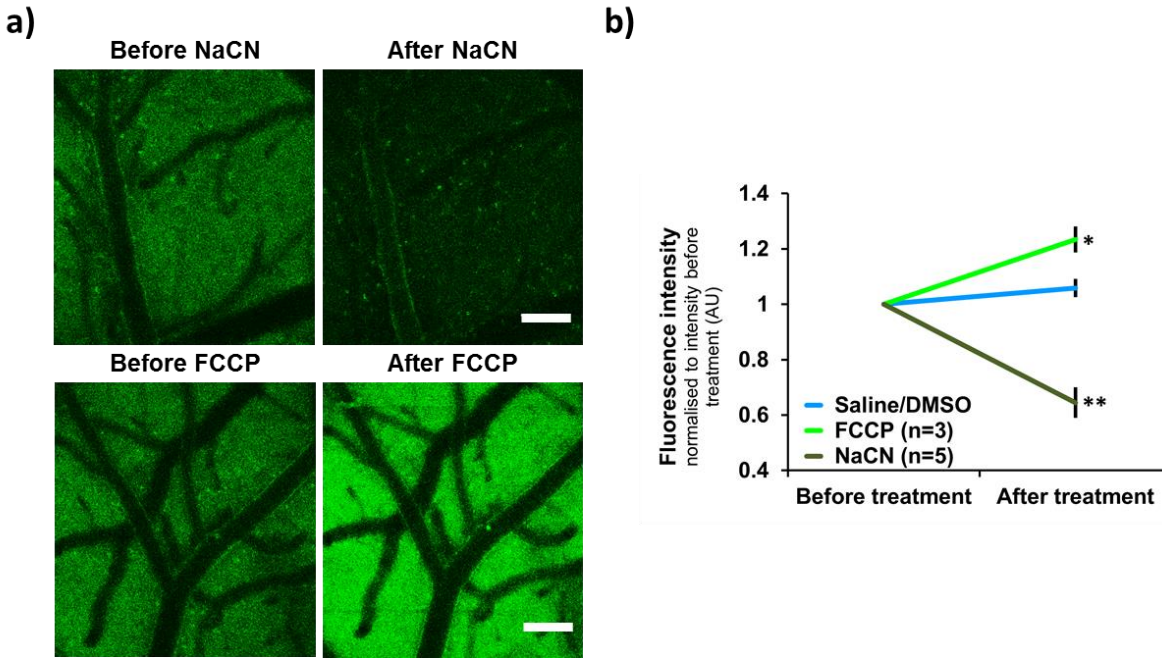

Figure 2.5.2.1: **Confirmation of the mitochondrial origin of endogenous green fluorescence. (a)** Representative images of flavoprotein fluorescence before and after the addition of NaCN and FCCP showing a decrease and increase in the flavoprotein signal respectively. Scale bar = 100µm. **(b)** Quantification of the change in fluorescence intensity before and after the addition of cyanide and FCCP. Data displayed as mean ± SEM. Significance is compared between the change in signal after application of DMSO vs FCCP, * = $p \leq 0.05$ and between the change in the signal after application of HEPES buffered saline vs NaCN, ** = $p \leq 0.01$.

2.5.3. Hypoxaemia affects the flavoprotein fluorescence

Increasing FiO_2 from 21% to 100% had no effect on the signal amplitude or distribution. Reducing FiO_2 (to ≤ 10%) however, resulted in a marked change in flavoprotein fluorescence. This change was characterised by a decrease in fluorescence intensity which preferentially affected areas around veins and tissue remote from arteries. This left a 'halo' of preserved autofluorescence in

tissue adjacent to arteries and arterioles (Figure 2.5.3.1 a). This pattern typically appeared at 5-10% inspired oxygen. In contrast, smaller decreases in FiO_2 (e.g. 15%) had no effect on the flavoprotein signal (Figure 2.5.3.1 b).

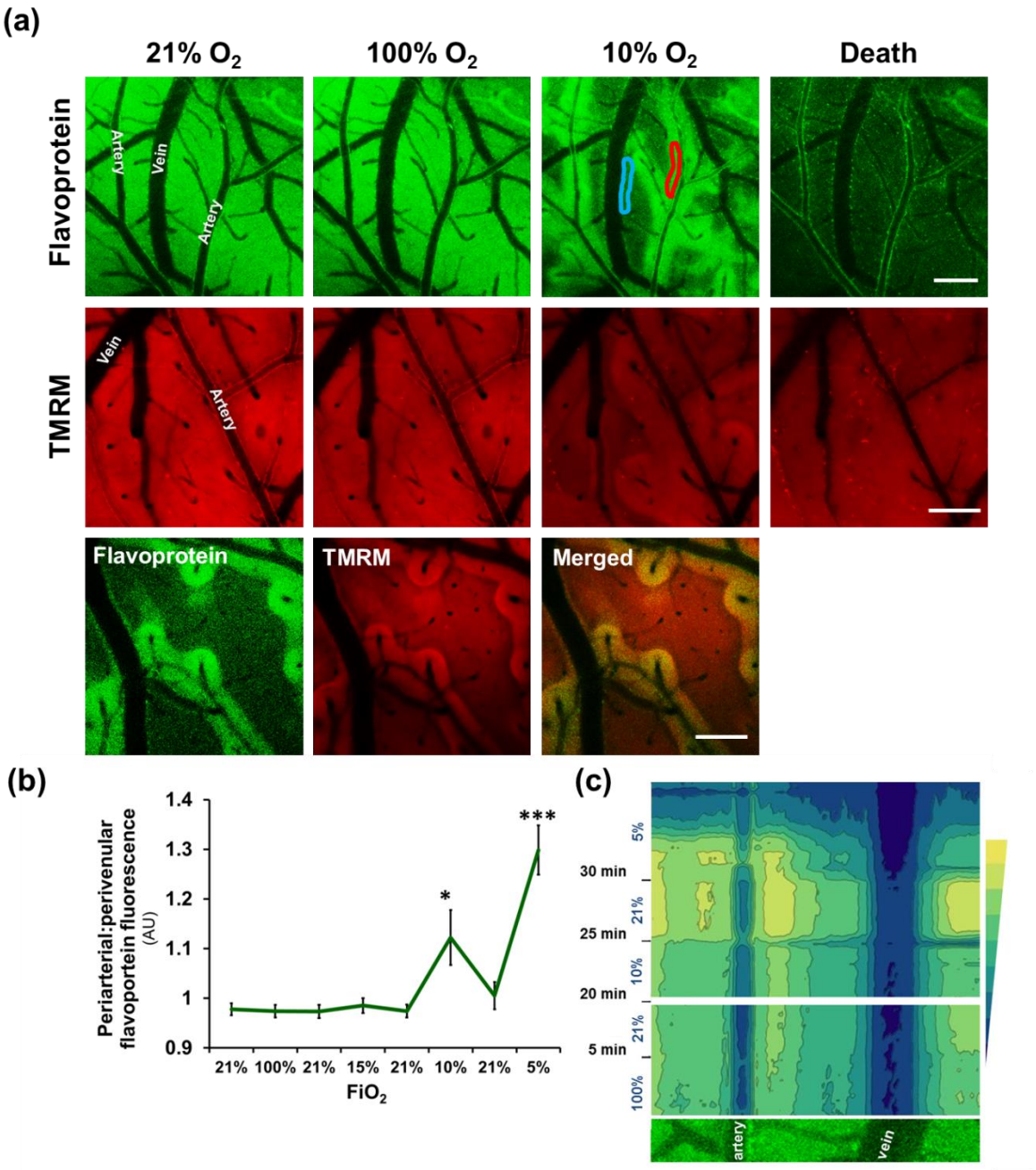

Figure 2.5.3.1: **Flavoprotein and TMRM fluorescence during hypoxaemia.**

(a) Representative images of changes in cortical flavoprotein and TMRM fluorescence in response to changes in FiO_2. An increase in inspired oxygen above 21% did not change the flavoprotein fluorescence or the TMRM fluorescence. However a decrease in FiO_2 to $\geq$ 10% O_2 reduces the flavoprotein and TMRM signal with preserved signal only around the arteries. Scale bar = 200µm. **(b)** Quantification of flavoprotein fluorescence represented as the ratio of periarterial over perivenular fluorescence intensity (representative selections displayed in **(a)**, red = periarterial selection, blue = perivenular selection). Data displayed as mean ± SEM. Significance was assessed between changes in inspired oxygen and the initial room air condition. * = $p \leq 0.05$, ** = $p \leq 0.01$, n = 21. **(c)** Profile plot showing the change in flavoprotein fluorescence during changes in FiO_2 in a representative tissue section (represented in the bottom). Blue indicates low fluorescence intensity, yellow represents high fluorescence intensity.

To confirm the accuracy of our quantification of the change in flavoprotein fluorescence with hypoxaemia, we compared the chosen method (hand selection of three periarterial and three perivenular areas and the creation of a ratio, see method, chapter 2.4.5) with a more detailed method. This method involved the hand selection of a 'halo' of 20-30µm around all vessels, instead of a selection of only six areas.

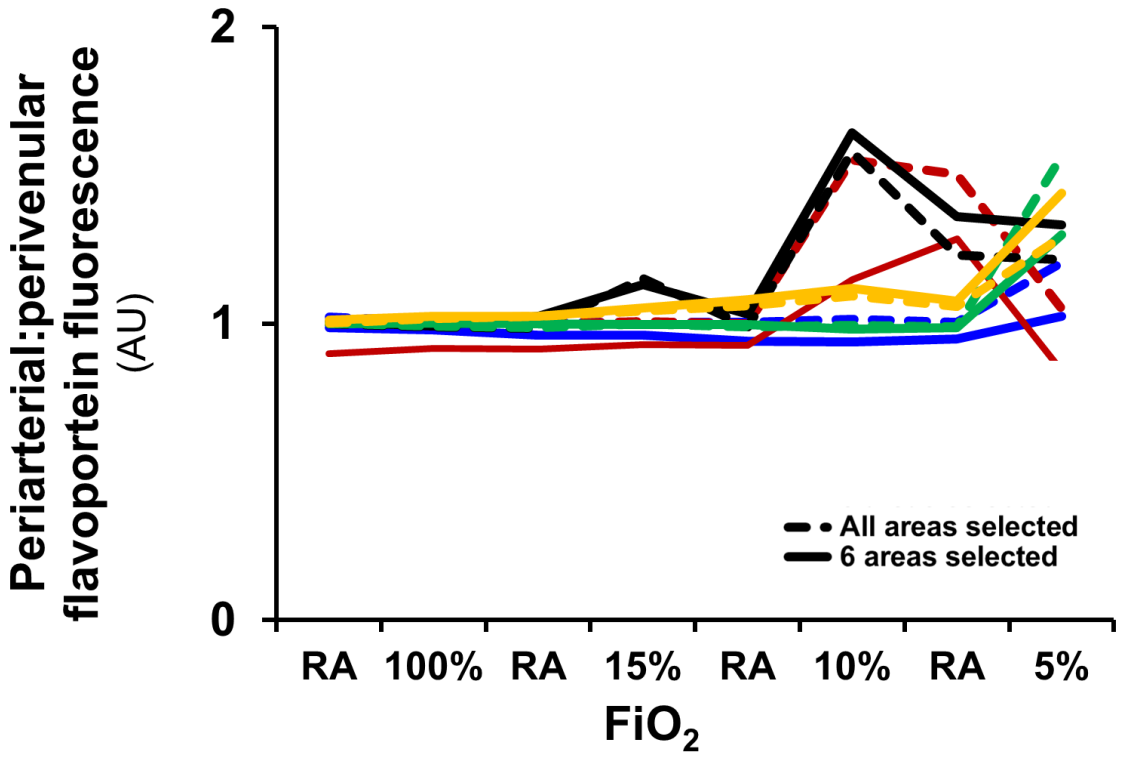

Figure 2.5.3.2: **Quantification of flavoprotein signal change.**
Assessment of the accuracy of the measure used to quantify the flavoprotein signal change with hypoxaemia. Two methods of quantification were compared. One method (solid lines) involved the hand selection of three periarterial and three perivenular areas and the creation of a ratio. The second method (dotted lines) is more exhaustive and involves the free hand selection of a 20-30µm halo around all vessels and the creation of a periarterial to perivenular ratio. Each colour represents one separate experiment with 5 experiments being compared in total.

In most cases no considerable difference between the two assessment methods was observed (Figure 2.5.3.2.). The occasional discrepancy between the two forms of quantification (red lines) could be due to surgical damage which could have left some areas of the brain non-responsive to hypoxaemia. Such areas can be avoided when selecting 6 areas. Therefore all further quantification of flavoprotein ratios will reflect the ratio of three hand selected areas around arteries and three hand selected areas around veins.

The relatively abrupt appearance of the change in fluorescence intensity (Figure 2.5.3.1 c) suggests a sharp threshold at which cortical mitochondrial function is affected by changes in

inspired oxygen. Indeed, when hypoxaemia was introduced more gradually, with a 1% decrease in inspired oxygen every 3 minutes, it became obvious that changes in flavoprotein fluorescence occur very abruptly between 7-9% inspired oxygen, despite a continuous and gradual decline in arterial oxygenation saturation (Figure 2.5.3.3). It seemed that arterial haemoglobin oxygen saturation (as assessed by arterial pulse oximetry) needed to be around 55% O_2 before an effect on cortical mitochondria can be visualised (Figure 2.5.3.3).

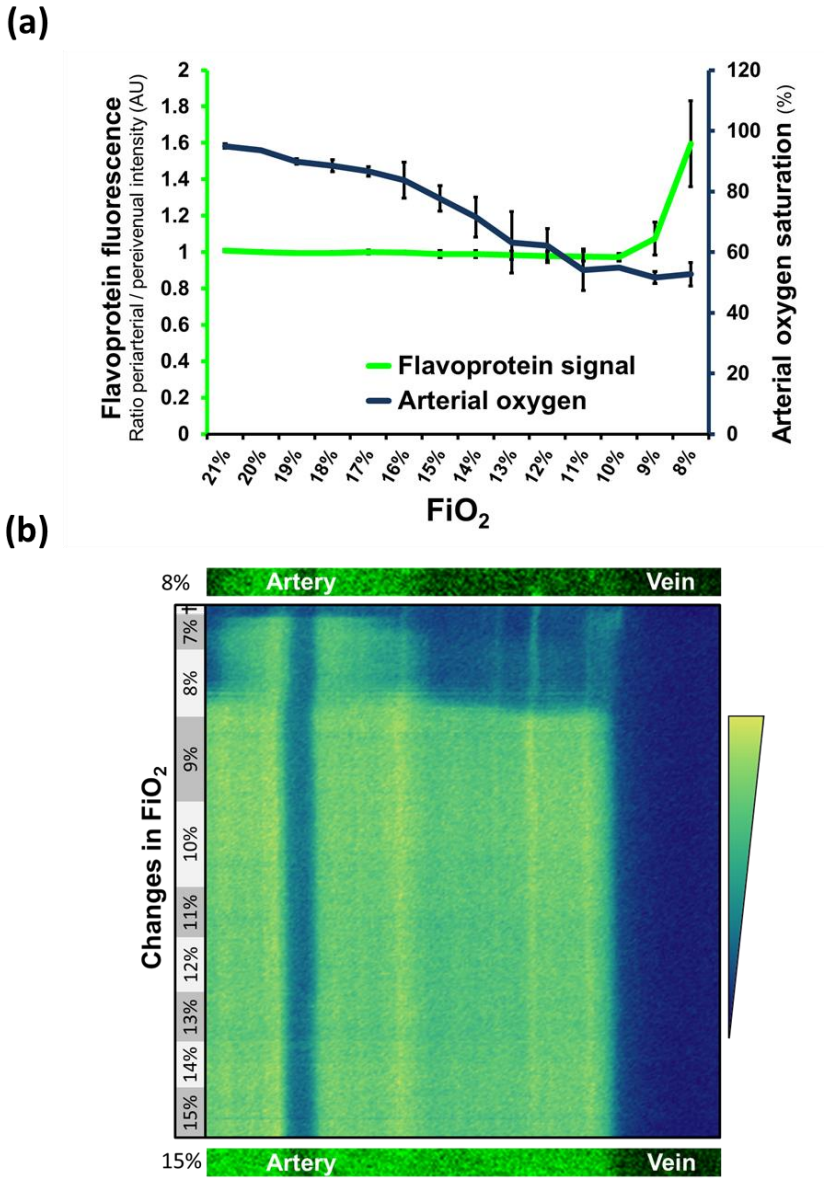

Figure 2.5.3.3: **Flavoprotein fluorescence and arterial haemoglobin saturation.**
(a) Change in flavoprotein fluorescence and arterial haemoglobin saturation with gradual increases in hypoxaemia. Data displayed as mean ± SEM. Flavoprotein signal n = 4; arterial oxygen saturation n = 2. **(b)** Profile plot showing the change in flavoprotein fluorescence during gradual changes in FiO_2 in a representative tissue section (represented in the bottom at 15% inspired O_2 and at the top at 8% inspired O_2). Blue indicates low fluorescence intensity, yellow represents high fluorescence intensity.

Additionally, reductions in flavoprotein fluorescence were reversible if the animals were returned to room air and were able to recover (Figure 2.5.3.1 b and c). It should also be noted that some animals showed an increased flavoprotein fluorescence following recovery (23% showed a very clear increase in flavoprotein signal upon recovery).

Further we explored whether changes in flavoprotein fluorescence were also associated with changes in mitochondrial membrane potential. To examine this we assessed the effects of hypoxaemia on TMRM fluorescence. We observed the same arterial 'halos' of preserved TMRM fluorescence at 5-10% FiO_2 as with flavoprotein autofluorescence (Figure 2.5.3.1 a). The change in the flavoprotein fluorescence in the merged image is not due to bleed through from TMRM as equivalent flavoprotein fluorescent changes occur also in the absence of TMRM loading (Figure 2.5.3.1 a).

The changes in the distribution of the flavoprotein fluorescence at reduced FiO_2 varied inversely with NAD(P)H fluorescence (Figure 2.5.3.4). This is because NAD(P)H can be visualised when it, and the mitochondrial ETC, are reduced. This pattern is in opposition to flavoprotein autofluorescence which only fluoresces in the oxidized state. However neither NAD(P)H nor flavoproteins are expected to provide significant signal inside vessels. Therefore it is not surprising that the absence of flavoprotein and NAD(P)H signals converge in vessels (Figure 2.5.3.4)

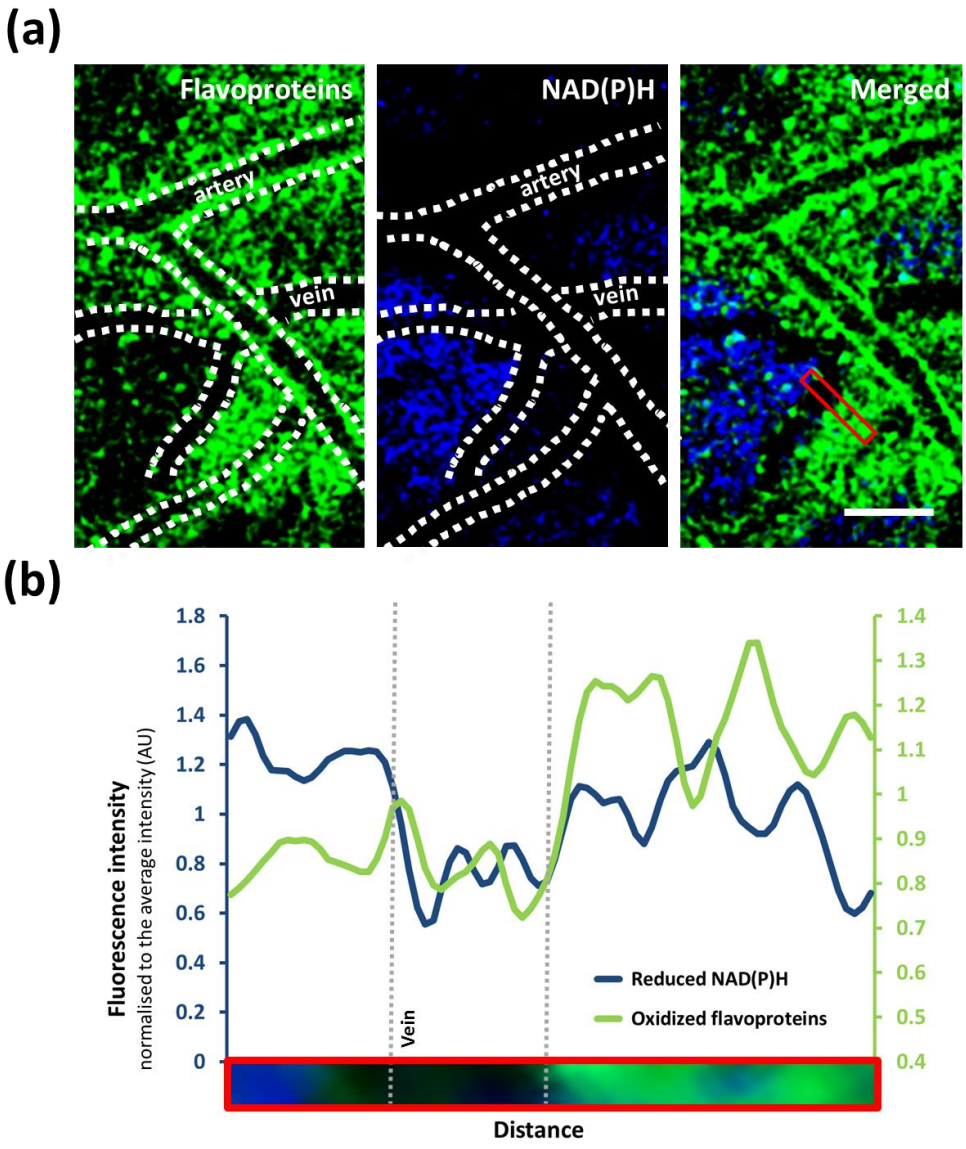

Figure 2.5.3.4. **Flavoprotein and pyridine nucleotide fluorescence during hypoxaemia** **(a)** Representative images of flavoprotein and NAD(P)H fluorescence during hypoxaemia. Scale bar = 60µm. **(b)** Graphical representation of a small section of tissue (highlighted in red in the merged image in **(a)** and at the bottom of the graph). In cortical parenchyma flavoprotein and NAD(P)H fluorescence tend to diverge as flavoprotein fluoresce when oxidized and NAD(P)H when reduced. In vessels the signals will converge due to absence of fluorescence.

Using oxygen-sensitive phosphorescent beads we were also able to show that changing the FiO_2 resulted in a corresponding change in cortical tissue oxygen, as expected (Figure 2.5.3.5). The

oxygen-sensitive beads increased in fluorescence intensity with a decrease in available oxygen, exhibiting an approximately 3-fold increase in the fluorescence intensity when O_2 is reduced from 21% to 0%.

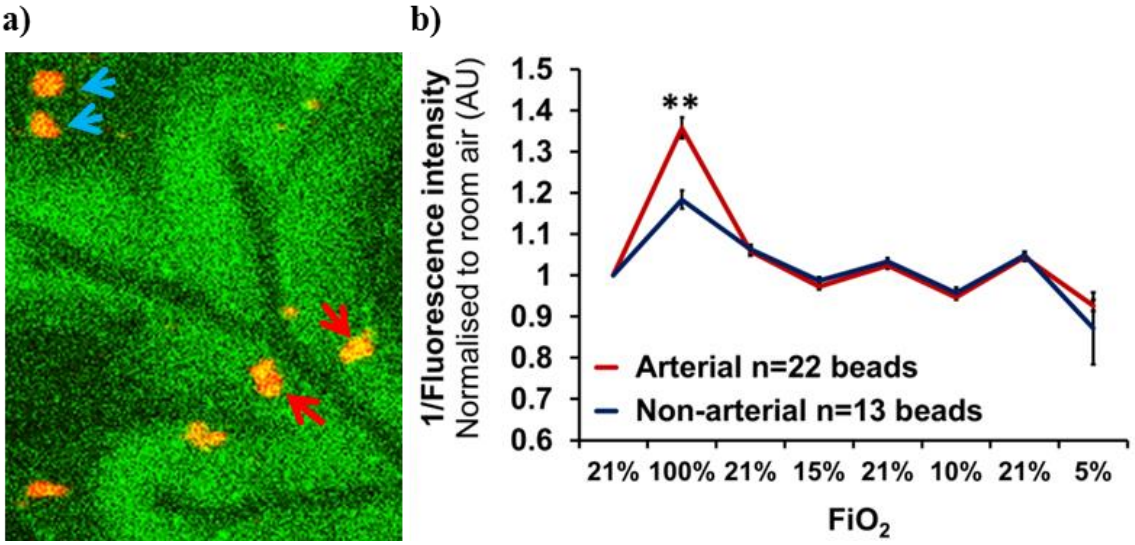

Figure 2.5.3.5. **Change in cortical oxygenation assessed by oxygen sensitive beads**
(a) Representative image of oxygen sensitive phosphorescent beads (orange beads) on a cortex imaged for flavoprotein fluorescence (green). Beads close to the arteries (red arrows) were analysed separately from beads further away (blue arrows). **(b)** Quantification of fluorescence intensity changes with changes in inspired oxygen. The reciprocal of the fluorescence intensity was graphed. Data displayed as mean ± SEM. ** = $p \leq 0.01$

When the FiO_2 was increased to 100%, a significantly larger decrease in fluorescent intensity was observed in periarterial beads which were defined as being within the 'halo' of preserved flavoprotein fluorescence, compared with beads located further away from arteries (Figure 2.5.3.5 b). However, other changes in FiO_2 did not lead to differences between the change of periarterial and the change of perivenular bead fluorescence, suggesting that oxygenation in areas around the arteries and areas further away responds similarly to reductions in inspired oxygen or that the beads were not sensitive enough to detect more subtle changes.

2.6. Discussion

We demonstrated that it is possible to use flavoprotein autofluorescence, imaged using standard confocal microscopy, in the cortex of anaesthetized mice, as a measure of mitochondrial redox potential. Using this measure we further showed that cortical mitochondrial function is selectively compromised at low concentrations of inspired oxygen. The impairment is selective for perivenular areas and tissues further away from arteries, with preservation of mitochondrial redox potential along arteries and arterioles. This pattern of selective mitochondrial dysfunction during hypoxaemia demonstrates the role of arteries and arterioles in the direct supply of oxygen to cerebral tissue.

2.6.1. Flavoprotein signal represents mitochondrial redox potential

The use of flavoprotein autofluorescence as an indicator of mitochondrial redox potential is well established (Chance et al. 1979; Huang et al. 2002; Reinert et al. 2004; Scholz et al. 1969) but its application in intravital fluorescence microscopy to assess mitochondrial function in the CNS has been limited. To our knowledge endogenous flavoprotein fluorescence has not been used previously to evaluate cortical redox state in response to changes in inspired oxygen with the high spatial and temporal resolutions of confocal microscopy shown here.

We used pharmacological interventions to vary the mitochondrial redox potential in cortical mitochondria in order to confirm the mitochondrial origin of the green autofluorescence. A variation in the redox state was achieved using the well characterised agents NaCN and FCCP. NaCN is known to block complex IV and thereby prevent the transfer of electrons to oxygen. This inhibitor therefore causes a build-up of electrons on the ETC and leads to reduction of the ETC and the mitochondrial redox potential. This reduction in the redox potential corresponds to a decrease in

flavoprotein fluorescence. FCCP instead acts as an uncoupling agent thereby allowing protons to cross the inner mitochondrial membrane without passing through complex V. This maximally stimulated mitochondrial respiration (Benz and Mclaughlin 1983) and thereby leads to the oxidation of mitochondria, including flavoproteins. And as a result we observed an increase in flavoprotein autofluorescence corresponding to an increase in its oxidation state.

The source of the endogenous flavoprotein fluorescence was further validated by simultaneous imaging of flavoprotein and NAD(P)H fluorescence. NAD(P)H is known to fluoresce when reduced and has been previously imaged in the cortex *in vivo* (Kasischke et al. 2011; Takano et al. 2007). Reduced pyridine nucleotides therefore provide the fluorescence counterpart of oxidized flavoproteins and are expected to vary inversely. This is indeed what we found when exposing the mouse to a reduction in inspired oxygen. In the absence of oxygen (the final electron acceptor) the electrons build up on the ETC and thereby lead to a reduction of mitochondrial redox potential, which results in a decrease in flavoprotein fluorescence concomitant with an increase in pyridine nucleotide fluorescence in the cerebral cortex *in vivo*.

2.6.2. Reductions in FiO_2 reveal arterial oxygenation of the cortex

Under normoxic conditions (21% inspired oxygen) we found that the oxygen supply to the brain was sufficient to sustain functional mitochondria uniformly throughout the cortex in agreement with previous reports (Erecinska and Silver 2001). Increasing the concentration of inspired oxygen had no effect on flavoprotein autofluorescence, suggesting that oxygen availability was not a rate limiting factor in flavoprotein oxidation under these conditions. This is in contrast to previous studies which found an increase in NAD(P)H fluorescence also under an FiO_2 of 21% (Kasischke et al. 2011), suggesting that also under normoxaemia the cortex exhibits tissue patches in which mitochondria are reduced. This can be explained by the use of different autofluorescent

fluorophores (namely pyridine nucleotides) or possibly also by differences in the preparation of the cranial window. Specifically Kasischke et al.'s experimental design involved the removal of the dura mater, while our set-up left this intact. The removal of the dura can lead to enhanced swelling of the cortex which can cause the obstruction of blood vessels along the edge of the cranial window hampering perfusion to the cranial window and thereby possibly resulting in unintentional cortical hypoxia.

In our experiment a small reduction in the FiO_2 to 15% also had little influence on the mitochondrial redox potential suggesting that an FiO_2 of 15% in a healthy, anaesthetised animal is still sufficient to maintain a healthy pool of oxidized mitochondria throughout the cortex. A further decrease in the concentration of inspired oxygen to less than 10%, however, resulted in a characteristic change in the flavoprotein signal. This consisted of a reduction of flavoprotein autofluorescence in avascular areas away from arterioles and areas close to venules with preservation of oxidized flavoprotein autofluorescence along pial arteries and arterioles, similar to previous investigations (Kasischke et al. 2011). The loss of flavoprotein fluorescence was further investigated by a gradual decrease in FiO_2. This revealed a sudden loss of flavoprotein fluorescence around 7-9% inspired oxygen which in our experiment corresponds to an approximately 55% arterial haemoglobin oxygen saturation. This is in line with previous findings showing that reductions in systemic oxygenation need to be severe before they have an influence on healthy cortical mitochondria (Chance et al. 1962; Macmillan and Siesjo 1972). Indeed, Chance et al, using fluorometry, found that the cortical NAD(P)H signal only increased at concentrations of inspired oxygen below 8% (Chance et al. 1962) which reflects our observations. This reduced level of oxygen happens to align well with the so called "death zone" experienced at extreme altitudes, above 30 000 feet (height of Everest), where sustained habitation and human acclimatisation have been said to be impossible (Huey and Eguskitza 2001). Here the oxygen concentration is approximately 34% of that at sea level leaving an oxygen concentration of around 7% (Huey and

Eguskitza 2001). Of course only limited parallels can be drawn between the extreme conditions endured on Mount Everest and those experienced by an anaesthetised rodent.

If hypoxaemia is sufficient it very abruptly leads to dysfunctional cortical mitochondria despite a gradual decrease in systemic oxygenation (as assessed by pulse oximetry). The spatial pattern seen with flavoprotein autofluorescence in response to changes in FiO_2 was also observed with TMRM fluorescence, suggesting that other measures of mitochondrial function such as membrane potential are also affected by hypoxaemia. We were able to assess TMRM and flavoprotein fluorescence simultaneously showing concordance between the two signals. We also imaged these separately in different populations of animals to show that the change in flavoprotein fluorescence does not correspond to TMRM signal bleed through. Preservation of flavoprotein/TMRM fluorescence and loss of NAD(P)H fluorescence in periarterial tissue is not consistent with the historical assumption that oxygen delivery to organs is limited to capillaries (Krogh 1919). Instead these data support more recent evidence that arteries and arterioles play a major role in delivering oxygen directly to tissue (Ivanov et al. 1982; Ivanov et al. 1999; Sakadzic et al. 2010; Vovenko 1999). Furthermore, our results also show that the oxygen delivered via cortical arteries and arterioles is physiologically relevant and maintains mitochondrial function during hypoxaemia, in line with previous work (Kasischke et al. 2011). Therefore, we have shown not only that oxygen delivery to tissue is not limited to capillaries but also that the delivery of the oxygen through arterioles is of relevance to tissue function.

It should also be noted, that if the animals were allowed to recover after a reduction in FiO_2, under $\geq 21\%$ O_2, the loss of flavoprotein signal was reversible. Additionally a subset of mice (23%) showed even an enhancement of the flavoprotein autofluorescence after recovery from the hypoxaemia. We were unable to find a correlate to this enhanced recovery. One might speculate that this increase in flavoprotein signal after recovery from hypoxaemia could be related to mitochondrial transition pore opening during ischemia/reperfusion injury (Honda et al. 2005) which

can lead to an uncoupling of mitochondrial oxidative phosphorylation (Brenner and Moulin 2012; Halestrap et al. 1998) and a resultant increase in oxidation of mitochondrial flavoproteins (as seen after the application of FCCP, described above). Indeed, it is known that mitochondrial membrane depolarisation, as seen here with TMRM, increases the probability of the opening of the permeability transition pore (Bernardi et al. 1993; Honda et al. 2005; Ly et al. 2003; Petronilli et al. 1993). However, formal testing of this hypothesis would be needed and might include the inhibition of permeability transition pore opening by e.g. cyclosporine A.

2.6.3. Cortical microglia/macrophages distribution can be visualized using endogenous green fluorescence

The uniform coverage of green autofluorescence seen in the cortex, originating from mitochondrial flavoprotein, is interspersed by bright fluorescent puncta throughout the parenchyma. This signal is unaffected by reductions in inspired oxygen or the addition of cyanide, suggesting that it is not mitochondrial in nature. Previous *in vitro* studies have also found such non-mitochondrial autofluorescence and have implicated lysosomes (Andersson et al. 1998). This is in line with our observations using high magnification time-lapse imaging which revealed that moving circular structures, consistent with lysosomes, make up the autofluorescent bodies. Furthermore, it is known that microglia/macrophages have autofluorescent properties (Edelson et al. 1985; Xu et al. 2008) which could originate from their lysosomes (Koenig 1963). To test whether the brightly fluorescent puncta seen in the cerebral cortex of anaesthetized mice do originate from microglia/macrophages we applied isolectin (which is known to label macrophages/microglia (Kaur and Ling 1991)) to the surface of the cortex. The co-labelling of isolectin with the autofluorescent puncta suggests that these are indeed cortical microglia/macrophages. This finding illustrates yet another opportunity for autofluorescent imaging: the assessment of microglia and macrophages

without the application of exogenous dyes. The origin of the fluorescence in the microglia/macrophages/lysosomes is not within the scope of this research but it has been suggested to derive from the accumulation of waste products such as lipofuscin (Xu et al. 2008) and/or non-mitochondrial flavoprotein autofluorescence, as both inducible nitric oxide synthase and the respiratory burst are associated with flavoproteins (Babior 1984; Clark 1990; Clark 1999; Hevel et al. 1991; Stuehr et al. 1991).

2.6.4. Changes in FiO_2 can be detected by oxygen sensitive microbeads

Changing the concentration of inspired oxygen resulted in a corresponding change in cortical oxygenation as assessed by oxygen-sensitive microbeads. Hyperoxia was found to have a differential effect on periarterial and perivenular tissue oxygenation while no measurable difference in the reduction in periarterial and non-arterial tissue oxygenation was detected at $\leq$ 21% FiO_2, despite the decrease in oxidized flavoprotein distal to arteries. This however does not mean that arterial and venous oxygenations are not different, as absolute measurements were not possible using oxygen sensitive microbeads. However, it does mean that, according to our oxygen sensitive microbeads, periarterial and non-arterial regions are similarly affected by reductions in inspired oxygen but that arterial regions are more affected by hyperoxic conditions. This is in line with previous studies (Bergofsk and Bertun 1966) and might be related to a decrease in blood flow with hyperoxia (Bergofsk and Bertun 1966; Kennedy et al. 1971; Lambertsen et al. 1953; Leahy et al. 1980; Watson et al. 2000) which can lead to a greater oxygen extraction by the tissue and a relatively reduced venous oxygen outflow (Bergofsk and Bertun 1966).

2.7. Limitations and further research

As mentioned in the introduction, both NAD(P)H and flavoprotein fluorescence originate from a number of different sources. However, our data does not differentiate between these sources. It is believed that flavoprotein fluorescence originates primarily from the FAD cofactor in α-lipoamide dehydrogenase and/or electron transfer flavoproteins together with some non-redox reactive fluorescence (Kunz and Gellerich 1993; Kunz and Kunz 1985). Small spectral variations in α-lipoamide dehydrogenase and electron transfer flavoprotein fluorescence allowed the differentiation of these signals (Lam et al. 2012; Rocheleau et al. 2004). However, spectral overlap remains extensive and more ready differentiation might be achieved with fluorescence lifetime imaging (FLIM). Briefly, FLIM records the decay rate of fluorophores from an excited state. Practically this involves excitation with a femtosecond laser and recording of the rate of release of photons after the excitation event. Different molecules will have different decay properties but even similar molecules can vary in their decay characteristics based on their immediate environment. The local environments and binding partners of flavoprotein cofactors in α-lipoamide dehydrogenase and electron transfer flavoproteins provide good theoretical grounds for the likely differentiation of these molecules with FLIM. Indeed, FLIM has been used to differentiate the phosphorylated and un-phosphorylated reduced pyridine nucleotides from each other both *in vitro* and *ex vivo* (Blacker et al. 2014) showing that the fluorescence originating from NADPH is not negligible (Blacker et al. 2014). The different environments and binding partners of NADH and NADPH allows for FLIM differentiation of these two molecules when bound to different structures (Blacker et al. 2014), while free NAD(P)H cannot be differentiated by FLIM imaging (Blacker et al. 2013).

Therefore, a future improvement of the current technique might include the use of FLIM to differentiate the origin of the flavoprotein and NAD(P)H signal *in vivo* in the

cortex and comparing the fluorescence lifetimes in the CNS with fluorescence lifetimes in other organs where the ratio of these fluorophores is expected to be different. It has been stated that neither NADPH nor electron transfer flavoproteins are extensively present in brain tissue (Klaidman et al. 1995; Kunz and Gellerich 1993; Shuttleworth 2010). This is in contrast to the liver where β-oxidation occurs more extensively and thereby the electron transfer flavoprotein content is expected to be higher compared to the brain (Kunz and Gellerich 1993). However as the signal generated by oxidized flavoproteins is weaker compared with that of reduced pyridine nucleotides (Chance et al. 1979; Koke et al. 1981) their assessment using two-photon excitation might be more difficult due to the localised excitation of two-photon lasers. Therefore, the use of pulsed single-photon lasers might be necessary which allows for greater signal collection following the loss of resolution in the z-plane by opening of the pinhole. The feasibility of this would have to be determined experimentally.

2.8. Conclusion

In conclusion, we demonstrated that it is possible to use flavoprotein autofluorescence to assess mitochondrial redox potential *in vivo* in the central nervous system with the spatial and temporal resolution afforded by fluorescence microscopy and that this signal is sensitive enough to reflect changes in mitochondrial redox state both in response to mitochondrial inhibitors and hypoxaemia. Changes in mitochondrial redox potential were revealed in the cerebral cortex of hypoxaemic mice, as demonstrated by a regionally selective decrease in flavoprotein fluorescence in areas away from arteries and tissue surrounding veins. These reductions in mitochondrial redox potential are associated

with corresponding changes in mitochondrial membrane potential. The preservation of oxidized flavoproteins and membrane potential in periarterial tissue is consistent with the direct supply of oxygen from arteries and arterioles to cortical tissue. Additionally endogenous green fluorescence can also be used to assess resident microglia without the application of dyes. However, further characterization of the autofluorescent signal is necessary to reveal the exact origin of mitochondrial flavoprotein fluorescence.

CHAPTER THREE

3. Mitochondrial function in the CNS during systemic inflammation

3.1. Introduction

Having characterised flavoprotein fluorescence in the cortex of naïve and hypoxaemic mice we were interested in assessing the relationship between mitochondrial redox potential and hypoxaemia during systemic inflammation as a murine model of sepsis.

3.1.1. Sepsis and the brain

Sepsis is a serious medical condition estimated to be the 11th most common cause of death in 2010 (Murphy et al. 2013). Furthermore the incidence of sepsis is expected to rise in the future with an increasingly aged and immunosuppressed population (Singer and Brealey 1999). Multiple organ dysfunction and failure is the leading cause of death during sepsis and other intensive care conditions (Gustot 2011; Thijs et al. 1996). The brain is not spared from sepsis related dysfunction and it is indeed common for septic patients to have brain dysfunction which can range from mild confusion to coma and these symptoms have been associated with increased mortality (Adam et al. 2013). Despite the wide reaching impact of sepsis, the mechanism by which it leads to multiple organ dysfunction and especially encephalopathy is still unclear.

As sepsis can be caused by a large number of bacterial, fungal or viral insults and displays a very broad clinical spectrum with large individual variation, it is a difficult disease to model (Wichterman et al. 1980). Not only the initial infection, but particularly the host immune response

has been consistently implicated in the disease pathology of sepsis and inflammatory response syndrome (Bone et al. 1997; Bopp et al. 2008; Flemming 2011; Goris et al. 1985). Given the immune system's dual nature of host protection and injury it is a very difficult pathway to target therapeutically (Bone et al. 1997). Given this inherent difficulty in the study of the immune response in sepsis and its clear importance in disease pathology, we decided to model the inflammatory component of sepsis without the complication of a true bacterial infection. For this we used a mild model of systemic endotoxemia, induced by a systemic injection of LPS which is a component of the cell wall of Gram-negative bacteria, known to induce a strong inflammatory reaction. Systemic LPS has frequently been used as a model of sepsis (Fink et al. 1987; Matsumoto et al. 2001; Peyssonnaux et al. 2007) and it presents a well characterised inflammatory model which mirrors some essential aspects of sepsis.

3.1.2. Sepsis and mitochondrial dysfunction

Extensive research has shown that sepsis is associated with mitochondrial dysfunction in several tissues, including skeletal muscle (Brealey et al. 2002; Brealey et al. 2004; Tavakoli and Mela 1982), liver (Brealey et al. 2004; Crouser et al. 2002a; Kantrow et al. 1997; Mela et al. 1971; Tavakoli and Mela 1982), and kidney (Mela and Miller 1983) and the idea of a bioenergetics failure has grown in acceptance in recent years. Even in a mild model of sub-acute septicaemia evidence of mitochondrial dysfunction has been reported (Tavakoli and Mela 1982) and early on in the induction of sepsis in rats Schaefer et al detected mitochondrial abnormalities using near infrared spectroscopy (Schaefer et al. 1991), suggesting that mitochondrial dysfunction is an early player in sepsis associated pathology. Indeed, a link has been established between disease severity, mitochondrial dysfunction and patient outcome (Brealey et al. 2002) and it has been suggested that patients may frequently die not of the initial infection *per se* (Bone et al. 1997) but rather because

of factors that persist even if the infection has been successfully combatted, such as a pronounced energy imbalance (Brealey and Singer 2003).

Mitochondrial dysfunction can result from an inadequate supply of oxygen and extensive evidence has linked sepsis and sepsis-related organ dysfunction to microvascular disturbances and poor organ perfusion (De Backer et al. 2013; De Backer et al. 2014; Lam et al. 1994). Indeed, dysfunction in sublingual microcirculation was associated with patient outcome as non-survivors showed more severe alterations compared to survivors (Bateman and Walley 2005; De Backer et al. 2013) and therapies aimed at microcirculatory recovery have shown promise (Anning et al. 1999; Bateman and Walley 2005; Spronk et al. 2002). Reduced cerebral blood flow has also been reported in patients (Bowton et al. 1989; Maekawa et al. 1991) and animal models (Crouser 2004; Ekstromjodal and Larsson 1982) although others have found no abnormalities (Lang et al. 1984; Pollard et al. 1997).

Given such evidence implicating mitochondrial dysfunction, inadequate perfusion and bioenergetic failure in sepsis it is expected that factors which reduce energy supply further, including hypoxaemia, could be particularly detrimental in sepsis. In contrast, it is expected that factors which reduce energy demand, such as hypothermia, may be protective.

Indeed, hypothermia has been successfully applied to several critical care conditions and has shown particular potential for neuroprotection (Bernard and Buist 2003; Polderman and Herold 2009). On the other hand, a recent clinical study of therapeutic hypothermia in bacterial meningitis had to be prematurely abandoned because of increased harm (Mourvillier et al. 2013). Murine models of sepsis have a rapid onset of hypothermia, with the magnitude of change being related to reduced oxygen consumption and increased mortality rates (Zolfaghari et al. 2013). Thus the impact of therapeutic hypothermia is uncertain.

3.2. Hypotheses

1) Systemic inflammation affects the CNS and can result in hypoxia which can affect mitochondrial resilience to additional energetic challenges (hypoxaemia)
2) Hypothermia can offer protection to CNS mitochondria during energetic challenges induced by systemic inflammation

3.3. Aims and objectives

In the previous chapter and in published work we have shown that the endogenous green fluorescence of flavoproteins can be used to assess mitochondrial redox potential *in vivo* in the CNS (Chisholm et al. 2015). We are now able to use this protocol to assess changes in cortical mitochondrial sensitivity to an energetic challenge (hypoxaemia) in a murine model of sepsis. Additionally we will assess whether cortical oxygenation is affected by endotoxemia thereby investigating a possible mechanism for putative increased mitochondrial vulnerability in cortices of endotoxic mice. Having assessed cortical mitochondrial vulnerability to hypoxaemia during systemic inflammation we can then test the efficacy of hypothermia to regulate this possible energetic imbalance and attenuate the enhanced sensitivity of endotoxic mice to reductions in inspired oxygen.

3.4. Methods

C57bl/6 mice (~20 g) were housed in a 12 hour light/dark cycle with food and water *ad libitum*. All experiments were performed in accordance with the UK Home Office Animals (Scientific Procedures) Act (1986).

3.4.1. Model

Following a pilot dosing experiment (described in chapter 4), mice were injected with LPS (from *Escherichia coli*, Sigma-Aldrich, USA; i.p. 5mg/kg in saline, 0.01ml/g) or saline alone. After the injection mice were placed back into normal housing conditions until surgery. 117 Mice were randomly allocated to one of nine conditions (Table 3.4.1.1) and a further fifteen mice were designated for assessment of cortical oxygenation (n = 5 (2 saline and 3 LPS) per time point: 6, 24, 48 hours post-injection)

	6 hrs post injection	24 hrs post injection	48 hrs post injection	Saline
Normothermia (37˚C)	n = 17	n = 13	n = 7	n = 21
Spontaneous temperature	n = 13	n = 13	-	n = 10
Induced hypothermia (32˚C)	n = 13	-	-	n = 10

Table 3.4.1.1: **Experimental conditions and n numbers**.
Nine conditions include different temperatures and times post-injection. It should be noted that an unequal distribution of numbers resulted from variable mortality rates with different disease and treatment conditions.

3.4.2. Craniotomy

Surgery was performed as described previously for the assessment of flavoprotein fluorescence in the cortices of anaesthetised mice (chapter 2). Briefly, isoflurane (~2%) was used to anaesthetise mice. A homeothermic heating mat maintained their rectal temperature at the desired level (either normothermia (37˚C), induced hypothermia (32˚C) or the spontaneous temperature exhibited immediately after anaesthesia). Following anaesthesia the skull was exposed and stabilised by fixation to a titanium bar (with dental cement and cyanoacrylate glue). A partial craniotomy over the right hemisphere exposed the underlying cortex which was cleaned and moistened with saline and covered with a circular glass coverslip, 6mm in diameter, and sealed with petroleum jelly. Following these preparations the mice were transferred to a custom-made stage for confocal microscopy. In a subset of mice (n = 27) oxygen-sensitive microbeads impregnated with a phosphorescent dye, PtPFPP, were added to partially cover the dura (5 µl of 5 mg/ml aqueous suspension).

3.4.3. Oxygen probe measurements

Fifteen mice were anaesthetised as above using isoflurane (~2% in room air) and core body temperature was measured and controlled at 37˚C via a rectal probe and homeothermic heating mat. A small opening of approximately 2mm in diameter was drilled into the skull of the right hemisphere to expose the underlying cortex. The dura mater was removed from a small area of the craniotomy for easier probe insertion. The fibre optic tip of an oxygen sensing probe (OxyMicro, World Precision Instruments, USA; assessing the phosphorescent quenching properties of oxygen) was inserted into the cortex using a micromanipulator. The probe was inserted to a depth of 700µm from the cortical surface, followed by a retraction of 100µm, to a final recoding depth of 600µm from the cortical surface. While measurements were continuously taken the FiO_2 was reduced by

the addition of nitrogen to room air for 5 minute intervals as follows: 0.21, 0.15, 0.21, 0.10, 0.21, 0.5, until death.

3.4.4. Microscopy

Confocal time-lapse recording were conducted using the LSM 5 Pascal laser-scanning confocal microscope (Zeiss, Germany) with an in-plane resolution of 512 by 512 pixels and an optical slice thickness of 896µm. Endogenous flavoprotein signal was excited using a multi-line argon laser with a 488nm wavelength. Emission was collected around a band of 505-570nm. The oxygen-sensitive phosphorescent beads were imaged using a helium-neon laser at an excitation wavelength of 543nm or a diode laser with an excitation wavelength of 405nm (the two lasers were used because of a change in the microscope system in our laboratory). Emission was collected with a 585nm long pass filter. During continuous time-lapse imaging the FiO_2 was varied as described above.

3.4.5. Electrocardiograms

Electrocardiograms (ECG) were recorded in a subset of animals (n = 53) using conventional electrophysiological equipment (Neurolog, Digitimer, UK). For this, a reference electrode (hypodermic needle) was placed in the right hind foot of the mouse and a ground and recording electrode (hypodermic needles) were inserted subcutaneously in the back and chest of the mouse respectively. The ECG record was displayed on a digital oscilloscope (Sigma 60, Nicolet Technologies, USA) and recorded manually at regular intervals.

3.4.6. Analysis

Images were processed as described in chapter 2 using Fiji/ImageJ Version 1.48v. Again time-lapse sequences were aligned and areas of interest selected. For flavoprotein analysis three regions of interest were selected immediately adjacent to arteries and three adjacent to veins followed by the calculation of the ratio of these averaged areas. A difference in the change in the ratio of periarterial over perivenous fluorescence in response to reductions in inspired oxygen was compared between groups. To assess the differential responsiveness of oxygen sensitive beads to changes in inspired oxygen between groups the average intensity of phosphorescent microbeads was determined for the last five cycles of each oxygen manipulation and compared across conditions. To assess absolute changes in cortical oxygenation the traces of the oxygen probe were averaged over the last minute of each oxygen manipulation and compared across conditions. Statistical significance was assessed using the IBM SPSS Statistics 22 package and a $p \leq 0.05$ was considered significant.

3.5. Results

3.5.1. Clinical signs

Systemic endotoxemia resulted in the appearance of clinical signs, including sedation, hunched appearance, piloerection, ocular discharge and hypothermia (Zolfaghari et al. 2013). Additionally weight loss was observed after LPS injection but not consistently after saline injection (Table, 3.5.1.1). Indeed, weight loss comparisons between saline and LPS injected mice were highly significant at all time-points (for 6 hours: $p \leq 0.01$, for 24 hours and 48 hours: $p \leq 0.001$, Table 3.5.1.1)

	Saline	LPS
6 hrs	- 0.35 (±0.08) gr	- 0.7 (±0.05) gr **
24 hrs	+ 0.42 (±0.36) gr	- 1.91 (±0.12) gr ***
48 hrs	+ 0.37 (±0.27) gr	- 2.01 (±0.44) gr ***

Table 3.5.1.1: **Change in weight of mice 6, 24 and 48 hrs after an injection of saline or LPS**. Mean ± SEM. Two-tailed t-test comparisons were made between LPS and saline injected groups. ** = $p \leq 0.01$, *** = $p \leq 0.001$.

Additionally core body temperature dropped significantly 6 hours (33.05˚C ± 0.4; $p \leq 0.001$) and 24 hours (32.98˚C ± 0.65; $p \leq 0.001$) but not 48 hours (35.57 ± 0.6; $p \geq 0.05$) after LPS injection when compared with saline controls (35.9˚C ± 0.14).

There was a significant positive correlation between weight loss and temperature 24 hours after LPS injection ($r=0.798$, $p \leq 0.001$ Spearman's rank correlation coefficient) such that animals with a higher core body temperature 24 hours after LPS injection had lost more weight (Figure 3.5.1.1). This was not the case 6 hours after LPS injection ($r=0.000$, $p \geq 0.05$).

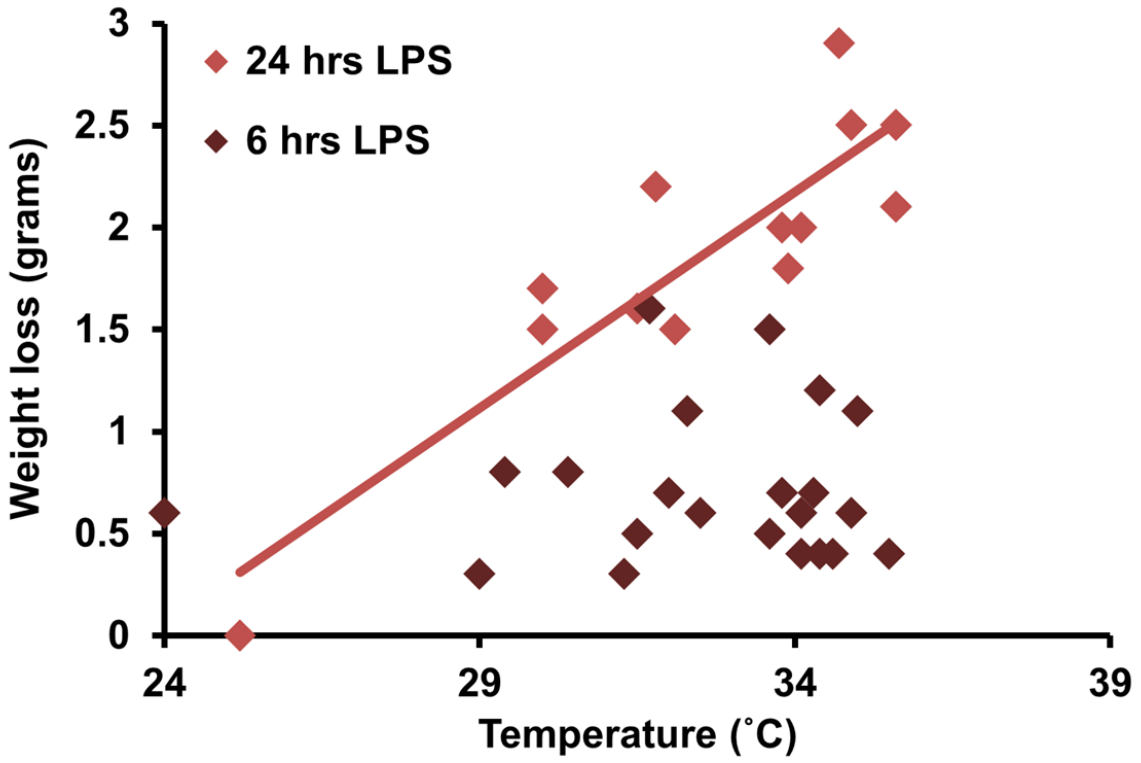

Figure 3.5.1.1: **Correlation between weight loss and core body temperature 6 and 24 hrs after LPS injection**.

Mortality was increased in endotoxic mice compared to saline-injected controls but hypothermia (both spontaneous and induced) significantly enhanced resilience to increased levels of hypoxaemia 6 hours after endotoxaemia (Figure 3.5.1.2 a): During progressive hypoxaemia, LPS-injected mice died at higher FiO_2 values compared to saline-injected controls. However, hypothermia (both *spontaneous* and *induced*) improved tolerance to hypoxaemia in endotoxic mice 6 hours after LPS (Figure 3.5.1.2 a).

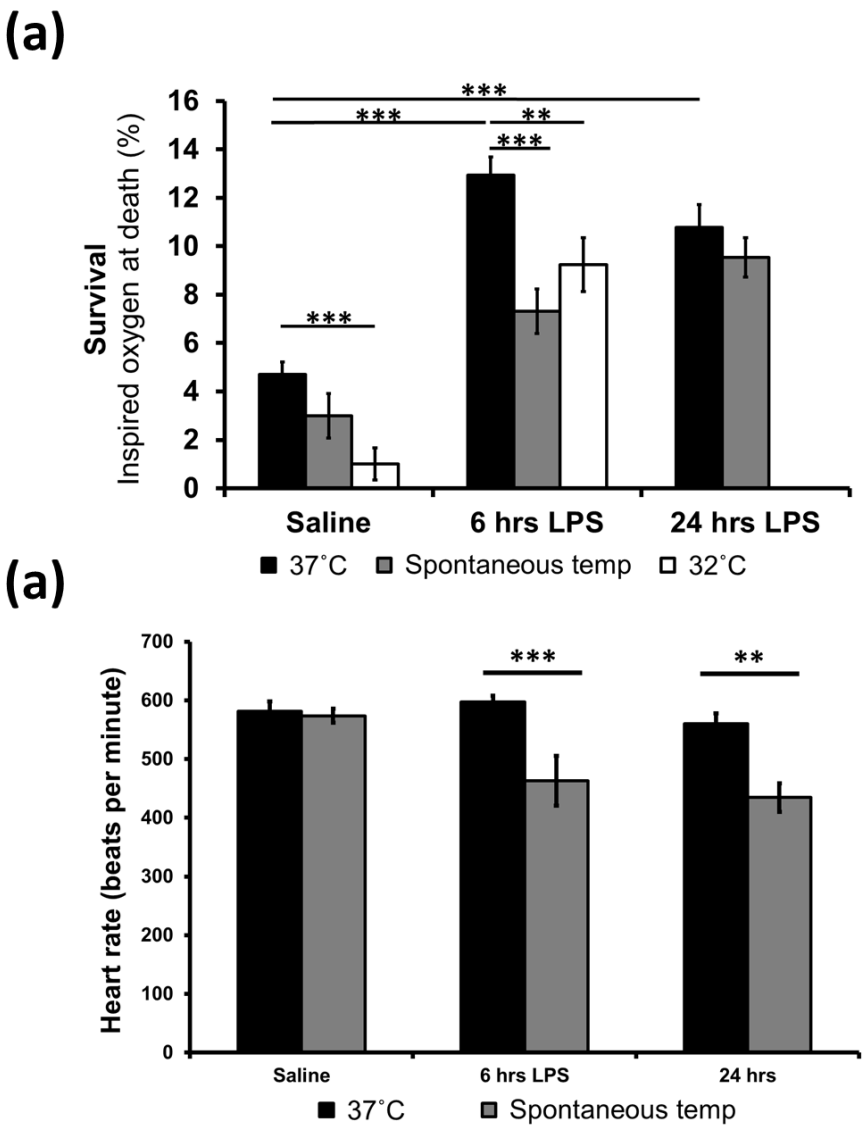

Figure 3.5.1.2: **Mortality and heart rate during systemic inflammation.**

(a) Survival of mice subjected to systemic inflammation/saline and hypoxaemia. **(b)** Changes in heart rate between groups. Data displayed as mean ± SEM. ** = $p \leq 0.01$; *** = $p \leq 0.001$.

There was no measurable difference in the heart rate between LPS and saline-injected mice. However, spontaneous hypothermia reduced the heart rate significantly, at both 6 and 24 hours after LPS injection (Figure 3.5.1.2 b).

3.5.2. Systemic inflammation affects flavoprotein signal in the cerebral cortex during hypoxaemia

In chapter 2 and a previous publication (Chisholm et al. 2015) we reported that healthy animals subjected to hypoxaemia showed a characteristic reduction in the cortical flavoprotein fluorescence revealing areas of vulnerability in tissues distant from arteries and close to veins, with a 'halo' of preserved flavoprotein fluorescence around arteries (*'arterial halo' pattern*). We show this here again (Figure 3.5.2.1). In saline-injected mice this *'arterial halo' pattern* appeared at the same FiO_2, regardless of the time from injection (data not shown). Therefore, the data collected from mice injected with saline were pooled. All mice exposed to room air showed a relatively even flavoprotein signal covering the cortex uniformly (Figure 3.5.2.1). Also an increase in inspired oxygen to 100% had no influence on the flavoprotein signal on animals in any groups (Figure 3.5.2.1), as discussed in the previous chapter. Also saline-injected animals exposed to 15% inspired oxygen did not show any variation in their cortical flavoprotein signal, in agreement with our previous data (chapter 2). If however, the amount of inspired oxygen was decreased further to 10%, a subset of mice (11 of 21) showed a characteristic change in the cortical flavoprotein fluorescence exemplified by the *'arterial halo' pattern*. If the FiO_2 was reduced further to 5% all but two saline injected animals showed this characteristic change in the flavoprotein signal. If however, the mice were injected with LPS 6 hours prior to the imaging session the flavoprotein signal decreased already at 15% inspired oxygen, notably a concentration at which the flavoprotein fluorescence does not change in healthy, saline-injected controls (Figure 3.5.2.1). Most animals (65%) injected with LPS 6 hours previously also did not survive 15% oxygen (Figure 3.5.1.2 a). By 24 hours after LPS injection, mice showed an attenuated sensitivity of the flavoprotein autofluorescence to reductions in inspired oxygen. At 24 hours after LPS injection 77% (10/13) of mice showed a change in the signal between 15% inspired oxygen and 10% inspired oxygen (Figure 3.5.2.1) which

was concomitant with improved survival when compared with the 6 hours post LPS injection group (Figure 3.5.1.2 a). At 48 hours after LPS injection clinical signs, survival and flavoprotein signal sensitivity to changes in inspired oxygen recovered back to saline control values (Figure 3.5.1.2 a and 3.5.2.1).

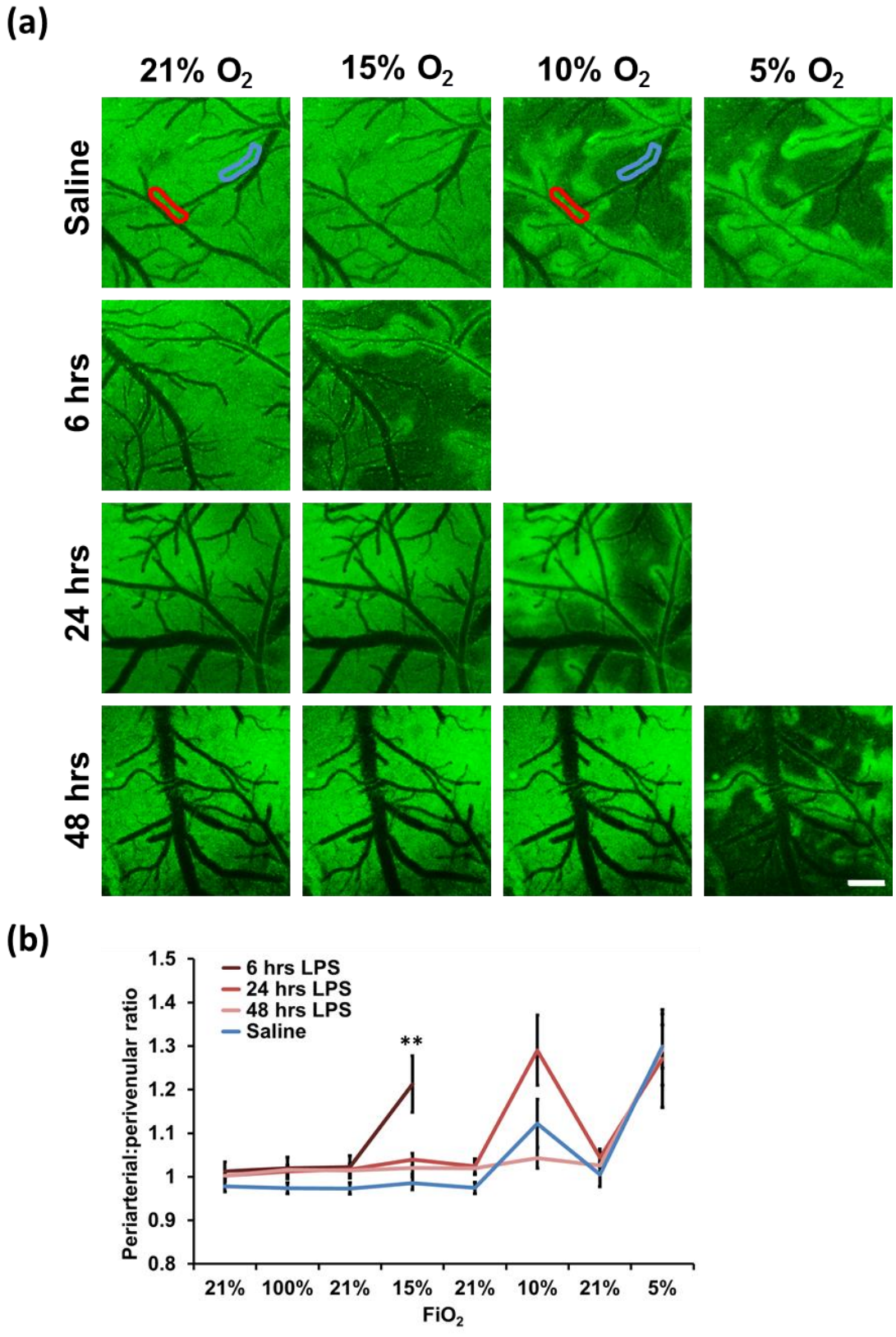
(a)
21% O2
15% O2
10% O2
5% O2
Saline
6 hrs
24 hrs
48 hrs
(b)
6 hrs LPS
24 hrs LPS
48 hrs LPS
Saline
**
Periarterial:perivenular ratio
1.5
1.4
1.3
1.2
1.1
1
0.9
0.8
21%
100%
21%
15%
21%
10%
21%
5%
FiO2

Figure 3.5.2.1: **The sensitivity of flavoprotein signal to changes in inspired oxygen is affected by systemic endotoxemia**.
(a) Flavoprotein signal changes in endotoxic and control mice with changes in inspired oxygen. In blue = representative selection of perivenular tissue, in red = representative selection of periarterial tissue. Scale bar = 200µm. (**b)** Quantification of the change in endogenous flavoprotein fluorescence around veins relative to arteries. An increase in the ratio of periarterial over perivenular fluorescence indicates the appearance of the *'arterial halo' pattern*. Data are displayed as means ± SEM. ** = p (Saline vs 6 hrs LPS) ≤ 0.01. It should be noted that where images or data are missing in the visual representation, a high mortality rate would have made these unrepresentative and as a result they were removed from the display but not from the analysis.

As mentioned in the previous chapter, the reduction in the flavoprotein fluorescence with hypoxaemia was reversible in animals that were allowed to recover from hypoxaemia during room air exposure. In these cases the 'halo' of preserved flavoprotein fluorescence expanded until it covered the cortex again, and the ratio returned back to ~1 (Figure 3.5.2.1 b).

3.5.3. Oxygenation of the cortex

Oxygenation of the cortex was assessed using an oxygen microsensor inserted into the cortex at a depth of 600µm. However, given the need for a separate cohort of animals when the oxygen microsensor was used, changes in oxygenation were also assessed using oxygen-sensitive microbeads (introduced in chapter 2) in the imaging cohort of animals. This allowed us to confirm changes in cortical oxygen with changes in FiO_2 while simultaneously assessing flavoprotein fluorescence.

The level of oxygen in the cortices of saline-injected control mice (46.5 ± 3.0 mmHg) was significantly higher compared with mice injected with LPS 6 hours (29.3 ± 5.6 mmHg; $p \leq 0.01$, single tailed t-test) and 24 hours (34.3 ± 6.1 mmHg; $p \leq 0.05$) prior, as assessed by oxygen probe

measurements at an FiO_2 of 0.21. This pattern continued also at lower concentrations of inspired oxygen although the differences did not always reach significance (Figure 3.5.3.1). By 48 hours the oxygen levels in cortices of LPS-injected animals had recovered to control levels (46.9 ± 5.9 mmHg, Figure 3.5.3.1).

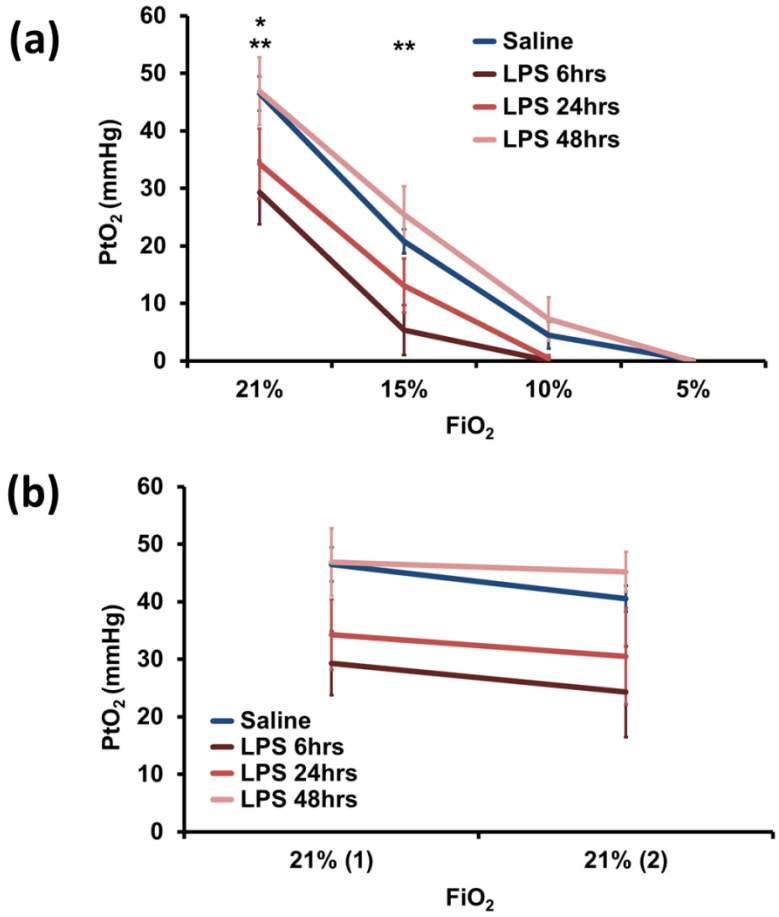

Figure 3.5.3.1: **Cortical oxygen during systemic endotoxemia**

(a) Oxygen concentration of the cortex during reductions in FiO_2. With a decrease in the amount of inspired oxygen the cortical oxygenation decreased in all groups. However, the overall cortical oxygenation was lower in endotoxic animals compared to saline injected controls at 6 and 24 hrs. This reduced cortical oxygenation in endotoxic animals recovered by 48hrs. **(b)** Change in cortical oxygen concentration between two room air conditions. The first room air exposure provided the initial baseline condition, before any change in inspired oxygen. The second room air exposure separated the 15% and 10% inspired oxygen conditions. This reveals that most

animals did not recover fully back to the baseline room air condition after a 5 minute exposure to hypoxaemia. However, the recovery rate is non-significantly different between groups, suggesting that the recovery from hypoxaemia to room air was achieved equally in all conditions (endotoxic and control). Data displayed as mean ± SEM. ** = p (saline vs 6 hrs LPS) ≤ 0.01, * = p (saline vs 24 hrs LPS) ≤ 0.05, one tailed t-test.

Although none of the groups recovered fully back to the original room air values following the initial reduction in inspired oxygen to 15%, the decrease in cortical oxygenation in the two room air conditions were not significantly different between groups (Figure 3.5.3.1 b, one-way ANOVA, $p \geq 0.05$ on the change in oxygenation between the two room air conditions across groups), suggesting that the recovery rate for all groups of animals was comparable.

The change in cortical oxygenation with changes in FiO_2 was also confirmed using oxygen-sensitive phosphorescent microbeads (Figure 3.5.3.2).

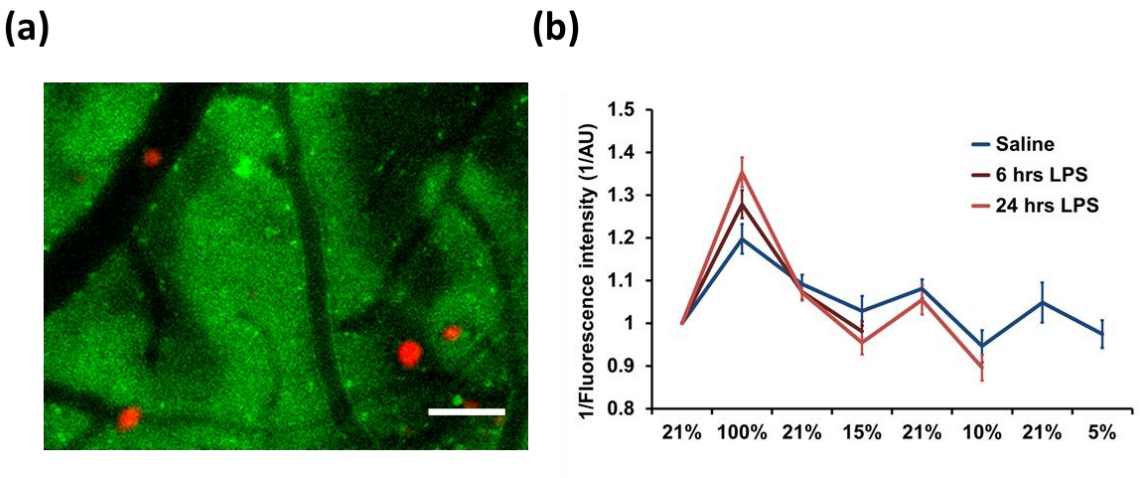

Figure 3.5.3.2: **Oxygen-sensitive beads in systemic inflammation**
(a) Example distribution of oxygen-sensitive microbeads on the cortical surface. Scale bar = 100µm **(b)** Relative changes in cortical oxygen (shown as the reciprocal of the fluorescence intensity of the sensor bead) with changes in FiO_2. The data are normalized to the initial room air condition. Data presented as mean ± SEM.

It should be noted that the fluorescence intensity of individual beads was influenced by their size and the focal plane. As a result absolute values were meaningless and instead the beads were normalized to the initial room air condition and only relative changes in the fluorescence intensity with changes in inspired oxygen are considered. Additionally, as a decrease in oxygenation resulted in an increase in fluorescence intensity of the oxygen-sensitive beads, the reciprocal of the fluorescence intensity is shown here, to allow an easier graphical representation and more accessible comparison with the data from the oxygen probe. Although endotoxic mice, particularly 24 hours after endotoxemia, seemed more reactive to changes in oxygen, particularly hyperoxia, this difference was not statistically significant.

3.5.4. Spontaneous hypothermia attenuates increased sensitivity of mice with systemic inflammation

In order to assess the effect of spontaneous temperature changes (known to occur in septic mice (Zolfaghari et al. 2013)) on the sensitivity of the flavoprotein fluorescence to hypoxaemia we conducted a study in which we kept all mice at their spontaneous temperature measured immediately after anaesthesia. The average core body temperature of saline injected mice was 35.9˚C (± 0.14). Accordingly, this group (saline-injected, spontaneous temperature) showed a very similar *'arterial halo' pattern* response to differences in FiO_2 as saline-injected mice kept at 37˚C. Instead mice injected with LPS 6 hours prior to the imaging session showed spontaneous hypothermia of 33.05˚C (± 0.4) shortly after anaesthesia. If this spontaneous hypothermia was maintained during imaging, the cortical mitochondria of these mice were protected from hypoxaemia relative to their normothermic, LPS injected counterparts, which were forcibly kept at 37˚C during the preparation and imaging session (Figure 3.5.4.1). Indeed, the *'arterial-halo pattern'* response to changes in FiO_2 in this group of animals (6 hours LPS imaged at their

spontaneous temperature) is similar to that seen in saline-injected controls (Figure 3.5.4.1). Also the resilience to increasing levels of hypoxaemia (hereafter termed "survival") of endotoxic mice after 6 hours was improved when they were kept under their spontaneous hypothermia and compared with normothermic counterparts, though mortality was still higher than in saline-injected controls (Figure 3.5.1.2 a).

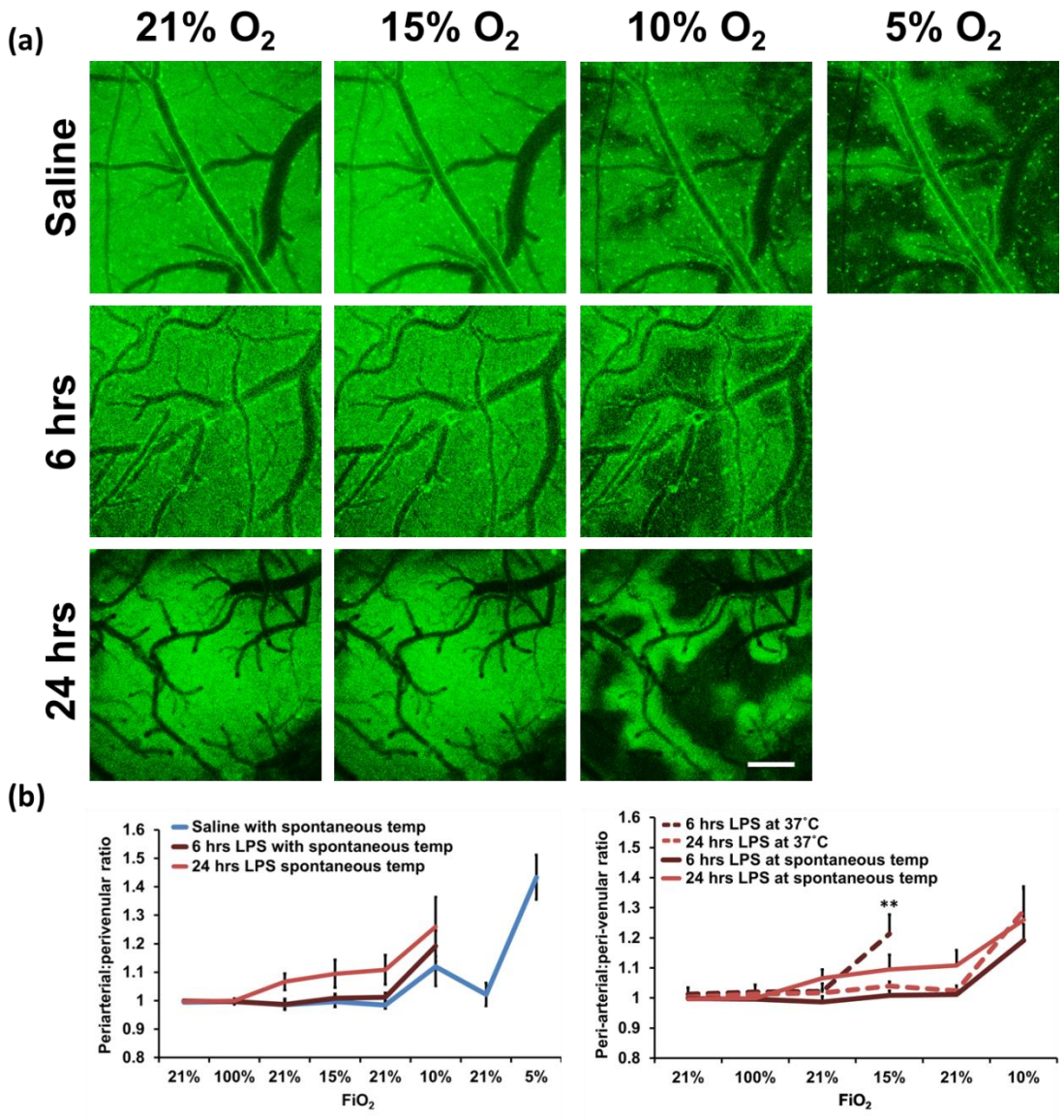

Figure 3.5.4.1: **Spontaneous hypothermia protects cortical mitochondria from hypoxaemia**.

(a) Changes in cortical flavoprotein signal during changes in FiO_2 in saline and LPS-injected animals kept at their spontaneous temperature. Scale bar = 200µm **(b)** Quantification of the ratio of periarterial over perivenular fluorescence in saline- and LPS-injected animals kept at their spontaneous temperature and at 37˚C. Data displayed as mean ± SEM. ** = p (6 hrs LPS 37˚C vs spontaneous temp) ≤ 0.01.

At 24 hours, LPS-injected mice also had an average hypothermic temperature of 32.98˚C ± 0.65. If they were kept at their spontaneous temperature during imaging they were not protected from hypoxaemia in terms of survival or cortical mitochondrial function (Figure 3.5.1.2 a and 3.5.4.1). However, it is noteworthy that fewer LPS-injected animals survived surgery 24 hours after LPS when kept at forced normothermia (37˚C) compared with animals left at their spontaneous hypothermic temperature. This group of animals was not included as no imaging data could be collected.

3.5.5. Induced hypothermia protects against hypoxaemia

As we observed a protective effect of spontaneous hypothermia in LPS-injected animals (both in terms of survival and *'arterial-halo' pattern* onset in response to reductions in FiO_2) at 6 hours, we sought to determine the effects of hypothermia on healthy, saline-injected control mice. To achieve this, both healthy and LPS-injected mice (6 hours post injection) were kept at an induced hypothermia of 32˚C during surgery and imaging. This hypothermia was protective for saline- and LPS-injected mice. Compared with their normothermic counterparts (37˚C), saline-injected mice, kept at 32˚C, showed an *'arterial-halo' pattern* response at lower FiO_2 (5%) and exhibited improved survival (Figure 3.5.5.1 and 3.5.1.2 a).

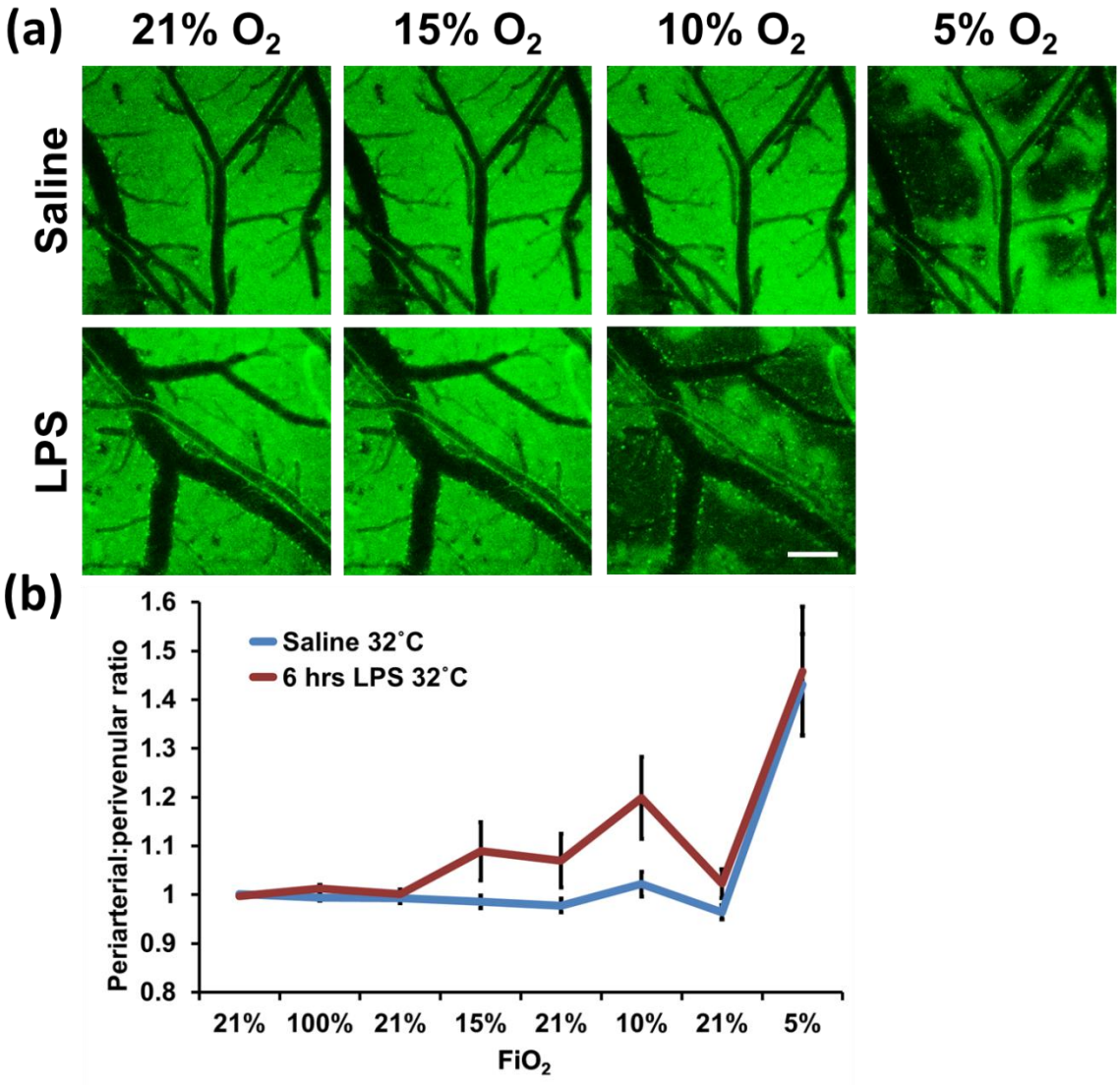

Figure 3.5.5.1: **Induced hypothermia protects cortical mitochondria from hypoxaemia.** **(a)** Changes in cortical flavoprotein signal during changes in FiO_2 in saline and LPS-injected animals 6 hours after endotoxemia kept at 32˚C. Scale bar = 200µm. **(b)** Quantification of the ratio of periarterial over perivenular fluorescence. Data displayed as mean ± SEM.

Also endotoxic mice were protected from hypoxaemia when hypothermia was induced (32˚C), both in terms of survival and *'arterial-halo' pattern* response to reductions in FiO_2, compared with their normothermic controls kept at 37˚C (Figure 3.5.1.2 a and 3.5.5.1). However

the protection afforded to LPS-injected mice (6 hours) by induced hypothermia (32˚C) was less than that provided to mice kept at their spontaneous temperature.

3.6. Discussion

Much evidence implicates bioenergetic failure in sepsis and multiple organ dysfunction, e.g. (Balestra et al. 2009). We therefore investigated whether hypoxaemia, which provides an additional energetic challenge, promoted mitochondrial dysfunction in the cortices of mice subjected to mild systemic endotoxemia. As shown in the previous chapter and a publication, we found that mitochondrial dysfunction, assessed by a selective loss of flavoprotein autofluorescence (Chisholm et al. 2015), is pronounced during hypoxaemia and reveals areas of cortical vulnerability between vessels and along veins, with protected 'halos' of preserved flavoprotein fluorescence close to arteries (Chisholm et al. 2015; Kasischke et al. 2011). Additionally we now report that such areas of vulnerability are more readily revealed at higher concentrations of inspired oxygen in endotoxic mice when compared with healthy, saline-injected counterparts. Such findings suggest an increased vulnerability towards hypoxaemia in the cortices of mildly endotoxic animals. However, due to the lack of baseline assessments combined with the clear presence of a clinical presentation even during room air conditions we are not able to rule out that this cortical vulnerability may be an epiphenomenon as far as the symptoms of the model are concerned. The increased vulnerability, with this non-lethal model of systemic inflammation, was only temporary with a peak observed at 6 hours and a complete recovery by 48 hours post LPS injection.

3.6.1. Vascular dysfunction in sepsis

The observation that mitochondrial vulnerability in the endotoxic brain conforms to the vascular anatomy, together with numerous previous reports of microvascular disturbances in sepsis and systemic inflammation (Bowton et al. 1989; Lam et al. 1994; Maekawa et al. 1991; Neviere et

al. 1996; Vincent and De Backer 2005) strongly implicate compromised oxygen availability in our findings. Therefore, oxygen probe measurements were taken of the cortex of a separate cohort of animals. These recordings revealed lower levels of oxygen in the cortices of sick animals compared to healthy control mice. Endotoxic animals had the lowest cortical oxygen level at 6 hours, showed an increase at 24 hours and a complete recovery at 48 hours after LPS injection. The change in cortical oxygenation with systemic inflammation therefore coincided with the increased cortical vulnerability of LPS injected mice towards hypoxaemia.

These findings are in line with evidence suggesting microvascular dysfunction as a leading cause of inadequate perfusion and eventually multiple organ dysfunction (Bateman et al. 2001; Bowton et al. 1989; Diaz et al. 1998; Drazenovic et al. 1992; Ellis et al. 2002; Gundersen et al. 1998; Hinshaw 1996; Lam et al. 1994; Levi et al. 1997; Maekawa et al. 1991; Neviere et al. 1996; Piper et al. 1996; Schmidt et al. 1997; Vincent and De Backer 2005). Numerous mechanisms can lead to inflammation-related changes in perfusion. For example, alterations in endothelial cells themselves, such as an increase in adhesion molecule expression or damaged glycocalyx, can lead to disordered flow and poor perfusion during sepsis (Bateman and Walley 2005; Cabrales et al. 2007; Hofmann-Kiefer et al. 2009; Nieuwdorp et al. 2009). Additionally, heterogeneity of the microvasculature between and within organs has been repeatedly implicated (Bateman et al. 2003; Bateman and Walley 2005; De Backer et al. 2013; De Backer et al. 2014; Ellis et al. 2002; Humer et al. 1996; Ince and Sinaasappel 1999; Lam et al. 1994; Piper et al. 1996). Lam et al suggested that increased heterogeneity in microvascular perfusion, observed in a normotensive rodent model of sepsis, prevented the microcirculation in the muscle from adapting to increases in oxygen demand after maximal twitch contraction (Lam et al. 1994). Similarly, it has been suggested that conducted vasoconstriction is affected by sepsis which is predicted to have a significant impact on blood flow control (Lidington et al. 2004; Tyml et al. 2001). Indeed, the inability to control blood flow and tissue oxygenation in sepsis, in response to changes in demand, has been well supported (Astiz et

al. 1991; Hartl et al. 1988; Neviere et al. 1996; Sibbald et al. 1991) and is in line with our current findings.

On the other hand, proponents of the cytopathic hypoxia hypothesis of sepsis suggest that organ dysfunction originates not from inadequate oxygen provision but rather from mitochondrial dysfunction preventing the consumption of readily available oxygen (Fink 1997; Fink 2001; Fink 2002a; Fink 2002b; Schwartz et al. 1999). This hypothesis originated in part from the inefficiency of treatments aiming to enhance oxygen delivery (Gattinoni et al. 1995; Hayes et al. 1994) and from findings of metabolic disturbances even in the presence of an apparently sufficient oxygen supply (Astiz et al. 1988; Boekstegers et al. 1991; Boekstegers et al. 1994; Crouser et al. 2002a; Crouser 2004; Rosser et al. 1995; Vandermeer et al. 1995). These data do not however take into account that mean arterial blood pressure, whole body oxygenation and cardiac output alone cannot determine microvascular perfusion (Bateman and Walley 2005; LeDoux et al. 2000; Neviere et al. 1996). Instead microvascular heterogeneity and shunting can lead to hypoxic patches in proximity to well-oxygenated areas (Bateman et al. 2003; Bateman and Walley 2005; De Backer et al. 2013; De Backer et al. 2014; Lam et al. 1994) resulting in an overall high level of oxygenation at the systemic and even organ level with small scale abnormalities causing significant tissue dysoxia and mitochondrial dysfunction. Indeed therapies aimed at improved microvascular function have shown promise in the treatment of sepsis-related dysfunction, including treatment with nitroglycerine (Spronk et al. 2002) or nitric oxide donors (Siegemund et al. 2000), together with appropriately administered fluid resuscitation.

Currently our method does not allow us to look at baseline measurement of mitochondrial function as preparation quality, laser intensity and imaging depth are too variable to allow the detection of subtle changes in mitochondrial redox potential. However, our data suggest that perfusion abnormalities result in increased mitochondrial vulnerability in the cortex of endotoxic animals as systemic inflammation resulted in less well-oxygenated cortices, and the pattern of

mitochondrial vulnerability is spatially related to the cerebral vasculature. These results are in line with suggestions of an initially compromised vasculature followed by mitochondrial vulnerability and dysfunction due to inadequate oxygenation and cellular dysoxia (Spronk et al. 2005). This however, does not exclude additional primary mitochondrial damage due to inflammatory mediators.

3.6.2. Hypothermia as a protection from an inflammation-induced energetic challenge

Our results therefore suggest that even mild systemic inflammation can lead to a supply demand imbalance of cortical oxygen that can be revealed during mild hypoxaemia. We therefore hypothesised that interventions which reduce metabolism and thereby energy demand (e.g. hypothermia (Erecinska et al. 2003; Pernerstorfer et al. 1995)) could offer protection to the cortices of endotoxic mice and prevent energetic failure during additional energetic challenges (e.g. hypoxaemia). In line with this we found that mild hypothermia, both spontaneous and induced, protected animals from hypoxaemia, both in terms of cortical flavoprotein fluorescence and survival. Mice that were injected with LPS 6 hours previously and were kept at their spontaneous hypothermic temperatures, showed attenuated vulnerability to hypoxaemia (both in terms of survival and *'arterial-halo' pattern onset*) when compared to LPS-injected animals kept at forced normothermia (37˚C), indeed almost to the same level of resilience as shown by saline-injected control animals. In contrast animals injected with LPS 24 hours prior to flavoprotein imaging were not protected from hypothermia. However, this could be attributable to the higher pre-imaging mortality rate in the 24 hours normothermic, LPS injected group, as a number of these animals could not be assessed. The experimental procedure required continuous anaesthesia for around 1 hour for the surgery alone, in addition to the imaging duration. Some of the sicker mice, especially

at 24 hours post LPS injection, did not survive the surgical anaesthetic depth and were therefore not imaged for cortical vulnerability.

Given the protection afforded by hypothermia to mice injected with LPS at 6 hours we further investigated the effect of induced hypothermia (32˚C) on healthy, saline-injected mice. Hypothermia was found to be protective (both in terms of preserved flavoprotein fluorescence and survival) during hypoxaemia also in healthy mice injected with saline. This further supports the protective role of hypothermia during an energetic imbalance and suggests that situations in which oxygenation is limited, might benefit from hypothermia or other energy conserving therapies. Induced hypothermia (32˚C) also offered protection to animals injected with LPS 6 hours prior to assessment. However, this protection was not as effective as spontaneous hypothermia either in terms of survival or cortical flavoprotein fluorescence. This result might be due to the variability of the disease severity and associated temperatures. In some endotoxic mice the core body temperature dropped below 32˚C at 6 hours post injection and these mice were therefore exposed to an increase in temperature to 32˚C. Notably lower core body temperatures were also associated with more severe clinical signs. These results suggest that the titration of hypothermia treatment is an important consideration to ensure adequate protection while reducing any putative negative side effects.

The protective effect of hypothermia was further evident in the preservation of body weight associated with more severe hypothermia 24 hours after LPS injection. Animals that were more hypothermic showed an attenuated loss in body weight compared with warmer animals of the same group, despite severe hypothermia usually being accompanied by more severe clinical signs. These data suggest that early onset hypothermia in mice subjected to systemic inflammation may be an attempt at energy preservation and protection in the face of a potential energetic imbalance. Therefore, forced recovery to normothermia might be detrimental for these animals and could lead to excessive energy consumption and an inability to sustain additional energetic insults. A reduction

in core body temperature and energy consumption, combined with preservation of body weight and slowed heart rate, as reported here, are hallmarks of hibernation which certain strains of mice can engage in for the conservation of resources during cold months (Protti and Singer 2006; Singer 2002). Such findings further support the notion of hypothermia as a possible protective response of the energetically challenged organism during endotoxemia.

3.7. Limitation and further research

As mentioned in the introduction, endotoxemia, initiated by a single LPS injection, results in a purely inflammatory and not pathogen-driven disease. This simplified model allowed us to focus on the inflammatory aspect of systemic inflammation and sepsis while it does not take into consideration the complexities of sepsis which can be driven by a various bacteria, viruses or fungi. Such factors have strong implications for the applicability of our research into the treatment of sepsis in humans. The dual nature of the immune system makes extrapolation to sepsis difficult as the pro-inflammatory mediators may be essential in combatting the initial infection and hypothermia has been associated with immunosuppression (Hildebrand et al. 2004). Additionally it will remain difficult to extrapolate any experimental findings onto a human septic population not only because of the varied nature of the pathogens involved in sepsis but also because of the marked inter-species variation in the inflammatory response (Bone et al. 1997) as well as the heterogeneity in the human patient population exhibiting a number of different underlying conditions (Bone 1991).

Additionally it is imperative to optimise the timing of the administration of any treatment, especially treatments that can suppress the host immune response, such as hypothermia (Hildebrand et al. 2004). Therefore, it is important to consider the different stages that characterise sepsis, including an early hyperdynamic, pro-inflammatory phase in which the immune system is both combatting the infection and possibly damaging the host, and a subsequent hypodynamic and anti-inflammatory phase (Bone et al. 1997). The latter phase is considered a compensatory response to the initial pro-inflammatory phase and can lead to suppression of the immune response sufficient to prevent adequate pathogen elimination and can even lead to immune deficiency (Bone et al. 1997). Early, titrated hypothermia together with appropriate anti-bacterial/fungal/viral treatment might help in preventing an oxygen supply/demand imbalance, while attenuating host damage by the immune system and preventing further compensatory anti-inflammatory immune derailment.

We note that neither fluid resuscitation was given, nor blood pressure measurements taken, so an underlying hypovolaemia in the endotoxic mice may have exacerbated the impact of the hypoxaemic insult. Additionally, no neuropathological studies were conducted on the animals imaged as the tissue could not be processed following surgery and imaging. Future studies could include a histochemical assessment of a separate cohort of animals for the investigation of neuropathological correlates.

Finally, we have not addressed whether the supply/demand imbalance in oxygenation in our endotoxic model is related to an inadequate supply, for example through damaged or heterogeneous cerebral vasculature (Bateman and Walley 2005; Bowton et al. 1989; De Backer et al. 2013; De Backer et al. 2014; Ellis et al. 2002; Humer et al. 1996; Ince and Sinaasappel 1999; Lam et al. 1994; Maekawa et al. 1991; Neviere et al. 1996; Piper et al. 1996; Schmidt et al. 1997; Vincent and De Backer 2005) or whether it is related to an increase in demand for oxygen, for example through increased consumption by mitochondria (d'Avila et al. 2008; Dahn et al. 1995; Dawson et al. 1988; Fredriksson et al. 2009; Poderoso et al. 1994; Sjovall et al. 2010; Tanaka et al. 1982). This could be investigated by a closer analysis of the cerebral vasculature in our model, including blood flow assessment (e.g. through laser Doppler measures) and/or vessel perfusion (e.g. assessment of number of perfused vessels through injection of fluorescent compounds). Additionally mitochondrial function in this model should be investigated in more detail, through isolation of mitochondria from the brains of endotoxic mice followed by *in vitro* assessment of their rate of oxygen consumption as well as further *in vivo* investigation of mitochondrial function that could provide baseline measurements and avoid false negatives related to the removal of the mitochondria from their pathogenic environment.

3.8. Conclusion

In summary, we observed that mild systemic endotoxemia can lead to increased mortality and increased sensitivity of cortical mitochondria (as assessed by flavoprotein fluorescence) to additional energetic insult (hypoxaemia). This increased sensitivity to hypoxaemia was accompanied by a decrease in cortical oxygenation. Given this imbalance in oxygen supply and/or demand, observed in our endotoxic model, a reduction in metabolic rate through, for example hypothermia, could attenuate increased mortality and the increased vulnerability of cortical mitochondria associated with mild systemic inflammation. These findings suggest that energy conserving therapies, like hypothermia, can be beneficial for patients suffering from an oxygen supply/demand imbalance as has been reported in sepsis (e.g. reviewed by (Brealey and Singer 2003)). Such treatment may protect this group of patients from increased vulnerability towards other insults that would leave healthy individuals unaffected. However, further research is needed to assess the applicability of these findings to a diverse disease in a diverse human population and to optimise administration and timing of energy conserving therapies.

CHAPTER FOUR

4. Retinal inflammation

4.1. Introduction

Given the association between systemic inflammation and cortical hypoxia, reported in chapter 3, together with published reports linking inflammation and hypoxia (Davies et al. 2013; Eltzschig and Carmeliet 2011; Karhausen et al. 2005) we sought to investigate the relationship between inflammation and hypoxia in other organs and during other inflammatory conditions. Therefore, we aimed to assess different models of retinal inflammation in terms of their reliability, reproducibility and applicability for the assessment of retinal flavoprotein fluorescence longitudinally.

4.1.1. Why the eye

The retina and the optic nerve are developmental outgrowths of the brain, originating from the neural tube (Silver and Robb 1979). Therefore, the retina and brain share the same tissue developmentally, making the retina part of the central nervous system (CNS). Indeed the retina has been used repeatedly as a model to characterize and exemplify phenomena implicated in the rest of the CNS (Ames and Nesbett 1981; Cordeiro et al. 2004; Dowling and Boycott 1966; Guo et al. 2010; Mcewen and Grafstein 1968). The eyes have therefore been considered as a "window on the brain" (Cordeiro et al. 2004).

The retina is a highly organized structure with different cell types grouped into different layers fed by a relatively simple vascular bed (Figure 4.1.1.1 a and b as well as (Yu and Cringle

2001)). Also the mitochondrial distribution within the retina is relatively well compartmentalized (Figure 4.1.1.1 c), with the inner and outer plexiform layer, the ganglion cell layer and the inner segment containing a high density of mitochondria. Given the limited nature of the retinal vasculature (which is constrained due to the need for clear optics (Yu and Cringle 2001)) and highly organised mitochondrial distribution, the retina provides a heterogeneous but organised organ in terms of oxygen consumption and provision. Indeed, parts of the retina (including the highly metabolically active inner segment of the photoreceptors (Yu and Cringle 2001)) are located in avascular regions (Figure 4.1.1.1 b). Additionally, it should be noted that the vascular support for the outer retina comes primarily from the choriocapillaris. Although this vascular bed is well oxygenated it lacks an adequate response to changes in the metabolic need of the photoreceptors which may prevent adequate vascular responses during changes in metabolic demand. The combination of a metabolically highly active tissue (Ames 1992; Anderson 1968; Toernquist and Alm 1979; Wangsa-Wirawan and Linsenmeier 2003) and a poor vascular supply (Yu and Cringle 2001; Zein et al. 2004) and resulting spatial heterogeneity in tissue oxygenation (Wangsa-Wirawan and Linsenmeier 2003) make this model system an excellent one in which to study the relationship between inflammation, oxygenation and functional deficits.

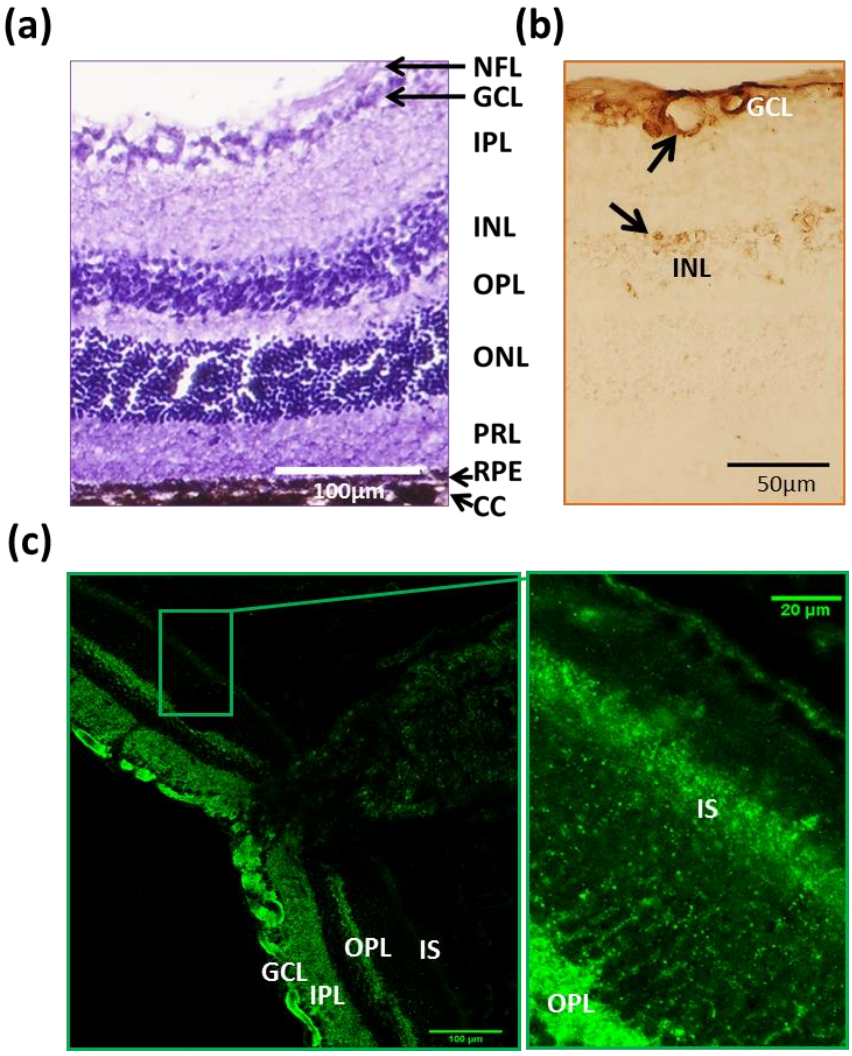

Figure 4.1.1.1: **Retinal structure, vasculature and mitochondrial distribution**

(a) C57bl/6 mouse retina stained with haematoxylin and eosin to exemplify the retinal structure. **(b)** C57bl/6 mouse retina labelled for laminin (component of the basement membrane which associates with endothelial cells (Timpl et al. 1979)). Arrows pointing towards retinal vessels. **(c)** C57bl/6 mouse retina labelled with Voltage-dependent anion-selective channel 1 (VDAC 1), a mitochondrial marker. NFL, nerve fibre layer; GCL, ganglion cell layer; IPL, inner plexiform layer; INL, inner nuclear layer; OPL, outer plexiform layer; ONL, outer nuclear layer; PRL, photoreceptor layer; RPE, Retinal Pigment Epithelium; CC, choriocapillaris; IS, inner segment (of photoreceptors); INL, inner nuclear layer.

The retina lacks myelin (Figure 4.1.1.2), and it therefore can provide an interesting model in which to distinguish the effects of inflammation from those arising from demyelination. Additionally, an absence of myelin provides clear optics through which to image the retina *in vivo*, using confocal microscopy, at greater depths.

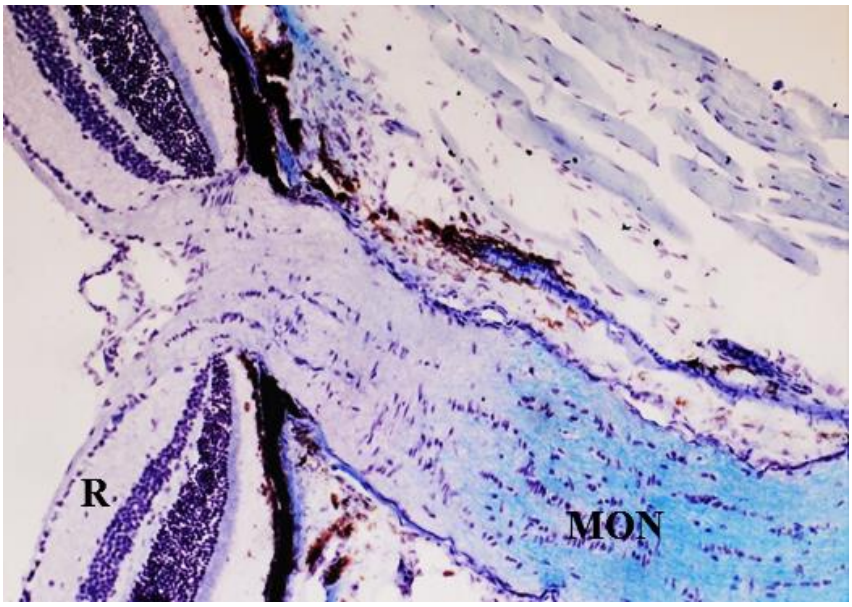

Figure 4.1.1.2: **The mouse retina and optic nerve stained with haematoxylin and luxol fast blue.**
Luxol fast blue straining reveals the lack of myelin in the retina**.** The myelinated part of the optic nerve is stained in blue. Abbreviations: R = retina, MON = myelinated optic nerve.

4.1.2. Endotoxin induced uveitis (EIU)

Uveitis is a generalised inflammation of the highly vascular and pigmented uvea which is composed of the iris, the ciliary body and the choroid, but with frequent spreading of the inflammation to the retina and vitreous (Rothova et al. 1992). It is considered to be the most common form of ocular inflammation with an incidence of 17-52 cases per 100,000 people (Wakefield and Chang 2005). Uveitis is associated with a number of diseases including MS (Zein

et al. 2004), juvenile rheumatoid arthritis (Wolf et al. 1987), inflammatory bowel disease (Orchard et al. 2002), Reiter's syndrome (Kiss et al. 2003) and others (Rothova et al. 1992).

As mentioned before, LPS are components of the cell walls of Gram-negative bacteria. Upon injection of LPS, this endotoxin binds to receptors on for example microglial cells, such as TLR4 (Chow et al. 1999; Henneke and Golenbock 2002), initiating an inflammatory cascade which includes the recruitment of further immune cells, secretion of cytokines and formation of NO. When injected systemically (intravenous, intraperitoneal or foot pad administration) or locally (into the vitreous of the eye) LPS can elicit strong, dose-dependent inflammatory reactions in the eye, termed endotoxin-induced uveitis (EIU) (Devos et al. 1994; Forrester et al. 1980; Hoekzema et al. 1992; Rosenbaum et al. 1980). EIU involves breakdown of the blood retinal barrier (Koizumi et al. 2003), infiltration of inflammatory cells (Hayashi et al. 1996), and a reduction in the A and B waves of the electroretinogram (ERG) (Del Sole et al. 2008; Franco et al. 2008), and can result in damage ranging from the cornea (Aslan et al. 2007), and anterior chamber (Allen et al. 1998) to the retina (Franco et al. 2008; Sasaki et al. 2009).

4.1.3. Visual defect in experimental autoimmune encephalomyelitis (EAE)

Experimental autoimmune encephalomyelitis (EAE) is a frequently used model of MS and is induced by immunisation with a myelin antigen, derived from homogenized CNS tissue or myelin proteins, in adjuvant ((in)complete Freud's adjuvant, serving as an immunopotentiator). This immunisation results in an inflammatory, demyelinating disease of the CNS, with variable characteristics and time course, depending on the animals and myelin epitope used. Typically, animals will show ascending paralysis and inflammation of the CNS, primarily in the spinal cord but also in the brain and optic nerve, together with demyelination and axonal damage (Rao and Segal 2004). Several different proteins have been used to induce EAE, including myelin basic

protein, proteolipid protein and myelin oligodendrocyte glycoprotein (MOG), in several different species, including mice, rats, guinea pigs and non-human primates (Rao and Segal 2004).

MOG is a protein believed to be involved in the pathogenesis of MS (Derosbo et al. 1993; Quarles 2002; Sun et al. 1991). MOG is preferentially found on the outside of CNS myelin sheaths (Quarles, 2002) and this distribution means that it is more strongly represented in tissues where the surface area to volume ratio is greater, such as the optic nerve. The exposed location of MOG could make it an important antigen in possible autoimmune diseases such as MS (Genain and Hauser 2001; Iglesias et al. 2001; t'Hart et al. 2000). Indeed it is possible to induce EAE in rodents by injecting MOG subcutaneously (Stefferl et al. 1999). For example it can be used to induce EAE in female Brown Norway (BN) rats resulting in a more pronounced visual involvement compared to immunisation of other strains (Meyer et al. 2001; Storch et al. 1998). Therefore, the induction of EAE via a subcutaneous injection of MOG in female BN rats results in a fulminant disease course which mimics the opticospinal form of MS (Collongues et al. 2012)

4.1.4. Age-related macular degeneration (AMD) and factor H transgenic mice

As mentioned in the introduction (chapter 1) ageing and its associated pathology are often characterised by neuroinflammation (Anderson et al. 2002; Buschini et al. 2011; Mcgeer et al. 2005; Mcgeer and Sibley 2005). The complement system, an essential part of the innate immune-inflammatory reaction, has been implicated in several inflammatory CNS diseases (Barnum 2002; Van Beek et al. 2003) and specifically in AMD (Coffey et al. 2007; Hageman et al. 2005; Hollyfield et al. 2008). AMD leads to the degeneration and damage of the central part of the retina and is the leading cause of visual loss in developed countries (Taylor and Keeffe 2001).

More specifically, complement factor H (CFH) deficiency has been associated with AMD (Coffey et al. 2007; Edwards et al. 2005; Hageman et al. 2005; Klein et al. 2005), with a link made between the AMD phenotypes and polymorphisms in Factor H encoding genes in humans (Edwards et al. 2005; Hageman et al. 2005) and CFH deficiency in mice resulting in visual defects that mimic certain aspects of the human disease (Coffey et al. 2007). CFH is a regulator of the alternative pathway of the complement system, primarily involved in inhibiting complement activation in response to host cells, thereby preventing autoimmunity. CFH recognizes heparin or sialic acid on host cells, and binds to any C3b present on such cells, thereby inactivating it. Therefore, a lack of Factor H can lead to excessive activation of the complement cascade, production of pro-inflammatory proteins and potentially the loss of host cells (Alexander et al. 2005). And indeed, aged $CFH^{-/-}$ mice show enhanced deposits of C3 on the basement membrane which also extend into the RPE and even into the outer retina, revealing excessive inflammatory activity in the retinas of aged $CFH^{-/-}$ mice (von Leithner et al. 2009).

4.2. Hypotheses

3) High levels of retinal inflammation result in functional deficits, as assessed by ERG recordings, and retinal hypoxia, as assessed by the intravenous probe, hypoxyprobe
4) The endogenous fluorescence of flavoproteins can be used to assess mitochondrial redox state *in vivo* in the retinas of anaesthetized mice

4.3. Aims and objectives

The aim of this chapter is to explore models of retinal inflammation, comparing their utility and reproducibility as well as their relationship with hypoxia. Additionally, we aim to test the use of flavoprotein fluorescence as a marker of mitochondrial redox potential in the retinas of anaesthetised mice.

Here we investigate four methods to induce retinal inflammation. The models include the classic induction of EAE in Brown Norway rats (a form of EAE that significantly involves the visual pathway), endotoxin-induced uveitis (intravitreal and systemic injection of LPS), and the use of transgenic factor H knockout mice ($CFH^{-/-}$; a model of AMD).

Using histochemical markers of hypoxia and inflammation together with electrophysiological readouts of retinal function we will explore the relationship between inflammation, visual function and hypoxia in the retina.

4.4. Methods

4.4.1. Hypoxyprobe injections

Hypoxyprobe, a marker of hypoxia ($pO_2 \leq 10mmHg$), was injected i.p. at a dose of 60mg/kg. In the absence of oxygen, hypoxyprobe becomes reductively activated and binds to sulfhydryl-containing macromolecules to form adducts which can be detected immunohistochemically.

Mice were kept in different ambient air conditions. Eight mice were kept in 10% oxygen and 90% nitrogen and two were kept in room air. Half of the mice from each group were culled after just one hour post injection and the other half after 4 hours. The cardiac perfusion (see below) was conducted under the same oxygenation as used for the experimental manipulation.

4.4.2. Flash Electroretinograms

To conduct the flash ERGs the animals were dark adapted for up to 60 minutes and anaesthetised with a mixture of ketamine (Ketaset, containing 100mg/ml ketamine, Animal Health Ltd, USA) and xylazine (Xylacare, containing 20mg/ml xylazine base, Animalcare Ltd, UK). Viscotears (BR Pharmaceuticals, USA) were applied to prevent corneal drying. The core body temperature was maintained at 37˚C with the use of a homeothermic heating mat and rectal probe. The recording electrode was formed from a monofilament platinum wire twisted into a coil and placed onto the cornea with a 'ground' and reference electrode (hypodermic needles) inserted subcutaneously in the back and scalp respectively. All adjustments to the recording arrangements were conducted under red light illumination.

4.4.3. *In vivo* retinal imaging

B6.Cg-Tg(Thy1-YFPH)2Jrs/J mice expressing yellow fluorescent protein (YFP) in a subset of neurons, including 10-30% of ganglion cells (http://jaxmice.jax.org/strain/003782.html), or their YFP negative litter mates, were anaesthetised with ~2% isoflurane in room air and subsequently placed on a homeothermic heating mat to maintain their rectal temperature at 37˚C. The eyes were kept moist and protected with Viscotears and the skin surrounding the eye was removed. The underlying bone and muscle were cleaned with saline and dried. A custom made titanium ring, attached to a stable base, was affixed to the skull surrounding the eye, using dental cement (Contemporary Ortho-Jet Powder, USA) mixed with cyanoacrylate glue (Loctite, Henkel Ltd., UK). After drying of the dental cement a circular coverslip (~10mm diameter) was placed over the cornea and stabilized and sealed using petroleum jelly (Vaseline, Unilever, UK). Following surgery, the mice were moved to a custom-made stage for confocal microscopy, and the inspired oxygen concentration was varied, as indicated, by changing the mixture of oxygen and nitrogen delivered via a nose cone.

4.4.4. Disease models

4.4.4.1. Experimental autoimmune encephalomyelitis (EAE)

Seven female BN rats were anaesthetised with isoflurane (IsoFlo, Abbott Laboratories, USA) and injected subcutaneously, with 100 µl of complete Freund's adjuvant (CFA) (Sigma-Aldrich, USA) containing 1mg/ml heat-killed and dried Mycobacterium tuberculosis with 100µg recombinant myelin oligodendrocyte glycoprotein (rMOG). ERG recordings were taken serially and the rats were weighed and assessed for clinical signs daily. Rats were scored in relation to the criteria in table 4.4.4.1.1. A cumulative score for each symptom (1 point per symptom) was

assigned. Additionally, a total score was given to each animal which consisted of the sum of all scores across the assessment time period. This score therefore took into account the severity and the rate of the disease progress.

	Tail tip weakness
	Tail weakness
	Tail paralysis
	Abnormal gait
	Abnormal toe spreading
	Unilateral hind limb weakness
	Bilateral hind limb weakness
	Unilateral hind limb paralysis
	Bilateral hind limb paralysis
	Moribund

Table 4.4.4.1.1: **Clinical disease scoring of EAE rats.** Each symptom is assigned one point with a cumulative score assigned daily.

During the peak of the disease (within 4 days of disease onset) rats were injected intravenously (via the saphenous vein) with hypoxyprobe (60 mg/kg) and left for 4 hours before intracardiac perfusion fixation.

4.4.4.2. Intravitreal LPS

Lipopolysaccharide (LPS) from *Salmonella abortus equi* (Sigma-Aldrich, USA) was used for intravitreal injections into mouse eyes. Twenty-one C57bl/6 mice were anaesthetised with ketamine/xylazine as before and a glass needle attached to a microsyringe, partly filled with mineral oil, was used to inject 0.5µl of variously diluted LPS or saline (control).

Dose trial: Six C57bl/6 mice were injected intravitreally with different doses of LPS (10ng, 100ng or 500ng) into one eye, while the other eye acted as a saline-injected control. ERG recordings were taken before termination 24 hours after intravitreal LPS injection.

Time trial: Control eyes were injected as above, and 40ng of LPS was injected into the contralateral eye. The animals were then injected i.p. with hypoxyprobe and ERG recordings were taken before termination 8, 24, 48, 72 hours or 7 days post injection (n=15, 3 per group).

4.4.4.3. Systemic LPS

LPS from *Escherichia coli* (Sigma Aldrich, USA) was dissolved in sterile saline and injected i.p. at various concentrations (from 1mg/kg – 5mg/kg) at a volume of 10ml/kg. Saline was injected in the same way. Following the injection the peritoneum was gently massaged to aid the distribution of the injection. Eight C57bl/6 mice were culled 10 hours after an i.p. injection of saline or LPS (1mg/kg, 3mg/kg or 5mg/kg, n = 2 per group) while a further 8 (same groups) were culled 24 hours after the injections.

4.4.4.4. CFH-/- mice

Twenty C57bl/6 mice (10 mice at 5-6 weeks and 10 mice at 16-24 months) and twenty-five $CFH^{-/-}$ mice on a C57bl/6 background (15 mice at 4 weeks and 10 mice at 14-15 months) were injected with hypoxyprobe i.p. and culled 2 hours post injection by cervical dislocation or perfusion.

All animals were purchased from Harlan, with the exception of the $CFH^{-/-}$ mice, which were provided by Matthew Pickering at Imperial College London. All animals were housed in a 12 hour light/dark cycle with food and water *ad libitum*. All experiments were performed in accordance with the UK Home Office Animals (Scientific Procedures) Act (1986).

4.4.5. Perfusion and fixation

Culmination of the experiments occurred either at an experimental endpoint or when the animal was suffering or could not reach food or water. Animals were culled via cervical dislocation or anaesthetised and culled via cardiac perfusion. For the cardiac perfusion, heparinised buffered saline was used to rinse away the blood from the vasculature which was followed by fixation with 4% paraformaldehyde (PFA) in phosphate buffered saline (PBS). The tissue was harvested and post fixed overnight in 4% PFA. It was then cryoprotected in 30% sucrose with 0.02% sodium azide, dissected, embedded in OCT (Optimal Cutting Temperature, Tissue Tek, UK) and frozen in dry ice. The tissue was then cut into 10µm thick sections and stored at -20°C until further use.

4.4.6. Immunohistochemistry

Fluorescent labelling of compounds was largely conducted in a similar fashion: after blocking with the appropriate serum (5%, Table 4.4.6.1, Vector Laboratories, USA) for more than 30 minutes the slides were incubated with the appropriate primary antibody diluted in 5% serum overnight at 4°C (Table 4.4.6.1). After a thorough wash the slides were incubated in a secondary antibody conjugated to a fluorophore diluted in 5% serum at room temperature for 1 hour. Slides were washed and mounted with Vectashield mounting medium (Vector Laboratories, USA) and sealed with nail varnish. They were then stored at 4°C until imaging.

To label slides using DAB (3,3'-diaminobenzidine) the slides were initially incubated with 0.3% hydrogen peroxide dissolved in methanol to saturate and thereby inactivate endogenous peroxidase activity. Following several washes slides were incubated with sodium borohydride twice for 5 minutes to uncover antigen by blocking free aldehydes. Following this, non-specific secondary antibody binding was blocked using the appropriate 5% serum or casein (only for hypoxyprobe antibody on rat tissue; see Table 4.4.6.1) for more than 30 minutes. Incubation of the primary

antibody followed, overnight at 4˚C. On the following day stringent washes preceded incubation with the appropriate biotinylated secondary antibody for one hour at room temperature. After this was washed off, slides were incubated with an avidin-biotin complex (Vectastain ABC kit, Vector Laboratories, USA) for thirty minutes. Following a further thorough wash the slides were briefly incubated with DAB which reacts with peroxidase enzymes included in the ABC kit to form a stable brown deposit. Slides were dehydrated in a series of alcohols and xylene and mounted with DPX (dibutyl phthalate xylene) mounting medium (VWR, UK) to be stored at room temperature.

1° antibody	Dilution 1°	Source	Company	Serum	2° antibody	Dilution 2°
Anti- ED1	1:200	Mouse, monoclonal	Sigma Aldrich	Horse	Horse anti-mouse	1:200
Anti-IBA1	1:500	Rabbit, polyclonal	Wako	Goat	Goat anti-rabbit	1:200
Anti-Hypoxyprobe (for mouse tissue)	1:200	Rabbit, polyclonal	HypoxyprobeTM	Goat	DAKO secondary anti-rabbit	NA
Anti-Hypoxyprobe (for rat tissue)	1:200	Mouse, monoclonal	HypoxyprobeTM	Casein	Horse anti-mouse	1:200
Anti-MHC class II	1:250	Mouse, monoclonal	Abcam	Donkey	Donkey anti-mouse	1:500
Anti-iNOS	1:200	Rabbit, polyclonal	BD transduction labs	Goat	Goat anti-rabbit	1:500

Table 4.4.6.1: **Primary antibodies used and their dilutions, specifications and further protocol information.**

DAB labelling of hypoxyprobe in mouse tissue involved the use of a DAKO blocking kit. Here the slides were initially agitated with 3% hydrogen peroxide in methanol after which citric acid (1:10 dilution, DAKO, Denmark) was used for antigen retrieval. Blocking was conducted with the DAKO blocking solution (Protein block, serum free) followed by incubation with the primary antibody (diluted 1:200 in 5% normal goat serum) overnight at 4°C. After a thorough wash the

slides were incubated with the secondary antibody (DAKO polymer HRP anti-rabbit). After 1 hour the DAKO substrate chromogen was dropped onto the slides and left for 3 minutes after which the slides were submerged in deionised water, dehydrated through a series of alcohols and xylene and mounted with DPX. The slides were subsequently stored at room temperature.

4.4.7. Image acquisition

Fluorescent image capture was conducted with the LSM 5 Pascal confocal microscope (Zeiss, Germany). Light microscopy was conducted with an Axiophot light microscope (Zeiss, Germany) including a Nikon D300 camera (Nikon, USA). Illumination conditions were stable throughout image acquisition.

4.4.8. Image quantification and statistical analysis

All image quantification was conducted using Fiji/ImageJ Version 1.48v (NIH, USA). Three analysis techniques were used: fluorescence intensity, particle count and percent area of positive labelling. The fluorescence intensity quantification was conducted through a Fiji/ImageJ plugin and particle counts were done manually. Percent areas of positive labelling involved the development of a threshold, which was chosen to be the mean intensity of an appropriate control image plus two standard deviations and everything above this threshold was considered positive labelling. This threshold then allowed the determination of the percentage of the selected area covered by positive labelling.

Statistical analysis was conducted via IBM SPSS Statistics 20. Standard Student t-tests and analyses of variance (ANOVA) were conducted in which the p-value cut off for statistical significance was 0.05.

4.5. Results

4.5.1. Electroretinograms

In order to optimize ERG recordings we investigated factors that could potentially influence the amplitude of the recorded flash ERG. These include stimulus intensity, dark adaptation, interpulse duration, electrode placement and the amount of Viscotears used. For simplicity averaged traces of the two eyes of different mice within the same group will be displayed, as there is limited variation between animals or between the two eyes of the same animal (Figure 4.5.1.1).

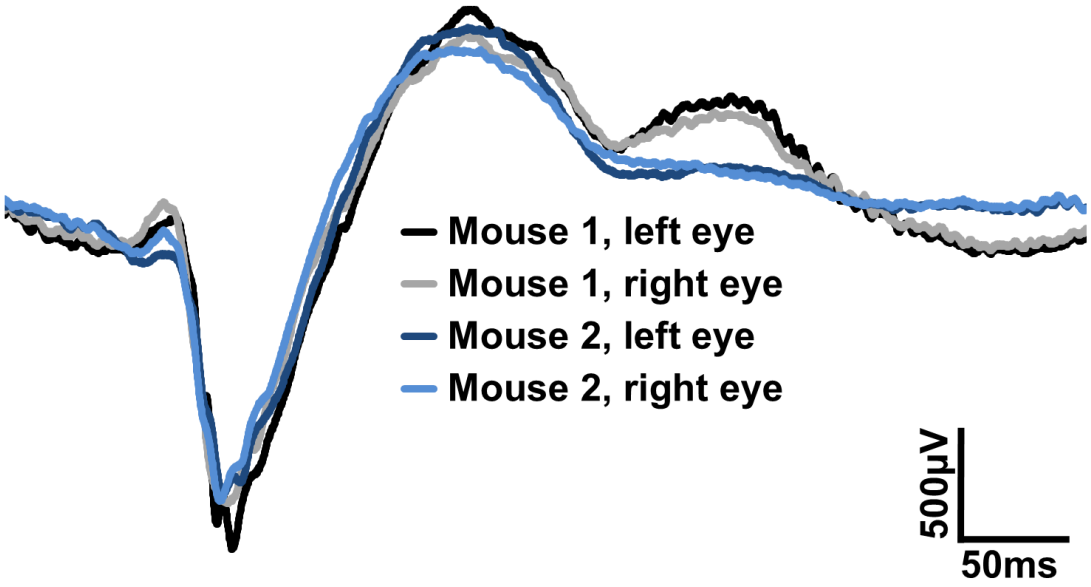

Figure 4.5.1.1: **Example traces of both eyes of two dark adapted mice subjected to 58mA light pulse stimuli**.

An increase in stimulus intensity increased the amplitude and decreased the latency of the ERG (Figure 4.5.1.2 a). It is possible that the increase in latency with decreased stimulus amplitude was a function of the stimulus arrangement, which might have had a delayed flash response at lower amplitudes. Additionally, it is evident that a longer dark adaptation of 1 hour resulted in a greater ERG amplitude compared to 30 minutes dark adaptation or 30 minutes light adaptation, while 30 minutes red light adaptation had approximately the same effect as 30 minutes dark adaptation (Figure 4.5.1.2 b). This allowed us to manipulate mice under red light without disturbing the dark adaptation. Additionally, a longer interpulse period resulted in more reproducible ERGs with greater amplitudes (Figure 4.5.1.2 c and d). This might be a result of light adaptation after frequent and repeated stimulation. The increased time span used in the 4 second interpulse periods, compared to the 1 second interpulse period, resulted from maintaining the number of stimulus averages consistent. Finally neither electrode placement (Figure 4.5.1.2 e) nor the amount of Viscotears used (Figure 4.5.1.2 f) seemed to have a significant effect on the ERG shape.

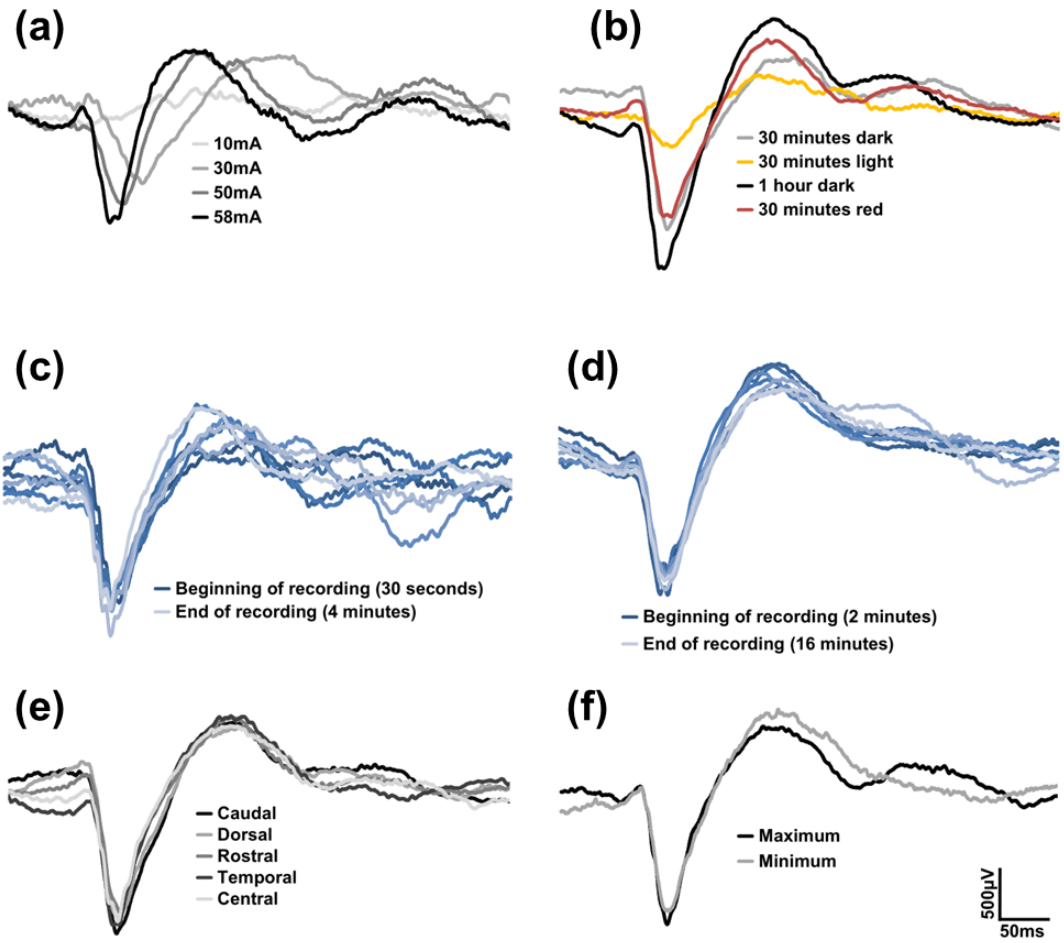

Figure 4.5.1.2: **An investigation of the factors affecting ERG amplitude and latency.**
The effect of stimulus intensity **(a)** and dark adaptation **(b)** on ERG amplitude. The effect of interpulse period duration on ERG amplitude and stability **(c)** and **(d)**. A series of ERG recordings with a 1 second interpulse period **(c)**. ERG recordings with a 4 second interpulse period **(d)**. ERGs of mice subjected to variations in electrode placement **(e)**. The effect of Viscotear application on ERG amplitude **(f)**; Maximum refers to the maximum possible usage of Viscotears and minimum refers to the least possible usage (without drying of the cornea). Each record is an average of 100 traces of 2 mice (mean of 4 eyes) with the exception of the electrode placement eyes which averaged of n = 3.

Given the above findings, any future recordings were presented in scotopic conditions, including dark adaptation, while the stimulus itself was relatively bright, with a 4 second inter pulse period, resulting in a response driven both by the rod and the cone pathways (Clark and Kraft 2012).

4.5.2. Hypoxyprobe labelling in the hypoxic murine retina

To characterise the use of hypoxyprobe as a marker of retinal hypoxia, we assessed the changes in labelling between mice maintained in room air, and mice placed into a reduced-oxygen environment (10% O_2).

Retinas of mice injected with hypoxyprobe and subjected to a fraction of inspired oxygen (FiO_2) of 10% for 4 hours are more strongly labelled compared with retinas subjected to hypoxyprobe and room air for 4 hours (Figure 4.5.2.1), suggesting that hypoxyprobe labelling is sufficient to detect a reduction in oxygen concentration for 4 hours. Also 1 hour after hypoxyprobe injection and hypoxia, the retina exhibits more labelling as compared to a room air control, despite a reduced difference in labelling between hypoxic and normoxic retinas as compared to the 4 hour condition.

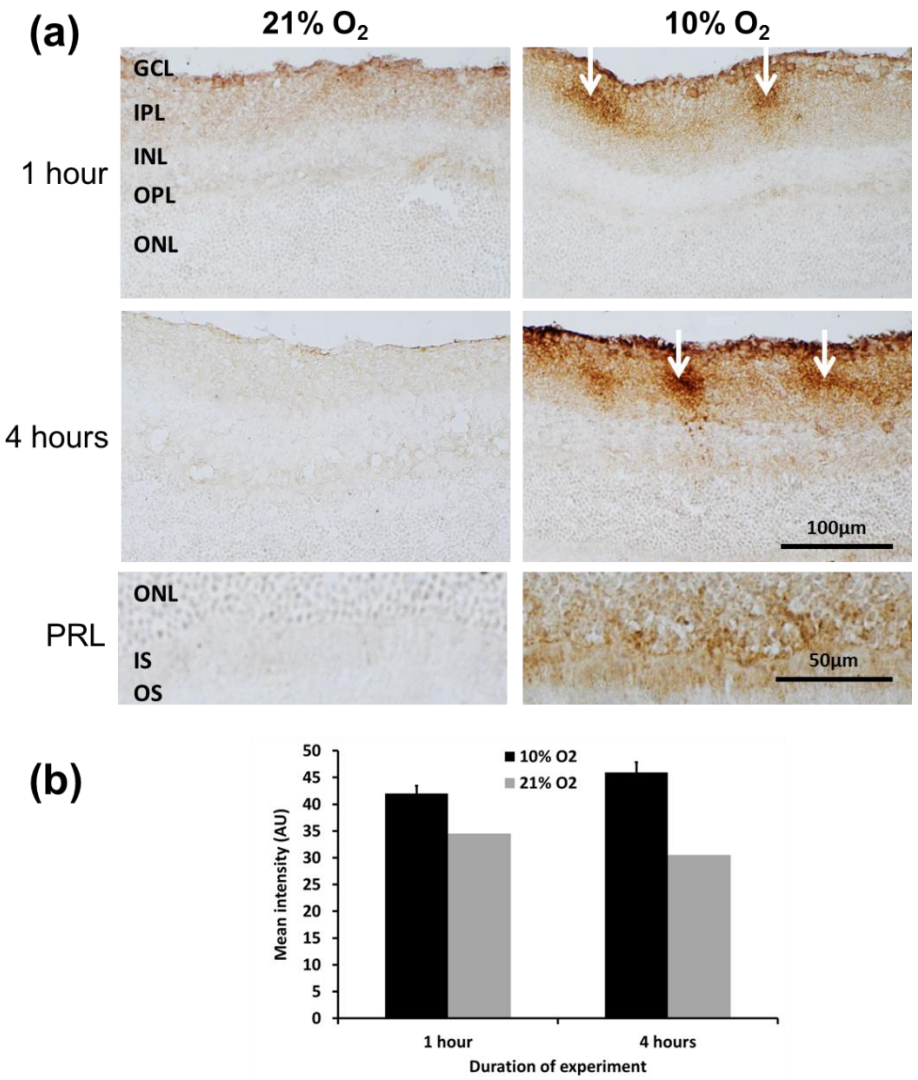

Figure 4.5.2.1: **Hypoxyprobe labelling in the retinas of hypoxaemic mice.**
(a) Retinas of mice injected with hypoxyprobe and kept in room air (21% O_2) or 10% oxygen for 1 hour or 4 hours. The white arrows indicate areas with intense hypoxyprobe labelling. Abbreviation: GCL, ganglion cell layer; IPL, inner plexiform layer; INL, inner nuclear layer; OPL, outer plexiform layer; ONL, outer nuclear layer; PRL, photoreceptor layer; IS, inner segment (of photoreceptors); OS, outer segment (of photoreceptors). **(b)** Quantification of the amount of labelling (average intensity from GCL to IS) displayed as mean ± SEM.

Labelling with DAB highlighted areas of intense hypoxia in the retina of hypoxaemic mice (Figure 4.5.2.1 a arrows). Such areas can be mainly seen in the inner plexiform layer but also the inner segment of the photoreceptors (though less consistently).

The difference in labelling between hypoxic and normoxic retinas, originates mainly from the inner retina. Indeed we found that there is a ~23% increase in hypoxyprobe labelling in the ganglion cell layer of hypoxic mice compared to normoxic mice and an approximately 19% increase in the inner plexiform layer as compared to a ~4% increase in the outer plexiform layer (data not shown).

4.5.3. EAE induction in Brown Norway rats

4.5.3.1. Clinical disease characterisation

Eight of eleven rats immunised with rMOG developed clinical disease characteristics. However, only five of them developed a quantifiable neurological deficit, ranging from tail tip weakness to hind limb paralysis, while three rats had severe vestibular problems, balance issues and lethargy. Due to the severity of these clinical signs they were given a score of 7-9, depending on the state of the animal. The incidence of clinical disease in the ERG control group (no ERG) was 100% (5 of 5) while only 50% of rats that were examined by ERG developed clinical deficits (3 of 6) by 29 days post immunisation. None of the CFA control rats showed any clinical deficits.

4.5.3.2. (Immuno)histochemical characterisation

Microglial morphology was assessed through IBA1 labelling. Microglia were divied into three groups of increasingly amoeboid morphology (Figure 4.5.3.2.1), based on the classification used in Desai (2013). Type I consisted of microglia with a ramified morphology with only the processess being labelled and visible. Type II microglia consisted of thickened processess and enlarged, clearly visible cell bodies. Type III microglia were amoeboid shaped with almost all processes retracted and only a rounded cell body being evident. Such changes in morphology have frequently been used as early indictaors of microglial activation (e.g. (Opie et al. 2012; Zhang et al.

2005), for review see for example (Streit et al. 1988) and figure 1 in (Hanisch and Kettenmann 2007)).

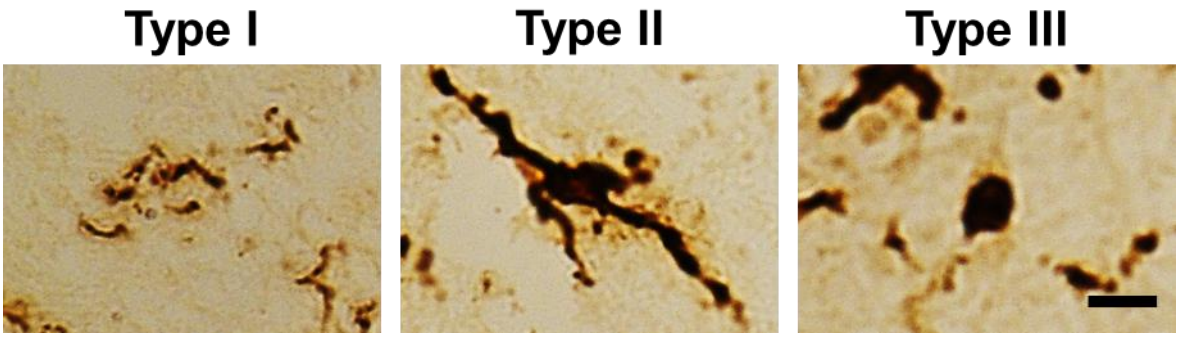

Figure 4.5.3.2.1: **Microglial morphology as assessed by IBA1 labelling.**
Microglia were divided into three groups (modified from (Desai 2013)). Type I microglia consisted of fine processes without cell body. Type II microglia consisted of enlarged processes and thickened cell bodies while type III microglia consisted of enlarged and rounded cell bodies with most processes completely retracted. Scale bar = 10µm.

Retinas and spinal cords of rats were assessed for the percentage of each microglial subtype. Asymptomatic and control rats exhibited less microglial activation compared to symptomatic rats in the grey matter of the spinal cord (Figure 4.5.3.2.2 a and c). However, these differences are not significant ($p \geq 0.05$ after Bonferroni correction). In contrast, the retinas of rMOG immunised rats show greater microglial activation as compared to control rats (Figure 4.5.3.2.2 b and d, $p \leq 0.05$ after Bonferroni correction when comparing type I and II microglial activation across groups). The microglial activation in the retina is limited to the inner retina with most activation evident in the ganglion cell layer (Figure 4.5.3.2.2 b).

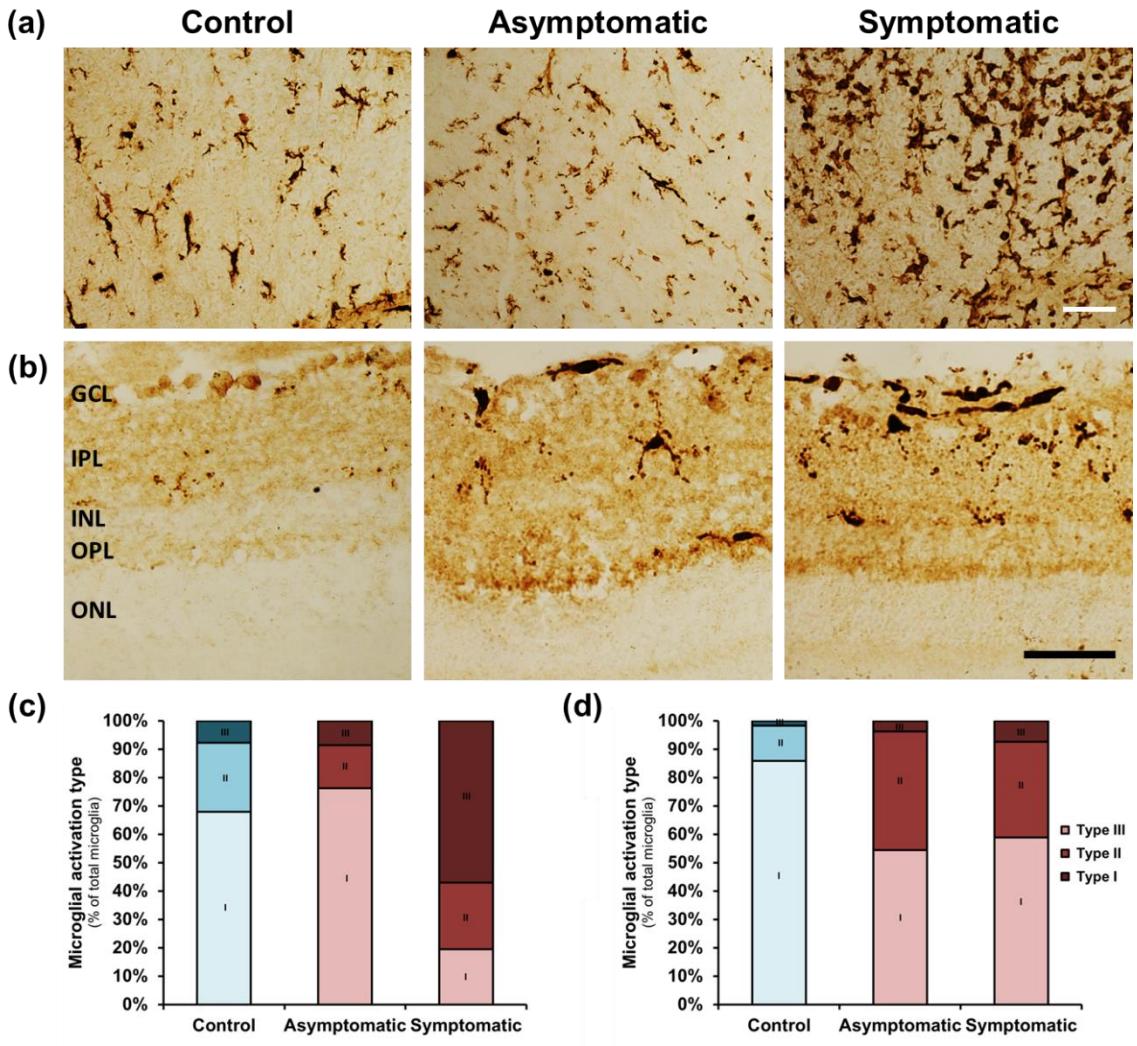

Figure 4.5.3.2.2: **Microglial activation in the spinal cords (a) and (c) and retinas (b) and (d) of rats with EAE and controls.**

Grey matter of spinal cords **(a)** and retinas **(b)** of control rats, asymptomatic rats and rats with clinical signs labelled for IBA1, indicating microglial morphology. Scale bar = 50µm. Quantification of microglial activation in the spinal cord grey matter **(c)** and retinas **(d)** of EAE and control animals. Data represented as percentage of types of microglial activation categories as defined in Figure 4.5.3.2.1. Abbreviations: GCL, ganglion cell layer; IPL, inner plexiform layer; INL, inner nuclear layer; OPL, outer plexiform layer; ONL, outer nuclear layer.

Histochemical labelling of ED1/CD68 (indicating the presence of phagocytic microglia or macrophages) revealed that optic nerve inflammation occurred even in animals lacking clinical

deficit, as assessed by tail and hind limb weakness/paralysis (Figure 4.5.3.2.3, in line with microglial morphology changes in asymptomatic retinas, Figure 4.5.3.2.2 b and d). This optic nerve inflammation was absent in adjuvant controls (Figure 4.5.3.2.3). No ED1 labelling could be found in the retina (data not shown).

There was a positive relationship between ED1 coverage in the optic nerve and the score at perfusion ($p \leq 0.001$, Spearman's rank correlation coefficient) as well as the total score ($p \leq 0.001$). There is also a significant difference between ED1 coverage in the optic nerves of control and symptomatic rats ($p \leq 0.01$, two-tailed t-test) while there is no relationship between ED1 coverage and the difference in ERG amplitude before and after symptom onset ($p \geq 0.05$, Spearman's rank correlation coefficient), (Figure 4.5.3.2.3).

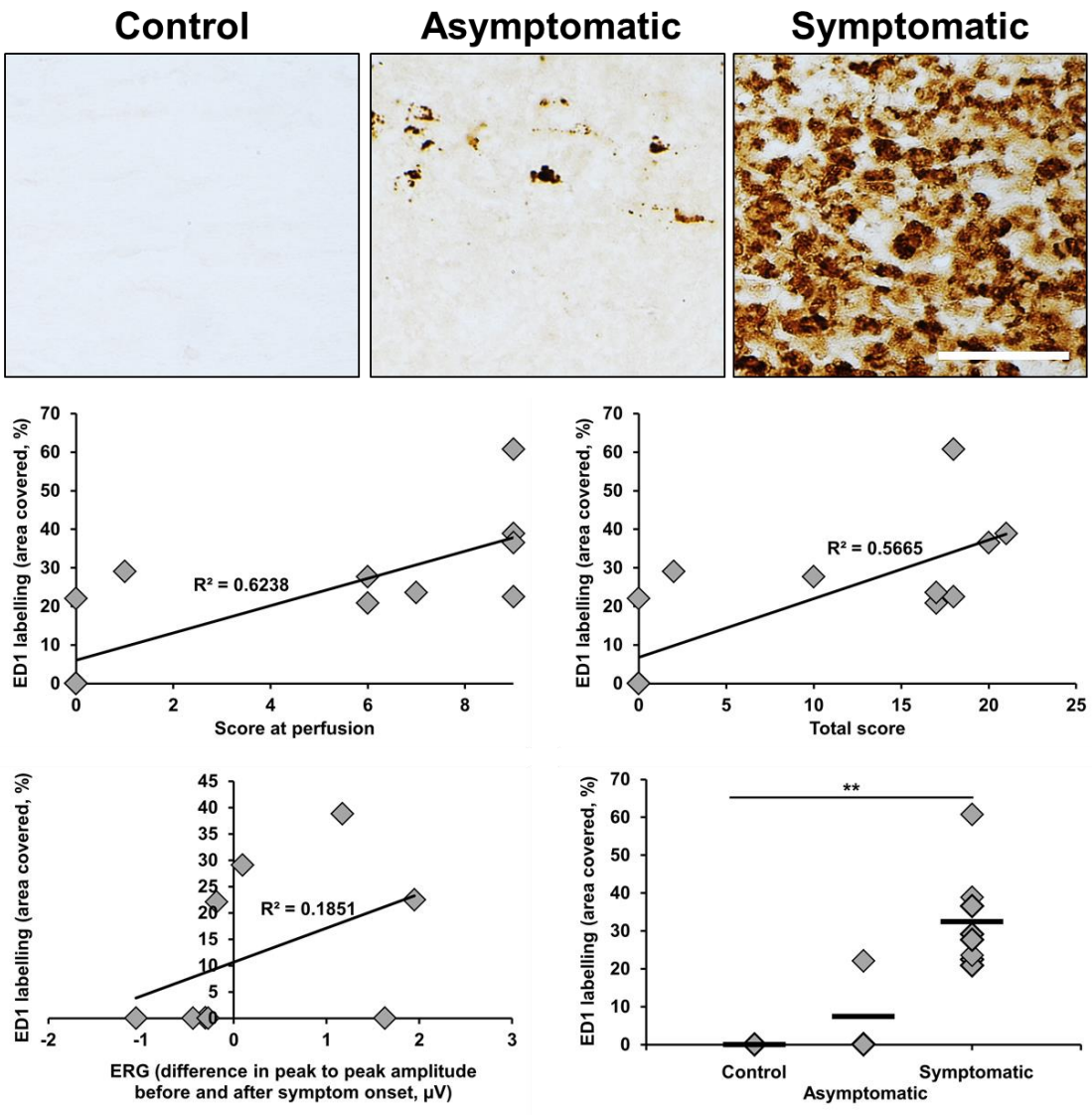

Figure 4.5.3.2.3: **ED1 positive cells in the optic nerve of control, asymptomatic and symptomatic rats.**

Scale bar = 50µm. Graphs: relationship between ED1 positive cell coverage and score at perfusion, total score, ERG amplitude difference before and after symptom onset and grouping. Data displayed as individual data points (grey diamonds) and means of groups (black lines). ** = $p \leq 0.01$.

There is a weak relationship between the clinical disease and hypoxyprobe labelling in the retinas of EAE rats (Figure 4.5.3.2.4) but this is not statictically significant ($p \geq 0.05$).

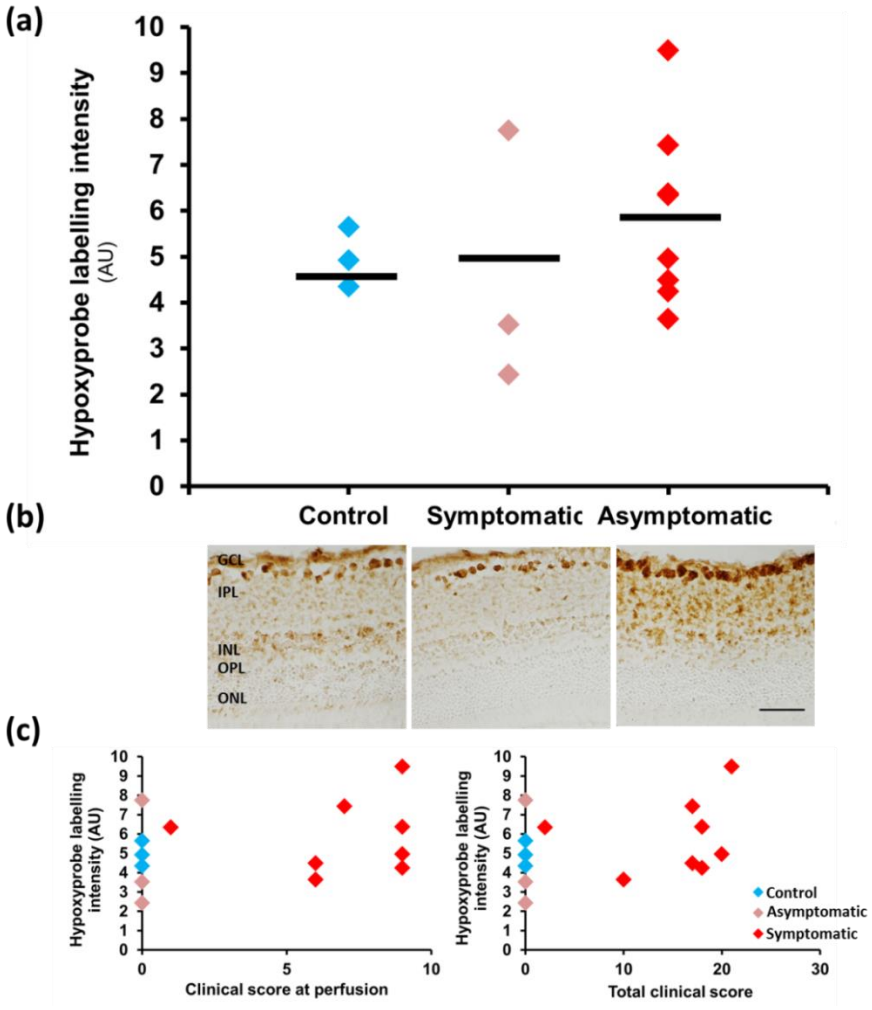

Figure 4.5.3.2.4: **Hypoxyprobe labelling in the rat retina in control animals and animals induced with EAE.**

(a) Quantification of hypoxyprobe associated DAB intensity in the retinas of rats in the different groups. **(b)** Sample images of hypoxyprobe labelling in the rat retina in the three groups. Scale bar = 50µm**. (c)** Relationship between hypoxyprobe labelling in the retina and the clinical score of the rat at perfusion and the total score of the animal. All $p \geq 0.05$.

There is no relationship between hypoxyprobe labelling in the retina and clinical score at perfusion or total score (defined by summing the daily scores of the animals until perfusion, Figure 4.5.3.2.4 c). This latter evaluation takes into account the score of the animal as well as the speed with which the animal succumbs to disease. Additionally there is no statistically significant

relationship between hypoxyprobe labelling and the level of inflammation (as assessed by microglial activation, data not shown).

4.5.3.3. Electroretinogram characterisation

As evident from the ERG records (Figure 4.5.3.3.1), the amplitude of both the A and the B wave in animals showing motor deficits is decreased relative to the other groups (Figure 4.5.3.3.1 a) when measured on the day of culling, as well as relative to the ERG amplitude before immunisation with rMOG (Figure 4.5.3.3.1 b and c).

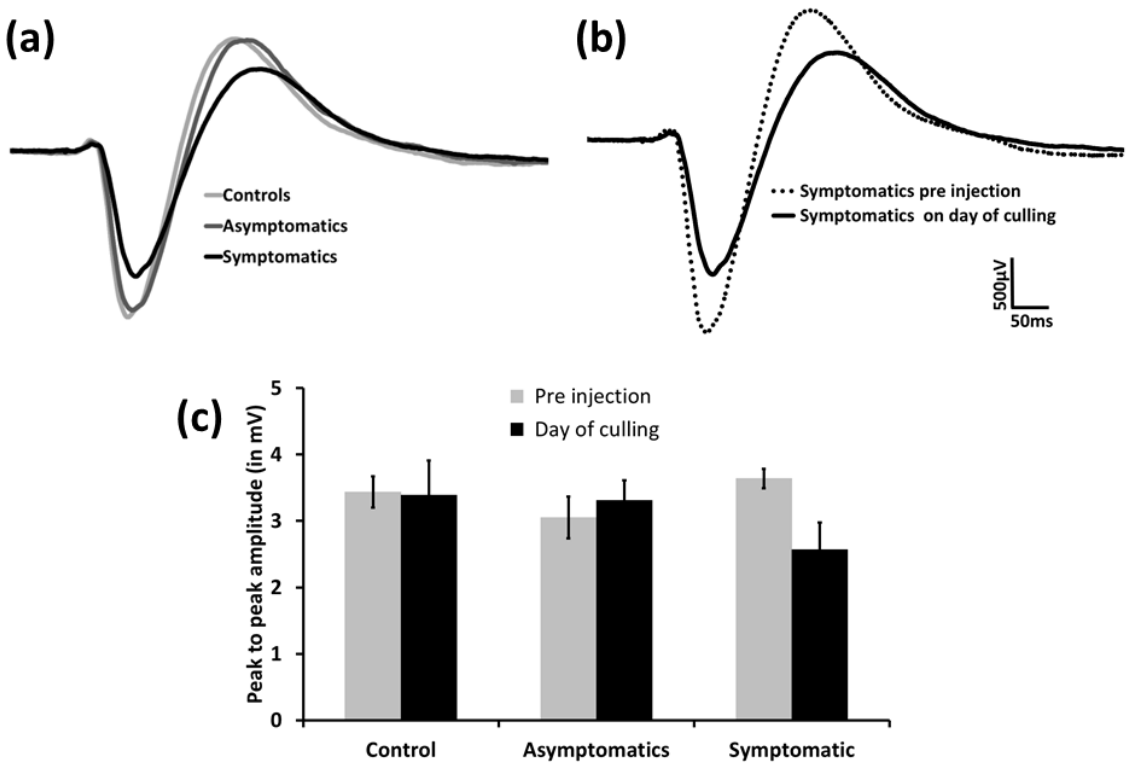

Figure 4.5.3.3.1: **ERGs collected in response to a 10ms flash of 58mA.**
(a) A comparison of the average ERG traces of symptomatic, asymptomatic and control rats on the day of culling. **(b)** Comparison of the ERG traces of symptomatic rats before injection and 24-72 hours after developing symptoms (day of culling). **(c)** The peak-to-peak amplitude in the three groups of rats, before injection and 24-72 hours after symptom onset (day of culling). Displayed as mean ± SEM. All $p \geq 0.05$

4.5.4. Intravitreal LPS injections

4.5.4.1. Concentration trial

One of the mice injected with 500ng LPS had to be excluded as the injection was not sufficiently accurate. None of the mice showed any obvious clinical symptoms.

4.5.4.1.1. (Immuno)histochemical characterisation

A haematoxylin and eosin (H&E) stain (Figure 4.5.4.1.1.1, top panel) reveals that saline injections caused no detectable pathology but that the eyes of the same animals, injected with various doses of LPS, show a dose dependent response, ranging from cellular infiltration in the vitreous along the surface of the retina, to haemorrhage and complete retinal disorganisation. Labelling for iNOS and major histocompatibility complex class II (MHCII) revealed that these infiltrating cells show inflammatory characteristics (Figure 4.5.4.1.1.1). However, it seems that iNOS only plays a significant role when complete retinal disorganisation is achieved. MHC class II bearing cells on the other hand seem to be present at each concentration of LPS near the surface of the retina and also further inside the retina after a 500ng injection of LPS (Figure 4.5.4.1.1.1).

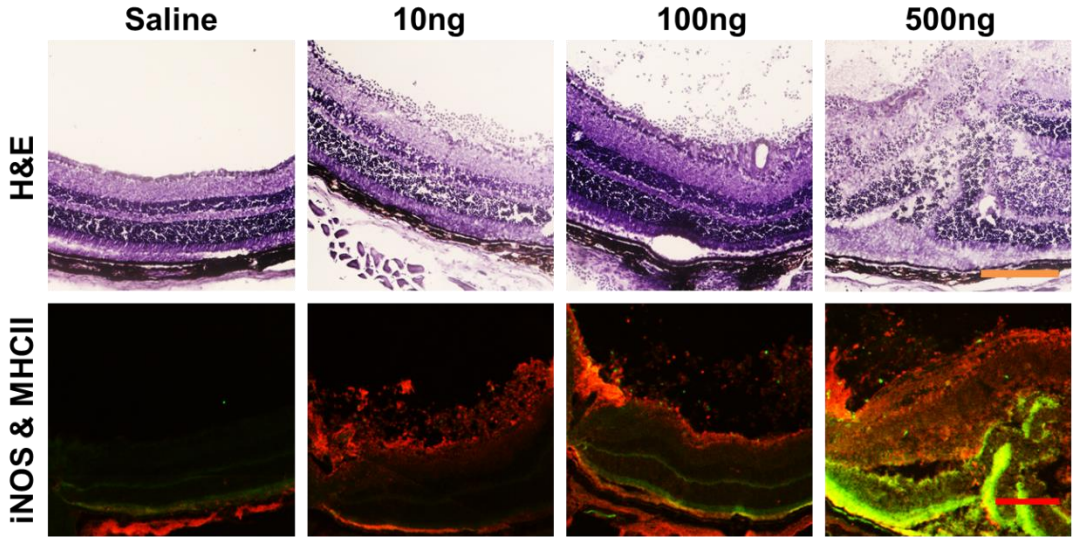

Figure 4.5.4.1.1.1: **Inflammation in retinas injected with 10ng, 100ng or 500ng LPS in one eye with the other eye acting as a saline control**.
Top panel: H&E stain. Lower panel: iNOS (green) and MHCII (red) immunofluorescence. Scale bar = 200μm

There does not seem to be much infiltration of cells into the retina at either 10ng or 100ng LPS injections. Instead cells tend to localise around the interface between retina and vitreous. However, at an injection of 500ng of LPS the retina becomes completely disorganised with cellular infiltration and severe haemorrhage. Haemorrhage also occurred to a lesser extent in some of the mice injected with 100ng.

4.5.4.1.2. Electroretinogram characterisation

LPS had a dose dependent effect on the ERG amplitude (Figure 4.5.4.1.2.1).

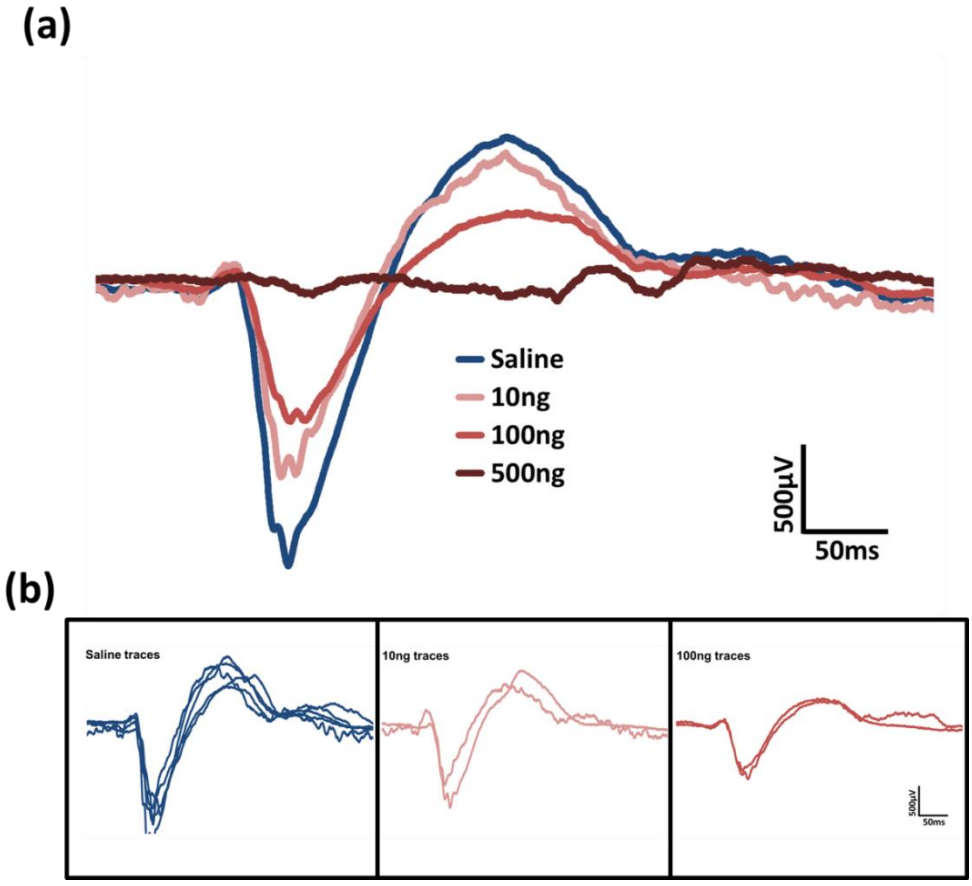

Figure 4.5.4.1.2.1: **ERGs collected 24 hours after injection of various doses of LPS into the vitreous of one eye, with the other eye acting as a saline control**.

Stimulus amplitude = 58mA. n=5. **(a)** averaged traces; **(b)** individual traces.

As can be seen, a higher injection dose led to a greater difference in ERG amplitude between the LPS injected eye and the control eye, with 500ng of LPS eliminating any ERG signal. However, this could also be due to haemorrhage, evident at higher doses of LPS, which could prevent the penetration of light onto the retina during recording of the ERG.

4.5.4.2. Time trial

Given the findings of the concentration trial it was decided that a time trial of intravitreal LPS injections should be conducted with 40ng of LPS, avoiding concentrations that cause severe haemorrhage but administering a high enough dose to provide a strong inflammatory response.

4.5.4.2.1. (Immuno)histochemical characterisation

Control eyes injected with saline show no abnormalities or infiltrating cells. Eyes injected with 40ng of LPS show cell infiltration after 24 hours with some eyes showing complete disorganisation after 24 hours, 3 days and 1 week, including haemorrhage and severe pathology. The haemorrhage may have been responsible for some of the severely attenuated ERG recordings, particularly at 3 days post injection.

The level of disorganisation of the retina and immune cell infiltration seemed not to be related to a particular time point (with the exception that no overt infiltration was evident at 8 hours post LPS injection, as assessed with H&E labelling) as the variation between mice of the same group is unexpectedly large (Figure 4.5.4.2.1.3 a). It is possible that extreme retinal disorganisation may be the result of slight mechanical damage to the retina during injection. However, given that none of the saline injected-eyes show any form of disorganisation it is likely that mechanical damage to the retina needs to be combined with LPS to cause severe retinal disorganisation.

As there was greater variation within groups compared to between groups of varying time points (Figure 4.5.4.2.1.3 a) the data will be presented in terms of inflammatory severity. Inflammation was rated by a blinded observer (based on H&E labelling) and grouped into retinas showing no, mild, moderate and severe disorganisation.

Severe retinal damage, including disorganisation of the retina and haemorrhage, led to iNOS upregulation (Figure 4.5.4.2.1.1). MHC class II molecules however, were also involved in less severe pathology, being located mainly along the retinal/vitreal interface (Figure 4.5.4.2.1.1).

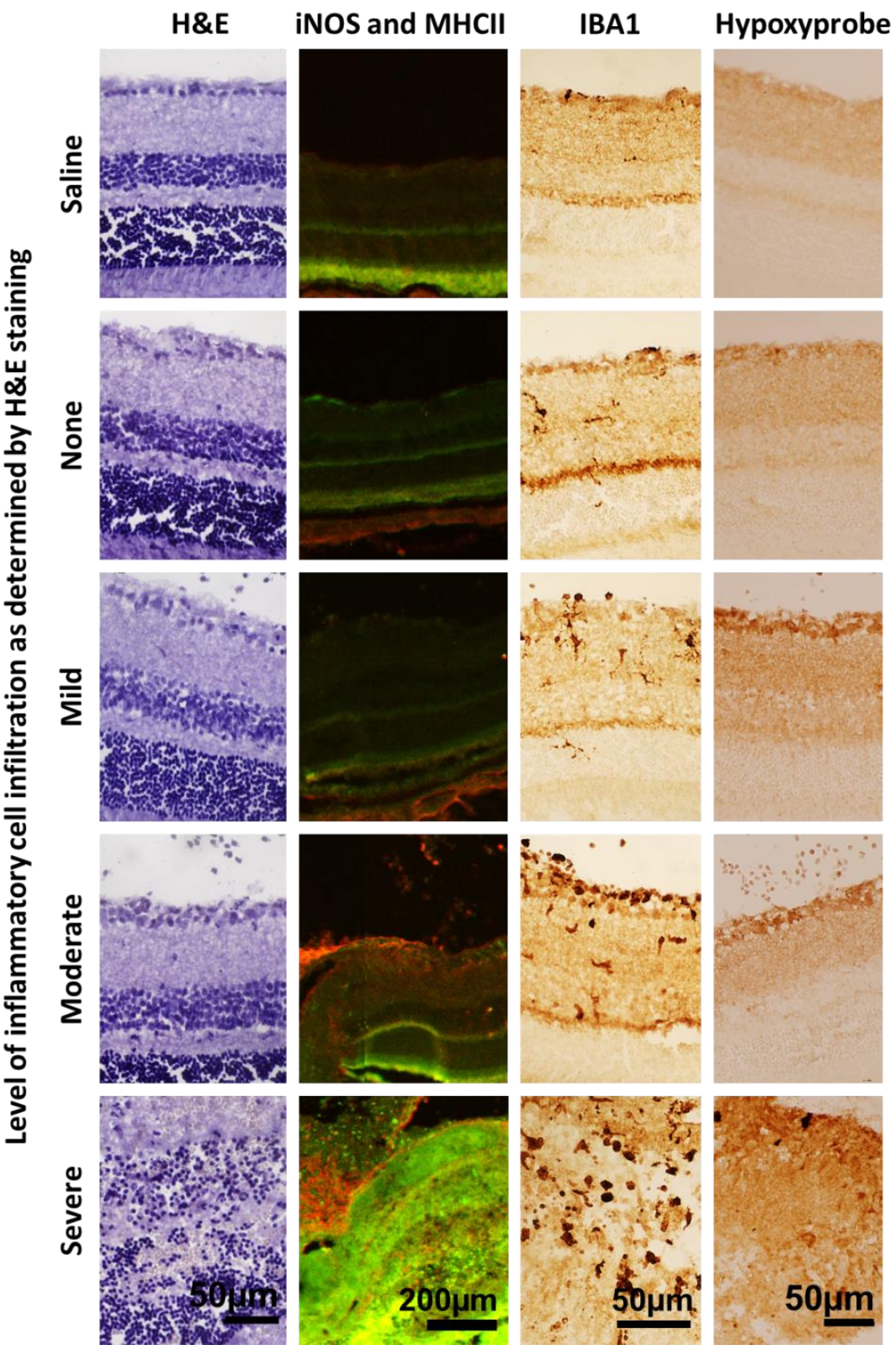
H&E
iNOS and MHCII
IBA1
Hypoxyprobe
Level of inflammatory cell infiltration as determined by H&E staining
Saline
None
Mild
Moderate
Severe
50µm
200µm
50µm
50µm

Figure 4.5.4.2.1.1: **Inflammation in retinas of mice injected with 40ng of LPS into one eye and saline into the other and culled at various time points** (see methods).
Retinas of eyes injected with LPS were divided into no-, mild-, moderate-, and severe inflammatory cell infiltration by a blinded observer. 1st panel: H&E stain. 2nd panel: iNOS (green) and MHCII (red) immunofluorescence. 3rd panel: Morphological microglial and macrophage label (IBA1), 4th panel: hypoxyprobe label.

Additionally, it can be seen that even in the absence of observable inflammatory cell infiltration (as determined by H&E staining) microglial morphology in the retina changes in response to an intravitreal LPS injection into a more activated phenotype (Figure 4.5.4.2.1.1). As the inflammation becomes more severe the microglial morphology changes from a ramified quiescent state to a more amoeboid and activated state (Figure 4.5.4.2.1.2a and also see Figure 4.5.3.2.1 for microglial morphological characterisation). Microglial activation does not only occur before noticeable inflammatory cell infiltration but also shortly after injection of LPS (8 hours after injection) (Figure 4.5.4.2.1.2 b).

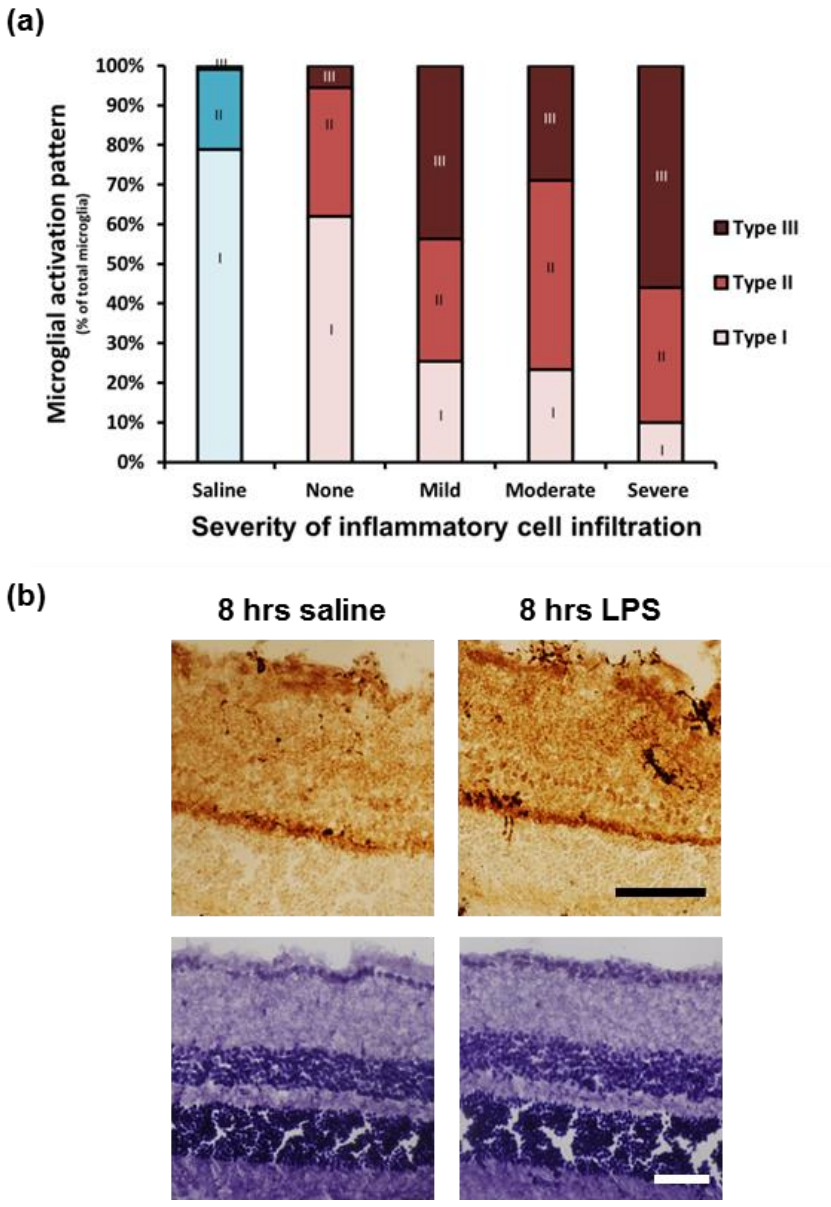

Figure 4.5.4.2.1.2: **Microglial activation after intravitreal LPS injections.**
(a) Quantification of microglial activation pattern grouped by the amount of inflammatory cell infiltration, as determined by blinded assessment of H&E labelling. **(b)** Upper panel: representative image showing enhanced microglial activation in retinas 8 hours after LPS injection as compared to saline-injected counterparts, despite an absence of inflammatory cell infiltration (H&E: lower panel). Scale bar = 50µm.

Also hypoxyprobe labelling increases with intravitreal LPS injections compared to saline injections (Figure 4.5.4.2.1.1 and Figure 4.5.4.2.1.3 c). There is a possibility that the retinas which

showed severe damage and disorganisation became detached from the supporting choriocapillaris. This could lead to reductions in oxygenation unrelated to LPS induced inflammation. Therefore, these animals were removed from the analysis. Nevertheless, the paired sample t-test revealed a significant difference between the labelling intensity of retinas of LPS-injected eyes when at least some inflammatory cell infiltration is present (as assessed by H&E labelling), and their vehicle-injected controls ($p \leq 0.05$).

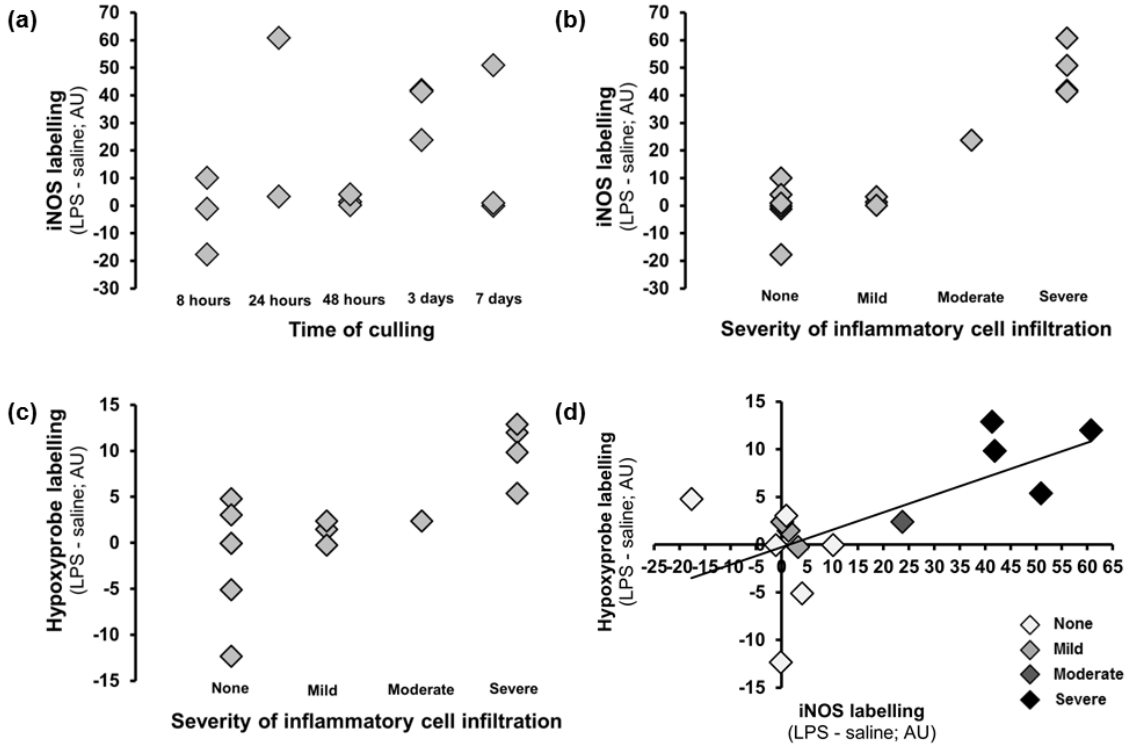

Figure 4.5.4.2.1.3: **iNOS and hypoxyprobe labelling after intravitreal LPS injections.** iNOS **(a)** and **(b)** and hypoxyprobe **(c)** labelling sorted by disease duration **(a)** and level of inflammatory cell infiltration, as assessed by H&E labelling by a blinded observer **(b)** and **(c)** **(a) – (c)** $p \geq 0.05$. Relationship between hypoxyprobe and iNOS labelling, Shapiro-Wilk test, $p \leq 0.05$ **(d)**. Data displayed as difference in labelling intensity between saline and LPS-injected eyes of the same animal.

There was a relationship between iNOS and hypoxyprobe labelling in this model (Figure 4.5.4.2.1.3 d). In the absence of a normal distribution (as assessed by the Shapiro-Wilk test, $p \leq$

0.05) a non-parametric Spearman's rank correlation coefficient revealed a significant relationship between iNOS and hypoxyprobe labelling ($p \leq 0.05$).

4.5.4.2.2. Electroretinogram characterisation

ERG recordings collected 8 hours after intravitreal injections were influenced either by the preceding injection or by the repeated anaesthesia, as both the saline and the LPS-injected eyes had attenuated ERGs (Figure 4.5.4.2.2.1). It is possible that 8 hours was not sufficient for the subject to recover completely from anaesthesia or increased intraocular pressure caused by the injection. Even after 24 hours the ERG amplitude of the saline eye was attenuated. After 24 hours the ERG recording was sufficiently sensitive to measure a relative reduction in ERG amplitude in the LPS-injected eye compared with the saline eye. Mice culled after 48 hours had almost indistinguishable ERGs in both eyes, while mice culled after 3 and 7 days show attenuated ERG amplitudes in LPS-injected eyes (Figure 4.5.4.2.2.1).

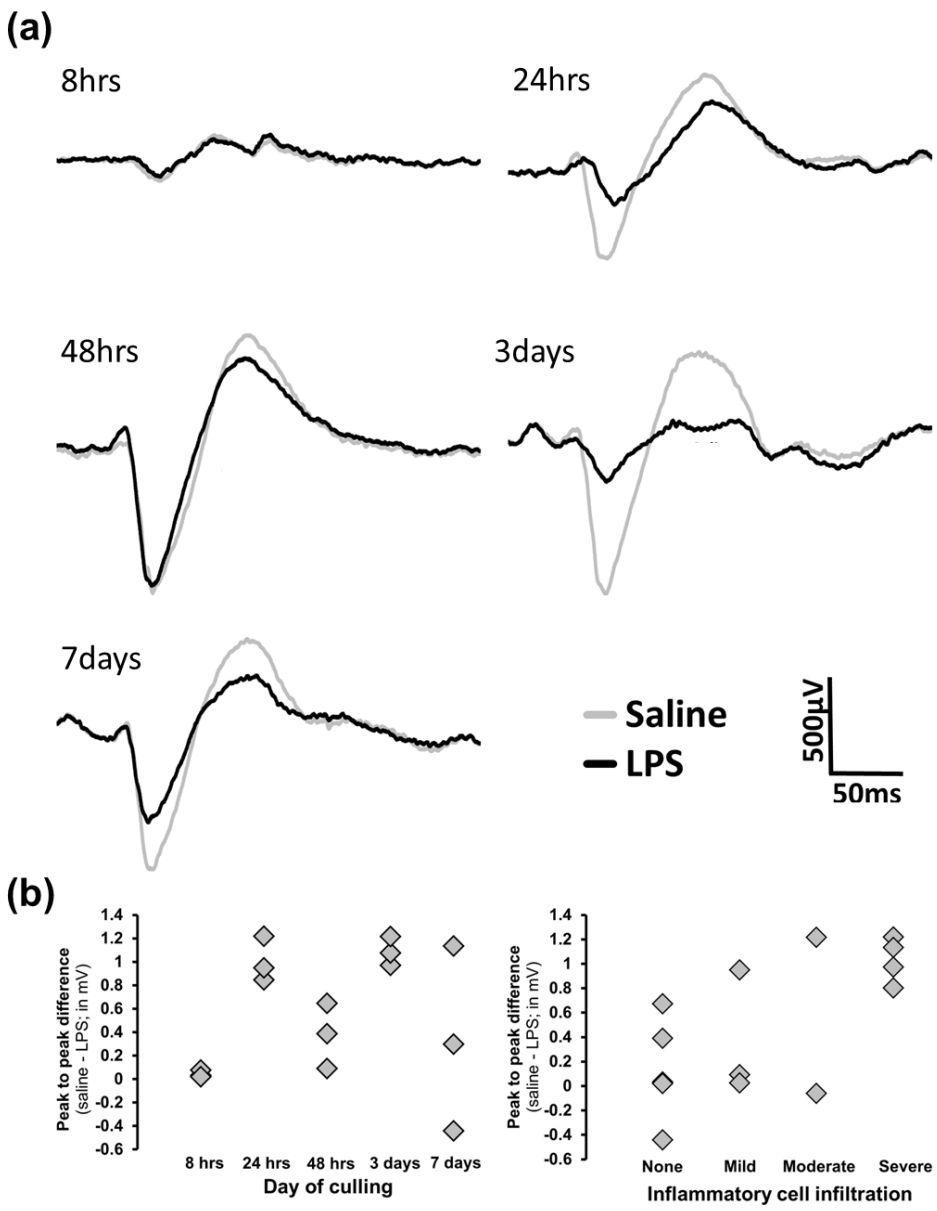

Figure 4.5.4.2.2.1: **ERG traces after intravitreal LPS/saline at different time points.**

(a) ERG traces of mice injected with 40ng of LPS into the vitreous of one eye and saline into the other, taken 8hrs, 24hrs, 48hrs, 3days and 7days post injection. **(b)** Difference in peak to peak difference between saline and LPS injected eyes sorted by day of culling, or by amount of inflammatory cell infiltration (as assessed by H&E labelling). All $p \geq 0.05$

4.5.5. Systemic LPS

Systemic inflammation was induced by an i.p. injection of LPS (1mg/kg, 3mg/kg, 5mg/kg). Mice showed a dose related clinical response ranging from mild sedation and decreased activity to somnolence, hunched appearance, piloerection and ocular discharge. They were culled 10 hours or 24 hours after injection with LPS.

4.5.5.1. (Immuno)histochemical characterisation

Inflammation in the retina and spinal cord (data not shown) was assessed using microglial morphology (Figure 4.5.5.1.1) and iNOS labelling (data not shown). Overt inflammation was not detected in the spinal cord or retina after systemic injection of LPS using either of these markers.

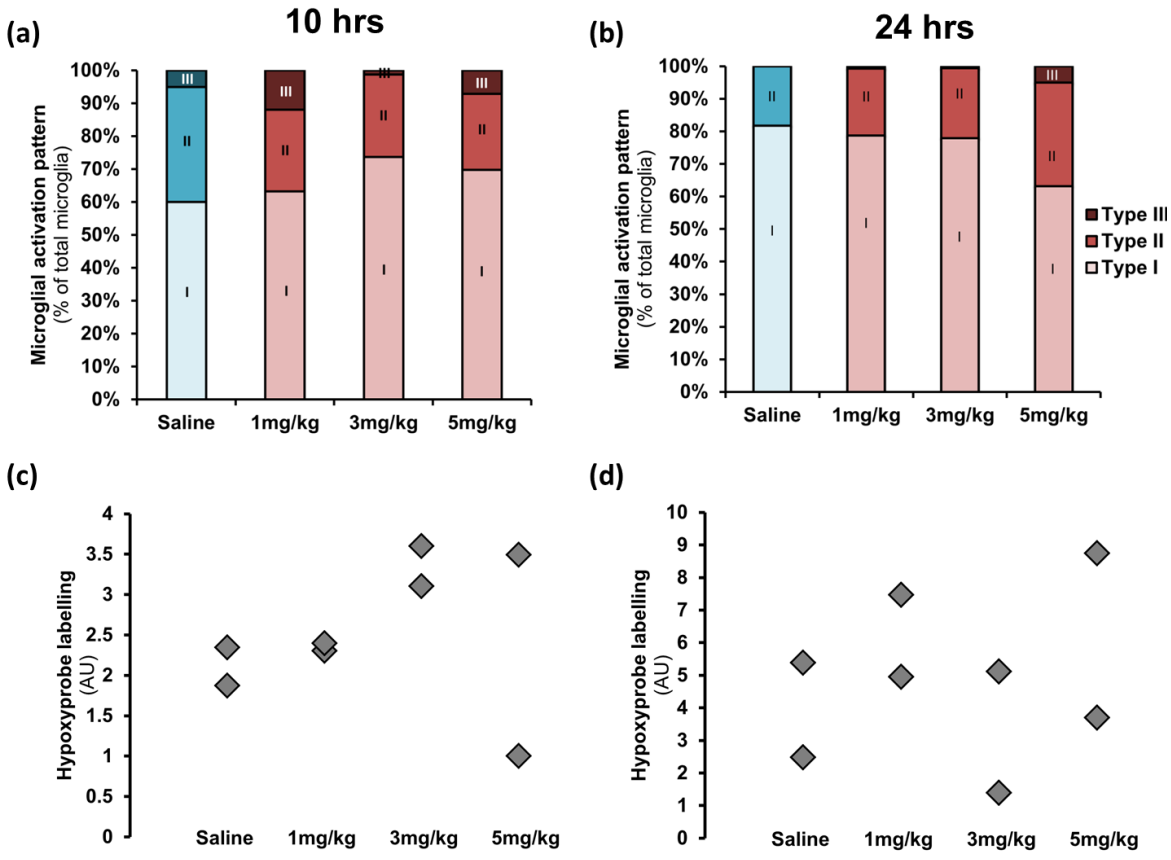

Figure 4.5.5.1.1: **Microglial activation and hypoxyprobe labelling in retinas after systemic LPS.**
Microglial activation **(a)** and **(b)** and hypoxyprobe labelling **(c)** and **(d)** in retinas of mice injected with LPS 10 hrs **(a)** and **(c)** or 24 hrs **(b)** and **(d)** prior. There is no microglial activation evident after systemic LPS injection and no relationship between LPS injection and hypoxyprobe labelling in the retina. All $p \geq 0.05$.

The slightly more activated morphology of microglia 10 hours as compared to 24 hours after saline and LPS injection (Figure 4.5.5.1.1 a and b) might be related to elevated stress levels shortly after handling and injection.

4.5.6. Normal and transgenic ($CFH^{-/-}$) ageing

In order to investigate the effect of age and factor H deficiency on retinal hypoxia we injected four groups of mice with hypoxyprobe and compared the amount of labelling between these groups (see methods for details). Two groups consisted of wild type animals (5-6 weeks vs 16-24 months) and two groups consisted of transgenic $CFH^{-/-}$ mice (4 weeks vs 14-15 months). There is no significant difference between hypoxyprobe labelling in old vs young wild type mice, while ageing in transgenic $CFH^{-/-}$ mice was associated with a significant increase in retinal hypoxyprobe labelling when compared with young $CFH^{-/-}$ mice (Figure 4.5.6.1)

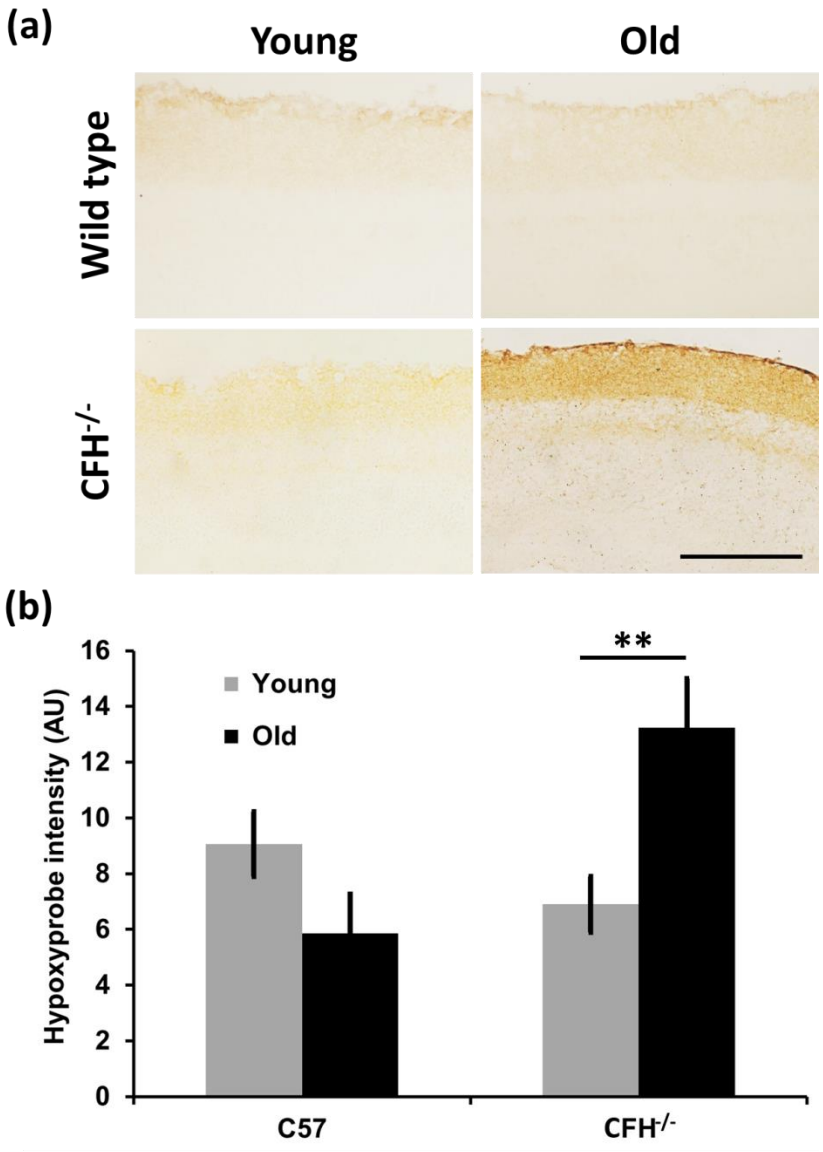

Figure 4.5.6.1: **Hypoxyprobe labelling in the retinas of old and young wild type and CFH$^{-/-}$ mice.**

(a) Example sections of old and young wild type C57bl/6 mice and CFH$^{-/-}$ mice. Scale bar = 100µm. **(b)** Quantification of the intensity of hypoxyprobe labelled retinas (from ganglion cell layer to inner segment of photoreceptors). Data displayed as mean ± SEM. ** = $p \leq 0.01$

4.5.7. Imaging flavoproteins in the retina

It was possible to image the retina using confocal microscopy (Figure 4.5.7.1 and 4.5.7.2). The oxygen inspired by a yellow fluorescent protein (YFP) positive mouse (expressing YFP in a subset of ganglion cells) was varied from 100% to 0% oxygen. The change in oxygenation caused a change in background green fluorescence, assumed to arise from flavoprotein autofluorescence. The focal plane did not change, as revealed by the consistency of the YFP positive ganglion cell body and axons (Figure 4.5.7.1).

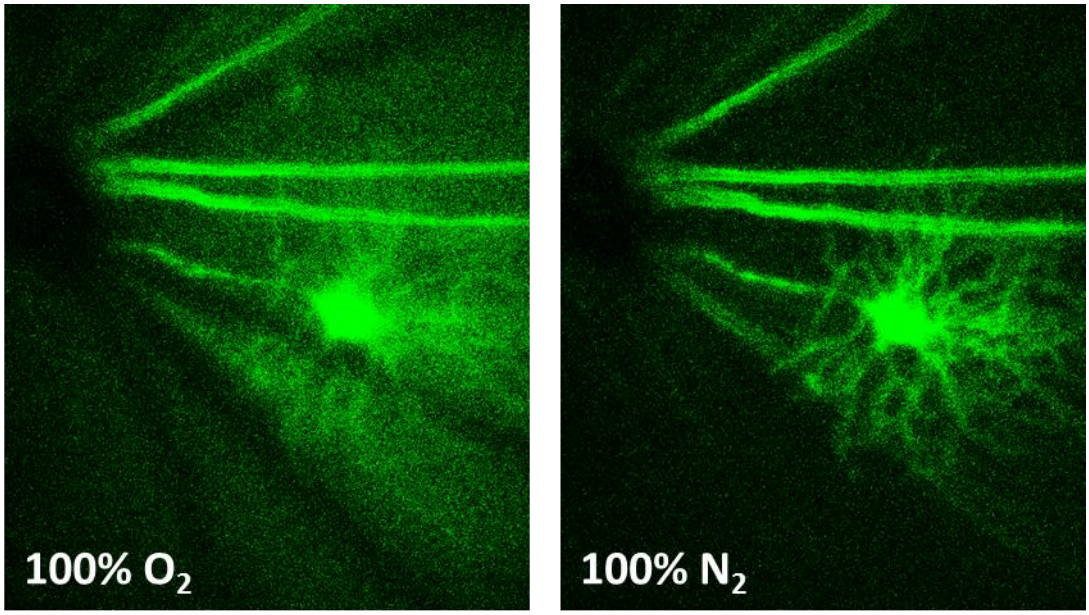

Figure 4.5.7.1: **Flavoprotein imaging in the retina of a YFP positive mouse.**
Mouse exposed to 100% O_2 and 0% O_2 (i.e. 100% nitrogen) reveals a change in the background green fluorescence. Scale bar is not determined as the optics of the eye do not allow accurate scale readings.

To allow an increase in background signal strength, YFP negative mice were imaged and confirmed the reduction in the retinal flavoprotein signal with a reduction in inspired oxygen (Figure 4.5.7.2).

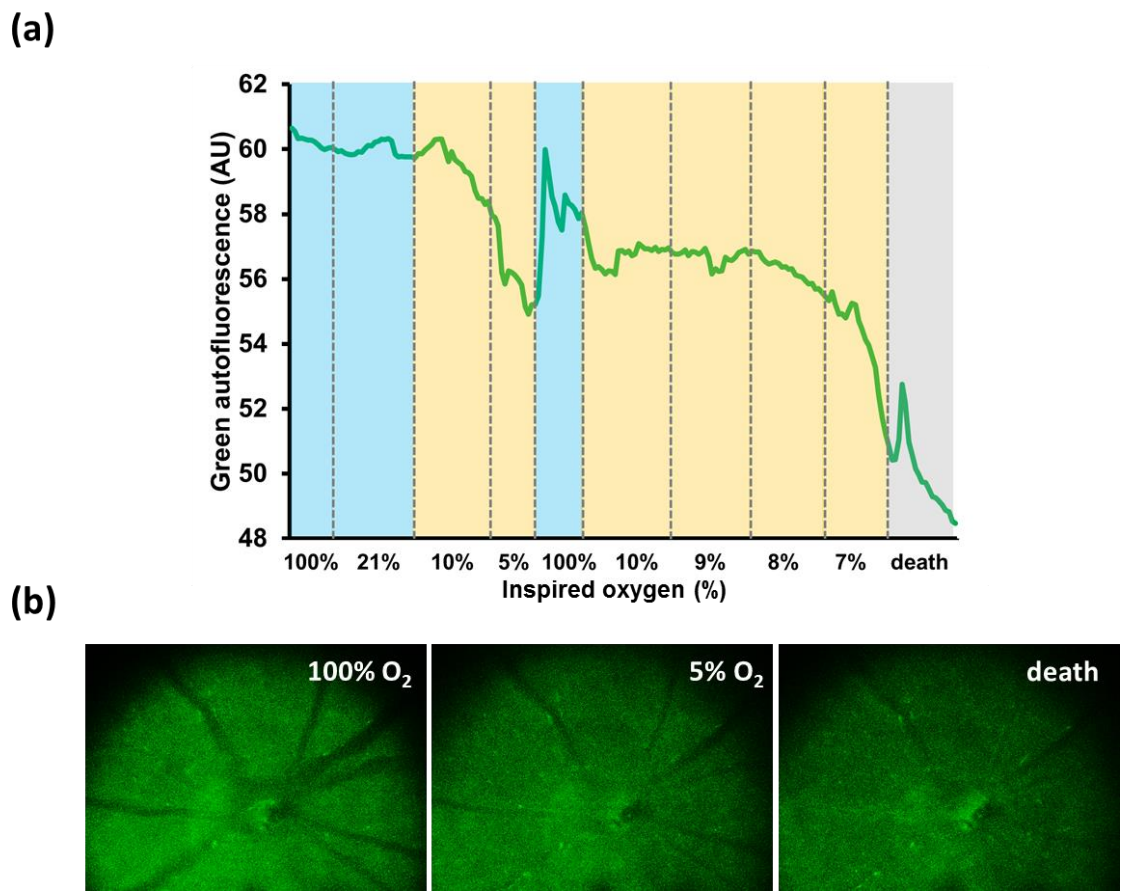

Figure 4.5.7.2: **Example of flavoprotein signal in the naïve and hypoxaemic mouse retina.** Quantification of flavoprotein signal with changes in inspired oxygen **(a)**. Representative example images of flavoprotein signal in a mouse exposed to 100% and 5% inspired oxygen, and after death **(b)**. Scale bar is not determined as the optics of the eye do not allow accurate scale readings.

4.6. Discussion

Four experimental models were examined for potential use in a project to assess the relationship between inflammation and hypoxia in the retina (EAE, local LPS, systemic LPS and $CFH^{-/-}$). We were able to demonstrate retinal inflammation in EAE and after intravitreal LPS injections and were able to show reduced amplitudes of the electroretinogram in these models. Furthermore, we found that the intravenous probe, hypoxyprobe, could indicate the presence of retinal hypoxia using the retinas of hypoxaemic mice as a positive control group. We were then able to assess hypoxyprobe labelling in the retina with inflammation during EAE, after intravitreal and systemic LPS injection and in transgenically aged $CFH^{-/-}$ knockout mice.

4.6.1. Induction of retinal inflammation

4.6.1.1. EAE

The clinical disease course of EAE induced in female BN rats using rMOG is known to result in a lethal disease with a fast onset and progression (Stefferl et al. 1999). It is furthermore known to induce opticospinal inflammation, demyelination and ganglion cell loss (Collongues et al. 2012; Meyer et al. 2001) which mimics frequently observed optical damage in MS patients (Leibowitz and Alter 1968; Mcdonald and Barnes 1992; Sorensen et al. 1999) and in neuromyelitis optica (Collongues et al. 2012; Storch et al. 1998). Therefore, this model is known to involve inflammation and demyelination of the optic nerve combined with functional visual deficits. This is in agreement with our findings. We see functional deficit (as measured by ERG) following the onset of clinical symptoms and observe immune cell activation and infiltration in the optic nerves of EAE induced rats even before observable neurological deficits. However, the involvement of the retina has as yet not been well document.

Here we report that in rMOG induced EAE, microglial morphology showed a more activated phenotype in the spinal cord compared to the retina. However, while microglial morphological changes in the spinal cord coincided with clinical symptom onset (which is manifest in tail and hind limb weakness/paralysis), changes in the retina, despite being less severe, could be seen in asymptomatic as well as symptomatic animals. This reflects a very weak correlation between retinal and spinal cord inflammation. Interestingly, most microglial activation seems to be limited to the inner retina, observed predominantly in the ganglion cell layer, suggesting that retinal inflammation may originate mainly from optic nerve inflammation. Indeed high levels of phagocytic inflammation, as assessed by ED1 expression, were found in the optic nerve of symptomatic and, to a lesser extent asymptomatic animals, but this was not seen in the retina. This suggests the possibility of severe optic nerve inflammation leading to low level secondary microglial activation in the retina. Interestingly microglial activation in the retina and microglial/macrophage activation in the optic nerve seem to precede functional deficit as measured by ERG recordings and clinical score, and there is no relationship between the level of optic nerve inflammation (as assessed by ED1 positive cell coverage) and visual deficit (as measured by ERG).

The ERG protocol was optimised to produce the strongest and most reliable signal. This includes dark adaptation for 1 hour and a stimulus intensity of 58mA with a stimulus interpulse period of 4 seconds. As shown in our experiments, this set-up was sufficient to distinguish pathological conditions from healthy vision.

The initial negative ‘A’ wave of the ERG trace is believed to reflect photoreceptor and Muller glia cell function in the form of the ‘light current’, a decrease in the dark current after absorption of the light stimulus (Penn and Hagins 1969). The positive ‘B’ wave is believed to be largely related to ON-centre bipolar cells (Dong and Hare 2002; Green and Kapousta-Bruneau 1999; Karwoski and Xu 1999) with contribution from amacrine cells and ganglion cells (Awatramani et al. 2001; Dong and Hare 2000; Dong and Hare 2002; Wurziger et al. 2001). It was

therefore not possible to localise the functional damage (as measured by ERG recordings) evident in our model to one retinal cell type, as both the 'A' and the 'B' wave component of the ERG are affected in rMOG induced EAE. The relative insensitivity of the ERG to localised changes in retinal function, due to the contribution of many layers towards the final trace, could explain the preservation of the ERG amplitude and latency in asymptomatic rats despite retinal and optic nerve inflammation. A more sensitive measure of, for example, ganglion cell function is the pattern ERG (Berardi et al. 1990) with alternating chequerboard patterns or sinusoidal gratings. This would be an interesting measure especially given the localisation of retinal inflammation to the inner retina in this model.

Additionally, we found that the development of clinical symptoms is influenced by repeated ERG measurements, reducing the number of rodents reaching clinical signs by 50%. This is likely to be related to the complex orchestra of hormones and cytokines released when an organism is stressed, e.g. following repeated anaesthetic episodes, which can include the release of anti-inflammatory steroids (Desborough 2000; Joels and Baram 2009).

4.6.1.2. Local LPS

As a component of Gram-negative bacteria, LPS can initiate an inflammatory reaction upon injection. To achieve retinal inflammation we injected mice with various concentrations of LPS into the vitreous of one eye (saline into the control eye) and culled them at different time points thereafter. The interpretation of the results was made more difficult by a large variation in the level of inflammation in the retinas of different subjects and the possibility of light physical damage to the retina, combined with LPS, resulting in complete retinal disorganisation and haemorrhage. Possibly as a result of inter-individual variation there was no demonstrable relationship between days post-injection and the level of inflammation.

It was possible to see a change in the morphology of microglia towards an activated/amoeboid phenotype following intravitreal LPS injections. Even in situations in which there was no obvious infiltration of inflammatory cells, activation of microglia was still present, confirming that the innate immune system provides the first line of defence *in situ*. Already 8 hours after an LPS injection microglial activation was evident, even without concomitant inflammatory cell infiltration. It was also evident that iNOS was upregulated in retinas during severe inflammation but was similar to saline injected counterparts in the absence of inflammatory cell infiltration or when infiltration was only mild.

ERG recordings, following intravitreal LPS injections, were effective in distinguishing retinas with severe inflammation from retinas with no inflammation, while mild or moderate inflammation did not consistently lead to reductions in ERG amplitude. However, ERG recordings were complicated by the effect of the intravitreal injection. It is possible that the anaesthetic used during the LPS injection or the increase in intraocular pressure reduced the ERG amplitude significantly at 8 hours and even 24 hours post intravitreal injection in saline and LPS injected animals. This attenuation of the healthy signal can influence the sensitivity of the ERG towards functional alterations with inflammation. Additionally *post mortem* histology revealed haemorrhage in cases with severe retinal inflammation. This, together with optical clouding from cellular infiltrates, could prevent light penetration to the retina and reduce the amplitude of the ERG traces without appropriate functional underpinnings. These factors taken together suggest that ERGs are not a good readout of retinal function after intavitreal injections of pro-inflammatory components.

4.6.1.3. Systemic LPS

Given the problems associated with the reproducibility and functional assessment of retinal inflammation induced by intravitreal LPS injections we decided to induce systemic inflammation

to assess the level of resulting retinal inflammation. Unfortunately systemic injections of all the concentrations assessed here (1mg/kg, 3mg/kg and 5mg/kg), despite resulting in a dose dependent increase in clinical signs, including ocular discharge and lethargy, did not result in any retinal inflammation. This is not in agreement with previous findings which suggested that systemic injections of LPS in the same strain of rodent can lead to retinal inflammation and damage as assessed by oxidative stress (Kubota et al. 2009; Sasaki et al. 2009), increased levels of IL-6 and iNOS mRNA (Nagai et al. 2005), leukocyte adhesion (Kubota et al. 2009; Nagai et al. 2005), astrocyte activation (Kurihara et al. 2006), reduction in retinal proteins (Kurihara et al. 2006), outer segment shortening (Sasaki et al. 2009) and function deficits (Kurihara et al. 2006; Sasaki et al. 2009). One possible explanation is that most studies used higher doses of LPS though some were only marginally higher (e.g. 6mg/kg (Kurihara et al. 2006)). Another possibility is that the previous studies used more sensitive techniques to assess retinal inflammation, including reverse transcription polymerase chain reaction enzyme-linked immunosorbent assay.

4.6.2. Hypoxia and retinal inflammation

The retina is believed to be one of the most metabolically active tissues in the body with photoreceptors consuming more oxygen than any other cell in the body (Arden et al. 2005; Hughes et al. 2010). Together with a relative avascularity this leads to a low oxygen tension in the retina under normal conditions (de Gooyer et al. 2006). This low oxygen concentration in the retina, has been suggested to be relevant in a range of visual diseases, including age-related macular degeneration and diabetic retinopathy (Arden et al. 2005; Lahdenranta et al. 2001). Hypoxia therefore, warrants a close investigation and characterisation in normal as well as pathological retinas and a histochemical investigation of hypoxia is of particular benefit as it has the potential to determine the distribution of hypoxic areas as well as their spatial and temporal correlates.

The intravenous probe, hypoxyprobe, thanks to its ability to penetrate easily into tissues and its relative safety and specificity (Lee et al. 2014), lends itself to the immunohistochemical study of hypoxia in the retina. We confirmed the applicability of hypoxyprobe to label retinal hypoxia by varying the atmospheric oxygen concentration that naïve mice were exposed to and quantifying the resulting change in DAB labelling in their retinas: A 50% decrease in environmental oxygen for 4 hours is sufficient to increase hypoxyprobe labelling in the retina. Results from this hypoxaemia study are in line with previous evidence suggesting that the inner plexiform layer is highly metabolically active and yet avascular (Yu and Cringle 2001). This putative disconnection between oxygen demand and supply would predict vulnerability towards hypoxaemia and is reflected in high levels of hypoxyprobe labelling in the inner plexiform layers of hypoxaemic mice. We also find increases in hypoxyprobe labelling in the inner segment (of photoreceptors) of mice subjected to hypoxaemia, as expected from this highly metabolic layer located in an avascular region (Figure 4.1.1.1 b (Yu and Cringle 2001)), although this finding is not as consistent as expected. Such a discrepancy might be related to the need for dark adaptation and the dark current to reach the full metabolic potential of the inner segment of the photoreceptors (Wangsa-Wirawan and Linsenmeier 2003). Additionally previous work also suggests that the nuclear layers as well as the outer segment are not highly metabolically active (Yu and Cringle 2001) which is in agreement with an absence of positive hypoxyprobe labelling in these layers, even during hypoxaemia. However, our work diverges from previous investigators who suggested that the inner retina is less prone to changes in oxygenation, compared to the outer retina, due to the adaptability of the retinal vasculature in contrast to the inflexible choroidal vasculature (Wangsa-Wirawan and Linsenmeier 2003). Instead, we find that hypoxaemia affects mainly the inner retina. This inconsistency with previous suggestions may be because the level of hypoxaemia was sufficiently high and prolonged to prevent the compensatory mechanisms offered by the retinal vasculature, or may be related to species differences.

Our results also suggest that after 1 hour there may be residual hypoxyprobe in the tissue causing spurious labelling in mice subjected to room air. Indeed the half-life of hypoxyprobe in mice is 25 minutes (Lee et al. 2014) suggesting that after 50 minutes there is approximately ¼ of the original amount in the blood of the animal. When tissue is harvested any residual amounts of hypoxyprobe may bind under the hypoxic conditions created during perfusion.

Having established hypoxyprobe as a marker of hypoxia in the retina we then explored the relationship between inflammation and hypoxia in the retina. Indeed, we found that retinas of eyes injected with LPS (into the vitreous) labelled significantly more strongly for hypoxyprobe, if inflammation was present (as assessed by inflammatory cell infiltration) as compared with their saline injected counterparts. Indeed, a positive correlation between retinal iNOS labelling (a marker of inflammation) and retinal hypoxyprobe labelling was revealed, following intravitreal LPS injection. In contrast we found only a very mild, non-significant relationship between the clinical presentation of EAE and hypoxyprobe labelling. Additionally, in the absence of retinal inflammation, during systemic endotoxemia, we found no increase in hypoxyprobe labelling. These findings strongly suggest that hypoxyprobe labelling is only robustly increased during high levels of inflammation.

While normally aged retinas were not significantly different from young retinas, enhanced hypoxyprobe labelling was observed in the aged $CFH^{-/-}$ retinas. This is in line with reports suggesting an essential role for complement factor H in the maintenance of retinal perfusion in age (von Leithner et al. 2009). Here the authors found significant deposits of the C3 and C3b complement components along retinal vessels and Bruch's membrane of aged knockout mice (von Leithner et al. 2009). Furthermore, C3b deposition was associated with vascular constrictions (von Leithner et al. 2009), suggesting a detrimental effect on local perfusion. Overall, there was a reduction in vessel density in aged $CFH^{-/-}$ mice together with a withering of the remaining network. Additionally perfusion rates, as assessed by fluorescein uptake and clearance, were reduced in aged

knockout mice and compromised perfusion was confirmed through reduced leakage of intravenous dextra (von Leithner et al. 2009) following laser lesions (von Leithner et al. 2009). These findings provide a reasonable explanation for enhanced hypoxyprobe labelling only in aged $CFH^{-/-}$ as vascular changes, indicative of hypoperfusion, were only evident in transgenic mice with aged wild type mice showing no obvious abnormalities. This has potential implications for age-related macular degeneration in which nucleotide substitutions of the CFH gene are common (Coffey et al. 2007; von Leithner et al. 2009). However, it should be noted that the CFH deficient mouse model only reflects some of the characteristic changes seen in human AMD with one of the major differences being reduced plasma C3 concentration in knockout mice, with preserved levels in human patients.

Inflammation could lead to hypoxia due to the increased energetic demand of an inflammatory environment (Eltzschig and Carmeliet 2011), which may include hypercellularity or increased use of oxygen for non-energetic needs, like free radical production. Additionally, inflammation may decrease the supply of oxygen via thrombosis or compression (Eltzschig and Carmeliet 2011) as well as leading to endothelial cell and vascular damage (von Leithner et al. 2009). Such factors may be particularly relevant in the eye where the blood supply is physiologically limited due to the need for clear optics (Yu and Cringle 2001).

4.6.3. *In vivo* retinal imaging

The assessment of the retina, even in humans, using confocal microscopy, has seen huge advances in recent years with the development and use of the (confocal) scanning laser ophthalmoscope (Helb et al. 2010; Wollstein et al. 1998). These advances also include the use of retinal autofluorescence, for example in the investigation of geographic atrophy in AMD (Holz et al. 2001). In the current work we have assessed the use of flavoprotein autofluorescence for the visualization of mitochondrial function in retinal inflammation.

It was possible to image the back of the eye, using standard confocal microscopy. The method was initially developed using transgenic mice expressing YFP in a subset of retinal ganglion cells. It was possible to show reductions in background green autofluorescence (also replicated in YFP negative mice) with a decrease in inspired oxygen, which, as in the cortex, was reversible upon re-oxygenation. However, it is also clear that the ratio of flavoprotein fluorescence (oxygen sensitive fluorescence) to other green autofluorescence (insensitive to change in inspired oxygen) in the retina is not as substantial as in the brain. This finding is in line with the high lipofuscin and melanin content in the retina (Bindewald et al. 2004; Wabbels et al. 2006). Lipofuscin, in particular, accumulates in the retinal pigment epithelium as a result of photoreceptor outer segment phagocytosis, and fluoresces strongly in the same wavelengths as flavoproteins (Bindewald et al. 2004; Delori et al. 1995; Wabbels et al. 2006). The relatively low signal (flavoprotein fluorescence) to noise (other green fluorescence) ratio, may prove particularly detrimental when assessing mitochondrial redox potential in conditions that could change the optics of the eye, including inflammation and ageing, which may reduce the signal to noise ratio even further. Therefore, longitudinal interventions and assessment may be necessary, including for example changes in retinal flavoprotein signal in response to hypoxaemia, but may limit the possible study designs applicable to retinal flavoprotein imaging.

4.7. Limitations and further research

It is evident that the induction of reliable and reproducible levels of retinal inflammation has encountered some problems. Local injection of endotoxin has provided the highest level of retinal inflammation but it was frequently concomitant with haemorrhage and other complications, leading to problems with ERG recordings and *in vivo* retinal imaging, resulting from optical clouding and the obstruction of light as well as possible alterations of aqueous fluid dynamics (Forrester 1991).

The effects of systemic LPS seem not to cross the blood retinal barrier effectively, thereby preventing the induction of retinal inflammation, at least with our detection methods. Instead, systemic endotoxemia may be more effective in inducing retinal inflammation when the blood retinal barrier is damaged, by for example co-injecting agents that can induce blood brain/retinal barrier breakdown (Argaw et al. 2009; Azmin et al. 1985; Saija et al. 1997). However, it should be noted that these agents may have effects outside the blood brain barrier which should be considered before administration. Blood brain/retinal barrier weakening also occurs in ageing (Chan-Ling et al. 2007; Hughes et al. 2006; Popescu et al. 2009) and could provide a feasible alternative for the induction of retinal inflammation using systemic injections of endotoxins. However, again several other factors change with ageing which need to be evaluated in the experimental design.

The use of an autoimmune disease model to study retinal inflammation has shown some promise by providing reproducible but very mild levels of retinal inflammation. This is likely to be related to the use of a myelin antigen which resulted in strong optic nerve inflammation (where myelin is abundant) with possibly secondary retinal inflammation. This could be counteracted by using a retinal antigen (for example interphotoreceptor binding protein (Fox et al. 1987), S-antigen (Dekozak et al. 1981), or rhodopsin (Schalken et al. 1988)) to induce experimental autoimmune uveitis.

In conditions in which strong retinal inflammation was induced we were also able to show an increase in hypoxyprobe labelling, suggesting a relationship between hypoxia and inflammation. However, it should be noted that to make firm conclusions on the relationship between hypoxia and inflammation other markers of hypoxia should be used, including the use of invasive oxygen probes. Nevertheless, we have gone one step further in assessing this relationship by replicating a finding from spinal cord inflammation, which has been validated using intraspinal oxygen probe measures (Davies et al. 2013), in the retina using different inflammatory insults. What we have not replicated however, is the relationship between hypoxia and functional deficits. A future project based on the therapeutic use of oxygen during retinal inflammation is necessary to comment on the causal role played by hypoxia in retina dysfunction during inflammation.

4.8. Conclusion

We find that retinal inflammation can be induced by inravitreal injections of LPS and, to a lesser extent, by immunisation with a MOG antigen. Such inflammation can lead to a corresponding decrease in ERG amplitude which however is complicated during severe retinal inflammation by possible haemorrhage and ocular opacity due to inflammatory cell infiltrates. Additionally, high levels of inflammation as well as transgenic $CFH^{-/-}$ ageing led to an increase in hypoxyprobe labelling which suggests the presence of hypoxia. Finally, we showed that it is possible to assess mitochondrial flavoprotein fluorescence in the naïve mouse retina, using standard confocal microscopy.

CHAPTER FIVE

5. Final discussion and clinical relevance

The work presented in this thesis provides evidence that certain types of inflammatory conditions can be associated with low oxygen levels in CNS organs and that this can have implications for mitochondrial function. Additionally, we show that it is possible to assess mitochondrial redox state *in vivo* with high spatial and temporal resolution in both the brain and the retina.

Following the observation that systemic inflammation can lead to cerebral hypoxia and resulting increases in mitochondrial vulnerability to hypoxaemia (as assessed by changes in flavoprotein fluorescence) we report an investigation of several models of retinal inflammation, assessing their reliability, their level of inflammation, and their applicability to confocal assessment of retinal flavoproteins. Overall the attempt to find a reliable model of retinal inflammation that would allow longitudinal assessment of changes in flavoprotein fluorescence was problematic as only very high levels of inflammation, or an aged transgenically induced model of AMD, led to tissue hypoxia (as assessed by hypoxyprobe labelling). These very high levels of inflammation and aged transgenic AMD models are not conducive to longitudinal assessment of flavoprotein fluorescence as the optical clouding associated with high level ocular inflammation and ageing can obscure clear vision of the retina. This does not however prevent the assessment of the differential vulnerability of mitochondria to additional insults (e.g. hypoxaemia) during inflammation.

There are two main reasons why considerable effort has been invested in the use of flavoprotein assessment during retinal inflammation. First of all the retina is highly sensitive to reductions in oxygen, given the necessarily limited nature of the retinal vasculature (constrained due to the need for clear optics (Yu and Cringle 2001)), combined with a high metabolic activity (Ames 1992; Anderson 1968; Toernquist and Alm 1979; Wangsa-Wirawan and Linsenmeier 2003). Indeed, as shown in chapter 4 parts of the retina (including the highly metabolically active inner segment of the photoreceptors (Yu and Cringle 2001)) are located in avascular regions. Therefore the consequences associated with inflammation-induced hypoxia would be predicted to have an even greater impact on the retina in comparison with more vascularised tissues. Secondly, the retina which has been considered as a 'window on the brain' (Cordeiro et al. 2004), provides significant clinical potential. It is the only CNS organ that can be visualised non-invasively giving potential for use in the clinic in which (confocal) scanning laser ophthalmoscopes are already in regular use (Helb et al. 2010; Wollstein et al. 1998). By determining correction factors for ocular clouding or by using longitudinal designs which include the introduction of additional insults (e.g. hypoxaemia) and assessing the response of the flavoprotein signal to these insults, it might still be possible to explore the use of flavoprotein fluorescence in human subjects.

Additionally, our findings on systemic inflammation and cortical hypoxia together with their implications on mitochondrial function provide clinically relevant information. We report that increased mitochondrial vulnerability towards hypoxaemia during systemic endotoxemia (as assessed by changes in flavoprotein fluorescence) can be attenuated by energy conserving treatments (such as hypothermia). Despite the limitations of the model used (described in chapter 2) these findings suggest that such treatments may provide potential in the clinical setting. As mentioned in the introduction (chapter 1) a clinical trial on L-NMMA (a nitric oxide synthase inhibitor) had to be terminated prematurely due to a higher mortality rate in the treatment group (Grover et al. 1999). Given that inhibition of NOS can lead to enhanced metabolism and oxygen

consumption, (Laycock et al. 1998; Shen et al. 1994) the failure of the trial could be explained using the results from this thesis which suggest that an increase in mitochondrial oxygen consumption (e.g. through induced normothermia or L-NMMA administration) may be detrimental during systemic inflammation and sepsis. Therefore, treatments which enhance organ perfusion, such as nitroglycerine (Spronk et al. 2002), together with mild inhibitors of metabolism, might restore the energetic imbalances reported in sepsis by us and others, e.g. (Balestra et al. 2009), and so provide patients the energetic capacity to survive and recover.

5.1. Future directions

The data reported here show that inflammation can cause tissue hypoxia in different organs, including the brain, during systemic inflammation, and in the retina during local intravitreal inflammation and inflammation-enhanced ageing. Furthermore the data reported here also link this inflammatory hypoxia with mitochondrial dysfunction in the cerebral cortex of endotoxic mice. However, several questions were not answered:

1) Does the inflammation-associated hypoxia originate from a compromised supply of oxygen, or from an excessive demand? To explore this question it would be interesting to investigate whether vascular dysfunction, including endothelial cell dysfunction, impaired red blood cell deformability, hypovolaemia and/or microcirculatory heterogeneity, increase the presence of hypoxic foci in the CNS during inflammation. Equally, enhanced oxygen demand may play a role in the presence of hypoxia, which could be related to an increase in metabolic rate, mitochondrial uncoupling, hypercellularity and/or increased consumption of oxygen for the production of reactive oxygen and reactive nitrogen species.
2) Although hypothermia was protective against the enhanced vulnerability of cortical mitochondria during systemic inflammation, the mechanism by which protection was

achieved has not been explored. There are multiple ways in which hypothermia may be protective in this model, including enhanced oxygenation of the hypoxic tissue by reducing metabolic demand for oxygen, or increasing blood flow. Additionally, hypothermia is known to suppress the immune system thereby potentially reducing immune-mediated damage.

3) Although hypoxia was assessed during inflammatory conditions both in the retina and the cortex through the use of hypoxyprobe labelling and oxygen probe measurements respectively, we did not specify the cell types exhibiting hypoxia (although a previous study associating spinal cord inflammation with hypoxia suggested global tissue hypoxia (Davies et al. 2013)), or which cell types are particularly vulnerable to hypoxia. It is known that glial cells are capable of generating ATP via glycolysis (Funfschilling et al. 2012; Pellerin and Magistretti 1994; Volobоueva et al. 2013) while neurons rely primarily on oxidative metabolism (Almeida et al. 2001; Belanger et al. 2011; Herrero-Mendez et al. 2009), which would place them in a potentially more vulnerable position.

4) As mentioned above, the clinical applications of the described work should be explored in more detail. This includes both the administration of hypothermia (or other energy conserving therapies in different models of sepsis) as well as the use of retinal flavoprotein imaging as a window on the energetics of the brain.

5.2. Conclusion

Overall, this thesis aimed to explore the possibility of flavoprotein imaging in the cerebral cortex and retina of anaesthetised mice, and to investigate the relationship between mitochondrial function, tissue oxygen and inflammation in these two CNS organs. The findings reveal that it is possible to use flavoprotein fluorescence to indicate mitochondrial redox potential *in vivo* in both

the brain and the retina. Using this technique, as well as other established methods, we have shown a relationship between systemic inflammation and cortical hypoxia, and the functional consequences with regard to mitochondrial vulnerability towards additional energetic insults such as hypoxaemia. We hypothesized that the enhanced sensitivity (both in terms of mitochondrial flavoprotein fluorescence and survival) was related to energetic dysfunction due to an imbalance between oxygen demand and supply. We further explored the hypothesis regarding an energetic imbalance by showing that hypothermia, known to decrease metabolic demand in a response suggestive of hibernation (Protti and Singer 2006), attenuated increased mitochondrial vulnerability towards hypoxaemia.

Having established this functionally relevant relationship between inflammation, hypoxia and mitochondrial function we wanted to explore the link between inflammation and hypoxia in another CNS organ, the retina. This investigation was combined with an attempt at assessing mitochondrial redox state (through flavoprotein fluorescence) in the retina *in vivo* in order to develop a 'window' to the inflamed brain with an aim at clinical applicability. However, the level of retinal inflammation achieved in our experiments was relatively binary, with very mild inflammation, primarily limited to the retinal-vitreal interface, or complete retinal disorganisation (including haemorrhage), being the predominant outcomes. In the case of very mild inflammation, hypoxia was not readily evident (as assessed by hypoxyprobe labelling), while higher levels of inflammation were not very encouraging for the purpose of *in vivo* imaging, as optical clouding would confound absolute measurements of flavoprotein fluorescence. However, as with cortical flavoprotein imaging it may be possible to utilize experimental designs with longitudinal manipulations which would allow for normalised readouts.

Our findings provide insight into the consequences of sepsis and systemic/CNS inflammation, and reveal an opportunity for therapies based on the correction of energetic

deficiencies reported in some inflammatory conditions. The observations also establish a tool for the investigation of mitochondrial function in both the brain and the retina.

References

Adam, N., Kandelman, S., Mantz, J., Chretien, F., & Sharshar, T. 2013. Sepsis-induced brain dysfunction. *Expert Review of Anti-Infective Therapy*, 11, (2) 211-221

Adib-Conquy, M. & Cavaillon, J.M. 2009. Compensatory anti-inflammatory response syndrome. *Thromb.Haemost.*, 101, (1) 36-47

Akiyama, H. 2000. Inflammation in Alzheimer's disease. *Brain Pathol.*, 10, (4) 707-708

Akiyama, H., Barger, S., Barnum, S., Bradt, B., Bauer, J., Cole, G.M., Cooper, N.R., Eikelenboom, P., Emmerling, M., Fiebich, B.L., Finch, C.E., Frautschy, S., Griffin, W.S.T., Hampel, H., Hull, M., Landreth, G., Lue, L.F., Mrak, R., Mackenzie, I.R., Mcgeer, P.L., O'Banion, M.K., Pachter, J., Pasinetti, G., Plata-Salaman, C., Rogers, J., Rydel, R., Shen, Y., Streit, W., Strohmeyer, R., Tooyoma, I., Van Muiswinkel, F.L., Veerhuis, R., Walker, D., Webster, S., Wegrzyniak, B., Wenk, G., & Wyss-Coray, T. 2000. Inflammation and Alzheimer's disease. *Neurobiol.Aging*, 21, (3) 383-421

Albelda, S.M., Smith, C.W., & Ward, P.A. 1994. Adhesion Molecules and Inflammatory Injury. *FASEB J.*, 8, (8) 504-512

Alberti, C., Brun-Buisson, C., Burchardi, H., Martin, C., Goodman, S., Artigas, A., Sicignano, A., Palazzo, M., Moreno, R., Boulme, R., Lepage, E., & Le Gall, J.R. 2002. Epidemiology of sepsis and infection in ICU patients from an international multicentre cohort study. *Intensive Care Med.*, 28, (2) 108-121

Alexander, J.J., Pickering, M.C., Haas, M., Osawe, I., & Quigg, R.J. 2005. Complement factor H limits immune complex deposition and prevents inflammation and scarring in glomeruli of mice with chronic serum sickness. *Journal of the American Society of Nephrology*, 16, (1) 52-57

Allen, J.B., Keng, T., & Privalle, C. 1998. Nitric oxide and peroxynitrite production in ocular inflammation. *Environmental Health Perspectives*, 106, 1145-1149

Almeida, A., Almeida, J., Bolanos, J.P., & Moncada, S. 2001. Different responses of astrocytes and neurons to nitric oxide: The role of glycolytically generated ATP in astrocyte protection. *Proc.Natl.Acad.Sci.U.S.A.*, 98, (26) 15294-15299

Ames, A. 1992. Energy-Requirements of Cns Cells As Related to Their Function and to Their Vulnerability to Ischemia - A Commentary Based on Studies on Retina. *Can.J.Physiol.Pharmacol.*, 70, S158-S164

Ames, A. & Nesbett, F.B. 1981. In vitro retina as an experimental model of the central nervous system. *J.Neurochem.*, 37, (4) 867-877

Anderson, B. 1968. Ocular effects of changes in oxygen and carbon dioxide tension. *Transactions of the American Ophthalmological Society*, 66, 423-474

Anderson, D.H., Mullins, R.F., Hageman, G.S., & Johnson, L.V. 2002. Perspective - A role for local inflammation in the formation of drusen in the aging eye. *Am.J.Ophthalmol.*, 134, (3) 411-431

Andersson, H., Baechi, T., Hoechl, M., & Richter, C. 1998. Autofluorescence of living cells. *Journal of Microscopy-Oxford*, 191, 1-7

Andreyev, A.I., Kushnareva, Y.E., & Starkov, A.A. 2005. Mitochondrial metabolism of reactive oxygen species. *Biochemistry-Moscow*, 70, (2) 200-214

Anesi, S.D. & Foster, C.S. 2012. Importance of Recognizing and Preventing Blindness From Juvenile Idiopathic Arthritis-Associated Uveitis. *Arthritis Care & Research*, 64, (5) 653-657

Anning, P.B., Sair, M., Winlove, C.P., & Evans, T.W. 1999. Abnormal tissue oxygenation and cardiovascular changes in endotoxemia. *Am.J.Respir.Crit.Care Med.*, 159, (6) 1710-1715

Arden, G.B., Sidman, R.L., Arap, W., & Schlingemann, R.O. 2005. Spare the rod and spoil the eye. *British Journal of Ophthalmology*, 89, (6) 764-769

Argaw, A.T., Gurfein, B., Zhang, Y., Zameer, A., & John, G. 2009. VEGF-mediated disruption of endothelial CLN-5 promotes blood-brain barrier breakdown. *Mult.Scler.*, 15, (9) S91

Aslan, M., Yucel, I., Ciftcioglu, A., Savas, B., Akar, Y., Yucel, G., & Sanlioglu, S. 2007. Corneal protein nitration in experimental uveitis. *Experimental Biology and Medicine*, 232, (10) 1308-1313

Astiz, M., Rackow, E.C., Weil, M.H., & Schumer, W. 1988. Early Impairment of Oxidative-Metabolism and Energy-Production in Severe Sepsis. *Circ.Shock*, 26, (3) 311-320

Astiz, M.E., Degent, G.E., Lin, R.Y., & Rackow, E.C. 1995. Microvascular Function and Rheological Changes in Hyperdynamic Sepsis. *Crit.Care Med.*, 23, (2) 265-271

Astiz, M.E., Tilly, E., Rackow, E.D., & Weil, M.H. 1991. Peripheral Vascular Tone in Sepsis. *Chest*, 99, (5) 1072-1075

Awatramani, G., Wang, J., & Slaughter, M.M. 2001. Amacrine and ganglion cell contributions to the electroretinogram in amphibian retina. *Vis.Neurosci.*, 18, (1) 147-156

Ayata, C., Jin, H.W., Kudo, C., Dalkara, T., & Moskowitz, M.A. 2006. Suppression of cortical spreading depression in migraine prophylaxis. *Ann.Neurol.*, 59, (4) 652-661

Azmin, M.N., Stuart, J.F.B., & Florence, A.T. 1985. The Distribution and Elimination of Methotrexate in Mouse-Blood and Brain After Concurrent Administration of Polysorbate-80. *Cancer Chemother.Pharmacol.*, 14, (3) 238-242

Babior, B.M. 1984. The Respiratory Burst of Phagocytes. *J.Clin.Invest.*, 73, (3) 599-601

Balestra, G.M., Legrand, M., & Ince, C. 2009. Microcirculation and mitochondria in sepsis: getting out of breath. *Curr.Opin.Anaesthesiol*, 22, (2) 184-190

Bamforth, S.D., Lightman, S., & Greenwood, J. 1996. The effect of TNF-alpha and IL-6 on the permeability of the rat blood-retinal barrier in vivo. *Acta Neuropathol.(Berl).*, 91, (6) 624-632

Banati, R.B., Gehrmann, J., Schubert, P., & Kreutzberg, G.W. 1993. Cytotoxicity of Microglia. *Glia*, 7, (1) 111-118

Bandy, B. & Davison, A.J. 1990. Mitochondrial Mutations May Increase Oxidative Stress - Implications for Carcinogenesis and Aging. *Free Radical Biol.Med.*, 8, (6) 523-539

Barnum, S.R. 2002. Complement in central nervous system inflammation. *Immunologic Research*, 26, (1-3) 7-13

Bateman, R.M., Jagger, J.E., Sharpe, M.D., Ellsworth, M.L., Mehta, S., & Ellis, C.G. 2001. Erythrocyte deformability is a nitric oxide-mediated factor in decreased capillary density during sepsis. *Am.J.Physiol-Heart.C.*, 280, (6) H2848-H2856

Bateman, R.M., Sharpe, M.D., & Ellis, C.G. 2003. Bench-to-bedside review: Microvascular dysfunction in sepsis - hemodynamics, oxygen transport, and nitric oxide. *Crit.Care*, 7, (5) 359-373

Bateman, R.M. & Walley, K.R. 2005. Microvascular resuscitation as a therapeutic goal in severe sepsis. *Crit.Care*, 9, S27-S32

Belanger, M., Allaman, I., & Magistretti, P.J. 2011. Brain Energy Metabolism: Focus on Astrocyte-Neuron Metabolic Cooperation. *Cell Metabolism*, 14, (6) 724-738

Bennett, J.L. & Stuve, O. 2009. Update on Inflammation, Neurodegeneration, and Immunoregulation in Multiple Sclerosis: Therapeutic Implications. *Clin.Neuropharmacol.*, 32, (3) 121-132

Benz, R. & Mclaughlin, S. 1983. The Molecular Mechanism of Action of the Proton Ionophore Fccp (Carbonylcyanide Para-Trifluoromethoxyphenylhydrazone). *Biophys.J.*, 41, (3) 381-398

Berardi, N., Domenici, L., Gravina, A., & Maffei, L. 1990. Pattern Erg in Rats Following Section of the Optic-Nerve. *Experimental Brain Research*, 79, (3) 539-546

Bergofsk, E.H. & Bertun, P. 1966. Response of Regional Circulations to Hyperoxia. *J.Appl.Physiol.*, 21, (2) 567-&

Bernard, S.A. & Buist, M. 2003. Induced hypothermia in critical care medicine: A review. *Crit.Care Med.*, 31, (7) 2041-2051

Bernardi, P., Veronese, P., & Petronilli, V. 1993. Modulation of the Mitochondrial Cyclosporine A-Sensitive Permeability Transition Pore .1. Evidence for 2 Separate Me2+ Binding-Sites with Opposing Effects on the Pore Open Probability. *J.Biol.Chem.*, 268, (2) 1005-1010

Bindewald, A., Jorzik, J.J., Loesch, A., Schutt, F., & Holz, F.G. 2004. Visualization of retinal pigment epithelial cells in vivo using digital high-resolution confocal scanning laser ophthalmoscopy. *Am.J.Ophthalmol.*, 137, (3) 556-558

Biousse, V., Trichet, C., Bloch-Michel, E., & Roullet, E. 1999. Multiple sclerosis associated with uveitis in two large clinic-based series. *Neurology*, 52, (1) 179-181

Blacker, T.S., Mann, Z.F., Gale, J.E., Ziegler, M., Bain, A.J., Szabadkai, G., & Duchen, M.R. 2014. Separating NADH and NADPH fluorescence in live cells and tissues using FLIM. *Nature Communications*, 5,

Blacker, T.S., Marsh, R.J., Duchen, M.R., & Bain, A.J. 2013. Activated barrier crossing dynamics in the non-radiative decay of NADH and NADPH. *Chem.Phys.*, 422, 184-194

Block, M.L. & Hong, J.S. 2005. Microglia and inflammation-mediated neurodegeneration: Multiple triggers with a common mechanism. *Prog.Neurobiol.*, 76, (2) 77-98

Boekstegers, P., Weidenhofer, S., Kapsner, T., & Werdan, K. 1994. Skeletal-Muscle Partial-Pressure of Oxygen in Patients with Sepsis. *Crit.Care Med.*, 22, (4) 640-650

Boekstegers, P., Weidenhofer, S., Pilz, G., & Werdan, K. 1991. Peripheral Oxygen Availability Within Skeletal-Muscle in Sepsis and Septic Shock - Comparison to Limited Infection and Cardiogenic-Shock. *Infection*, 19, (5) 317-323

Bolanos, J.P., Heales, S.J.R., Land, J.M., & Clark, J.B. 1995. Effect of Peroxynitrite on the Mitochondrial Respiratory-Chain - Differential Susceptibility of Neurons and Astrocytes in Primary Culture. *J.Neurochem.*, 64, (5) 1965-1972

Bone, R.C. 1991. The Pathogenesis of Sepsis. *Ann.Intern.Med.*, 115, (6) 457-469

Bone, R.C., Grodzin, C.J., & Balk, R.A. 1997. Sepsis: A new hypothesis for pathogenesis of the disease process. *Chest*, 112, (1) 235-243

Bopp, C., Bierhaus, A., Hofer, S., Bouchon, A., Nawroth, P.P., Martin, E., & Weigand, M.A. 2008. Bench-to-bedside review: The inflammation-perpetuating pattern-recognition receptor RAGE as a therapeutic target in sepsis. *Crit.Care*, 12, (1)

Bouzier-Sore, A.K., Voisin, P., Bouchaud, V., Bezancon, E., Franconi, J.M., & Pellerin, L. 2006. Competition between glucose and lactate as oxidative energy substrates in both neurons and astrocytes: a comparative NMR study. *Eur.J.Neurosci.*, 24, (6) 1687-1694

Boveris, A. & Chance, B. 1973. The Mitochondrial Generation of Hydrogen Peroxide. *Biochem.J.*, 134, 707-716

Bowton, D.L., Bertels, N.H., Prough, D.S., & Stump, D.A. 1989. Cerebral Blood-Flow Is Reduced in Patients with Sepsis Syndrome. *Crit.Care Med.*, 17, (5) 399-403

Brealey, D., Brand, M., Hargreaves, I., Heales, S., Land, J., Smolenski, R., Davies, N.A., Cooper, C.E., & Singer, M. 2002. Association between mitochondrial dysfunction and severity and outcome of septic shock. *Lancet*, 360, (9328) 219-223

Brealey, D., Karyampudi, S., Jacques, T.S., Novelli, M., Stidwill, R., Taylor, V., Smolenski, R.T., & Singer, M. 2004. Mitochondrial dysfunction in a long-term rodent model of sepsis and organ failure. *American Journal of Physiology-Regulatory Integrative and Comparative Physiology*, 286, (3) R491-R497

Brealey, D. & Singer, M. 2003. Mitochondrial dysfunction in sepsis. *Curr.Infect.Dis.Rep*, 5, (5) 365-371

Brennan, A.M., Connor, J.A., & Shuttleworth, C.W. 2006. NAD(P)H fluorescence transients after synaptic activity in brain slices: predominant role of mitochondrial function. *J.Cereb.Blood Flow Metab.*, 26, (11) 1389-1406

Brenner, C. & Moulin, M. 2012. Physiological Roles of the Permeability Transition Pore. *Circul.Res.*, 111, (9) 1237-1247

Bressler, N.M., Bressler, S.B., & Fine, S.L. 1988. Age-Related Macular Degeneration. *Surv.Ophthalmol.*, 32, (6) 375-413

Brookes, P.S., Land, J.M., Clark, J.B., & Heales, S.J.R. 1998. Peroxynitrite and brain mitochondria: Evidence for increased proton leak. *J.Neurochem.*, 70, (5) 2195-2202

Brown, G.C. 1995. Nitric-Oxide Regulates Mitochondrial Respiration and Cell Functions by Inhibiting Cytochrome-Oxidase. *FEBS Lett.*, 369, (2-3) 136-139

Brown, G.C. 2001. Regulation of mitochondrial respiration by nitric oxide inhibition of cytochrome c oxidase. *Biochimica et Biophysica Acta-Bioenergetics*, 1504, (1) 46-57

Brown, G.C. & Bal-Price, A. 2003. Inflammatory neurodegeneration mediated by nitric oxide, glutamate, and mitochondria. *Mol.Neurobiol.*, 27, (3) 325-355

Brown, G.C. & Cooper, C.E. 1994. Nanomolar Concentrations of Nitric-Oxide Reversibly Inhibit Synaptosomal Respiration by Competing with Oxygen at Cytochrome-Oxidase. *FEBS Lett.*, 356, (2-3) 295-298

Bruins, M.J., Lamers, W.H., Meijer, A.J., Soeters, P.B., & Deutz, N.E.P. 2002. In vivo measurement of nitric oxide production in porcine gut, liver and muscle during hyperdynamic endotoxaemia. *Br.J.Pharmacol.*, 137, (8) 1225-1236

Buschini, E., Piras, A., Nuzzi, R., & Vercelli, A. 2011. Age related macular degeneration and drusen: Neuroinflammation in the retina. *Progress in Neurobiology*, 95, (1) 14-25

Cabrales, P., Vazquez, B.Y.S., Tsai, A.G., & Intaglietta, M. 2007. Microvascular and capillary perfusion following glycocalyx degradation. *J.Appl.Physiol.*, 102, (6) 2251-2259

Cadenas, E., Boveris, A., Ragan, C.I., & Stoppani, A.O.M. 1977. Production of Superoxide Radicals and Hydrogen-Peroxide by Nadh-Ubiquinone Reductase and Ubiquinol-Cytochrome C Reductase from Beef-Heart Mitochondria. *Arch.Biochem.Biophys.*, 180, (2) 248-257

Calabresi, P.A., Balcer, L.J., & Frohman, E.M. 2010. Retinal pathology in multiple sclerosis: insight into the mechanisms of neuronal pathology. *Brain*, 133, 1575-1577

Carmo, A., Cunha-Vaz, J.G., Carvalho, A.P., & Lopes, M.C. 2000. Nitric oxide synthase activity in retinas from non-insulin-dependent diabetic Goto-Kakizaki rats: Correlation with blood-retinal barrier permeability. *Nitric Oxide-Biology and Chemistry*, 4, (6) 590-596

Carson, M.J., Doose, J.M., Melchior, B., Schmid, C.D., & Ploix, C.C. 2006. CNS immune privilege: hiding in plain sight. *Immunol.Rev.*, 213, 48-65

Carter, C.S., Hofer, T., Seo, A.Y., & Leeuwenburgh, C. 2007. Molecular mechanisms of life- and health-span extension: role of calorie restriction and exercise intervention. *Applied Physiology Nutrition and Metabolism-Physiologie Appliquee Nutrition et Metabolisme*, 32, (5) 954-966

Cassina, A. & Radi, R. 1996. Differential inhibitory action of nitric oxide and peroxynitrite on mitochondrial electron transport. *Arch.Biochem.Biophys.*, 328, (2) 309-316

Cernadas, M.R., de Miguel, L.S., Garcia-Duran, M., Gonzalez-Fernandez, F., Millas, I., Monton, M., Rodrigo, J., Rico, L., Fernandez, P., de Frutos, T., Rodriguez-Feo, J.A., Guerra, J., Caramelo, C., Casado, S., & Lopez-Farre, A. 1998. Expression of constitutive and inducible nitric oxide synthases in the vascular wall of young and aging rats. *Circul.Res.*, 83, (3) 279-286

Chan, C.C. & Li, Q. 1998. Immunopathology of uveitis. *Br.J.Ophthalmol.*, 82, (1) 91-96

Chan, C.C., Wetzig, R.P., Palestine, A.G., Kuwabara, T., & Nusenblatt, R.B. 1987. Immunohistopathology of Ocular Sarcoidosis - Report of A Case and Discussion of Immunopathogenesis. *Arch.Ophthalmol.*, 105, (10) 1398-1402

Chan-Ling, T., Hughes, S., Baxter, L., Rosinova, E., McGregor, I., Morcos, Y., Van Nieuwenhuyzen, P., & Hu, P. 2007. Inflammation and breakdown of the blood-retinal

barrier during "physiological aging" in the rat retina: A model for CNS aging. *Microcirculation*, 14, (1) 63-76

Chance, B. & Baltscheffsky, H. 1958. Respiratory Enzymes in Oxidative Phosphorylation .7. Binding of Intramitochondrial Reduced Pyridine Nucleotide. *J.Biol.Chem.*, 233, (3) 736-739

Chance, B., Cohen, P., Jobsis, F., & Schoener, B. 1962. Intracellular Oxidation-Reduction States in Vivo. *Science*, 137, (3529) 499-508

Chance, B. & Connelly, C.M. 1957. Method for the Estimation of the Increase in Concentration of Adenosine Diphosphate in Muscle Sarcosomes Following A Contraction. *Nature*, 179, (4572) 1235-1237

Chance, B. & Jobsis, F. 1959. Changes in Fluorescence in A Frog Sartorius Muscle Following A Twitch. *Nature*, 184, (4681) 195-196

Chance, B., Schoener, B., Oshino, R., Itshak, F., & Nakase, Y. 1979. Oxidation-Reduction Ratio Studies of Mitochondria in Freeze-Trapped Samples - Nadh and Flavoprotein Fluorescence Signals. *J.Biol.Chem.*, 254, (11) 4764-4771

Chaudry, I.H., Wichterman, K.A., & Baue, A.E. 1979. Effect of Sepsis on Tissue Adenine-Nucleotide Levels. *Surgery*, 85, (2) 205-211

Chih, C.P. & Roberts, E.L. 2003. Energy substrates for neurons during neural activity: a critical review of the astrocyte-neuron lactate shuttle hypothesis. *J.Cereb.Blood Flow Metab.*, 23, (11) 1263-1281

Chisholm, K.I., Ida, K.K., Davies, A.L., Papkovsky, D.B., Singer, M., Dyson, A., Tachtsidis, I., Duchen, M.R., & Smith, K.J. 2015. In Vivo Imaging Of Flavoprotein Fluorescence During Hypoxia Reveals The Importance Of Direct Arterial Oxygen Supply To Cerebral Cortex Tissue. *Oxygen Transport to Tissue XXXVII (in press)*

Cho, C.G., Kim, H.J., Chung, S.W., Jung, K.J., Shim, K.H., Yu, B.P., Yodoi, J., & Chung, H.Y. 2003. Modulation of glutathione and thioredoxin systems by calorie restriction during the aging process. *Exp.Gerontol.*, 38, (5) 539-548

Chorinchath, B.B., Kong, L.Y., Mao, L., & McCallum, R.E. 1996. Age-associated differences in TNF-alpha and nitric oxide production in endotoxic mice. *J.Immunol.*, 156, (4) 1525-1530

Chow, J.C., Young, D.W., Golenbock, D.T., Christ, W.J., & Gusovsky, F. 1999. Toll-like receptor-4 mediates lipopolysaccharide-induced signal transduction. *J.Biol.Chem.*, 274, (16) 10689-10692

Chung, H.Y., Cesari, M., Anton, S., Marzetti, E., Giovannini, S., Seo, A.Y., Carter, C., Yu, B.P., & Leeuwenburgh, C. 2009. Molecular inflammation: Underpinnings of aging and age-related diseases. *Ageing Research Reviews*, 8, (1) 18-30

Chung, H.Y., Sung, B., Jung, K.J., Zou, Y., & Yu, B.P. 2006. The molecular inflammatory process in aging. *Antioxidants & Redox Signaling*, 8, (3-4) 572-581

Chwastiak, L., Ehde, D.M., Gibbons, L.E., Sullivan, M., Bowen, J.D., & Kraft, G.H. 2002. Depressive symptoms and severity of illness in multiple sclerosis: Epidemiologic study of a large community sample. *Am.J.Psychiatry*, 159, (11) 1862-1868

Clark, M. E. & Kraft, T. W. 2012, "Measuring Rodent Electroretinograms to Assess Retinal Function," *In Retinal Development, Methods in Molecular Biology*, pp. 265-276.

Clark, R.A. 1990. The Human Neutrophil Respiratory Burst Oxidase. *J.Infect.Dis.*, 161, (6) 1140-1147

Clark, R.A. 1999. Activation of the neutrophil respiratory burst oxidase. *J.Infect.Dis.*, 179, S309-S317

Claudio, L., Martiney, J.A., & Brosnan, C.F. 1994. Ultrastructural Studies of the Blood-Retina Barrier After Exposure to Interleukin-1-Beta Or Tumor-Necrosis-Factor-Alpha. *Lab.Invest.*, 70, (6) 850-861

Clayton, D.A. 1982. Replication of Animal Mitochondrial-Dna. *Cell*, 28, (4) 693-705

Clayton, D.A., Doda, J.N., & Friedberg, E.C. 1974. The absence of a pyrimidine dimer repair mechanism in mammalian mitochondria. *Proceedings of the National Academy of Sciences*, 71, (7) 2777-2781

Cleeter, M.W.J., Cooper, J.M., Darleyusmar, V.M., Moncada, S., & Schapira, A.H.V. 1994. Reversible Inhibition of Cytochrome-C-Oxidase, the Terminal Enzyme of the Mitochondrial Respiratory-Chain, by Nitric-Oxide - Implications for Neurodegenerative Diseases. *FEBS Lett.*, 345, (1) 50-54

Clementi, E., Brown, G.C., Feelisch, M., & Moncada, S. 1998. Persistent inhibition of cell respiration by nitric oxide: Crucial role of S-nitrosylation of mitochondrial complex I and protective action of glutathione. *Proc.Natl.Acad.Sci.U.S.A.*, 95, (13) 7631-7636

Coffey, P.J., Gias, C., McDermott, C.J., Lundh, P., Pickering, M.C., Sethi, C., Bird, A., Fitzke, F.W., Maass, A., Chen, L.L., Holder, G.E., Luthert, P.J., Salt, T.E., Moss, S.E., & Greenwood, J. 2007. Complement factor H deficiency in aged mice causes retinal abnormalities and visual dysfunction. *Proceedings of the National Academy of Sciences of the USA*, 104, (42) 16651-16656

Cohen, J. 2002. The immunopathogenesis of sepsis. *Nature*, 420, (6917) 885-891

Collongues, N., Chanson, J.B., Blanc, F., Steibel, J., Lam, C.D., Shabbir, A., Trifilieff, E., Honnorat, J., Pham-Dinh, D., Ghandour, M.S., & de Seze, J. 2012. The Brown Norway opticospinal model of demyelination: Does it mimic multiple sclerosis or neuromyelitis optica? *Int.J.Dev.Neurosci.*, 30, (6) 487-497

Cordeiro, M.F., Guo, L., Luong, V., Harding, G., Wang, W., Jones, H.E., Moss, S.E., Sillito, A.M., & Fitzke, F.W. 2004. Real-time imaging of single nerve cell apoptosis in retinal neurodegeneration. *Proceedings of the National Academy of Sciences of the United States of America*, 101, (36) 13352-13356

Crouser, E.D. 2004. Mitochondrial dysfunction in septic shock and multiple organ dysfunction syndrome. *Mitochondrion*, 4, (5-6) 729-741

Crouser, E.D., Julian, M.W., Blaho, D.V., & Pfeiffer, D.R. 2002a. Endotoxin-induced mitochondrial damage correlates with impaired respiratory activity. *Crit.Care Med.*, 30, (2) 276-284

Crouser, E.D., Julian, M.W., Joshi, M.S., Bauer, J.A., Wewers, M.D., Hart, J.M., & Pfeiffer, D.R. 2002b. Cyclosporin A ameliorates mitochondrial ultrastructural injury in the ileum during acute endotoxemia. *Crit.Care Med.*, 30, (12) 2722-2728

d'Avila, J.C., Santiago, A.P.S.A., Amancio, R.T., Galina, A., Oliveira, M.F., & Bozza, F.A. 2008. Sepsis induces brain mitochondrial dysfunction. *Crit.Care Med.*, 36, (6) 1925-1932

da Silva-Santos, J.E., Terluk, M.R., & Assreuy, J. 2002. Differential involvement of guanylate cyclase and potassium channels in nitric oxide-induced hyporesponsiveness to phenylephrine in endotoxemic rats. *Shock*, 17, (1) 70-76

Dahn, M.S., Lange, M.P., Mccurdy, B., & Mahaffey, S. 1995. Metabolic Function of the Isolated-Perfused Rat-Liver in Chronic Sepsis. *J.Surg.Res.*, 59, (2) 287-291

Davies, A.L., Desai, R.A., Bloomfield, P.S., McIntosh, P.R., Chapple, K.J., Linington, C., Fairless, R., Diem, R., Kasti, M., Murphy, M.P., & Smith, K.J. 2013. Neurological Deficits Caused by Tissue Hypoxia in Neuroinflammatory Disease. *Ann.Neurol.*, 74, (6) 815-825

Davis, J.B., Mcmurray, H.F., & Schubert, D. 1992. The Amyloid Beta-Protein of Alzheimers-Disease Is Chemotactic for Mononuclear Phagocytes. *Biochem.Biophys.Res.Commun.*, 189, (2) 1096-1100

Dawson, K.L., Geller, E.R., & Kirkpatrick, J.R. 1988. Enhancement of Mitochondrial-Function in Sepsis. *Arch.Surg.*, 123, (2) 241-244

De Backer, D., Cortes, D.O., Donadello, K., & Vincent, J.L. 2014. Pathophysiology of microcirculatory dysfunction and the pathogenesis of septic shock. *Virulence*, 5, (1) 73-79

De Backer, D., Creteur, J., Preiser, J.C., Dubois, M.J., & Vincent, J.L. 2002. Microvascular blood flow is altered in patients with sepsis. *Am.J.Respir.Crit.Care Med.*, 166, (1) 98-104

De Backer, D., Donadello, K., Sakr, Y., Ospina-Tascon, G., Salgado, D., Scolletta, S., & Vincent, J.L. 2013. Microcirculatory Alterations in Patients With Severe Sepsis: Impact of Time of Assessment and Relationship With Outcome. *Crit.Care Med.*, 41, (3) 791-799

de Gooyer, T.E., Stevenson, K.A., Humphries, P., Simpson, D.A.C., Curtis, T.M., Gardiner, T.A., & Stitt, A.W. 2006. Rod photoreceptor loss in Rho(-/-) mice reduces retinal hypoxia and hypoxia-regulated gene expression. *Investigative Ophthalmology & Visual Science*, 47, (12) 5553-5560

Dekozak, Y., Sakai, J., Thillaye, B., & Faure, J.P. 1981. S-Antigen-Induced Experimental Autoimmune Uveo-Retinitis in Rats. *Curr.Eye Res.*, 1, (6) 327-337

Del Sole, M.J., Sande, P.H., Felipe, A.E., Fernandez, D.C., Sarmiento, M.I.K., Aba, M.A., & Rosenstein, R.E. 2008. Characterization of uveitis induced by use of a single intravitreal injection of bacterial lipopolysaccharide in cats. *American Journal of Veterinary Research*, 69, (11) 1487-1495

Delori, F.C., Dorey, C.K., Staurenghi, G., Arend, O., Goger, D.G., & Weiter, J.J. 1995. In-Vivo Fluorescence of the Ocular Fundus Exhibits Retinal-Pigment Epithelium Lipofuscin Characteristics. *Investigative Ophthalmology & Visual Science*, 36, (3) 718-729

Derosbo, N.K., Milo, R., Lees, M.B., Burger, D., Bernard, C.C.A., & Bennun, A. 1993. Reactivity to Myelin Antigens in Multiple-Sclerosis - Peripheral-Blood Lymphocytes Respond Predominantly to Myelin Oligodendrocyte Glycoprotein. *Journal of Clinical Investigation*, 92, (6) 2602-2608

Desai, R.A. 2013.
The Role of Hypoxia in Neuroinflammatory Disease.

Desborough, J.P. 2000. The stress response to trauma and surgery. *Br.J.Anaesth.*, 85, (1) 109-117

Deschenes, J., Char, D.H., & Kaleta, S. 1988. Activated Lymphocytes-T in Uveitis. *Br.J.Ophthalmol.*, 72, (2) 83-87

Desmet, M.D., Yamamoto, J.H., Mochizuki, M., Gery, I., Singh, V.K., Shinohara, T., Wiggert, B., Chader, G.J., & Nussenblatt, R.B. 1990. Cellular Immune-Responses of Patients with Uveitis to Retinal Antigens and Their Fragments. *Am.J.Ophthalmol.*, 110, (2) 135-142

Devos, A.F., Vanharen, M.A.C., Verhagen, C., Hoekzema, R., & Kijlstra, A. 1994. Kinetics of Intraocular Tumor-Necrosis-Factor and Interleukin-6 in Endotoxin-Induced Uveitis in the Rat. *Investigative Ophthalmology & Visual Science*, 35, (3) 1100-1106

Diaz, N.L., Finol, H.J., Torres, S.H., Zambrano, C.I., & Adjounian, H. 1998. Histochemical and ultrastructural study of skeletal muscle in patients with sepsis and multiple organ failure syndrome (MOFS). *Histol.Histopathol.*, 13, (1) 121-128

DiMauro, S. & Schon, E.A. 2003. Mechanisms of disease: Mitochondrial respiratory-chain diseases. *New Engl.J.Med.*, 348, (26) 2656-2668

DiMauro, S. & Schon, E.A. 2008. Mitochondrial disorders in the nervous system. *Annu.Rev.Neurosci.*, 31, 91-123

Dinarello, C.A. 1997. Proinflammatory and anti-inflammatory cytokines as mediators in the pathogenesis of septic shock. *Chest*, 112, (6) 321S-329S

Dirnagl, U., Lindauer, U., & Villringer, A. 1993. Role of Nitric-Oxide in the Coupling of Cerebral Blood-Flow to Neuronal Activation in Rats. *Neurosci.Lett.*, 149, (1) 43-46

Dombeck, D.A., Khabbaz, A.N., Collman, F., Adelman, T.L., & Tank, D.W. 2007. Imaging large-scale neural activity with cellular resolution in awake, mobile mice. *Neuron*, 56, (1) 43-57

Dong, C.J. & Hare, W.A. 2000. Contribution to the kinetics and amplitude of the electroretinogram b-wave by third-order retinal neurons in the rabbit retina. *Vision Res.*, 40, (6) 579-589

Dong, C.J. & Hare, W.A. 2002. GABAc feedback pathway modulates the amplitude and kinetics of ERG b-wave in a mammalian retina in vivo. *Vision Res.*, 42, (9) 1081-1087

Dowling, J.E. & Boycott, B.B. 1966. Organization of the primate retina: Electron microscopy. *Proceedings of the Royal Society of London*

Drazenovic, R., Samsel, R.W., Wylam, M.E., Doerschuk, C.M., & Schumacker, P.T. 1992. Regulation of Perfused Capillary Density in Canine Intestinal-Mucosa During Endotoxemia. *J.Appl.Physiol.*, 72, (1) 259-265

Duling, B.R. & Berne, R.M. 1970. Longitudinal Gradients in Periarteriolar Oxygen Tension in Hamster Cheek Pouch. *Fed.Proc.*, 29, (2) A320-&

Duling, B.R., Kuschinsky, W., & Wahl, M. 1979. Measurements of the Perivascular Po2 in the Vicinity of the Pial Vessels of the Cat. *Pflugers Archiv-European Journal of Physiology*, 383, (1) 29-34

Dutta, R., McDonough, J., Yin, X.G., Peterson, J., Chang, A., Torres, T., Gudz, T., Macklin, E.B., Lewis, D.A., Fox, R.J., Rudick, R., Mirnics, K., & Trapp, B.D. 2006. Mitochondrial dysfunction as a cause of axonal degeneration in multiple sclerosis patients. *Annals of Neurology*, 59, (3) 478-489

Edelson, J.D., Macfadden, D.K., Klein, M., & Rebuck, A.S. 1985. Autofluorescence of Alveolar Macrophages - Problems and Potential Solutions. *Med.Hypotheses*, 17, (4) 403-407

Edwards, A.O., Ritter, R., Abel, K.J., Manning, A., Panhuysen, C., & Farrer, L.A. 2005. Complement factor H polymorphism and age-related macular degeneration. *Science*, 308, (5720) 421-424

Eidelman, L.A., Putterman, D., Putterman, C., & Sprung, C.L. 1996. The spectrum of septic encephalopathy - Definitions, etiologies, and mortalities. *Jama-Journal of the American Medical Association*, 275, (6) 470-473

Ekstromjodal, B. & Larsson, L.E. 1982. Effects of Dopamine on Cerebral-Circulation and Oxygen-Metabolism in Endotoxic-Shock - An Experimental-Study in Dogs. *Crit.Care Med.*, 10, (6) 375-377

Ellis, C.G., Bateman, R.M., Sharpe, M.D., Sibbald, W.J., & Gill, R. 2002. Effect of a maldistribution of microvascular blood flow on capillary O-2 extraction in sepsis. *Am.J.Physiol-Heart.C.*, 282, (1) H156-H164

Eltzschig, H.K. & Carmeliet, P. 2011. Mechanisms of Disease: Hypoxia and Inflammation. *New Engl.J.Med.*, 364, (7) 656-665

Englander, M. & Singh, R.P. 2013. Treatment Paradigms in Neovascular AMD. *Current Ophthalmology Reports*, 1, 12-19

Erecinska, M. & Silver, I.A. 2001. Tissue oxygen tension and brain sensitivity to hypoxia. *Respir.Physiol.*, 128, (3) 263-276

Erecinska, M., Thoresen, M., & Silver, I.A. 2003. Effects of hypothermia on energy metabolism in mammalian central nervous system. *J.Cereb.Blood Flow Metab.*, 23, (5) 513-530

Federico, A., Cardaioli, E., Da Pozzo, P., Formichi, P., Gallus, G.N., & Radi, E. 2012. Mitochondria, oxidative stress and neurodegeneration. *J.Neurol.Sci.*, 322, (1-2) 254-262

Fein, A. & Tsacopoulos, M. 1988. Activation of Mitochondrial Oxidative-Metabolism by Calcium-Ions in Limulus Ventral Photoreceptor. *Nature*, 331, (6155) 437-440

Fernandes, D. & Assreuy, J. 2008. Nitric oxide and vascular reactivity in sepsis. *Shock*, 30, 10-13

Fink, M.P. 1997. Cytopathic hypoxia in sepsis. *Acta Anaesthesiol.Scand.*, 41, (S110) 87-94

Fink, M.P. 2001. Cytopathic hypoxia - Mitochondrial dysfunction as mechanism contributing to organ dysfunction in sepsis. *Crit.Care Clin.*, 17, (1) 219-+

Fink, M.P. 2002a. Bench-to-bedside review: Cytopathic hypoxia. *Crit.Care*, 6, (6) 491-499

Fink, M.P. 2002b. Cytopathic hypoxia - Is oxygen use impaired in sepsis as a result of an acquired intrinsic derangement in cellular respiration? *Crit.Care Clin.*, 18, (1) 165-+

Fink, M.P., Fiallo, V., Stein, K.L., & Gardiner, W.M. 1987. Systemic and Regional Hemodynamic-Changes After Intraperitoneal Endotoxin in Rabbits - Development of A New Model of the Clinical Syndrome of Hyperdynamic Sepsis. *Circ.Shock*, 22, (1) 73-81

Fisher, J.B., Jacobs, D.A., Markowitz, C.E., Galetta, S.L., Volpe, N.J., Nano-Schiavi, M.L., Baier, M.L., Frohman, E.M., Winslow, H., Frohman, T.C., Calabresi, P.A., Maguire, M.G., Cutter, G.R., & Balcer, L.J. 2006. Relation of visual function to retinal nerve fiber layer thickness in multiple sclerosis. *Ophthalmology*, 113, (2) 324-332

Fleming, I., Julouschaeffer, G., Gray, G.A., Parratt, J.R., & Stoclet, J.C. 1991. Evidence That An L-Arginine Nitric-Oxide Dependent Elevation of Tissue Cyclic-Gmp Content Is Involved in Depression of Vascular Reactivity by Endotoxin. *Br.J.Pharmacol.*, 103, (1) 1047-1052

Flemming, A. 2011. SEPSIS DAMPening inflammation. *Nature Reviews Drug Discovery*, 10, (6) 416

Forrester, J.V. 1991. Uveitis - Pathogenesis. *Lancet*, 338, (8781) 1498-1501

Forrester, J.V., Worgul, B.V., & Merriam, G.R. 1980. Endotoxin-Induced Uveitis in the Rat. *Albrecht Von Graefes Archiv fur Klinische und Experimentelle Ophthalmologie*, 213, (4) 221-233

Fox, G.M., Kuwabara, T., Wiggert, B., Redmond, T.M., Hess, H.H., Chader, G.J., & Gery, I. 1987. Experimental Autoimmune Uveoretinitis (Eau) Induced by Retinal Interphotoreceptor Retinoid-Binding Protein (Irbp) - Differences Between Eau Induced by Irbp and by S-Antigen. *Clin.Immunol.Immnopathol.*, 43, (2) 256-264

Franco, P.J., Fernandez, D.C., Sande, P.H., Sarmiento, M.I.K., Chianelli, M., Sanez, D.A., & Rosenstein, R.E. 2008. Effect of bacterial lipopolysaccharide on ischemic damage in the rat retina. *Investigative Ophthalmology & Visual Science*, 49, (10) 4604-4612

Fredriksson, K., Flaring, U., Guillet, C., Wernerman, J., & Rooyackers, O. 2009. Muscle mitochondrial activity increases rapidly after an endotoxin challenge in human volunteers. *Acta Anaesthesiol.Scand.*, 53, (3) 299-304

Frey, E.A. & Finlay, B.B. 1998. Lipopolysaccharide induces apoptosis in a bovine endothelial cell line via a soluble CD14 dependent pathway. *Microb.Pathog.*, 24, (2) 101-109

Fujita, H., Morita, I., & Murota, S. 1991. Involvement of Adhesion Molecules (Cd11A-Icam-1) in Vascular Endothelial-Cell Injury Elicited by Pma-Stimulated Neutrophils. *Biochem.Biophys.Res.Commun.*, 177, (2) 664-672

Fukushima, A., Lai, J.C., Chanaud, N.P., Shiloach, J., Whitcup, S.M., Nussenblatt, R.B., & Gery, I. 1997. Permissive recognition of immunodominant determinants of the retinal S-antigen in different rat strains, primates and humans. *Int.Immunol.*, 9, (1) 169-177

Funfschilling, U., Supplie, L.M., Mahad, D., Boretius, S., Saab, A.S., Edgar, J., Brinkmann, B.G., Kassmann, C.M., Tzvetanova, I.D., Mobius, W., Diaz, F., Meijer, D., Suter, U., Hamprecht, B., Sereda, M.W., Moraes, C.T., Frahm, J., Goebbels, S., & Nave, K.A. 2012.

Glycolytic oligodendrocytes maintain myelin and long-term axonal integrity. *Nature*, 485, (7399) 517-U130

Galea, I., Bechmann, I., & Perry, V.H. 2007. What is immune privilege (not)? *Trends Immunol.*, 28, (1) 12-18

Gao, W.C., Chen, G., Reinert, K.C., & Ebner, T.J. 2006. Cerebellar cortical molecular layer inhibition is organized in parasagittal zones. *J.Neurosci.*, 26, (32) 8377-8387

Gattinoni, L., Brazzi, L., Pelosi, P., Latini, R., Tognoni, G., Pesenti, A., & Fumagalli, R. 1995. A Trial of Goal-Oriented Hemodynamic Therapy in Critically Ill Patients. *New Engl.J.Med.*, 333, (16) 1025-1032

Gehrmann, J., Matsumoto, Y., & Kreutzberg, G.W. 1995. Microglia - Intrinsic Immuneffector Cell of the Brain. *Brain Res.Rev.*, 20, (3) 269-287

Genain, C.P. & Hauser, S.L. 2001. Experimental allergic encephalomyelitis in the New World monkey Callithrix jacchus. *Immunological Reviews*, 183, 159-172

Gibson, C.L., Coughlan, T.C., & Murphy, S.P. 2005. Glial nitric oxide and ischemia. *Glia*, 50, (4) 417-426

Giovannini, M.G., Scali, C., Prosperi, C., Bellucci, A., Vannucchi, M.G., Rosi, S., Pepeu, G., & Casamenti, F. 2002. beta-amyloid-induced inflammation and cholinergic hypofunction in the rat brain in vivo: Involvement of the p38MAPK pathway. *Neurobiol.Dis.*, 11, (2) 257-274

Goldman, D., Bateman, R.M., & Ellis, C.G. 2004. Effect of sepsis on skeletal muscle oxygen consumption and tissue oxygenation: interpreting capillary oxygen transport data using a mathematical model. *Am.J.Physiol-Heart.C.*, 287, (6) H2535-H2544

Goode, H.F., Cowley, H.C., Walker, B.E., Howdle, P.D., & Webster, N.R. 1995. Decreased Antioxidant Status and Increased Lipid-Peroxidation in Patients with Septic Shock and Secondary Organ Dysfunction. *Crit.Care Med.*, 23, (4) 646-651

Goris, R.J.A., Teboekhorst, T.P.A., Nuytinck, J.K.S., & Gimbrere, J.S.F. 1985. Multiple-Organ Failure - Generalized Autodestructive Inflammation. *Arch.Surg.*, 120, (10) 1109-1115

Graham, E.M., Francis, D.A., Sanders, M.D., & Rudge, P. 1989. Ocular Inflammatory Changes in Established Multiple-Sclerosis. *Journal of Neurology Neurosurgery and Psychiatry*, 52, (12) 1360-1363

Graham, E.M., Stanford, M.R., Shilling, J.S., & Sanders, M.D. 1987. Neovascularization Associated with Posterior Uveitis. *Br.J.Ophthalmol.*, 71, (11) 826-833

Green, A.J., McQuaid, S., Hauser, S.L., Allen, I.V., & Lyness, R. 2010. Ocular pathology in multiple sclerosis: retinal atrophy and inflammation irrespective of disease duration. *Brain*, 133, 1591-1601

Green, D.G. & Kapousta-Bruneau, N.V. 1999. A dissection of the electroretinogram from the isolated rat retina with microelectrodes and drugs. *Vis.Neurosci.*, 16, (4) 727-741

Grover, R., Lopez, A., Lorente, J., Steingrub, J., Bakker, J., Willatts, S., McLuckie, A., & Takala, J. 1999. Multi-center, randomized, placebo-controlled, double blind study of the nitric oxide synthase inhibitor 546C88: Effect on survival in patients with septic shock. *Crit.Care Med.*, 27, (1) A33

Gundersen, Y., Corso, C.O., Leiderer, R., Dorger, M., Lilleaasen, P., Aasen, A.O., & Messmer, K. 1998. The nitric oxide donor sodium nitroprusside protects against hepatic microcirculatory dysfunction in early endotoxaemia. *Intensive Care Med.*, 24, (12) 1257-1263

Guo, L., Duggan, J., & Cordeiro, M.F. 2010. Alzheimer's disease and retinal neurodegeneration. *Current Alzheimer Research*

Gupta, D., Singh, V.K., Rajasingh, J., Shinohara, T., Misra, R., & Agarwal, S.S. 1996. Cellular immune responses of patients with juvenile chronic arthritis to retinal antigens and their synthetic peptides. *Immunol.Res.*, 15, (1) 74-83

Gustot, T. 2011. Multiple organ failure in sepsis: prognosis and role of systemic inflammatory response. *Current Opinion in Critical Care*, 17, (2) 153-159

Hackenbr, CR. 1968. Ultrastructural Bases for Metabolically Linked Mechanical Activity in Mitochondria .2. Electron Transport-Linked Ultrastructural Transformations in Mitochondria. *Journal of Cell Biology*, 37, (2) 345-&

Hageman, G.S., Anderson, D.H., Johnson, L.V., Hancox, L.S., Taiber, A.J., Hardisty, L.I., Hageman, J.L., Stockman, H.A., Borchardt, J.D., Gehrs, K.M., Smith, R.J.H., Silvestri, G., Russell, S.R., Klaver, C.C.W., Barbazetto, I., Chang, S., Yannuzzi, L.A., Barile, G.R., Merriam, J.C., Smith, R.T., Olsh, A.K., Bergeron, J., Zernant, J., Merriam, J.E., Gold, B., Dean, M., & Allikmets, R. 2005. A common haplotype in the complement regulatory gene factor H (HF1/CFH) predisposes individuals to age-related macular degeneration. *Proc.Natl.Acad.Sci.U.S.A.*, 102, (20) 7227-7232

Halestrap, A.P., Kerr, P.M., Javadov, S., & Woodfield, K.Y. 1998. Elucidating the molecular mechanism of the permeability transition pore and its role in reperfusion injury of the heart. *Biochimica et Biophysica Acta-Bioenergetics*, 1366, (1-2) 79-94

Hall, C.N., Klein-Flugge, M.C., Howarth, C., & Attwell, D. 2012. Oxidative Phosphorylation, Not Glycolysis, Powers Presynaptic and Postsynaptic Mechanisms Underlying Brain Information Processing. *J.Neurosci.*, 32, (26) 8940-8951

Hamanaka, R.B. & Chandel, N.S. 2010. Mitochondrial reactive oxygen species regulate cellular signaling and dictate biological outcomes. *Trends Biochem.Sci.*, 35, (9) 505-513

Handa, O., Stephen, J., & Cepinskas, G. 2008. Role of endothelial nitric oxide synthase-derived nitric oxide in activation and dysfunction of cerebrovascular endothelial cells during early onsets of sepsis. *Am.J.Physiol-Heart.C.*, 295, (4) H1712-H1719

Hanisch, U.K. & Kettenmann, H. 2007. Microglia: active sensor and versatile effector cells in the normal and pathologic brain. *Nat.Neurosci.*, 10, (11) 1387-1394

Hannestad, J., Gallezot, J.D., Schafbauer, T., Lim, K., Kloczynski, T., Morris, E.D., Carson, R.E., Ding, Y.S., & Cosgrove, K.P. 2012. Endotoxin-induced systemic inflammation activates microglia: [C-11]PBR28 positron emission tomography in nonhuman primates. *Neuroimage*, 63, (1) 232-239

Harman, D. 1956. Aging - A Theory Based on Free-Radical and Radiation-Chemistry. *Journals of Gerontology*, 11, (3) 298-300

Harman, D. 1992. Free-Radical Theory of Aging. *Mutat.Res.*, 275, (3-6) 257-266

Hartl, W.H., Gunther, B., Inthorn, D., & Heberer, G. 1988. Reactive Hyperemia in Patients with Septic Conditions. *Surgery*, 103, (4) 440-444

Hawkins, R.A. 1986. Transport of Essential Nutrients Across the Blood-Brain-Barrier of Individual Structures. *Fed.Proc.*, 45, (7) 2055-2059

Hayashi, S., GuexCrosier, Y., Delvaux, A., Velu, T., & Roberge, F.G. 1996. Interleukin 10 inhibits inflammatory cells infiltration in endotoxin-induced uveitis. *Graefes Archive for Clinical and Experimental Ophthalmology*, 234, (10) 633-636

Hayes, M.A., Timmins, A.C., Yau, E.H.S., Palazzo, M., Hinds, C.J., & Watson, D. 1994. Elevation of Systemic Oxygen Delivery in the Treatment of Critically Ill Patients. *New Engl.J.Med.*, 330, (24) 1717-1722

Helb, H.M., Issa, P.C., Fleckenstein, M., Schmitz-Valckenberg, S., Scholl, H.P.N., Meyer, C.H., Eter, N., & Holz, F.G. 2010. Clinical evaluation of simultaneous confocal scanning laser ophthalmoscopy imaging combined with high-resolution, spectral-domain optical coherence tomography. *Acta Ophthalmol.(Copenh).*, 88, (8) 842-849

Helenius, M., Hanninen, M., Lehtinen, S.K., & Salminen, A. 1996. Changes associated with aging and replicative senescence in the regulation of transcription factor nuclear factor-kappa B. *Biochem.J.*, 318, 603-608

Henderson, A.P.D., Trip, S.A., Schlottmann, P.G., Altmann, D.R., Garway-Heath, D.F., Plant, G.T., & Miller, D.H. 2008. An investigation of the retinal nerve fibre layer in progressive multiple sclerosis using optical coherence tomography. *Brain*, 131, 277-287

Henneke, P. & Golenbock, D.T. 2002. Innate immune recognition of lipopolysaccharide by endothelial cells. *Crit.Care Med.*, 30, (5) S207-S213

Herrero-Mendez, A., Almeida, A., Fernandez, E., Maestre, C., Moncada, S., & Bolanos, J.P. 2009. The bioenergetic and antioxidant status of neurons is controlled by continuous degradation of a key glycolytic enzyme by APC/C-Cdh1. *Nat.Cell Biol.*, 11, (6) 747-U105

Hevel, J.M., White, K.A., & Marletta, M.A. 1991. Purification of the Inducible Murine Macrophage Nitric-Oxide Synthase - Identification As A Flavoprotein. *J.Biol.Chem.*, 266, (34) 22789-22791

Hildebrand, F., Giannoudis, P.V., van Griensven, M., Chawda, M., & Pape, H.C. 2004. Pathophysiologic changes and effects of hypothermia on outcome in elective surgery and trauma patients. *Am.J.Surg.*, 187, (3) 363-371

Hinshaw, L.B. 1996. Sepsis/septic shock: Participation of the microcirculation: An abbreviated review. *Crit.Care Med.*, 24, (6) 1072-1078

Hobbs, M.V., Weigle, W.O., Noonan, D.J., Torbett, B.E., Mcevilly, R.J., Koch, R.J., Cardenas, G.J., & Ernst, D.N. 1993. Patterns of Cytokine Gene-Expression by Cd4+ T-Cells from Young and Old Mice. *J.Immunol.*, 150, (8) 3602-3614

Hoekzema, R., Verhagen, C., Vanharen, M., & Kijlstra, A. 1992. Endotoxin-Induced Uveitis in the Rat - the Significance of Intraocular Interleukin-6. *Investigative Ophthalmology & Visual Science*, 33, (3) 532-539

Hofmann-Kiefer, K.F., Kemming, G.I., Chappell, D., Flondor, M., Kisch-Wedel, H., Hauser, A., Pallivathukal, S., Conzen, P., & Rehm, M. 2009. Serum Heparan Sulfate Levels Are Elevated in Endotoxemia. *Eur.J.Med.Res.*, 14, (12) 526-531

Hollyfield, J.G., Bonilha, V.L., Rayborn, M.E., Yang, X.P., Shadrach, K.G., Lu, L., Ufret, R.L., Salomon, R.G., & Perez, V.L. 2008. Oxidative damage-induced inflammation initiates age-related macular degeneration. *Nat.Med.*, 14, (2) 194-198

Holtmaat, A., Bonhoeffer, T., Chow, D.K., Chuckowree, J., De Paola, V., Hofer, S.B., Hubener, M., Keck, T., Knott, G., Lee, W.C.A., Mostany, R., Mrsic-Flogel, T.D., Nedivi, E., Portera-Cailliau, C., Svoboda, K., Trachtenberg, J.T., & Wilbrecht, L. 2009. Long-term, high-resolution imaging in the mouse neocortex through a chronic cranial window. *Nature Protocols*, 4, (8) 1128-1144

Holz, F.G., Bellman, C., Staudt, S., Schutt, F., & Volcker, H.E. 2001. Fundus autofluorescence and development of geographic atrophy in age-related macular degeneration. *Investigative Ophthalmology & Visual Science*, 42, (5) 1051-1056

Honda, H.M., Korge, P., & Weiss, J.N. 2005. Mitochondria and ischemia/reperfusion injury. *Communicative Cardiac Cell*, 1047, 248-258

Hortelano, S., Dallaporta, B., Zamzami, N., Hirsch, T., Susin, S.A., Marzo, I., Bosca, L., & Kroemer, G. 1997. Nitric oxide induces apoptosis via triggering mitochondrial permeability transition. *FEBS Lett.*, 410, (2-3) 373-377

Huang, D., Swanson, E.A., Lin, C.P., Schuman, J.S., Stinson, W.G., Chang, W., Hee, M.R., Flotte, T., Gregory, K., Puliafito, C.A., & Fujimoto, J.G. 1991. Optical Coherence Tomography. *Science*, 254, (5035) 1178-1181

Huang, S.H., Heikal, A.A., & Webb, W.W. 2002. Two-photon fluorescence spectroscopy and microscopy of NAD(P)H and flavoprotein. *Biophys.J.*, 82, (5) 2811-2825

Huey, R.B. & Eguskitza, X. 2001. Limits to human performance: elevated risks on high mountains. *J.Exp.Biol.*, 204, (18) 3115-3119

Hughes, J.M., Groot, A.J., van der Groep, P., Sersansie, R., Vooijs, M., van Diest, P.J., Van Noorden, C.J.F., Schlingemann, R.O., & Klaassen, I. 2010. Active HIF-1 in the Normal Human Retina. *Journal of Histochemistry & Cytochemistry*, 58, (3) 247-254

Hughes, S., Gardiner, T., Hu, P., Baxter, L., Rosinova, E., & Chan-Ling, T. 2006. Altered pericyte-endothelial relations in the rat retina during aging: Implications for vessel stability. *Neurobiol.Aging*, 27, (12) 1838-1847

Humer, M.F., Phang, P.T., Friesen, B.P., Allard, M.F., Goddard, C.M., & Walley, K.R. 1996. Heterogeneity of gut capillary transit times and impaired gut oxygen extraction in endotoxemic pigs. *J.Appl.Physiol.*, 81, (2) 895-904

Husson, T.R., Mallik, A.K., Zhang, J.X., & Issa, N.P. 2007. Functional imaging of primary visual cortex using flavoprotein autofluorescence. *J.Neurosci.*, 27, (32) 8665-8675

Iglesias, A., Bauer, J., Litzenburger, T., Schubart, A., & Linington, C. 2001. T- and B-cell responses to myelin oligodendrocyte glycoprotein in experimental autoimmune encephalomyelitis and multiple sclerosis. *Glia*, 36, (2) 220-234

Ince, C. 2005. The microcirculation is the motor of sepsis. *Crit.Care*, 9, S13-S19

Ince, C. & Sinaasappel, M. 1999. Microcirculatory oxygenation and shunting in sepsis and shock. *Crit.Care Med.*, 27, (7) 1369-1377

Ivanov, K.P., Derry, A.N., Vovenko, E.P., Samoilov, M.O., & Semionov, D.G. 1982. Direct Measurements of Oxygen-Tension at the Surface of Arterioles, Capillaries and Venules of the Cerebral-Cortex. *Pflugers Archiv-European Journal of Physiology*, 393, (1) 118-120

Ivanov, K.P., Sokolova, I.B., & Vovenko, E.P. 1999. Oxygen transport in the rat brain cortex at normobaric hyperoxia. *European Journal of Applied Physiology and Occupational Physiology*, 80, (6) 582-587

Jeppsson, B., Freund, H.R., Gimmon, Z., James, J.H., Vonmeyenfeldt, M.F., & Fischer, J.E. 1981. Blood-Brain-Barrier Derangement in Sepsis - Cause of Septic Encephalopathy. *Am.J.Surg.*, 141, (1) 136-142

Joels, M. & Baram, T.Z. 2009. OPINION The neuro-symphony of stress. *Nature Reviews Neuroscience*, 10, (6) 459-U84

Kam, J.H., Lenassi, E., & Jeffery, G. 2010. Viewing Ageing Eyes: Diverse Sites of Amyloid Beta Accumulation in the Ageing Mouse Retina and the Up-Regulation of Macrophages. *Plos One*, 5, (10)

Kang, D.C. & Hamasaki, N. 2005. Alterations of mitochondrial DNA in common diseases and disease states: Aging, neurodegeneration, heart failure, diabetes and cancer. *Curr.Med.Chem.*, 12, (4) 429-441

Kann, O., Schuchmann, S., Buchheim, K., & Heinemann, U. 2003. Coupling of neuronal activity and mitochondrial metabolism as revealed by NAD(P)H fluorescence signals in organotypic hippocampal slice cultures of the rat. *Neuroscience*, 119, (1) 87-100

Kantrow, S.P., Taylor, D.E., Carraway, M.S., & Piantadosi, C.A. 1997. Oxidative metabolism in rat hepatocytes and mitochondria during sepsis. *Arch.Biochem.Biophys.*, 345, (2) 278-288

Kapin, M.A., Yanni, J.M., Brady, M.T., McDonough, T.J., Flanagan, J.G., Rawji, M.H., Dahlin, D.C., Sanders, M.E., & Gamache, D.A. 2003. Inflammation-mediated retinal edema in the rabbit is inhibited by topical nepafenac. *Inflammation*, 27, (5) 281-291

Karhausen, J., Haase, V.H., & Colgan, S.P. 2005. Inflammatory hypoxia - Role of hypoxia-inducible factor. *Cell Cycle*, 4, (2) 256-258

Karwoski, C.J. & Xu, X.J. 1999. Current source-density analysis of light-evoked field potentials in rabbit retina. *Vis.Neurosci.*, 16, (2) 369-377

Kasischke, K.A., Lambert, E.M., Panepento, B., Sun, A., Gelbard, H.A., Burgess, R.W., Foster, T.H., & Nedergaard, M. 2011. Two-photon NADH imaging exposes boundaries of oxygen diffusion in cortical vascular supply regions. *J.Cereb.Blood Flow Metab.*, 31, (1) 68-81

Kasischke, K.A., Vishwasrao, H.D., Fisher, P.J., Zipfel, W.R., & Webb, W.W. 2004. Neural activity triggers neuronal oxidative metabolism followed by astrocytic glycolysis. *Science*, 305, (5680) 99-103

Kaur, C. & Ling, E.A. 1991. Study of the Transformation of Ameboid Microglial Cells Into Microglia Labeled with the Isolectin Griffonia-Simplicifolia in Postnatal Rats. *Acta Anat.*, 142, (2) 118-125

Kennedy, C., Grave, G.D., & Jehle, J.W. 1971. Effect of Hyperoxia on the Cerebral Ciculation of the Newborn Puppy. *Pediatr.Res.*, 5, 659-667

Kerrison, J.B., Flynn, T., & Green, W.R. 1994. Retinal Pathological-Changes in Multiple-Sclerosis. *Retina-the Journal of Retinal and Vitreous Diseases*, 14, (5) 445-451

Kim, H.J., Kim, K.W., Yu, B.P., & Chung, H.Y. 2000. The effect of age on cyclooxygenase-2 gene expression: NF-kappa b activation and I kappa B alpha degradation. *Free Radical Biol.Med.*, 28, (5) 683-692

Kiss, S., Letko, E., Qamruddin, S., Baltatzis, S., & Foster, C.S. 2003. Long-term progression, prognosis, and treatment of patients with recurrent ocular manifestations of Reiter's syndrome. *Ophthalmology*, 110, (9) 1764-1769

Kitaura, H., Uozumi, N., Tohmi, M., Yamazaki, M., Sakimura, K., Kudoh, M., Shimizu, T., & Shibuki, K. 2007. Roles of nitric oxide as a vasodilator in neurovascular coupling of mouse somatosensory cortex. *Neurosci.Res.*, 59, (2) 160-171

Klaidman, L.K., Leung, A.C., & Adams, J.D. 1995. High-Performance Liquid-Chromatography Analysis of Oxidized and Reduced Pyridine Dinucleotides in Specific Brain-Regions. *Anal.Biochem.*, 228, (2) 312-317

Klein, R.J., Zeiss, C., Chew, E.Y., Tsai, J.Y., Sackler, R.S., Haynes, C., Henning, A.K., SanGiovanni, J.P., Mane, S.M., Mayne, S.T., Bracken, M.B., Ferris, F.L., Ott, J., Barnstable, C., & Hoh, J. 2005. Complement factor H polymorphism in age-related macular degeneration. *Science*, 308, (5720) 385-389

Koenig, H. 1963. The autofluorescence of lysosomes. Its value for the identification of lysosomal constituents. *Journal of Histochemistry & Cytochemistry*, 11, (4) 556-557

Koizumi, K., Poulaki, V., Doehmen, S., Welsandt, G., Radetzky, S., Lappas, A., Kociok, N., Kirchhof, B., & Joussen, A.M. 2003. Contribution of TNF-alpha to leukocyte adhesion, vascular leakage, and apoptotic cell death in endotoxin-induced uveitis in vivo. *Investigative Ophthalmology & Visual Science*, 44, (5) 2184-2191

Koke, J.R., Wylie, W., & Wills, M. 1981. Sensitivity of Flavoprotein Fluorescence to Oxidative State in Single Isolated Heart-Cells. *Cytobios*, 32, (127-) 139-145

Kongyai, N., Pathanapitoon, K., Sirirungsi, W., Kunavisarut, P., de Groot-Mijnes, J.D.F., & Rothova, A. 2012. Infectious causes of posterior uveitis and panuveitis in Thailand. *Jpn.J.Ophthalmol.*, 56, (4) 390-395

Korhonen, P., Helenius, M., & Salminen, A. 1997. Age-related changes in the regulation of transcription factor NF-kappa B in rat brain. *Neurosci.Lett.*, 225, (1) 61-64

Kreutzberg, G.W. 1996. Microglia: A sensor for pathological events in the CNS. *Trends Neurosci.*, 19, (8) 312-318

Krogh, A. 1919. The number and distribution of capillaries in muscles with calculations of the oxygen pressure head necessary for supplying the tissue. *Journal of Physiology-London*, 52, (6) 409-415

Kroll, J. & Waltenberger, J. 1998. VEGF-A induces expression of eNOS and iNOS in endothelial cells via VEGF receptor-2 (KDR). *Biochem.Biophys.Res.Commun.*, 252, (3) 743-746

Kubota, S., Kurihara, T., Mochimaru, H., Satofuka, S., Noda, K., Ozawa, Y., Oike, Y., Ishida, S., & Tsubota, K. 2009. Prevention of Ocular Inflammation in Endotoxin-Induced Uveitis with Resveratrol by Inhibiting Oxidative Damage and Nuclear Factor-kappa B Activation. *Investigative Ophthalmology & Visual Science*, 50, (7) 3512-3519

Kubota, Y., Kamatani, D., Tsukano, H., Ohshima, S., Takahashi, K., Hishida, R., Kudoh, M., Takahashi, S., & Shibuki, K. 2008. Transcranial photo-inactivation of neural activities in the mouse auditory cortex. *Neurosci.Res.*, 60, (4) 422-430

Kumar, A., Roberts, D., Wood, K.E., Light, B., Parrillo, J.E., Sharma, S., Suppes, R., Feinstein, D., Zanotti, S., Taiberg, L., Gurka, D., Kumar, A., & Cheang, M. 2006. Duration of hypotension before initiation of effective antimicrobial therapy is the critical determinant of survival in human septic shock. *Crit.Care Med.*, 34, (6) 1589-1596

Kunz, W.S. & Gellerich, F.N. 1993. Quantification of the Content of Fluorescent Flavoproteins in Mitochondria from Liver, Kidney Cortex, Skeletal-Muscle, and Brain. *Biochem.Med.Metab.Biol.*, 50, (1) 103-110

Kunz, W.S. & Kunz, W. 1985. Contribution of Different Enzymes to Flavoprotein Fluorescence of Isolated Rat-Liver Mitochondria. *Biochimica et Biophysica Acta*, 841, (3) 237-246

Kurihara, T., Ozawa, Y., Shinoda, K., Nagai, N., Inoue, M., Oike, Y., Tsubota, K., Ishida, S., & Okano, H. 2006. Neuroprotective effects of angiotensin II type 1 receptor (AT1R) blocker, telmisartan, via modulating AT1R and AT2R signaling in retinal inflammation. *Investigative Ophthalmology & Visual Science*, 47, (12) 5545-5552

Lahdenranta, J., Pasqualini, R., Schlingemann, R.O., Hagedorn, M., Stallcup, W.B., Bucana, C.D., Sidman, R.L., & Arap, W. 2001. An anti-angiogenic state in mice and humans with retinal photoreceptor cell degeneration. *Proc.Natl.Acad.Sci.U.S.A.*, 98, (18) 10368-10373

Lam, A.K., Silva, P.N., Altamentova, S.M., & Rocheleau, J.V. 2012. Quantitative imaging of electron transfer flavoprotein autofluorescence reveals the dynamics of lipid partitioning in living pancreatic islets. *Integrative Biology*, 4, (8) 838-846

Lam, C., Tyml, K., Martin, C., & Sibbald, W. 1994. Microvascular Perfusion Is Impaired in A Rat Model of Normotensive Sepsis. *J.Clin.Invest.*, 94, (5) 2077-2083

Lambertsen, C.J., Kough, R.H., Cooper, D.Y., Emmel, G.L., Loeschcke, H.H., & Schmidt, C.F. 1953. Oxygen Toxicity. Effects in Man of Oxygen Inhalation at 1 and 3.5 Atmospheres Upon Blood Gas Transport, Cerebral Circulation and Cerebral Metabolism. *J.Appl.Physiol.*, 5, (9) 471-486

Lang, C.H., Bagby, G.J., Ferguson, J.L., & Spitzer, J.J. 1984. Cardiac-Output and Redistribution of Organ Blood-Flow in Hypermetabolic Sepsis. *Am.J.Physiol.*, 246, (3) R331-R337

Larsson, N.G. & Clayton, D.A. 1995. Molecular genetic aspects of human mitochondrial disorders. *Annu.Rev.Genet.*, 29, 151-178

Lassen, N.A. 1959. Cerebral Blood Flow and Oxygen Consumption in Man. *Physiol.Rev.*, 39, (2) 183-238

Lauritzen, M., Dreier, J.P., Fabricius, M., Hartings, J.A., Graf, R., & Strong, A.J. 2011. Clinical relevance of cortical spreading depression in neurological disorders: migraine, malignant stroke, subarachnoid and intracranial hemorrhage, and traumatic brain injury. *J.Cereb.Blood Flow Metab.*, 31, (1) 17-35

Laycock, S.K., Vogel, T., Forfia, P.R., Tuzman, J., Xu, X.B., Ochoa, M., Thompson, C.I., Nasjletti, A., & Hintze, T.H. 1998. Role of nitric oxide in the control of renal oxygen consumption and the regulation of chemical work in the kidney. *Circul.Res.*, 82, (12) 1263-1271

Le Scanff, J., Seve, P., Renoux, C., Broussolle, C., Confavreux, C., & Vukusic, S. 2008. Uveitis associated with multiple sclerosis. *Mult.Scler.*, 14, (3) 415-417

Leahy, F.A.N., Cates, D., MacCallum, M., & Rigatto, H. 1980. Effect of CO2 and 100% 02 on cerebral blood flow in preterm infants. *American Physiological Society*, 48, 468-472

Leal, E.C., Manivannan, A., Hosoya, K.I., Terasaki, T., Cunha-Vaz, J., Ambrosio, A.F., & Forrester, J.V. 2007. Inducible nitric oxide synthase isoform is a key mediator of leukostasis and blood-retinal barrier breakdown in diabetic retinopathy. *Investigative Ophthalmology & Visual Science*, 48, (11) 5257-5265

Lebon, V., Petersen, K.F., Cline, G.W., Shen, J., Mason, G.F., Dufour, S., Behar, K.L., Shulman, G.I., & Rothman, D.L. 2002. Astroglial contribution to brain energy metabolism in humans revealed by C-13 nuclear magnetic resonance spectroscopy: Elucidation of the dominant pathway for neurotransmitter glutamate repletion and measurement of astrocytic oxidative metabolism. *J.Neurosci.*, 22, (5) 1523-1531

LeDoux, D., Astiz, M.E., Carpati, C.M., & Rackow, E.C. 2000. Effects of perfusion pressure on tissue perfusion in septic shock. *Crit.Care Med.*, 28, (8) 2729-2732

Lee, L., Raleigh, J. A., & Ji, X. History of Hypoxyprobe Development. 28-10-2014. Ref Type: Online Source

Leibowitz, U. & Alter, M. 1968. Optic Nerve Involvement and Diplopia As Initial Manifestations of Multiple Sclerosis. *Acta Neurol.Scand.*, 44, (1) 70-&

Leist, M., Single, B., Naumann, H., Fava, E., Simon, B., Kuhnle, S., & Nicotera, P. 1999. Inhibition of mitochondrial ATP generation by nitric oxide switches apoptosis to necrosis. *Exp.Cell Res.*, 249, (2) 396-403

Levi, M., VanderPoll, T., TenCate, H., & VanDeventer, S.J.H. 1997. The cytokine-mediated imbalance between coagulant and anticoagulant mechanisms in sepsis and endotoxaemia. *Eur.J.Clin.Invest.*, 27, (1) 3-9

Lewis, D.V. & Schuette, W.H. 1976. Nadh Fluorescence, [K+]0 and Oxygen-Consumption in Cat Cerebral-Cortex During Direct Cortical Stimulation. *Brain Res.*, 110, (3) 523-535

Lidington, D., Ouellette, Y., Li, F., & Tyml, K. 2004. Conducted vasoconstriction is reduced in a mouse model of sepsis. *J.Vasc.Res.*, 41, (1) 107-108

Lightman, S., Mcdonald, W.I., Bird, A.C., Francis, D.A., Hoskins, A., Batchelor, J.R., & Halliday, A.M. 1987. Retinal Venous Sheathing in Optic Neuritis - Its Significance for the Pathogenesis of Multiple-Sclerosis. *Brain*, 110, 405-414

LihBrody, L., Powell, S.R., Collier, K.P., Reddy, G.M., Cerchia, R., Kahn, E., Weissman, G.S., Katz, S., Floyd, R.A., McKinley, M.J., Fisher, S.E., & Mullin, G.E. 1996. Increased oxidative stress and decreased antioxidant defenses in mucosa of inflammatory bowel disease. *Dig.Dis.Sci.*, 41, (10) 2078-2086

Lin, M.T. & Beal, M.F. 2006. Mitochondrial dysfunction and oxidative stress in neurodegenerative diseases. *Nature*, 443, (7113) 787-795

Lothman, E., LaManna, J., Cordingley, G., Rosenthal, M., & Somjen, G. 1975. Responses of electrical potential, potassium levels, and oxidative metabolic activity of the cerebral neocortex of cats. *Brain Res.*, 88, (1) 15-36

Lowenstein, C.J., Dinerman, J.L., & Snyder, S.H. 1994. Nitric-Oxide - A Physiological Messenger. *Ann.Intern.Med.*, 120, (3) 227-237

Lowes, D.A., Thottakam, B.M.V., Webster, N.R., Murphy, M.P., & Galley, H.F. 2008. The mitochondria-targeted antioxidant MitoQ protects against organ damage in a lipopolysaccharide-peptidoglycan model of sepsis. *Free Radical Biol.Med.*, 45, (11) 1559-1565

Luna, J.D., Chan, C.C., Derevjanik, N.L., Mahlow, J., Chiu, C., Peng, B., Tobe, T., Campochiaro, P.A., & Vinores, S.A. 1997. Blood-retinal barrier (BRB) breakdown in experimental autoimmune uveoretinitis: Comparison with vascular endothelial growth factor, tumor necrosis factor alpha, and interleukin-1 beta-mediated breakdown. *J.Neurosci.Res.*, 49, (3) 268-280

Ly, J.D., Grubb, D.R., & Lawen, A. 2003. The mitochondrial membrane potential (Delta psi m) in apoptosis; an update. *Apoptosis*, 8, (2) 115-128

Machiedo, G.W., Powell, R.J., Rush, B.F., Swislocki, N.I., & Dikdan, G. 1989. The Incidence of Decreased Red Blood-Cell Deformability in Sepsis and the Association with Oxygen Free-Radical Damage and Multiple-System Organ Failure. *Arch.Surg.*, 124, (12) 1386-1389

Macmillan, V. & Siesjo, B.K. 1972. Brain Energy Metabolism in Hypoxemia. *Scandinavian Journal of Clinical & Laboratory Investigation*, 30, (2) 127-&

Maekawa, T., Fujii, Y., Sadamitsu, D., Yokota, K., Soejima, Y., Ishikawa, T., Miyauchi, Y., & Takeshita, H. 1991. Cerebral-Circulation and Metabolism in Patients with Septic Encephalopathy. *Am.J.Emerg.Med.*, 9, (2) 139-143

Magistretti, P.J. & Pellerin, L. 1999. Cellular mechanisms of brain energy metabolism and their relevance to functional brain imaging. *Philosophical Transactions of the Royal Society of London Series B-Biological Sciences*, 354, (1387) 1155-1163

Magistretti, P.J., Pellerin, L., Rothman, D.L., & Shulman, R.G. 1999. Neuroscience - Energy on demand. *Science*, 283, (5401) 496-497

Mahad, D., Lassmann, H., & Turnbull, D. 2008. Review: Mitochondria and disease progression in multiple sclerosis. *Neuropathol.Appl.Neurobiol.*, 34, (6) 577-589

Mander, P., Borutaite, V., Moncada, S., & Brown, G.C. 2005. Nitric oxide from inflammatory-activated glia synergizes with hypoxia to induce neuronal death. *J.Neurosci.Res.*, 79, (1-2) 208-215

Marchant, A., Deviere, J., Byl, B., Degroote, D., Vincent, J.L., & Goldman, M. 1994. Interleukin-10 Production During Septicemia. *Lancet*, 343, (8899) 707-708

Marie, C., Cavaillon, J.M., & Losser, M.R. 1996. Elevated levels of circulating transforming growth factor-beta 1 in patients with the sepsis syndrome. *Ann.Intern.Med.*, 125, (6) 520-521

Masters, B.R., So, P.T.C., & Gratton, E. 1997. Multiphoton excitation fluorescence microscopy and spectroscopy of in vivo human skin. *Biophys.J.*, 72, (6) 2405-2412

Matsumoto, T., Dolgor, B., Ninomiya, K., Bandoh, T., Yoshida, T., & Kitano, S. 2001. Effect of CO2 pneumoperitoneum on the systemic and peritoneal cytokine response in a LPS-induced sepsis model. *Eur.Surg.Res.*, 33, (2) 71-76

Matsuo, T., Nakayama, T., Koyama, T., Koyama, M., Fujimoto, S., & Matsuo, N. 1986. Immunological Studies of Uveitis .3. Cell-Mediated-Immunity to Interphoto-Receptor Retinoid-Binding Protein. *Jpn.J.Ophthalmol.*, 30, (4) 487-494

Maurer, M. & Rieckmann, P. 2000. Relapsing-remitting multiple sclerosis - What is the potential for combination therapy? *Biodrugs*, 13, (3) 149-158

Mayevsky, A. 1984. Brain NADH Redox State Monitored In Vivo by Fiber Optic Surface Fluorometry. *Brain Reserach Reviews*, 7, 49-68

Mayevsky, A. & Chance, B. 1973. A new long-term method for the measurement of NADH fluorescence in intact rat brain with chronically implanted cannula. *Oxygen Transport to Tissue Advances in Experimental Medicine and Biology*, 37, 239-244

Mayevsky, A. & Chance, B. 1974. Repetitive Patterns of Metabolic Changes During Cortical Spreading Depression of Awake Rat. *Brain Res.*, 65, (3) 529-533

Mayevsky, A., Zeuthen, T., & Chance, B. 1974. Measurements of Extracellular Potassium, Ecog and Pyridine-Nucleotide Levels During Cortical Spreading Depression in Rats. *Brain Res.*, 76, (2) 347-349

Mcdonald, W.I. & Barnes, D. 1992. The Ocular Manifestations of Multiple-Sclerosis .1. Abnormalities of the Afferent Visual-System. *Journal of Neurology Neurosurgery and Psychiatry*, 55, (9) 747-752

Mcewen, B.S. & Grafstein, B. 1968. Fast and Slow Components in Axonal Transport of Protein. *Journal of Cell Biology*, 38, (3) 494-&

Mcgeer, E.G., Klegeris, A., & Mcgeer, P.L. 2005. Inflammation, the complement system and the diseases of aging. *Neurobiology of Aging*, 26, S94-S97

Mcgeer, P.L. & Mcgeer, E.G. 2004. Inflammation and neurodegeneration in Parkinson's disease. *Parkinsonism & Related Disorders*, 10, S3-S7

Mcgeer, P.L. & Sibley, J. 2005. Sparing of age-related macular degeneration in rheumatoid arthritis. *Neurobiology of Aging*, 26, (8) 1199-1203

Mecocci, P., Macgarvey, U., Kaufman, A.E., Koontz, D., Shoffner, J.M., Wallace, D.C., & Beal, M.F. 1993. Oxidative Damage to Mitochondrial-Dna Shows Marked Age-Dependent Increases in Human Brain. *Ann.Neurol.*, 34, (4) 609-616

Meda, L., Bonaiuto, C., Szendrei, G.I., Ceska, M., Rossi, F., & Cassatella, M.A. 1995a. Beta-Amyloid(25-35) Induces the Production of Interleukin-8 from Human Monocytes. *J.Neuroimmunol.*, 59, (1-2) 29-33

Meda, L., Cassatella, M.A., Szendrei, G.I., Otvos, L., Baron, P., Villalba, M., Ferrari, D., & Rossi, F. 1995b. Activation of Microglial Cells by Beta-Amyloid Protein and Interferon-Gamma. *Nature*, 374, (6523) 647-650

Mela, L., Bacalzo, L.V., & Miller, L.D. 1971. Defective Oxidative Metabolism of Rat Liver Mitochondria in Hemorrhagic and Endotoxin Shock. *Am.J.Physiol.*, 220, (2) 571-&

Mela, L. & Miller, L.D. 1983. Efficacy of Glucocorticoids in Preventing Mitochondrial Metabolic Failure in Endotoxemia. *Circ.Shock*, 10, (4) 371-381

Meyer, R., Weissert, R., Diem, R., Storch, M.K., de Graaf, K.L., Kramer, B., & Bahr, M. 2001. Acute neuronal apoptosis in a rat model of multiple sclerosis. *J.Neurosci.*, 21, (16) 6214-6220

Meyrick, B., Christman, B., & Jesmok, G. 1991. Effects of Recombinant Tumor-Necrosis-Factor-Alpha on Cultured Pulmonary-Artery and Lung Microvascular Endothelial Monolayers. *Am.J.Pathol.*, 138, (1) 93-101

Minson, C.T., Berry, L.T., & Joyner, M.J. 2001. Nitric oxide and neurally mediated regulation of skin blood flow during local heating. *J.Appl.Physiol.*, 91, (4) 1619-1626

Mogensen, P.H. 1990. Histopathology of Anterior Parts of the Optic Pathway in Patients with Multiple-Sclerosis. *Acta Ophthalmol.(Copenh).*, 68, (2) 218-220

Moseley, M.L., Zu, T., Ikeda, Y., Gao, W.C., Mosemiller, A.K., Daughters, R.S., Chen, G., Weatherspoon, M.R., Clark, H.B., Ebner, T.J., Day, J.W., & Ranum, L.P.W. 2006. Bidirectional expression of CUG and CAG expansion transcripts and intranuclear polyglutamine inclusions in spinocerebellar ataxia type 8. *Nat.Genet.*, 38, (7) 758-769

Mourvillier, B., Tubach, F., van de Beek, D., Garot, D., Pichon, N., Georges, H., Lefevre, L.M., Bollaert, P.E., Boulain, T., Luis, D., Cariou, A., Girardie, P., Chelha, R., Megarbane, B., Delahaye, A., Chalumeau-Lemoine, L., Legriel, S., Beuret, P., Brivet, F., Bruel, C., Camou, F., Chatellier, D., Chillet, P., Clair, B., Constantin, J.M., Duguet, A., Galliot, R., Bayle, F., Hyvernat, H., Ouchenir, K., Plantefeve, G., Quenot, J.P., Richecoeur, J., Schwebel, C., Sirodot, M., Esposito-Farese, M., Le Tulzo, Y., & Wolff, M. 2013. Induced Hypothermia in Severe Bacterial Meningitis A Randomized Clinical Trial. *J.Am.Med.Assoc.*, 310, (20) 2174-2183

Murakami, H., Kamatani, D., Hishida, R., Takao, T., Kudoh, M., Kawaguchi, T., Tanaka, R., & Shibuki, K. 2004. Short-term plasticity visualized with flavoprotein autofluorescence in the somatosensory cortex of anaesthetized rats. *Eur.J.Neurosci.*, 19, (5) 1352-1360

Murphy, M.P. 2009. How mitochondria produce reactive oxygen species. *Biochem.J.*, 417, 1-13

Murphy, S.L., Xu, J., & Kochanek, K.D. 2013. Deaths: Final Data for 2010. *Natl.Vital Stat.Rep.*, 61, (4) 1-118

Nagai, N., Oike, Y., Noda, K., Urano, T., Kubota, Y., Ozawa, Y., Shinoda, H., Koto, T., Shinoda, K., Inoue, M., Tsubota, K., Yamashiro, K., Suda, T., & Ishida, S. 2005. Suppression of ocular inflammation in endotoxin-induced uveitis by blocking the angiotensin II type 1 receptor. *Investigative Ophthalmology & Visual Science*, 46, (8) 2925-2931

Nakajima, K. & Kohsaka, S. 2005, "Resposne of microglia to brain injury," *In Neuroglia*, 2nd ed. H. Kettenmann & B. R. Ransom, eds., New York: Oxford University Press, pp. 443-453.

Neviere, R., Mathieu, D., Chagnon, J.L., Lebleu, N., Millien, J.P., & Wattel, F. 1996. Skeletal muscle microvascular blood flow and oxygen transport in patients with severe sepsis. *Am.J.Respir.Crit.Care Med.*, 153, (1) 191-195

Nieuwdorp, A., Melawese, M.C., Mooij, H.L., van Lieshout, M.H.P., Hayden, A., Levi, M., Meijers, J.C.M., Ince, C., Kastelein, J.J.P., Vink, H., & Stroes, E.S.G. 2009. Tumor necrosis factor-alpha inhibition protects against endotoxin-induced endothelial glycocalyx perturbation. *Atherosclerosis*, 202, (1) 296-303

Nowak, J.Z. 2006. Age-related macular degeneration (AMD): pathogenesis and therapy. *Pharmacological Reports*, 58, (3) 353-363

Nussenblatt, R.B. 1990. The Natural-History of Uveitis. *Int.Ophthalmol.*, 14, (5-6) 303-308

Nussenblatt, R.B., Gery, I., Ballintine, E.J., & Wacker, W.B. 1980. Cellular Immune Responsiveness of Uveitis Patients to Retinal S-Antigen. *Am.J.Ophthalmol.*, 89, (2) 173-179

Nussler, A.K. & Billiar, T.R. 1993. Inflammation, Immunoregulation, and Inducible Nitric-Oxide Synthase. *J.Leukocyte Biol.*, 54, (2) 171-178

Opie, N.L., Greferath, U., Vessey, K.A., Burkitt, A.N., Meffin, H., Grayden, D.B., & Fletcher, E.L. 2012. Retinal Prosthesis Safety: Alterations in Microglia Morphology due to Thermal Damage and Retinal Implant Contact. *Investigative Ophthalmology & Visual Science*, 53, (12) 7802-7812

Orchard, T.R., Chua, C.N., Ahmad, T., Cheng, H., Welsh, K.I., & Jewell, D.P. 2002. Uveitis and erythema nodosum in inflammatory bowel disease: Clinical features and the role of HLA genes. *Gastroenterology*, 123, (3) 714-718

Palmer, R.M.J., Ferrige, A.G., & Moncada, S. 1987. Nitric-Oxide Release Accounts for the Biological-Activity of Endothelium-Derived Relaxing Factor. *Nature*, 327, (6122) 524-526

Panek, W.C., Holland, G.N., Lee, D.A., & Christensen, R.E. 1990. Glaucoma in Patients with Uveitis. *Br.J.Ophthalmol.*, 74, (4) 223-227

Papadopoulos, M.C., Lamb, F.J., Moss, R.F., Davies, D.C., Tighe, D., & Bennett, E.D. 1999. Faecal peritonitis causes oedema and neuronal injury in pig cerebral cortex. *Clin.Sci.*, 96, (5) 461-466

Parent, C. & Eichacker, P.Q. 1999. Neutrophil and endothelial cell interactions in sepsis - The role of adhesion molecules. *Infect.Dis.Clin.North Am.*, 13, (2) 427-+

Patterson, G.H., Knobel, S.M., & Piston, D.W. 2000. Separation of the glucose-stimulated cytoplasmic and mitochondrial NAD(P)H responses in pancreatic islet beta cells. *Biophys.J.*, 78, (1) 445A

Pellerin, L. & Magistretti, P.J. 1994. Glutamate Uptake Into Astrocytes Stimulates Aerobic Glycolysis - A Mechanism Coupling Neuronal-Activity to Glucose-Utilization. *Proc.Natl.Acad.Sci.U.S.A.*, 91, (22) 10625-10629

Penn, R.D. & Hagins, W.A. 1969. Signal Transmission along Retinal Rods and the Origin of the Electroretinographic a-Wave. *Nature*, 223, 201-205

Pernerstorfer, T., Krafft, P., Fitzgerald, R., Fridrich, P., Koc, D., Hammerle, A.F., & Steltzer, H. 1995. Optimal Values for Oxygen-Transport During Hypothermia in Sepsis and Ards. *Acta Anaesthesiol.Scand.*, 39, 223-227

Petronilli, V., Cola, C., Massari, S., Colonna, R., & Bernardi, P. 1993. Physiological Effectors Modify Voltage Sensing by the Cyclosporine A-Sensitive Permeability Transition Pore of Mitochondria. *J.Biol.Chem.*, 268, (29) 21939-21945

Peyssonnaux, C., Cejudo-Martin, P., Doedens, A., Zinkernagel, A.S., Johnson, R.S., & Nizet, V. 2007. Cutting edge: Essential role of hypoxia inducible factor-1 alpha in development of lipopolysaccharide-induced sepsis. *J.Immunol.*, 178, (12) 7516-7519

Pickkers, P., Sprong, T., van Eijk, L., van der Hoeven, H., Smits, P., & van Deuren, M. 2005. Vascular endothelial growth factor is increased during the first 48 hours of human septic shock and correlates with vascular permeability. *Shock*, 24, (6) 508-512

Piper, R.D., Pitt-Hyde, M., Li, F.Y., Sibbald, W.J., & Potter, R.F. 1996. Microcirculatory changes in rat skeletal muscle in sepsis. *Am.J.Respir.Crit.Care Med.*, 154, (4) 931-937

Piston, D.W., Bennett, B.D., & Ying, G. 1995. Imaging of Cellular Dynamics by Two-Photon Excitation Miscoscopy. *Microsc.Microanal.* (1) 25-34

Poderoso, J.J., Fernandez, S., Carreras, M.C., Tchercanski, D., Acevedo, C., Rubio, M., Peralta, J., & Boveris, A. 1994. Liver Oxygen-Uptake Dependence and Mitochondrial-Function in Septic Rats. *Circ.Shock*, 44, (4) 175-182

Polderman, K.H. & Herold, I. 2009. Therapeutic hypothermia and controlled normothermia in the intensive care unit: Practical considerations, side effects, and cooling methods. *Crit.Care Med.*, 37, (3) 1101-1120

Pollard, V., Prough, D.S., Deyo, D.J., Conroy, B., Uchida, T., Daye, A., Traber, L.D., & Traber, D.L. 1997. Cerebral blood flow during experimental endotoxemia in volunteers. *Crit.Care Med.*, 25, (10) 1700-1706

Popescu, B.O., Toescu, E.C., Popescu, L.M., Bajenaru, O., Muresanu, D.F., Schultzberg, M., & Bogdanovic, N. 2009. Blood-brain barrier alterations in ageing and dementia. *J.Neurol.Sci.*, 283, (1-2) 99-106

Powell, R.J., Machiedo, G.W., Rush, B.F., & Dikdan, G. 1991. Oxygen Free-Radicals - Effect on Red-Cell Deformability in Sepsis. *Crit.Care Med.*, 19, (5) 732-735

Poynter, M.E. & Daynes, R.A. 1999. Age-associated alterations in splenic iNOS regulation: Influence of constitutively expressed IFN-gamma and correction following supplementation with PPAR alpha activators or vitamin E. *Cell.Immunol.*, 195, (2) 127-136

Protti, A. & Singer, M. 2006. Bench-to-bedside review: Potential strategies to protect or reverse mitochondrial dysfunction in sepsis-induced organ failure. *Crit.Care*, 10, (5)

Qi, X.P., Lewin, A.S., Sun, L., Hauswirth, W.W., & Guy, J. 2007. Suppression of mitochondrial oxidative stress provides long-term neuroprotection in experimental optic neuritis. *Investigative Ophthalmology & Visual Science*, 48, (2) 681-691

Quarles, R.H. 2002. Myelin sheaths: glycoproteins involved in their formation, maintenance and degeneration. *Cellular and Molecular Life Sciences*, 59, (11) 1851-1871

Quistorff, B., Haselgrove, J.C., & Chance, B. 1985. High Spatial-Resolution Readout of 3-D Metabolic Organ Structure - An Automated, Low-Temperature Redox Ratio-Scanning Instrument. *Anal.Biochem.*, 148, (2) 389-400

Ragan, C.I. & Garland, P.B. 1969. The Intra-Mitochondrial Localization of Flavoproteins Previously Assigned to the Respiratory Chain. *Eur.J.Biochem.*, 10, (3) 399-410

Raichle, M.E. & Gusnard, D.A. 2002. Appraising the brain's energy budget. *Proc.Natl.Acad.Sci.U.S.A.*, 99, (16) 10237-10239

Rao, P. & Segal, B. M. 2004, "Experimental Autoimmune Encephalomyelitis," *In Autoimmunity, Methods in Molecular Medicine*, pp. 363-375.

Reinert, K.C., Dunbar, R.L., Gao, W.C., Chen, G., & Ebner, T.J. 2004. Flavoprotein autofluorescence imaging of neuronal activation in the cerebellar cortex in vivo. *J.Neurophysiol.*, 92, (1) 199-211

Reinert, K.C., Gao, W.C., Chen, G., & Ebner, T.J. 2007. Flavoprotein autofluorescence imaging in the cerebellar cortex in vivo. *J.Neurosci.Res.*, 85, (15) 3221-3232

Reinert, K.C., Gao, W.C., Chen, G., Wang, X.M., Peng, Y.P., & Ebner, T.J. 2011. Cellular and Metabolic Origins of Flavoprotein Autofluorescence in the Cerebellar Cortex in vivo. *Cerebellum*, 10, (3) 585-599

Riancho, J.A., Zarrabeitia, M.T., Amado, J.A., Olmos, J.M., & Gonzalezmacias, J. 1994. Age-Related Differences in Cytokine Secretion. *Gerontology*, 40, (1) 8-12

Richter, C., Park, J.W., & Ames, B.N. 1988. Normal Oxidative Damage to Mitochondrial and Nuclear-Dna Is Extensive. *Proc.Natl.Acad.Sci.U.S.A.*, 85, (17) 6465-6467

Rocheleau, J.V., Head, W.S., & Piston, D.W. 2004. Quantitative NAD(P)H/flavoprotein autofluorescence imaging reveals metabolic mechanisms of pancreatic islet pyruvate response. *J.Biol.Chem.*, 279, (30) 31780-31787

Rosenbaum, J.T., Mcdevitt, H.O., Guss, R.B., & Egbert, P.R. 1980. Endotoxin-Induced Uveitis in Rats As A Model for Human-Disease. *Nature*, 286, (5773) 611-613

Rossen, R., Kabat, H., & Anderson, J.P. 1943. Acute arrest of cerebral circulation in man. *Archives of Neurology and Psychiatry*, 50, (5) 510-528

Rosser, D.M., Stidwill, R.P., Jacobson, D., & Singer, M. 1995. Oxygen tension in the bladder epithelium rises in both high and low cardiac output endotoxemic sepsis. *J.Appl.Physiol.*, 79, (6) 1878-1882

Rothova, A., Buitenhuis, H.J., Meenken, C., Brinkman, C.J.J., Linssen, A., Alberts, C., Luyendijk, L., & Kijlstra, A. 1992. Uveitis and Systemic-Disease. *British Journal of Ophthalmology*, 76, (3) 137-141

Roubenoff, R., Harris, T.B., Abad, L.W., Wilson, P.W.F., Dallal, G.E., & Dinarello, C.A. 1998. Monocyte cytokine production in an elderly population: Effect of age and inflammation. *Journals of Gerontology Series A-Biological Sciences and Medical Sciences*, 53, (1) M20-M26

Saija, A., Princi, P., Trombetta, D., Lanza, M., & DePasquale, A. 1997. Changes in the permeability of the blood-brain barrier following sodium dodecyl sulphate administration in the rat. *Exp.Brain Res.*, 115, (3) 546-551

Sakadzic, S., Roussakis, E., Yaseen, M.A., Mandeville, E.T., Srinivasan, V.J., Arai, K., Ruvinskaya, S., Devor, A., Lo, E.H., Vinogradov, S.A., & Boas, D.A. 2010. Two-photon high-resolution measurement of partial pressure of oxygen in cerebral vasculature and tissue. *Nat.Methods*, 7, (9) 755-U125

Sasaki, M., Ozawa, Y., Kurihara, T., Noda, K., Imamura, Y., Kobayashi, S., Ishida, S., & Tsubota, K. 2009. Neuroprotective Effect of an Antioxidant, Lutein, during Retinal Inflammation. *Investigative Ophthalmology & Visual Science*, 50, (3) 1433-1439

Sato, K., Miyakawa, K., Takeya, M., Hattori, R., Yui, Y., Sunamoto, M., Ichimori, Y., Ushio, Y., & Takahashi, K. 1995. Immunohistochemical Expression of Inducible Nitric-Oxide Synthase (Inos) in Reversible Endotoxic-Shock Studied by A Novel Monoclonal-Antibody Against Rat Inos. *J.Leukocyte Biol.*, 57, (1) 36-44

Schaefer, C.F., Biber, B., Lerner, M.R., Jobsisvandervliet, F.F., & Fagraeus, L. 1991. Rapid Reduction of Intestinal Cytochrome-A,A3 During Lethal Endotoxemia. *J.Surg.Res.*, 51, (5) 382-391

Schalken, J.J., Winkens, H.J., Vanvugt, A.H.M., Boveegeurts, P.H.M., Degrip, W.J., & Broekhuyse, R.M. 1988. Rhodopsin-Induced Experimental Autoimmune Uveoretinitis - Dose-Dependent Clinicopathological Features. *Exp.Eye Res.*, 47, (1) 135-145

Schapira, A.H.V., Gu, M., Taanman, J.W., Tabrizi, S.J., Seaton, T., Cleeter, M., & Cooper, J.M. 1998. Mitochondria in the etiology and pathogenesis of Parkinson's disease. *Ann.Neurol.*, 44, (3) S89-S98

Schmidt, H., Schmidt, W., Muller, T., Bohrer, H., Gebhard, M.M., & Martin, E. 1997. N-acetylcysteine attenuates endotoxin-induced leukocyte endothelial cell adhesion and macromolecular leakage in vivo. *Crit.Care Med.*, 25, (5) 858-863

Scholz, R., Thurman, R.G., Williams, J.R., Chance, B., & Bucher, T. 1969. Flavin and Pyridine Nucleotide Oxidation-Reduction Changes in Perfused Rat Liver .I. Anoxia and Subcellular Localization of Fluorescent Flavoproteins. *J.Biol.Chem.*, 244, (9) 2317-&

Schouten, M., Wiersinga, W.J., Levi, M., & van der Poll, T. 2008. Inflammation, endothelium, and coagulation in sepsis. *J.Leukocyte Biol.*, 83, (3) 536-545

Schurr, A. 2006. Lactate: the ultimate cerebral oxidative energy substrate? *J.Cereb.Blood Flow Metab.*, 26, (1) 142-152

Schwartz, D.R., Malhtora, A., & Fink, M.P. 1999. Cytopathic Hypoxia in Sepsis: An Overview. *Sepsis*, 2, (4) 279-289

Schweizer, M. & Richter, C. 1994. Nitric-Oxide Potently and Reversibly Deenergizes Mitochondria at Low-Oxygen Tension. *Biochem.Biophys.Res.Commun.*, 204, (1) 169-175

Selmi, C. 2014. Diagnosis and classification of autoimmune uveitis. *Autoimmun.Rev.*, 13, (4-5) 591-594

Semmler, A., Okulla, T., Sastre, M., Dumitrescu-Ozimek, L., & Heneka, M.T. 2005. Systemic inflammation induces apoptosis with variable vulnerability of different brain regions. *J.Chem.Neuroanat.*, 30, (2-3) 144-157

Semmler, A., Widmann, C.N., Okulla, T., Urbach, H., Kaiser, M., Widman, G., Mormann, F., Weide, J., Fliessbach, K., Hoeft, A., Jessen, F., Putensen, C., & Heneka, M.T. 2013. Persistent cognitive impairment, hippocampal atrophy and EEG changes in sepsis survivors. *Journal of Neurology Neurosurgery and Psychiatry*, 84, (1) 62-70

Shen, W.Q., Xu, X.B., Ochoa, M., Zhao, G., Wolin, M.S., & Hintze, T.H. 1994. Role of Nitric-Oxide in the Regulation of Oxygen-Consumption in Conscious Dogs. *Circul.Res.*, 75, (6) 1086-1095

Shibuki, K. 1989. Calcium-Dependent and Ouabain-Resistant Oxygen-Consumption in the Rat Neurohypophysis. *Brain Res.*, 487, (1) 96-104

Shibuki, K., Hishida, R., Murakami, H., Kudoh, M., Kawaguchi, T., Watanabe, M., Watanabe, S., Kouuchi, T., & Tanaka, R. 2003. Dynamic imaging of somatosensory cortical activity in the rat visualized by flavoprotein autofluorescence. *Journal of Physiology-London*, 549, (3) 919-927

Shibuki, K., Ono, K., Hishida, R., & Kudoh, M. 2006. Endogenous fluorescence imaging of somatosensory cortical activities after discrimination learning in rats. *Neuroimage*, 30, (3) 735-744

Shigenaga, M.K., Hagen, T.M., & Ames, B.N. 1994. Oxidative Damage and Mitochondrial Decay in Aging. *Proc.Natl.Acad.Sci.U.S.A.*, 91, (23) 10771-10778

Shorb, S.R., Irvine, A.R., Kimura, S.J., & Morris, B.W. 1976. Optic Disk Neovascularization Associated with Chronic Uveitis. *Am.J.Ophthalmol.*, 82, (2) 175-178

Shuttleworth, C.W. 2010. Use of NAD(P)H and flavoprotein autofluorescence transients to probe neuron and astrocyte responses to synaptic activation. *Neurochem.Int.*, 56, (3) 379-386

Shuttleworth, C.W., Brennan, A.M., & Connor, J.A. 2003. NAD(P)H fluorescence imaging of postsynaptic neuronal activation in murine hippocampal slices. *J.Neurosci.*, 23, (8) 3196-3208

Sibbald, W.J., Fox, G., & Martin, C. 1991. Abnormalities of Vascular Reactivity in the Sepsis Syndrome. *Chest*, 100, (3) S155-S159

Siegemund, M., van Bommel, J., Vollebrecht, K., Dries, J., & Ince, C. 2000. Influence of NO donor SIN-1 on the gut oxygenation in a normodynamic, porcine model of low-dose endotoxaemia. *Intensive Care Med.*, 26, S362-S363

Silver, J. & Robb, R.M. 1979. Studies on the Development of the Eye Cup and Optic-Nerve in Normal Mice and in Mutants with Congenital Optic-Nerve Aplasia. *Developmental Biology*, 68, (1) 175-190

Singer, D. 2002. Phylogeny of mammalian metabolism. *Anasthesiologie Intensivmedizin Notfallmedizin Schmerztherapie*, 37, (8) 441-460

Singer, M. & Brealey, D. 1999. Mitochondrial dysfunction in sepsis. *Mitochondria and Cell Death*, 66, 149-166

Sjovall, F., Morota, S., Hansson, M.J., Friberg, H., Gnaiger, E., & Elmer, E. 2010. Temporal increase of platelet mitochondrial respiration is negatively associated with clinical outcome in patients with sepsis. *Crit.Care*, 14, (6)

Smith, C.W. 1993. Endothelial Adhesion Molecules and Their Role in Inflammation. *Can.J.Physiol.Pharmacol.*, 71, (1) 76-87

Sonneville, R., Verdonk, F., Rauturier, C., Klein, I.F., Wolff, M., Annane, D., Chretien, F., & Sharshar, T. 2013. Understanding brain dysfunction in sepsis. *Annals of Intensive Care*, 3,

Sorensen, T.L., Frederiksen, J.L., Bronnum-Hansen, H., & Petersen, H.C. 1999. Optic neuritis as onset manifestation of multiple sclerosis - A nationwide, long-term survey. *Neurology*, 53, (3) 473-478

Sperlagh, B. & Vizi, E.S. 1996. Neuronal synthesis, storage and release of ATP. *Seminars in Neuroscience*, 8, (4) 175-186

Spronk, P.E., Ince, C., Gardien, M.J., Mathura, K.R., Oudemans-van Straaten, H.M., & Zandstra, D.F. 2002. Nitroglycerin in septic shock after intravascular volume resuscitation. *Lancet*, 360, (9343) 1395-1396

Spronk, P. E., Kanoore-Edul, V. S., & Ince, C. 2005, "Microcirculatory and Mitochondrial Distress Syndrome (MMDS): A New Look at Sepsis," *In Functional Hemodynamic Monitoring*, 42 ed. pp. 47-67.

Sprung, C.L., Peduzzi, P.N., Shatney, C.H., Wilson, M.F., & Hinshaw, L.B. 1988. The Impact of Encephalopathy on Mortality and Physiologic Derangements in the Sepsis Syndrome. *Crit.Care Med.*, 16, (4) 398

Stefferl, A., Brehm, U., Storch, M., Lambracht-Washington, D., Bourquin, C., Wonigeit, K., Lassmann, H., & Linington, C. 1999. Myelin oligodendrocyte glycoprotein induces experimental autoimmune encephalomyelitis in the "resistant" brown Norway rat: Disease susceptibility is determined by MHC and MHC-linked effects on the B cell response. *J.Immunol.*, 163, (1) 40-49

Storch, M.K., Stefferl, A., Brehm, U., Weissert, R., Wallstrom, E., Kerschensteiner, M., Olsson, T., Linington, C., & Lassmann, H. 1998. Autoimmunity to myelin oligodendrocyte glycoprotein in rats mimics the spectrum of multiple sclerosis pathology. *Brain Pathol.*, 8, (4) 681-694

Strauss, O. 2005. The retinal pigment epithelium in visual function. *Physiol.Rev.*, 85, (3) 845-881

Streit, W. J. 2005, "Microglial cells," *In Neuroglia*, 2nd ed. H. Kettenmann & B. R. ansom, eds., New York: Oxford University Press, pp. 60-71.

Streit, W.J., Graeber, M.B., & Kreutzberg, G.W. 1988. Functional Plasticity of Microglia - A Review. *Glia*, 1, (5) 301-307

Stuehr, D.J., Cho, H.J., Kwon, N.S., Weise, M.F., & Nathan, C.F. 1991. Purification and Characterization of the Cytokine-Induced Macrophage Nitric-Oxide Synthase - An Fad-Containing and Fmn-Containing Flavoprotein. *Proc.Natl.Acad.Sci.U.S.A.*, 88, (17) 7773-7777

Sugano, T., Oshino, N., & Chance, B. 1974. Mitochondrial functions under hypoxic conditions: The steady states of cytochrome c reduction and of energy metabolism. *Biochimica et Biophysica Acta (BBA) - Bioenergetics*, 347, (3) 340-358

Sun, J.B., Link, H., Olsson, T., Xiao, B.G., Andersson, G., Ekre, H.P., Linington, C., & Diener, P. 1991. T-Cell and B-Cell Responses to Myelin-Oligodendrocyte Glycoprotein in Multiple-Sclerosis. *Journal of Immunology*, 146, (5) 1490-1495

t'Hart, B.A., van Meurs, M., Brok, H.P.M., Massacesi, L., Bauer, J., Boon, L., Bontrop, R.E., & Laman, J.D. 2000. A new primate model for multiple sclerosis in the common marmoset. *Immunology Today*, 21, (6) 290-297

Taccone, F.S., Castanares-Zapatero, D., Peres-Bota, D., Vincent, J.L., Berre, J., & Melot, C. 2010. Cerebral Autoregulation is Influenced by Carbon Dioxide Levels in Patients with Septic Shock. *Neurocritical Care*, 12, (1) 35-42

Takahashi, K., Hishida, R., Kubota, Y., Kudoh, M., Takahashi, S., & Shibuki, K. 2006. Transcranial fluorescence imaging of auditory cortical plasticity regulated by acoustic environments in mice. *Eur.J.Neurosci.*, 23, (5) 1365-1376

Takano, T., Tian, G.F., Peng, W.G., Lou, N.H., Lovatt, D., Hansen, A.J., Kasischke, K.A., & Nedergaard, M. 2007. Cortical spreading depression causes and coincides with tissue hypoxia. *Nat.Neurosci.*, 10, (6) 754-762

Tanaka, J., Kono, Y., Shimahara, Y., Sato, T., Jones, R.T., Cowley, R.A., & Trump.B.F. 1982. A study of oxidative phosphorylative activity and calcium-induced respiration of rat liver mitochondria following living Escherichia coli injection. *Adv.Shock Res.*, 7, 77-90

Tavakoli, H. & Mela, L. 1982. Alterations of mitochondrial metabolism and protein concentrations in subacute septicemia. *Infect.Immun.*, 38, (2) 536-541

Taylor, H.R. & Keeffe, J.E. 2001. World blindness: a 21st century perspective. *British Journal of Ophthalmology*, 85, (3) 261-266

Thijs, L.G., Groeneveld, A.B.J., & Hack, C.E. 1996. Multiple organ failure in septic shock. *Pathology of Septic Shock*, 216, 209-237

Thompson, A.J., Polman, C.H., Miller, D.H., Mcdonald, W.I., Brochet, B., Filippi, M., Montalban, X., & Desa, J. 1997. Primary progressive multiple sclerosis. *Brain*, 120, 1085-1096

Timpl, R., Rohde, H., Robery, P.G., Rennard, S.I., Foidart, J.M., & Martin, G.R. 1979. Laminin-a glycoprotein from basement membranes. *The Journal of Biological Chemistry*, 254, 9933-9937

Todd, J.C., Poulos, N.D., Davidson, L.W., & Mollitt, D.L. 1993. Role of the Leukocyte in Endotoxin-Induced Alterations of the Red-Cell Membrane. *Am.Surg.*, 59, (1) 9-12

Toernquist, P. & Alm, A. 1979. Retinal and choroidal contribution to retinal metabolism in vivo. A study in pigs. *Acta Physiol.Scand.*, 106, (3) 351-357

Tohmi, M., Kitaura, H., Komagata, S., Kudoh, M., & Shibuki, K. 2006. Enduring critical period plasticity visualized by transcranial flavoprotein imaging in mouse primary visual cortex. *J.Neurosci.*, 26, (45) 11775-11785

Toledo, J., Sepulcre, J., Salinas-Alaman, A., Garcia-Layana, A., Murie-Fernandez, M., Bejarano, B., & Villoslada, P. 2008. Retinal nerve fiber layer atrophy is associated with physical and cognitive disability in multiple sclerosis. *Mult.Scler.*, 14, (7) 906-912

Toussaint, D., Perier, O., Verstappen, A., & Bervoets, S. 1983. Clinicopathological Study of the Visual Pathways, Eyes, and Cerebral Hemispheres in 32 Cases of Disseminated Sclerosis. *J.Clin.Neuroophthalmol.*, 3, (3) 211-220

Trapp, B.D., Peterson, J., Ransohoff, R.M., Rudick, R., Mork, S., & Bo, L. 1998. Axonal transection in the lesions of multiple sclerosis. *New Engl.J.Med.*, 338, (5) 278-285

Trip, S.A., Schlottmann, P.G., Jones, S.J., Altmann, D.R., Garway-Heath, D.F., Thompson, A.J., Plant, G.T., & Miller, D.H. 2005. Retinal nerve fiber layer axonal loss and visual dysfunction in optic neuritis. *Ann.Neurol.*, 58, (3) 383-391

Turrens, J.F. 1997. Superoxide production by the mitochondrial respiratory chain. *Biosci.Rep.*, 17, (1) 3-8

Turrens, J.F. 2003. Mitochondrial formation of reactive oxygen species. *Journal of Physiology-London*, 552, (2) 335-344

Turrens, J.F. & Boveris, A. 1980. Generation of Superoxide Anion by the Nadh Dehydrogenase of Bovine Heart-Mitochondria. *Biochem.J.*, 191, (2) 421-427

Tyml, K., Wang, X.W., Lidington, D., & Ouellette, Y. 2001. Lipopolysaccharide reduces intercellular coupling in vitro and arteriolar conducted response in vivo. *Am.J.Physiol-Heart.C.*, 281, (3) H1397-H1406

Ulrich, J. & Groebkelorenz, W. 1983. The Optic-Nerve in Multiple-Sclerosis - A Morphological-Study with Retrospective Clinicopathological Correlations. *Neuro-Ophthalmology*, 3, (3) 149-159

Vallance, P., Collier, J., & Moncada, S. 1989. Effects of Endothelium-Derived Nitric-Oxide on Peripheral Arteriolar Tone in Man. *Lancet*, 2, (8670) 997-1000

Vallet, B., Lund, N., Curtis, S.E., Kelly, D., & Cain, S.M. 1994. Gut and Muscle-Tissue Po2 in Endotoxemic Dogs During Shock and Resuscitation. *J.Appl.Physiol.*, 76, (2) 793-800

Van Beek, J., Elward, K., & Gasque, P. 2003. Activation of complement in the central nervous system - Roles in neurodegeneration and neuroprotection. *Neuroendocrine and Neural Regulation of Autoimmune and Inflammatory Disease: Molecular, Systems, and Clinical Insights*, 992, 56-71

van den Maagdenberg, A.M.J.M., Pietrobon, D., Pizzorusso, T., Kaja, S., Broos, L.A.M., Cesetti, T., van de Ven, R.C.G., Tottene, A., van der Kaa, J., Plomp, J.J., Frants, R.R., & Ferrari, M.D. 2004. A Cacna1a knockin migraine mouse model with increased susceptibility to cortical spreading depression. *Neuron*, 41, (5) 701-710

Vandermeer, T.J., Wang, H.L., & Fink, M.P. 1995. Endotoxemia Causes Ileal Mucosal Acidosis in the Absence of Mucosal Hypoxia in A Normodynamic Porcine Model of Septic Shock. *Crit.Care Med.*, 23, (7) 1217-1226

Vincent, J.L. & De Backer, D. 2005. Microvascular dysfunction as a cause of organ dysfunction in severe sepsis. *Crit.Care*, 9, S9-S12

Volobоueva, L.A., Emery, J.F., Sun, X.Y., & Giffard, R.G. 2013. Inflammatory response of microglial BV-2 cells includes a glycolytic shift and is modulated by mitochondrial glucose-regulated protein 75/mortalin. *FEBS Lett.*, 587, (6) 756-762

von Leithner, P.L., Kam, J.H., Bainbridge, J., Catchpole, I., Gough, G., Coffey, P., & Jeffery, G. 2009. Complement Factor H Is Critical in the Maintenance of Retinal Perfusion. *Am.J.Pathol.*, 175, (1) 412-421

Vovenko, E. 1999. Distribution of oxygen tension on the surface of arterioles, capillaries and venules of brain cortex and in tissue in normoxia: an experimental study on rats. *Pflugers Archiv-European Journal of Physiology*, 437, (4) 617-623

Wabbels, B., Demmler, A., Paunescu, K., Wegscheider, E., Preising, M.N., & Lorenz, B. 2006. Fundus autofluorescence in children and teenagers with hereditary retinal diseases. *Graefes Arch.Clin.Exp.Ophthalmol.*, 244, (1) 36-45

Wakefield, D. & Chang, J.H. 2005. Epidemiology of uveitis. *International Ophthalmology Clinics*

Wang, J., Xiong, S., Xie, C., Markesbery, W.R., & Lovell, M.A. 2005. Increased oxidative damage in nuclear and mitochondrial DNA in Alzheimer's disease. *J.Neurochem.*, 93, (4) 953-962

Wangsa-Wirawan, N.D. & Linsenmeier, R.A. 2003. Retinal oxygen - Fundamental and clinical aspects. *Arch.Ophthalmol.*, 121, (4) 547-557

Watson, N.A., Beards, S.C., Altaf, N., Kassner, A., & Jackson, A. 2000. The effect of hyperoxia on cerebral blood flow: a study in healthy volunteers using magnetic resonance phase-contrast angiography. *Eur.J.Anaesthesiol.*, 17, (3) 152-159

Webb, R.H., Hughes, G.W., & Delori, F.C. 1987. Confocal Scanning Laser Ophthalmoscope. *Appl.Opt.*, 26, (8) 1492-1499

Weber, B., Burger, C., Wyss, M.T., von Schulthess, G.K., Scheffold, F., & Buck, A. 2004. Optical imaging of the spatiotemporal dynamics of cerebral blood flow and oxidative metabolism in the rat barrel cortex. *Eur.J.Neurosci.*, 20, (10) 2664-2670

Wedmore, C.V. & Williams, T.J. 1981. Control of Vascular-Permeability by Polymorphonuclear Leukocytes in Inflammation. *Nature*, 289, (5799) 646-650

Wichterman, K.A., Baue, A.E., & Chaudry, I.H. 1980. Sepsis and Septic Shock - A Review of Laboratory Models and A Proposal. *J.Surg.Res.*, 29, (2) 189-201

Wilhelm, D.L. 1962. Mediation of Increased Vascular Permeability in Inflammation. *Pharmacol.Rev.*, 14, (2) 251-&

Wilson, R.F., Sarver, E.J., & Leblanc, P.L. 1971. Factors Affecting Hemodynamics in Clinical Shock with Sepsis. *Ann.Surg.*, 174, (6) 939-&

Wolf, M.D., Lichter, P.R., & Ragsdale, C.G. 1987. Prognostic Factors in the Uveitis of Juvenile Rheumatoid-Arthritis. *Ophthalmology*, 94, (10) 1242-1248

Wollstein, G., Garway-Heath, D.F., & Hitchings, R.A. 1998. Identification of early glaucoma cases with the scanning laser ophthalmoscope. *Ophthalmology*, 105, (8) 1557-1563

Wong, M.L., Rettori, V., AlShekhlee, A., Bongiorno, P.B., Canteros, G., Mccann, S.M., Gold, P.W., & Licinio, J. 1996. Inducible nitric oxide synthase gene expression in the brain during systemic inflammation. *Nat.Med.*, 2, (5) 581-584

Wurziger, K., Lichtenberger, T., & Hanitzsch, R. 2001. On-bipolar cells and depolarising third-order neurons as the origin of the ERG-b-wave in the RCS rat. *Vision Res.*, 41, (8) 1091-1101

Xu, H.P., Chen, M., Manivannan, A., Lois, N., & Forrester, J.V. 2008. Age-dependent accumulation of lipofuscin in perivascular and subretinal microglia in experimental mice. *Aging Cell*, 7, (1) 58-68

Xu, H.P., Forrester, J.V., Liversidge, J., & Crane, I.J. 2003. Leukocyte trafficking in experimental autoimmune uveitis: Breakdown of blood-retinal barrier and upregulation of cellular adhesion molecules. *Investigative Ophthalmology & Visual Science*, 44, (1) 226-234

Yakes, F.M. & VanHouten, B. 1997. Mitochondrial DNA damage is more extensive and persists longer than nuclear DNA damage in human cells following oxidative stress. *Proc.Natl.Acad.Sci.U.S.A.*, 94, (2) 514-519

Yalcin, A., Telang, S., Clem, B., & Chesney, J. 2009. Regulation of glucose metabolism by 6-phosphofructo-2-kinase/fructose-2,6-bisphosphatases in cancer. *Exp.Mol.Pathol.*, 86, (3) 174-179

Yang, G., Pan, F., Parkhurst, C.N., Grutzendler, J., & Gan, W.B. 2010. Thinned-skull cranial window technique for long-term imaging of the cortex in live mice. *Nature Protocols*, 5, (2) 201-208

Yang, S.Y., He, X.Y., & Schulz, H. 1987. Fatty-Acid Oxidation in Rat-Brain Is Limited by the Low Activity of 3-Ketoacyl-Coenzyme-A Thiolase. *J.Biol.Chem.*, 262, (27) 13027-13032

Ying, W.H. 2008. NAD(+)/ NADH and NADP(+)/NADPH in cellular functions and cell death: Regulation and biological consequences. *Antioxidants & Redox Signaling*, 10, (2) 179-206

Young, G.B., Bolton, C.F., Archibald, Y.M., Austin, T.W., & Wells, G.A. 1992. The Electroencephalogram in Sepsis-Associated Encephalopathy. *J.Clin.Neurophysiol.*, 9, (1) 145-152

Young, G.B., Bolton, C.F., Austin, T.W., Archibald, Y.M., Gonder, J., & Wells, G.A. 1990. The Encephalopathy Associated with Septic Illness. *Clinical and Investigative Medicine-Medecine Clinique et Experimentale*, 13, (6) 297-304

Yu, D.Y. & Cringle, S.J. 2001. Oxygen distribution and consumption within the retina in vascularised and avascular retinas and in animal models of retinal disease. *Prog.Retin.Eye Res.*, 20, (2) 175-208

Zapelini, P.H., Rezin, G.T., Cardoso, M.R., Ritter, C., Klamt, F., Moreira, J.C.F., Streck, E.L., & Dal-Pizzol, F. 2008. Antioxidant treatment reverses mitochondrial dysfunction in a sepsis animal model. *Mitochondrion*, 8, (3) 211-218

Zein, G., Berta, A., & Foster, C.S. 2004. Multiple sclerosis-associated uveitis. *Ocular Immunology and Inflammation*, 12, (2) 137-142

Zhang, C., Lam, T.T., & Tso, M.O.M. 2005. Heterogeneous populations of microglia/macrophages in the retina and their activation after retinal ischemia and reperfusion injury. *Exp.Eye Res.*, 81, (6) 700-709

Zolfaghari, P.S., Pinto, B.B., Dyson, A., & Singer, M. 2013. The metabolic phenotype of rodent sepsis: cause for concern. *Intensive Care Medicine Experimental*, 1, (6) 1-13